MAPPING OF FUSARIUM HEAD BLIGHT RESISTANCE IN TWO WINTER WHEAT POPULATIONS AND GENE EXPRESSION ANALYSIS OF PUTATIVE GENES RELATED TO THE HOST-PATHOGEN INTERACTION

BY

YANG LIN

A Thesis submitted to the Faculty of Graduate Studies of

The University of Manitoba

In partial fulfilment of the requirements of the degree of

DOCTOR OF PHILOSOPHY

Department of Plant Science

University of Manitoba

Winnipeg, Manitoba

Lin, Yang. PhD Thesis. The University of Manitoba, 2022. Mapping of Fusarium head blight resistance in two winter wheat populations and gene expression analysis of putative genes related to the host-pathogen interaction. Ph.D. Supervisor: Dr. Anita Brûlé-Babel

ABSTRACT

Fusarium graminearum (*Fg*) is the primary causal agent of Fusarium head blight (FHB) in wheat. Resistance to FHB is complex and involves multiple genes with relatively small effects. A winter wheat line, 32c*17, demonstrated strong FHB and deoxynivalenol (DON) resistance. Two quantitative trait loci (QTL) mapping studies were conducted using two doubled haploid populations (32c*17/Peregrine (3CPR) and 18I*45/32c*17 (8I3C)) tested for FHB resistance in field and greenhouse trials. In the 3CPR population, three main QTL for FHB resistance on chromosomes 4D, 6A and 6D were detected. Markers for QTL on chromosomes 4D, 6B and 6D accurately predicted FHB resistance in the reciprocal cross. In the 8I3C population, two major 4B and 6D QTL for disease incidence (Inc) and DON content and one major 7A QTL for disease severity (Sev) were identified. The 32c*17 allele on chromosome 4B in the 8I3C population increased height, reduced anther retention, Inc and DON content, while no 4B QTL was detected in the 3CPR population. The 32c*17-derived 6D QTL was identified in both 8I3C and 3CPR populations. Moreover, the 8I3C 4D QTL for height and the 3CPR 4D QTL for FHB resistance were detected in the similar region. Height QTL on chromosomes 1D, 2B and 7B in the 8I3C population were not associated with FHB resistance.

A gene expression study was conducted to wheat- *Fg* interaction on five genotypes which included two near isogenic lines carrying either the *Rht-B1a* or *Rht-B1b* allele and three checks Sumai 3, 32c*17 and Caledonia. For four *Trichothecene* (*TRI*) genes (*TRI5*, *TRI6*, *TRI12* and *TRI101*)

examined, lower gene expression in genotypes with high disease severity were found in the inoculated spikelets in the point-inoculated *Fg* treatment. Higher expression of the three genes (*ABCC6*, *AOS* and *PR4*) at earlier time points (3 dai) and a lower expression level of *NFXL1* at the late time point may be associated with FHB resistance in all three inoculation treatments, while late expression of the same three genes might be insufficient to reduce disease severity.

ACKNOWLEDGEMENTS

First of all, I am deeply grateful to have Dr. Anita Brûlé-Babel as my Ph.D. supervisor for all the valuable guidance, strong support and continuous encouragement over these years. It was a great privilege to be one of your students. Not only have I received wonderful academic and science training, critical thinking, and team management skills, but I also hope I have developed great personal characteristics you model, like hard work, trustworthiness, humility, open-mindedness, thoughtfulness, patience, and endurance.

I acknowledge all of my committee members for their support and advice; Dr. Curt McCartney, Dr. Dilantha Fernando and Dr. Georg Hausner. A special thanks to Dr. McCartney for his great support, in particular teaching linkage and QTL mapping, providing additional marker tests, and always quickly and kindly answering my questions. I thank Dr. Aaron Beattie for serving as the external examiner. I also would like to thank Dr. Michele C. Loewen and her technician Kerry Boyle from for genotyping three winter wheat populations. I am very thankful to Dr. Paul Nicholson (John Innes Centre, United Kingdom) for kindly providing all near isogenic lines in the gene expression project. I appreciate Dr. Robert Duncan for allowing me to use his lab space and equipment for gene expression work and his wonderful technician Ralph Kowatsch for his advice and support. I would like to thank Dr. Jeannie Gilbert for providing *Fusarium* isolates and Dr. Gavin Humphreys for testing materials in Ottawa.

I am very grateful to be a part of the wheat breeding and genetics lab and greatly appreciate the technical assistance, support and encouragement from all lab staff: Mary Meleshko, Zesong Ye,

Dr. Maria Stoimenova, Epifania Austria, Roger Larios, Kaitlyn Pidherny and Vanessa Clemis. I also thank all my great fellow lab mates: Anjan Neupane, Younyoung Lee, Gabrielle Nowakowski, Duoduo Wang and Alice Mwaniki. I thank Xiaohan Zhu, Aihua Liu, Zhongwei Zou, Rhodesia Celoy, Mohammad Mira and Doug Durnin for their advice on the gene expression project.

Thank you to all fellow graduate students in the department for their friendship, especially to Kenny So, Jia Sun, Ashley Ammeter, Xiaohan Zhu, Chami Amarasinghe and Gabriel Linski. I thank the greenhouse staff Cathy Bay and Rob Visser for their hard work. I would also like to thank Martha Blouw for her support, Cunchun Yang and Valeria Lobos-Sujo for being great office mates and Jon Rosset for explaining SAS coding.

Special thanks to the funding agencies that supported this work: Western Grains Research Foundation, Manitoba Wheat and Barley Growers Association, Growing Forward 2, Natural Sciences and Engineering Research Council of Canada, and Willy Wiebe Graduate Fellowship.

Finally, my gratitude goes to my wonderful wife Dr. Donica Janzen for her continuous support, love, and encouragement and my beloved parents and family members for their love and support. I would like to remember my beloved grandma 陈淑英 in heaven for raising me.

TABLE OF CONTENTS

ABSTRACT I
ACKNOWLEDGEMENTS III
TABLE OF CONTENTS V
LIST OF TABLES VIII
LIST OF FIGURES X
LIST OF APPENDICES XIII
LIST OF ABBREVIATIONS XV
FOREWORD XVIII
CONTRIBUTIONS OF AUTHORS XIX
CHAPTER 1 1
GENERAL INTRODUCTION 1
CHAPTER 2 5
LITERATURE REVIEW 5
2.1 Wheat 5
2.1.1 Canadian wheat production 5
2.1.2 Wheat genome and genetics 6
2.2 *Fusarium graminearum* 9
2.2.1 Taxonomy and genome of *Fusarium graminearum* 9
2.2.2 Disease symptoms and epidemics of FHB in Canada 11
2.2.3 The life cycle of *Fusarium graminearum* 12
2.3 Fusarium head blight mycotoxins - Deoxynivalenol 13
2.3.1 Fusarium chemotypes 13
2.3.2 Deoxynivalenol biosynthesis pathway and important *TRI* genes 15
2.3.3 Toxicity of deoxynivalenol and its role in pathogenicity 17
2.4 Management of Fusarium head blight 19
2.4.1 Cultural practices 19
2.4.2 Chemical control 20
2.4.3 Biological control 23
2.5 FHB disease resistance breeding in wheat 24
2.5.1 Active host defense mechanisms of FHB resistance 24
2.5.1.1 Five types of FHB resistance 24
2.5.1.2 Sources of genetic resistance to FHB 24
2.5.1.3 Common QTL for Type I, II and V resistance 27
2.5.1.4 Common *Fhb* genes 29
2.5.1.5 The association of FHB susceptibility 30
2.5.2 Morphological traits affecting FHB 31
2.5.2.1 Association between plant height and FHB 31
2.5.2.2 Association between anther retention and FHB 33
2.6 Cross talk among different phytohormones during host defense 34
2.6.1 The regulation of gibberellin on plant height and the gibberellin-dependent dwarfing 34
2.6.2 Role of jasmonic acid signalling in wheat FHB resistance 37
2.6.3 Crosstalk between GA and JA pathways affecting wheat FHB resistance 39
CHAPTER 3 42

QTL MAPPING OF FUSARIUM HEAD BLIGHT RESISTANCE IN AN ELITE DOUBLED HAPLOID WINTER WHEAT CROSS 32C*17/PEREGRINE AND EVALUATION OF MARKER ASSISTED SELECTION EFFICIENCY OF DETECTED QTL IN THE RECIPROCAL CROSS 42
3.1 Abstract....42
3.2 Introduction....44
3.3 Materials and Methods....48
3.3.1 Plant material....48
3.3.2 Inoculum preparation....49
3.3.3 Field experiments for the 3CPR population....50
3.3.4 Greenhouse experiment for the 3CPR population....51
3.3.5 Linkage and QTL mapping in the 3CPR population....53
3.3.6 Statistical analyses....55
3.3.7 Estimation of prediction accuracy of resistant PR3C DHs by using the markers located within the putative 3CPR QTL....56
3.4 Results....57
3.4.1 Phenotyping for the 3CPR population, parental lines and checks....57
3.4.2 Linkage mapping....62
3.4.3 QTL mapping....63
3.4.3.1 QTL for anthesis date....64
3.4.3.2 QTL for plant height....64
3.4.3.3 QTL for FHB resistance....65
3.4.3.3.1 Visual FHB traits (Inc, Sev, VRI)....65
3.4.3.3.2 FDK and DON content....68
3.4.4 Marker prediction of 3CPR QTL in the reciprocal population PR3C....76
3.5 Discussion....78
3.6 Conclusions....89
CHAPTER 4....91
CHARACTERIZATION AND VALIDATION OF FUSARIUM HEAD BLIGHT RESISTANCE QTL IN AN ELITE DOUBLED HAPLOID WINTER WHEAT CROSS 18I*45/32C*17....91
4.1 Abstract....91
4.2 Introduction....92
4.3 Materials and Methods....96
4.3.1 Plant material....96
4.3.2 Inoculum preparation....97
4.3.3 Field experiments for the 8I3C population....98
4.3.4 Greenhouse experiment for FHB resistance for the 8I3C population....99
4.3.5 Greenhouse experiment for anther retention for the 8I3C population....101
4.3.6 Linkage and QTL mapping in the 8I3C population....102
4.3.7 Statistical analyses....104
4.4 Results....105
4.4.1 Phenotyping for the 8I3C population, parental lines and checks....105
4.4.2 Linkage mapping....114
4.4.3 QTL mapping....114
4.4.3.1 QTL for anthesis date....115

4.4.3.2 QTL for anther retention....116
4.4.3.3 QTL for plant height....116
4.4.3.4 QTL for FHB resistance....117
4.4.3.4.1 Visual FHB traits (Inc, Sev, VRI)....118
4.4.3.4.2 FDK and DON content....120
4.5 Discussion....128
4.5.1 QTL for agronomic traits (Anth, GAnth and Ht)....129
4.5.2 QTL for FHB resistance....133
4.6 Conclusions....141
CHAPTER 5....143
GENE EXPRESSION ANALYSIS OF PUTATIVE GENES RELATED TO THE HOST-PATHOGEN INTERACTION....143
5.1 Abstract....143
5.2 Introduction....145
5.2 Materials and Methods....150
5.2.1 Plant material....150
5.2.2 Fusarium inoculum and deoxynivalenol solution....151
5.2.3 Experiment design for four different inoculation methods....152
5.2.4 Measurement of phenotypic data and spike sampling....156
5.2.5 RNA purification and quantitative reverse transcription PCR....157
5.2.6 Statistical Analysis....159
5.3 Results....161
5.3.1 Phenotypic data....161
5.3.2 Relative expression of genes in qPCR tests....164
5.3.2.1 Four Fusarium *TRI* genes involved in the deoxynivalenol biosynthesis pathway in the iF and sF treatments....164
5.3.2.2 Response of two wheat genes, *ABCC6* and *NFXL1*, to the iF, sF and iD treatments....170
5.3.2.3 Two wheat genes (*AOS* and *JAZ1*) related to jasmonic acid hormone biosynthesis and signaling pathway and three wheat genes (*PR1b, PR4* and *PDF1.2*) involved in defense responses in the iF, sF and iD treatments....171
5.4 Discussion....181
5.4.1 Expression of *TRI* genes in the five genotypes in the iF treatment....181
5.4.2 Expression of *TRI* genes in the five genotypes in the sF treatment....185
5.4.3 Expression of seven wheat genes (*ABCC6*, *NFXL1*, *AOS*, *JAZ1*, *PR1b*, *PR4* and *PDF1.2*) in the five genotypes in the iF treatment....186
5.4.4 Expression of seven wheat genes (*ABCC6*, *NFXL1*, *AOS*, *JAZ1*, *PR1b*, *PR4* and *PDF1.2*) in the two genotypes in the iD treatment....189
5.4.5 Expression of seven wheat genes (*ABCC6*, *NFXL1*, *AOS*, *JAZ1*, *PR1b*, *PR4* and *PDF1.2*) in the five genotypes in the sF treatment....190
5.5 Conclusions....191
CHAPTER 6....193
GENERAL DISCUSSION AND CONCLUSION....193
References....203

LIST OF TABLES

Table 2.1 Location and function of all *Trichothecene* (*TRI*) genes involved in the deoxynivalenol (DON) biosynthesis pathway in *Fusarium* genome. Data were obtained and modified from multiple sources (Brown et al. 2002; McCormick et al. 2004; Gale et al. 2005; Kulik 2008; Lee et al. 2008; Foroud et al. 2019).....17
Table 2.2 Summary of previously reported major QTL for Fusarium head blight (FHB) resistance and morphological traits associated with these major FHB resistance in 21 wheat chromosomes based on information adapted from the two reviews (Buerstmayr et al. 2009, 2019). 28
Table 2.3 Current *Fhb* genes in characterized in wheat or wheat relatives, their chromosomal location, type of resistance and source. 30
Table 3.1 Combined analysis of variance for anthesis date (Anth), height (Ht), incidence (Inc), severity (Sev), visual rating index (VRI), Fusarium damaged kernel (FDK) and deoxynivalenol (DON) for the 3CPR population tested in field experiments conducted in six site years in Manitoba and analysis of variance for greenhouse anthesis (GAnth) and greenhouse severity (GSev1 and GSev2) conduced in a greenhouse trial in 2015. Replicate nested within each site year for the combined field analysis. 59
Table 3.2 Broad sense heritability and descriptive statistics of parental lines and the 3CPR doubled haploid (DH) population for traits measured in the combined six site year field trials and one greenhouse test. Traits include anthesis date (Anth), height (Ht), incidence (Inc), severity (Sev), visual rating index (VRI), Fusarium damaged kernel (FDK), deoxynivalenol (DON), greenhouse anthesis date (GAnth) and greenhouse severity (GSev1 and GSev2). 60
Table 3.3 Summary of linkage map for the 3CPR population including numbers of markers, genetic and physical distance, and average spacing between markers for genetic and physical map 71
Table 3.4 Summary of 3CPR QTL detected for all traits measured in field and greenhouse experiments using the following four methods: interval mapping (IM), inclusive composite interval mapping (ICIM), simple interval mapping (SIM) and composite interval mapping (CIM). 73
Table 3.5 Validation of markers under peaks of 3CRP QTL in the reciprocal population PR3C for field FHB incidence (Inc), field FHB severity (Sev) and FHB visual rating index (VRI) in 2015 and 2016 by using single marker analyses (T-test) between PR3C phenotypic data and the selected markers. 77
Table 3.6 A summary of QTL for FHB resistance previously reported in bi-parental QTL studies in other studies using the different FHB parameters, including incidence (Inc), greenhouse or field severity (Sev), visual rating index (VRI), Fusarium damaged kernel (FDK) and deoxynivalenol (DON) content. 87
Table 4.1 Analysis of variance for anthesis date (Anth), height (Ht), incidence (Inc), severity (Sev), visual rating index (VRI), Fusarium damaged kernel (FDK) and deoxynivalenol (DON) for the 8I3C population based on the combination of all six site years in Manitoba, analysis of variance for greenhouse anthesis (GAnth) and greenhouse severity (GSev1 and GSev2) in 2016, and analysis of variance for greenhouse anthesis (GAnth2), greenhouse height (GHt) and greenhouse anther retention (GAR) in 2019. Replicate nested within each site year was analyzed when all site years were combined. 108
Table 4.2 Broad sense heritability and descriptive statistics of parental lines and the 8I3C doubled haploid (DH) population for traits measured in combined six site year field trials and two

greenhouse tests. Traits include anthesis date (Anth), height (Ht), incidence (Inc), severity (Sev), visual rating index (VRI), Fusarium damaged kernel (FDK), deoxynivalenol (DON), 2016 greenhouse anthesis date (GAnth), 2016 greenhouse severity (GSev1 and GSev2), 2019 greenhouse anthesis date (GAnth2), 2019 greenhouse height (GHt) and anther retention (GAR). 109
Table 4.3 Summary of linkage map for the 8I3C population including numbers of markers, genetic and physical distance, and average spacing between markers for genetic and physical map. 123
Table 4.4 Summary of 8I3C QTL detected for all traits measured in field and greenhouse experiments using the following four methods: interval mapping (IM), inclusive composite interval mapping (ICIM), simple interval mapping (SIM) and composite interval mapping (CIM). 124
Table 4.5 Comparison of QTL detected in the two populations 8I3C (18I*45/32c*17) and 3CPR (32c*17/Peregrine) and the effect of the 32c*17 allele for specific traits associated with the QTL. 139
Table 5.1 The detailed information for the collection time points for different genotypes in different treatments in this experiment.....155
Table 5.2 Analysis of variance of plant height and disease severity under a controlled environment on five genotypes (G) at five time points (T) under four treatments including mock (Trt). 162

LIST OF FIGURES

Figure 2.1 A schematic diagram of main structure of type A and type B trichothecene, which was adapted from Foroud et al (2019). The "OAc" and "OIsoval" refer to O-acetyl and O-isovalerate, respectively. 14
Figure 2.2 A schematic diagram of the biosynthesis pathway of deoxynivalenol with several important *Trichothecene* (*TRI*) genes in *F. graminearum* (adapted from McCormick et al 2011). 16
Figure 2.3 A schematic diagram of the formation of GA (gibberellic acid)-GID1 (GA-insensitive dwarf1)-DELLA (D-E-L-L-A; Asp-Glu-Leu-Leu-Ala) complex for the regulation of gibberellin on plant height, which was adapted from Nelson and Steber (2016) and Hedden and Sponsel (2015). (a) A GID1 protein binds a bioactive GA molecule by using its N-terminal extension and the pocket-like core domain, which forms a GA-GID1 complex. (b) A wildtype allele *Rht-B1a* produces a normal DELLA protein with an intact DELLA domain and a C-terminal GRAS functional domain, which enables interaction with GA-GID1 complex to form a GA-GID1-DELLA complex. (c) A dwarf allele *Rht-B1b* encodes a truncated DELLA protein, which the partial DELLA domain cannot bind with GA-GID1 complex. 36
Figure 3.1 Frequency distributions of measured traits for the 3CPR doubled haploid (DH) lines based on means from six site year field trials and one year greenhouse test: anthesis date (a), height (b), incidence (c), severity (d), visual rating index (e), Fusarium damaged kernel (f), deoxynivalenol (g), greenhouse anthesis (h), greenhouse severity1 (i) and greenhouse severity2 (j). Means of parental lines for these traits were included. Anthesis date in field tests were calculated based on Julian calendar, while greenhouse anthesis date was calculated as the number of days between the date of transplanting into pots and the date at 30-50% anthesis stage.....62
Figure 4.1 Frequency distributions of measured traits for the 8I3C doubled haploid (DH) lines based on means from six site year field trials and greenhouse tests conducted in 2016 and 219: anthesis date (a), height (b), incidence (c), severity (d), visual rating index (e), Fusarium damaged kernel (f), deoxynivalenol (g), 2016 greenhouse anthesis (h), 2016 greenhouse severity1 (i), 2016 greenhouse severity2 (j), 2019 greenhouse anthesis (k), 2019 greenhouse height (l), and 2019 greenhouse anther retention (m). Means of parental lines for these traits were included. Anthesis date in field tests were calculated based on Julian calendar, while greenhouse anthesis date in 2016 and 2019 were calculated as the number of days between the date of transplanting into pots and the date at 30-50% anthesis stage. 113
Figure 5.1 A schematic diagram of the *Rht-B1b* NIL under the following four inoculation methods. (a) the spikelet labelled with the black mark, the spikelet above and the alternate spikelets on the other side of the picture were the four inoculated spikelets in the Mock treatment 0 days after inoculation (dai); (b, c) the spikelet labelled with black mark and the alternate spikelet were the two inoculated spikelets in the point inoculated *Fusarium* treatment (iF) or the point injected DON treatment (iD) 14 dai; (d) the spikelets labelled with black marks were the flowering spikelets in the spray inoculated *Fusarium* treatment (sF) 14 dai. 155
Figure 5.2 Disease severity of infected wheat spikes of five genotypes under the following three inoculation methods: (a) point inoculated with a macroconidal mixture of two 3ADON *F. graminearum* isolates (iF treatment), (b) point injected with a pure deoxynivalenol solution (iD treatment) and (c) spray inoculated with the same mixture (sF treatment). The five genotypes (G) are Maris Huntsman *Rht-B1a* NIL (1a) and *Rht-B1b* NIL (1b), 32c*17(32c), Caledonia (Cal) and Sumai 3 (Su3). The four time points are 1.5, 3, 7, 14 days after inoculation (dai). Letters indicate

significant differences ($P < 0.05$) among genotypes across all time points in individual treatments using Fisher's LSD test. 163
Figure 5.3 Relative expression of four *TRI* genes (*TRI5*, *TRI6*, *TRI12* and *TRI101*) related to DON biosynthesis pathway under a two-way interaction among genotype and time point in the following individual treatments: (a, c, e, g) point inoculated *Fusarium* (iF) and (b, d, f, h) spray inoculated *Fusarium* (sF). No significant expression difference for *TRI12* in the sF treatment and *TRI101* in the iF treatment indicates as "No diff" and "ns" (f and g). The five genotypes (G) are Maris Huntsman *Rht-B1a* NIL (1a) and *Rht-B1b* NIL (1b), 32c*17(32c), Caledonia (Cal) and Sumai 3 (Su3). The four time points are 1.5, 3, 7, 14 days after inoculation (dai). Expression of (a, b) *TRI5* and (g, h) *TRI101* were related to an early and middle stage of the biosynthesis pathway, respectively. Expression of (b, c) *TRI6* and (e, f) *TRI12* were related to a global transcription regulator mediating cellular metabolism and the entire DON biosynthesis pathway and toxin efflux pump, respectively. Mean of relative expression with log10 transformation for each genotype at each time point is shown, and least significant difference (LSD) values are shown. Letters indicate significant differences ($P < 0.05$) among means comparisons of the G*T interaction using Fisher's LSD test in each treatment. 167
Figure 5.4 Relative expression of all four *TRI* genes (*TRI5*, *TRI6*, *TRI12* and *TRI101*) related to DON biosynthesis pathway under a three-way interaction among part, genotype and time point in the point inoculated *Fusarium* treatments (a-d). No significant expression difference for *TRI12* indicates as "No diff" and "ns" (c). The two parts (IS and BIS part) were the inoculated spikelets and the spikelets below the inoculation points. The five genotypes (G) are Maris Huntsman *Rht-B1a* NIL (1a) and *Rht-B1b* NIL (1b), 32c*17(32c), Caledonia (Cal) and Sumai 3 (Su3). The four time points are 1.5, 3, 7, 14 days after inoculation (dai). Mean of relative expression with log10 transformation for each part of each genotype at each time point is shown, and least significant difference (LSD) values are shown. Letters indicate significant differences ($P < 0.05$) among means comparisons of the G*T*Part interaction using Fisher's LSD test in each treatment. Lines belonging to the IS part are shown in the left side and lines belonging to the BIS part are shown in right side. Y axis labels in the BIS part are the same as y axis in IS part. 169
Figure 5.5 Relative expression of seven wheat genes (*ABCC6*, *NFXL1*, *AOS*, *JAZ1*, *PR1b*, *PR4* and *PDF1.2*) under a two-way interaction among genotype and time point in the following individual treatments: (a1-g1) point inoculated *Fusarium* (iF), (a2-g2) point injected DON (iD) and (a3-g3) spray inoculated *Fusarium* (sF). The five genotypes (G) are Maris Huntsman *Rht-B1a* NIL (1a) and *Rht-B1b* NIL (1b), 32c*17 (32c), Caledonia (Cal) and Sumai 3 (Su3). The four time points are 1.5, 3, 7, 14 days after inoculation (dai). Mean of relative expression with log10 transformation for each genotype at each time point is shown, and least significant difference (LSD) values are shown. Letters indicate significant differences ($P < 0.05$) among means comparisons of the G*T interaction using Fisher's LSD test in each treatment. Due to missing data, there was no expression of *PDF1.2* in the *Rht-B1a* NIL at 14 dai in the iD treatment.....178
Figure 5.6 Relative expression of four wheat genes (*PR4*, *PDF1.2*, *JAZ1* and *PR1b*) under a three-way interaction among part, genotype and time point in individual treatments: (a) *PR4* and (b) *PDF1.2* in the point inoculated *Fusarium* treatment (iF), (c) *JAZ1* in the point inoculated deoxynivalenol treatment (iD) and (d) *PR1b* in spray inoculated *Fusarium* treatment (sF). The two parts (IS and BIS part) are the inoculated and neighboring spikelets. The four time points are 1.5, 3, 7 and 14 days after inoculation (dai). The five genotypes (G) are Maris Huntsman *Rht-B1a* NIL (1a) and *Rht-B1b* NIL (1b), 32c*17(32c), Caledonia (Cal) and Sumai 3 (Su3). Mean of relative expression with log10 transformation for each part of each genotype at each time point is shown,

and least significant difference (LSD) values are shown. Letters indicate significant differences ($P < 0.05$) among means comparisons of the G*T*Part interaction using Fisher's LSD test in each treatment. To improve readability, lines belonging to the IS part are shown in the left side and lines belonging to the BIS part are shown in right side. Due to missing date, lines in certain time points for different genotypes are shortened, especially in the IS part for *PDF1.2*, where Cal only had one time point at 3 dai with a highlighted dotted square and both the *Rht-B1b* NIL and Su3 had shorter lines. Y axis labels in the BIS are the same as y axis in IS part. 180

LIST OF APPENDICES

Appendix 3.1 Markers associated with common semi-dwarf genes or common FHB resistance genes/QTL screened on the parental lines and 3CPR doubled haploid population where appropriate. 224
Appendix 3.2 Analysis of variance for anthesis date (Anth), height (Ht), incidence (Inc), severity (Sev) and visual rating index (VRI) for the 3CPR population in each of six site years in Manitoba. 225
Appendix 3.3 Mean phenotype for anthesis date (Anth), height (Ht), incidence (Inc), severity (Sev), visual rating index (VRI), Fusarium damaged kernel (FDK), deoxynivalenol (DON), greenhouse anthesis (GAnth) and greenhouse severity (GSev1 and GSev2) or six checks based on least squares means in the combined field data and one year greenhouse data. 227
Appendix 3.4 Pearson correlation of anthesis date (Anth), height (Ht), incidence (Inc), severity (Sev), visual rating index (VRI), Fusarium damaged kernel (FDK), deoxynivalenol (DON), greenhouse anthesis (GAnth) and greenhouse severity (GSev1 and GSev2) for the 3CPR population based on means in the combined field data and one year greenhouse data. 228
Appendix 3.5 Boxplot distribution of genotypic classes grouped according to presence of specific allele combinations at QTL located on chromosomes 4D and 6D for FHB visual rating index (VRI) (a) and deoxynivalenol content (DON) (b). The boxplots are based on number of DHs with the corresponding allele combination for each trait in the 3CPR population. Data of each trait is based on QTL analysis on the combined site years. Boxes show 1st and 3rd quartiles (as top and bottom edges, respectively), median values (as solid middle lines) and mean values (indicated by x as well as numbers above boxes). Outliers are dots outside the boxes. 229
Appendix 4.1 Markers associated with common semi-dwarf genes or common FHB resistance genes/QTL screened on the parental lines and 8I3C doubled haploid population where appropriate. 230
Appendix 4.2 Analysis of variance for anthesis date (Anth), height (Ht), incidence (Inc), severity (Sev) and visual rating index (VRI) for the 8I3C population in each of six site years in Manitoba. 231
Appendix 4.3 Mean phenotype for anthesis date (Anth), height (Ht), incidence (Inc), severity (Sev), visual rating index (VRI), Fusarium damaged kernel (FDK), deoxynivalenol (DON), 2016 greenhouse anthesis (GAnth), 2016 greenhouse severity (GSev1 and GSev2), 2019 greenhouse anthesis (GAnth2), 2019 greenhouse height (GHt) and anther retention (GAR) of six checks based on least squares means in the combined field data and two year greenhouse data. 233
Appendix 4.4 Pearson correlation of anthesis date (Anth), height (Ht), incidence (Inc), severity (Sev), visual rating index (VRI), Fusarium damaged kernel (FDK), deoxynivalenol (DON), 2016 greenhouse anthesis (GAnth), 2016 greenhouse severity (GSev1 and GSev2), 2019 greenhouse anthesis (GAnth2), 2019 greenhouse height (GHt) and anther retention (GAR) for the 8I3C population based on means in the combined field data and two year greenhouse data. 234
Appendix 4.5 Boxplot distribution of the 8I3C population genotypic classes grouped according to presence of specific allele combinations at QTL of interest for phenotypic traits. The boxplots are based on number of DHs with the corresponding allele combination for each trait in the 8I3C population. Data of each trait are based on QTL analysis on the combined site years. Boxes show 1st and 3rd quartiles (as top and bottom edges, respectively), median values (as solid middle lines) and mean values (indicated by x as well as numbers above boxes). Outliers are dots outside the boxes. 238

Appendix 5.1 Selected genes studied for gene expression in the *Fusarium*-wheat pathosystem. Four genes in deoxynivalenol (DON) biosynthesis were tested for pathogen genes, while seven genes involved in DON response and jasmonic acid (JA) pathway were examined for wheat genes. 239
Appendix 5.2 Height (Ht) of infected wheat spikes of five genotypes in a series of time points (0, 1.5, 3, 7 and 14 days after inoculation (dai)). The five genotypes are Maris Huntsman *Rht-B1a* NIL (1a) and *Rht-B1b* NIL (1b), 32c*17(32c), Caledonia (Cal) and Sumai 3 (Su3). The multiple means comparison test for the interaction between genotype and time points on height was conducted in a combined analysis across all treatments. Letters indicate significant differences ($P < 0.05$) among genotypes at individual time points using Fisher's least significant difference (LSD) test. Means of Ht across all time points for each genotype were also included.....240
Appendix 5.3 Analysis of variance of log10 transformed relative expression of four *Fusarium* and seven wheat genes under a controlled environment on two parts (Part) of five genotypes (G) at four time points (T) under different treatments (Trt). *Fusarium* gene (*TRI5*, *TRI6*, *TRI12* and *TRI101*) were tested under both spray and point inoculated Fg treatments, while wheat genes (*ABCC6*, *NFXL1*, *AOS*, *JAZ1*, *PR1b*, *PR4* and *PDF1.2*) were tested under all four treatments. The four treatments were point inoculated *Fusarium* spore suspension, point injected deoxynivalenol solution, point injected water and spray inoculated *Fusarium* suspension. 241
Appendix 5.4 Analysis of variance of log10 transformed relative expression of four *Fusarium* genes (*TRI5*, *TRI6*, *TRI12* and *TRI101*) under a controlled environment on two parts (Part) of five genotypes (G) at four time points (T) under the following individual treatments: point inoculated Fusarium (iF) and spray inoculated Fusarium (sF).....242
Appendix 5.5 Analysis of variance of log10 transformed relative expression of seven wheat genes (*ABCC6*, *NFXL1*, *AOS*, *JAZ1*, *PR1b*, *PR4* and *PDF1.2*) under a controlled environment on two parts (Part) of five genotypes (G) at four time points (T) under the following individual treatments: point inoculated Fusarium (iF), point injected DON (iD) and spray inoculated Fusarium (sF). 243
Appendix 5.6 Relative expression of wheat genes (*JAZ1* and *PR1b*) under a two-way interaction among part and genotype in individual treatments: (a) *JAZ1* and (b) *PR1b* in the point inoculated *Fusarium* treatment (iF) and (c) *PR1b* in the point inoculated deoxynivalenol treatment (iD). The two parts (IS and BIS part) are the inoculated and neighboring spikelets. The five genotypes (G) are Maris Huntsman *Rht-B1a* NIL (1a) and *Rht-B1b* NIL (1b), 32c*17(32c), Caledonia (Cal) and Sumai 3 (Su3). Mean of relative expression with log10 transformation for each part of each genotype is shown, and least significant difference (LSD) values are shown. Letters indicate significant differences ($P < 0.05$) among means comparisons of the G*Part interaction using Fisher's LSD test in each treatment. 246

LIST OF ABBREVIATIONS

Abbreviation	Description
32c	32c*17
3ADON	3-acetyl-deoxynivalenol
3CPR	32c*17/Peregrine
8I3C	18i*45/32c*17
15ADON	15-acetyl-deoxynivalenol
AAFC	Agriculture and Agri-Food Canada
ABCC	*ATP-binding cassette sub-family C member*
AE	Anther extrusion
Anth	Anthesis date
AOS	*Allene oxide synthase*
AR	Anther retention
BCA	Biocontrol agent
BIS	Below inoculated spikelet
Cal	Caledonia
CIM	Composite interval mapping
cM	Centimorgan
CMC	Carboxymethyl cellulose
COI	Coronatine insensitive 1
Cyp51	*Cytochrome P450 sterol 14α-demethylase*
Cq	Quantification cycle
dai	Days after inoculation
DArT	Diversity arrays technology
DEG	Differentially expressed gene
DELLA	D-E-L-L-A; Asp-Glu-Leu-Leu-Ala
DH	Doubled haploid
DMI	Demethylation inhibitor
DON	Deoxynivalenol
EF-1α	*Elongation factor-1 alpha*
ELISA	Enzyme-linked immunosorbent assay
FDK	Fusarium damaged kernel
Fg	*Fusarium graminearum*
FGSC	*F. graminearum species complex*
Fs	*F. sporotrichioides*
FHB	Fusarium head blight
G	Genotype
GA	Gibberellic acid
GAPDH	*Glyceraldehyde-3-phosphate dehydrogenase*
GAnth	Greenhouse anthesis date
GAR	Greenhouse anther retention
Gbp	Giga base pairs
GBS	Genotyping-by-sequencing
GHt	Greenhouse height
GID	GA-insensitive dwarf1

GRAS	GA insensitive, Repressor of GA1 and SARECROW
GSev	Greenhouse disease severity
h^2	Broad sense heritability
His	Histidine-rich calcium-binding
Ht	Height
ICIM	Inclusive composite interval mapping
iD	Point injected deoxynivalenol
iF	Point inoculated *Fg*
IM	Interval mapping
Inc	Incidence
IS	Inoculated spikelet
JA	Jasmonic acid
Jas	Jasmonic acid-associated
JA-Ile	Jasmonoyl-isoleucine
JAZ	JASMONATE ZIM-DOMAIN
KASP	Kompetitive allele-specific PCR
LOD	Logarithm of the odds
LRR-RLK	Leucine rich repeat receptor like kinase
LSD	Least significant difference
MAS	Marker assisted selection
Mbp	Million base pairs
ml	Milliliter
MYB	*Myeloblastosis*
MYC	*Myelocytomatosis oncogenes*
NAC	No apical meristem, Arabidopsis transcription activation factor and cup-shaped cotyledon
NFXL	*Nuclear transcription factor, X-box binding like 1*
NIL	Near isogenic line
NIV	Nivalenol
NRC	National Research Council Canada
NT	N-terminal
PCR	Polymerase chain reaction
PDA	Potato dextrose agar
PDF	*Plant defensin*
ppm	parts per million
PPR	PureLink™ Plant RNA Reagent
PR	*Pathogenesis-related*
PR3C	Peregrine/32c*17
qPCR	Quantitative polymerase chain reaction
qRT-PCR	Real time polymerase chain reaction
QTL	Quantitative trait loci
RNA-seq	RNA sequencing
SA	Salicylic acid
SCAR	Sequence characterized amplified region
Sev	Severity
sF	spray *Fg*

SIM	Single interval mapping
SNA	Spezieller Nährstoffarmer agar
SNP	Single nucleotide polymorphism
SSR	Simple sequence repeat
Su3	Sumai 3
T	Time point
TF	Transcriptional factor
TRI	*Trichothecene*
Trt	Treatment
uM	Micromolar
ug	Microgram
ul	Millimeter
VRI	Visual rating index
ZIM	Zinc-finger inflorescence meristem

FOREWORD

The thesis includes a general introduction, literature review and three research chapters followed by general discussion and conclusion. The research chapters are currently written in the format of Theoretical and Applied Genetics and follow the guidelines defined by the Faculty of Graduate Studies, University of Manitoba. All three research chapters will be published in future as peer reviewed journal articles.

CONTRIBUTIONS OF AUTHORS

CHAPTER 3 QTL MAPPING OF FUSARIUM HEAD BLIGHT RESISTANCE IN AN ELITE DOUBLED HAPLOID WINTER WHEAT CROSS 32C*17/PEREGRINE AND EVALUATION OF MARKER ASSISTED SELECTION EFFICIENCY OF DETECTED QTL IN THE RECIPROCAL CROSS

Lin Y, McCartney C, Loewen M, Fernando D, Hausner G, Brûlé-Babel A

Author Contributions: Lin Y: Conceptualization, Methodology, Formal analysis, Writing-original draft. **McCartney C:** Genotyping, Methodology, Formal analysis, Writing-review. **Loewen M:** Genotyping. **Fernando D:** Writing-review. **Hausner G:** Writing-review. **Brûlé-Babel A:** Conceptualization, Funding acquisition, Investigation, Methodology, Project administration, Resources, Supervision, Formal analysis, Writing-review & editing.

CHAPTER 4 CHARACTERIZATION AND VALIDATION OF FUSARIUM HEAD BLIGHT RESISTANCE QTL IN AN ELITE DOUBLED HAPLOID WINTER WHEAT CROSS 18I*45/32C*17

Lin Y, McCartney C, Loewen M, Fernando D, Hausner G, Brûlé-Babel A

Author Contributions: Lin Y: Conceptualization, Methodology, Formal analysis, Writing-original draft. **McCartney C:** Genotyping, Methodology, Formal analysis, Writing-review. **Loewen M:** Genotyping. **Fernando D:** Writing-review. **Hausner G:** Writing-review. **Brûlé-Babel A:** Conceptualization, Funding acquisition, Investigation, Methodology, Project administration, Resources, Supervision, Formal analysis, Writing-review & editing.

CHAPTER 5 GENE EXPRESSION ANALYSIS OF PUTATIVE GENES RELATED TO THE HOSTPATHOGEN INTERACTION

Lin Y, McCartney C, Nicholson P, Fernando D, Hausner G, Brûlé-Babel A

Author Contributions: Lin Y: Conceptualization, Methodology, Formal analysis, Writing-original draft. **McCartney C:** Formal analysis, Writing-review. **Nicholson P:** Resources. **Fernando D:** Writing-review. **Hausner G:** Writing-review. **Brûlé-Babel A:** Conceptualization, Funding acquisition, Investigation, Methodology, Project administration, Resources, Supervision, Formal analysis, Writing-review & editing.

CHAPTER 1

GENERAL INTRODUCTION

Fusarium head blight (FHB) is one of most common diseases of wheat (*Triticum aestivum* L.) worldwide and can be caused by multiple fungal pathogens *Fusarium spp*. (McMullen et al. 1997; Gilbert and Tekauz 2000). In North America, *Fusarium graminearum sensu stricto* Schwabe (teleomorph: *Gibberella zeae* (Schwein.) Petch) (*Fg*) is the predominant causal species of FHB in wheat. High yield loss, poor grain quality, seedling blight, reduced kernel weight, and low germination rates are common negative impacts of FHB in wheat (Dexter and Nowicki, 2003; McMullen *et al.*, 1997; Parry *et al.*, 1995). Also, the mycotoxin, deoxynivalenol (DON), released by *Fg* is toxic to human and animal cells and poses a threat to food and feed safety (Proctor et al. 1995; Bai et al. 2002; Jansen et al. 2005; Sobrova et al. 2010; Buhrow et al. 2016; Mayer et al. 2017). In western Canada, since the first major FHB epidemic occurred in 1993, FHB has become a common problem to wheat growers in most of years (Clear and Abramson 1986; Gilbert and Tekauz 2000; Aboukhaddour et al. 2020). Great economic losses due to FHB infection have been widely reported (Canadian grain commission 2021; Government of Alberta 2021).

Integrated FHB management in Canada includes the uses of resistant cultivars, fungicides and cultural practices (such as including crop rotation and tillage) (Gilbert and Haber 2013). Common sources of FHB resistance come from Asian spring wheat genotypes including Sumai 3 and its derivates and Wangshuibai, but these alleles are also functional in winter wheat (Buerstmayr et al. 2009, 2019). More than 100 FHB quantitative trait loci (QTL) for FHB resistance have been identified and are distributed across all 21 wheat chromosomes. To date, seven *Fhb* genes have

been characterized from wheat and its related species (Liu et al. 2006; Cuthbert et al. 2007; Qi et al. 2008; Xue et al. 2010a, 2011; Cainong et al. 2015; Guo et al. 2015; Rawat et al. 2016). However, FHB resistance is a complex of traits and often involves multiple genes with relatively small effects. Expression of resistance is influenced by many environmental factors. No single resistance gene is sufficient to completely resist FHB (Gilbert and Haber 2013). The current breeding strategy is to combine different types of resistance into a single genotype and to continue the identification and characterization of more FHB resistance from potential new sources/germplasms through genetic studies.

Several morphological traits, especially plant height, are associated with FHB resistance (Mesterházy 1995; Buerstmayr et al. 2009; Yan et al. 2011; Saville et al. 2012). In particular, the *Rht-B1a* and *Rht-D1a* alleles in two gibberellic acid (GA)-insensitive dwarfing loci *Rht-B1* and *Rht-D1* were associated with increases in height and FHB resistance in several QTL studies (Lu et al. 2013; He et al. 2016; Xu et al. 2020). In addition to height, floral traits contribute to FHB resistance. In particular, anther retention (anthers retained between the lemma and palea) is associated with FHB susceptibility by providing a path for the fungus to enter and infect the host tissues (Buerstmayr et al. 2019). The *Rht-B1a* or *Rht-D1a* alleles were also associated with lower anther retention.

However, the *Rht-B1b* and *Rht-D1b* alleles in the two common wheat dwarfing loci reduce plant height, which allows wheat growers to increase fertilizer use to achieve high yield without the risk of lodging (Hedden 2003). The introduction of dwarf alleles *Rht-B1b* or *Rht-D1b* has increased grain yield and lodging resistance, but has been associated with FHB susceptibility. Thus, the use

of wildtype *Rht-B1a* or *Rht-D1a* alleles for improving FHB resistance has been discouraged due to the associated height increase leading to lodging and yield reduction (Verma et al. 2005; Voss et al. 2008; Guedira et al. 2010; Lanning et al. 2012; Chen et al. 2016). The ideal breeding goal is to maintain optimal height and improve FHB resistance.

Saville et al. (2012) reported that a Maris Huntsman near-isogenic line (NIL) carrying the *Rht-B1b* allele had less FHB symptoms than its NIL carrying the *Rht-B1a* allele in both indoor point inoculation and direct DON injection tests, while the *Rht-B1a* NIL had less bleached spikelets than the *Rht-B1b* NIL in a field spray experiment. Plants carrying the wildtype *Rht-B1a* allele are able to encode an intact DELLA protein as an important negative regulator in GA pathway. The name of DELLA protein comes from the abbreviation of a conserved amino acid sequence (Asp-Glu-Leu-Leu-Ala; D-E-L-L-A) in its N-terminal motif. The degradation of DELLA protein releases DELLA-suppressed transcriptional factors to promote plant height growth. Compared with wildtype *Rht-B1a* allele, the *Rht-B1b* allele encodes a truncated DELLA protein that is unable to be degraded; consequently, plant height fails to increase leading to semi-dwarfness (Nelson and Steber 2016; Thomas 2017). The host-pathogen interaction relying on salicylic acid (SA) or jasmonic acid (JA) pathway can be affected by crosstalk with other phytohormones (Berens et al. 2017; Yang et al. 2019; Liu and Timko 2021). DELLA protein in the GA pathway is able to bind with a key JA-repressor JASMONATE ZIM-DOMAIN (JAZ) protein, resulting in enhancing the JA signaling pathway, where the ZIM domain is named from zinc-finger protein expressed in inflorescence meristem. Thus, Saville et al. (2012) hypothesized that the *Rht-B1b* allele might promote the JA signalling pathway and inhibit the SA signalling pathway, resulting in susceptibility to biotrophic pathogens and resistance to necrotrophic pathogens.

An elite winter wheat breeding line (named 32c*17) was developed by the University of Manitoba, Canada breeding program and demonstrated strong FHB and DON resistance under severe disease pressure in both Canada and Germany. Based on a haplotyping study (unpublished data), this line does not carry any common Sumai3 FHB resistance alleles (*Fhb1, Qfhs.ifa-5AS* and *Fhb2*), which indicated that this line has inherited non-common useful FHB resistance from its parents and possesses a potential breeding value for FHB resistance. To better understand the resistance carried by 32c*17, two QTL mapping population (32c*17/Peregrine (3CPR) and 18I*45/32c*17 (8I3C)) with the common parental line 32c*17 were generated. The first two objectives of this research project were to: 1) identify QTL of FHB resistance and other agronomic traits associated with FHB resistance in both populations, and 2) estimate the efficiency of markers closely linked with 3CPR FHB QTL to predict resistant lines in the reciprocal population (PR3C) for marker-assisted selection (MAS).

Moreover, in order to further understand how the truncated DELLA protein encoded by the *Rht-B1b* allele plays a role in the JA and GA pathways with the *Fg*-wheat pathosystem, a gene-expression study on five genotypes was conducted. The five genotypes consisted of the same two NILs used in the study of Saville et al. (2012) and three wheat checks, including Sumai 3, 32c*17 and Caledonia. The objectives of this research project were: 1) to study expression of important DON biosynthesis four *TRI* (*Trichothecene*) genes (*TRI5*, *TRI6*, *TRI12* and *TRI101*) using different inoculation methods and 2) determine expression levels of selected genes involved (*ABCC6*, *NFXL1*, *AOS, JAZ1*, *PR1b*, *PR4* and *PDF1.2*) by time series.

CHAPTER 2

LITERATURE REVIEW

2.1 Wheat

2.1.1 Canadian wheat production

Wheat is one of the most important crops in Canadian agriculture. In 2020, Canada produced more than 35 million metric tonnes of wheat, which consisted of 25.84 million metric tonnes of spring wheat, 6.57 million metric tonnes of durum wheat, and 2.77 million metric tonnes of winter wheat (Statistics Canada 2020). Based on grain end use characteristics, Canadian wheat varieties are designated into six eastern Canadian wheat classes and nine western Canadian wheat classes for international and domestic markets (Canadian Grain Commission 2019). The most commonly grown wheat classes in western Canada were the Canada western red spring (4.54 million hectares) and the Canada western amber durum (1.51 million hectares) classes, which accounted for 92 percent of commercial wheat area in western Canada in 2020 (Canadian Grain Commission 2020). Canada Western Red Winter wheat was produced on 0.049 million hectares in western Canada in the same year. Canada exported 24.35 million metric tonnes of wheat, domestically used 9.14 million metric tonnes and imported 0.275 million metric tonnes in 2020 (Agriculture and Agri-Food Canada 2021).

2.1.2 Wheat genome and genetics

Triticum aestivum L. (AABBDD) consists of three sub-genomes with seven chromosomes on each sub-genome (Shewry 2009; Charmet 2011; Peng et al. 2011; Marcussen et al. 2014; El Baidouri et al. 2017). The origin of the A sub-genome is thought to be an ancestral progenitor closely related to a diploid wheat *T. urartu* (AA), while an ancient progenitor of the B sub-genome remains unknown and could be a distant relative of a diploid goat grass *Aegilops speltoides* (SS) (El Baidouri et al. 2017). Another diploid goat grass *Ae. tauschii* is considered as the origin of the D sub-genome and was recently sequenced (Luo et al. 2017).

The genome size of hexaploid wheat *T. aestivum* was estimated to be around 16 giga base pairs (Gbp) (Walkowiak et al. 2020). The first draft genome assembly of hexaploid wheat on the cultivar, Chinese Spring, was published in 2014 (IWGSC 2014). In 2018, the first fully assembled and annotated Chinese Spring wheat reference sequence was released. This reference sequence (IWGSC RefSeq v1.0) contained a 14.5 Gbp assembly of genomic information and provided 107,891 high confidence genes. It also revealed that a high proportion (11.91 Gbp) of the wheat genome consisted of transposable elements (International Wheat Genome Sequencing Consortium (IWGSC) 2018). The latest version for the Chinese Spring wheat reference sequence is IWGSC RefSeq v2.1 (Zhu et al. 2021). Besides Chinese Spring, fifteen diverse wheat lines from different countries, including two Canadian cultivars, were further sequenced to form the first global wheat pangenome (Walkowiak et al. 2020). The first online graphing tool for the wheat pangenome assembly was recently released to researchers to better visualize regions of interest across all sixteen wheat lines including the Chinese Spring (Bayer et al. 2022). With more precise sequence

level genomic and genetic information in this reference sequence, breeders and scientists can accelerate their basic science studies and applied research by better understanding important traits at the chromosome level (International Wheat Genome Sequencing Consortium (IWGSC) 2018).

In applied wheat genetics, various molecular marker types have been used to generate wheat linkage maps and detect quantitative trait loci (QTL) of traits of interest over time. Prior to the early 1990s, several linkage groups were constructed using restriction fragment length polymorphisms markers (Chao et al. 1989; Nelson et al. 1995). Simple sequence repeats (SSRs), one type of polymerase chain reaction (PCR)-based markers, was widely used in linkage and QTL mapping in the early 2000s (Röder et al. 1998; McCartney et al. 2004; Cuthbert et al. 2007). One of the early *T. aestivum* consensus maps was constructed with 1,235 SSRs (Somers et al. 2004). Sequence characterized amplified region (SCAR) markers, which are also PCR-based, were developed to link with certain genes of interest, such as disease resistance genes (Liu et al. 1999). A common fluorescence-based PCR genotyping method, Kompetitive allele-specific PCR (KASP), has recently been used to validate single-nucleotide polymorphisms (SNPs) linked to a genomic region of interest (like a gene or QTL) (Allen et al. 2011; Singh et al. 2019; Xiong et al. 2021). The KASP system has a high SNP assay conversion rate (from chip-based SNPs to PCR-based SNPs) and has been used as a high throughput, cost-effective PCR-based genotyping method for marker assisted selection (Semagn et al. 2014; Makhoul et al. 2020). In current wheat marker-assisted selection in Canada, SNPs derived from KASP assays, SSRs and SCARs linked with important traits (i.e. agronomic, grain quality and disease resistance) have been widely adapted for use in breeding programs (Randhawa et al. 2013; Goutam et al. 2015; Toth et al. 2019).

Compared with relatively low throughput PCR-based assays, high throughput genotyping methods in wheat enabled the screening of hundreds of thousands of SNP markers for various genetic studies, including linkage and QTL mapping (Wang et al. 2014). Diversity arrays technology (DArT) was one of the early generation high-throughput genotyping methods used in linkage mapping (Akbari et al. 2006). DArT technology combined with SSRs was used to generate a high-density consensus map for durum wheat (Marone et al. 2012). The 90K Infinium iSelect SNP custom beadchip is an SNP-based genotyping platform developed from 19 hexaploid wheat accessions and 18 tetraploid wheat accessions (Wang et al. 2014). It was designed to be used in worldwide wheat accessions and has become popular in linkage mapping (Wang et al. 2014). Using the 90K array, a new SNP based high density consensus map was generated (Wang et al. 2014). The 90K array significantly increased the number of markers in linkage mapping from hundreds or thousands of SSRs or DArTs, to tens of thousands SNPs (Somers et al. 2004; Marone et al. 2012; Cabral et al. 2014). In 2016 and 2017, two Affymetrix Axiom SNP arrays (820K and 660K) designed by United Kingdom and Chinese scientists, respectively, were available for high-throughput wheat SNP genotyping (Winfield et al. 2016; Cui et al. 2017). In addition to the PCR-based and array-based methods, genotyping-by-sequencing (GBS) was another approach for genotyping in wheat for QTL mapping and genome-wide association study (Elshire et al. 2011; Akram et al. 2021; Blackburn et al. 2021). With the available wheat reference sequences (like IWGSC RefSeq v1.0), numbers of usable SNPs from GBS have been dramatically increased by using an imputation algorithm to reduce missing data (Alipour et al. 2019).

2.2 *Fusarium graminearum*

2.2.1 Taxonomy and genome of *Fusarium graminearum*

Morphological and molecular genetic studies have been conducted for taxonomic classification of *Fusarium* species. *Fusarium pseudograminearum*, previously named *F. graminearum* Group 1, is currently considered a different species from *F. graminearum*, because it only causes crown rot on cereals and not head blight (Aoki and O'Donnell 1999). *Fusarium graminearum sensu stricto* Schwabe (teleomorph: *Gibberella zeae* (Schwein.) Petch) (*Fg*), which produces the mycotoxin deoxynivalenol (DON) and causes bleached cereal head blight symptoms, was previously named *F. graminearum* Group 2. With the help of molecular markers, 27 strains of *F. graminearum* collected globally were perfectly separated into seven lineages corresponding to their geographic regions. This grouping refined the relationships in *F. graminearum* that could not be identified using traditional methods that mainly relied on morphological characterization (O'Donnell et al. 2000). Nine new *Fusarium* species within the *F. graminearum* clade were further identified based on their biogeographical distribution (O'Donnell et al. 2004). Furthermore, several novel species have been described and added into this *F. graminearum* species complex (FGSC) (Starkey et al. 2007; O'Donnell et al. 2008; Yli-Mattila et al. 2009; Sarver et al. 2011). What was initially described as *F. graminearum* was found to be fifteen distinct *Fusarium* species within the FGSC based on molecular phylogenetic data (Valverde-Bogantes et al. 2019). Morphologically, these fifteen species were indistinguishable based on their phenotypic characters and were only separated based on their genotypic information (Valverde-Bogantes et al. 2019). *F. graminearum s.s.* (lineage 7) is the only species within the FGSC to have a cosmopolitan distribution, however, all 15 species are self-fertile and produce Type B trichothecene mycotoxins (such as DON) to

cause disease symptoms on infected cereal florets (Valverde-Bogantes et al. 2019). Any *Fg* species within the FGSC is capable of producing the same mycotoxin components and cause the same level of disease infections in both resistant and susceptible wheat cultivars (Amarasinghe et al. 2019).

Additional *Fusarium spp.* not within the FGSC are commonly found in the Canadian prairies and can cause disease in wheat (Henriquez et al. 2018a, b, 2019a, b, 2020a, b; Ziesman et al. 2018, 2019). The frequency of different *Fusarium spp.* in the prairies has been regularly monitored in spring and winter wheat fields (Henriquez et al. 2018a, b, 2019a, b, 2020a, b; Ziesman et al. 2018, 2019). Currently, the two most predominant *Fusarium* species in the Manitoba and Saskatchewan are *F. graminearum* and *F. poae* (Henriquez et al. 2018a, b, 2019a, b, 2020a, b; Ziesman et al. 2018, 2019). Due to the absence of annual disease surveys, the diversity and occurrence of *Fusarium spp.* in Alberta remains unknown. *Fusarium* species can be genetically differentiated using multilocus genotyping which uses six primer pairs to amplify species-specific genes (Ward et al. 2008). Globally, *F. graminearum* and *F. culmorum* are the most widely occurring species that cause FHB (Foroud et al. 2019).

The genome of *Fg* consisted of four chromosomes totaling approximately 36 Mbp and with a genetic map length of 1,234 cM (in Kosambi) (Gale et al. 2005; King et al. 2015; Walkowiak et al. 2016). An updated linkage map totaling 1,140 cM in length was reported by Lee et al. (2008) which aligned nine linkage groups of the genetic map to the physical map of *G. zeae*. The *Fg* genome sequence contains few repetitive sequences and duplicated sequences with high identity (Cuomo et al. 2007). A *Fusarium* pan genome was constructed using a total of ten isolates spanning

three *Fusarium* species within the FGSC (*Fg, F. asiaticum* and *F. meridionale*) to enable further genomic studies of the pathogen (Walkowiak et al. 2016). High density SNPs were found in all proximal regions of the telomeres (Cuomo et al. 2007; Walkowiak et al. 2016).

2.2.2 Disease symptoms and epidemics of FHB in Canada

Infection of susceptible cereals by *Fusarium spp*. leads to Fusarium head blight (FHB). Infected wheat spikes initially appear water soaked and later appear to be bleached as disease progresses (Trail 2009). Infected grain appears shrivelled due to either direct infection by the pathogen, or insufficient supply of water and nutrients caused by *Fusarium* mycelia blocking the rachis (Bai and Shaner 2004). Severe FHB infection reduces both grain yield and grain quality. In addition infected grain can be contaminated with the mycotoxin DON that is toxic to humans and animals (Windels 2000). Ultimately, severe FHB epidemics can be financially devastating to farmers (Windels 2000). Historical FHB epidemics and their associated economic losses have been reviewed by several authors (McMullen et al. 1997; Gilbert and Tekauz 2000; Bai and Shaner 2004; Trail 2009; Aboukhaddour et al. 2020).

Although FHB has been prevalent in eastern Canada, the first record of FHB in wheat on the Canadian prairies was reported in southern Manitoba in 1984 and the first major outbreak in 1993 (Clear and Abramson 1986; Gilbert and Tekauz 2000; Aboukhaddour et al. 2020). To date, FHB remains a common wheat disease across western Canada, likely due to the switch from conventional tillage to conservation tillage (Aboukhaddour et al. 2020). The estimated economic

losses was more than $1.5 billion (CAD) in Canada since the middle of 1990s (Innovation Express 2014).

2.2.3 The life cycle of *Fusarium graminearum*

The *Fusarium* disease cycle has been extensively reviewed by several authors (Gilbert and Fernando 2004; Trail et al. 2005a; Trail 2009; Gilbert and Haber 2013). Briefly, the pathogen overwinters as dikaryotic mycelia and perithecial initials in infected crop residues. Warm spring weather induces perithecia to develop from the mycelia (Guenther and Trail 2005; Trail et al. 2005a; Trail 2009). Ascospores produced by perithecia become airborne and serve as primary inoculum for FHB infection in wheat fields (Trail et al. 2005b). Infection begins when ascospores land on flowering wheat spikes, germinate and produce mycelia which enter the floret (Trail 2009). Upon successful colonization of the floret, the mycelia then secrete the mycotoxin DON which enables infection of neighbouring spikelets through the vascular bundles of the rachis (Jansen et al. 2005; Trail et al. 2005a; Trail 2009). Colonized spikelets become necrotic and develop a bleached appearance typical of FHB symptoms (Guenther and Trail 2005; Trail 2009). Severe disease results in shriveled Fusarium damaged kernels (FDK) that contain high amounts of DON (Trail 2009). In the final stage of the life cycle, mycelia travel through the xylem vessels to the stems where they form the lipid rich dikaryotic hyphae to overwinter (Guenther and Trail 2005; Trail et al. 2005a; Trail 2009; Gilbert and Haber 2013).

2.3 Fusarium head blight mycotoxins - Deoxynivalenol

2.3.1 Fusarium chemotypes

In the life cycle of *Fusarium*, mycotoxins play an important role during colonization. Mycotoxins in *Fusarium* belong to a class of compounds called trichothecenes. These compounds are characterized by a core three ring structure containing an epoxide functional group (**Figure 2.1**) (Foroud and Eudes 2009; McCormick et al. 2011; Foroud et al. 2019). Of the four classes of trichothecenes, only two, type A and type B, are produced by *Fusarium spp.* (Foroud and Eudes 2009; McCormick et al. 2011; Foroud et al. 2019). Generally, the distinguishing feature between type A and type B trichothecene is observed at the C-8 position: a carbonyl group is present in type B, while various other functional groups are present in type A (**Figure 2.1**) (McCormick et al. 2011). Type A trichothecenes encompass T-2 toxin, HT-2 toxin and the recently discovered NX-2 and NX-3 mycotoxins (Foroud et al. 2019). Type B trichothecenes include nivalenol (NIV), DON, 3-acetyldeoxynivalenol (3ADON) and 15-acetyldeoxynivalenol (15ADON) (**Figure 2.1**). Different *Fusarium* species produce a different array of trichothecenes: *F. poae* and *F. sporotrichioides* typically produce type A trichothecenes while *F. culmorum* and *F. graminearum* produce type B trichothecenes (Foroud and Eudes 2009). Interestingly, *F. avenaceum* produces moniliformin mycotoxins that are not in the trichothecene class (Foroud et al. 2019). Overall, DON is the most common trichothecene mycotoxin found in FHB infected cereal grains (Foroud et al. 2019).

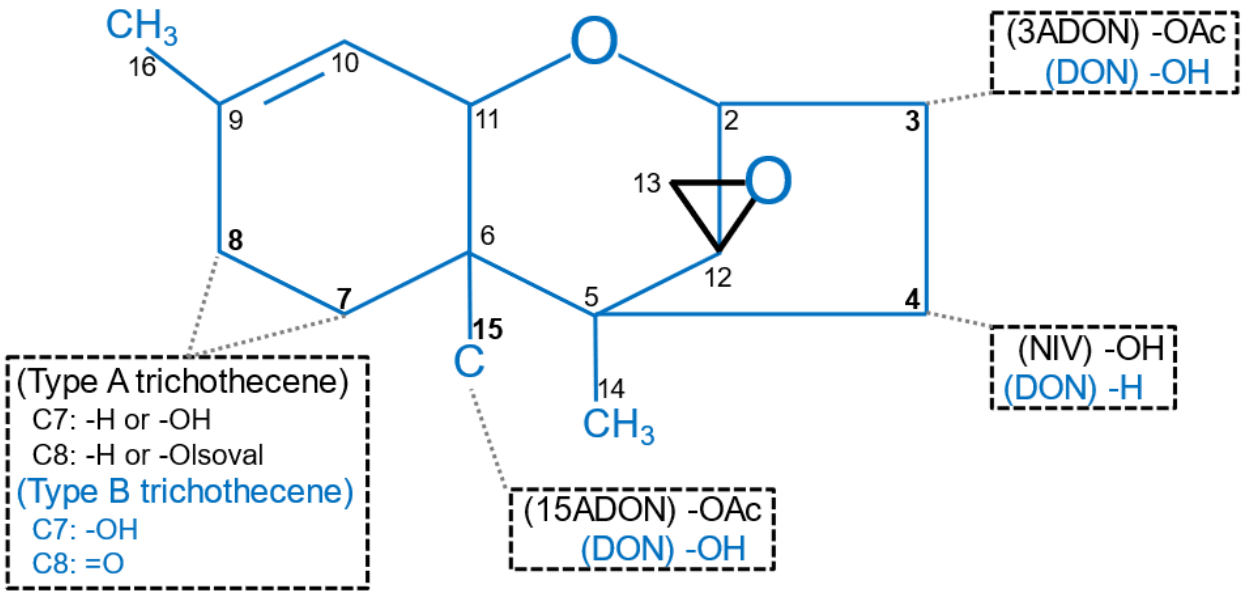

Figure 2.1 A schematic diagram of main structure of type A and type B trichothecene, which was adapted from Foroud et al (2019). The "OAc" and "OIsoval" refer to O-acetyl and O-isovalerate, respectively.

Given the diversity of mycotoxins produced by *Fusarium* species, pathogenic isolates are classified by chemotype (Foroud and Eudes 2009). The presence of a C-4 hydroxyl group distinguishes NIV from DON and its attachment is catalyzed by the trichothecene biosynthesis genes *TRI7* (*Trichothecene*) and *TRI1*3. The presence of functional *TRI7* and *TRI1*3 genes differentiates NIV from DON chemotypes that have non-functional forms of these genes (McCormick et al. 2011). DON chemotypes are further distinguished by their biosynthesis pathway. Although the 3ADON chemotype and 15ADON chemotype both ultimately produce DON, small amounts of DON precursor acetylated at the C-3 and C-15 position are present in the respective chemotypes (Puri and Zhong 2010; Alexander et al. 2011). Genetic variation in the trichothecene biosynthesis gene *TRI8* differentiates the two chemotypes (Alexander et al. 2011). In Canada, the *Fg* 3ADON and 15ADON chemotypes are dominant, while the NIV producing *Fg* has been not documented (Amarasinghe et al. 2015, 2019). The *Fg* NIV chemotype has been detected with low frequency in wheat in North Carolina (Cowger et al. 2020).

In addition to producing different mycotoxins, 3ADON and 15ADON chemotypes differ in their aggressiveness and resilience. 3ADON isolates typically produce more mycotoxin compared to 15ADON isolates under both *in vitro* and *in vivo* tests (Ward et al. 2008; Puri and Zhong 2010). Under *in vitro* conditions, 3ADON isolates accumulated greater biomass and produced both larger spores and higher spore counts than 15ADON isolates (Ward et al. 2008; Amarasinghe et al. 2019). Furthermore, 3ADON isolates grew better at extreme temperatures compared to 15ADON isolates, suggesting the former has better abiotic stress tolerance than the latter (Vujanovic et al. 2012; Gilbert et al. 2014). Given the increased-apparent fitness of 3ADON isolates, it is of interest to monitor changes in the frequency of this chemotype in western Canadian wheat fields. Although the 15ADON chemotype was historically predominant in western Canada, the more aggressive 3ADON chemotype had risen to account for approximately one third of the pathogen population in the early 2000s (Ward et al. 2008). By the early 2010s, the 3ADON chemotype had become the dominant chemotype in Manitoba (Gilbert et al. 2014); A similar shift in chemotype abundance was observed in North Dakota in the same period (Puri and Zhong 2010). To date, the mechanisms underlying the shift to 3ADON dominance in western Canadian wheat fields remain uncertain (Gilbert et al. 2014).

2.3.2 Deoxynivalenol biosynthesis pathway and important *TRI* genes

The biosynthesis pathways for type A and type B trichothecenes begin with the common conversion of farnesyl pyrophosphate to calonectrin before diverging to form individual mycotoxins. The DON biosynthesis pathway has been thoroughly reviewed (a graphical summary is presented in **Figure 2.2**) and a summary of all known *TRI* biosynthesis genes is presented in

Table 2.1 (Foroud and Eudes 2009; McCormick et al. 2011; Foroud et al. 2019). For DON biosynthesis, calonectrin is further converted into 3,15-acetyldeoxynivalenol which is then selectively de-acetylated into either 3ADON or 15ADON, depending on the chemotype, through the action of *TRI8* (Foroud et al. 2019). The differential de-acetylation action of *TRI8* is a direct result of two genetic variants of the same gene which show 78% nucleotide sequence homology (85% peptide sequence homology) to each other (Alexander et al. 2011). A final de-acetylation step converts 3ADON or 15ADON into DON (Foroud and Eudes 2009; McCormick et al. 2011; Foroud et al. 2019).

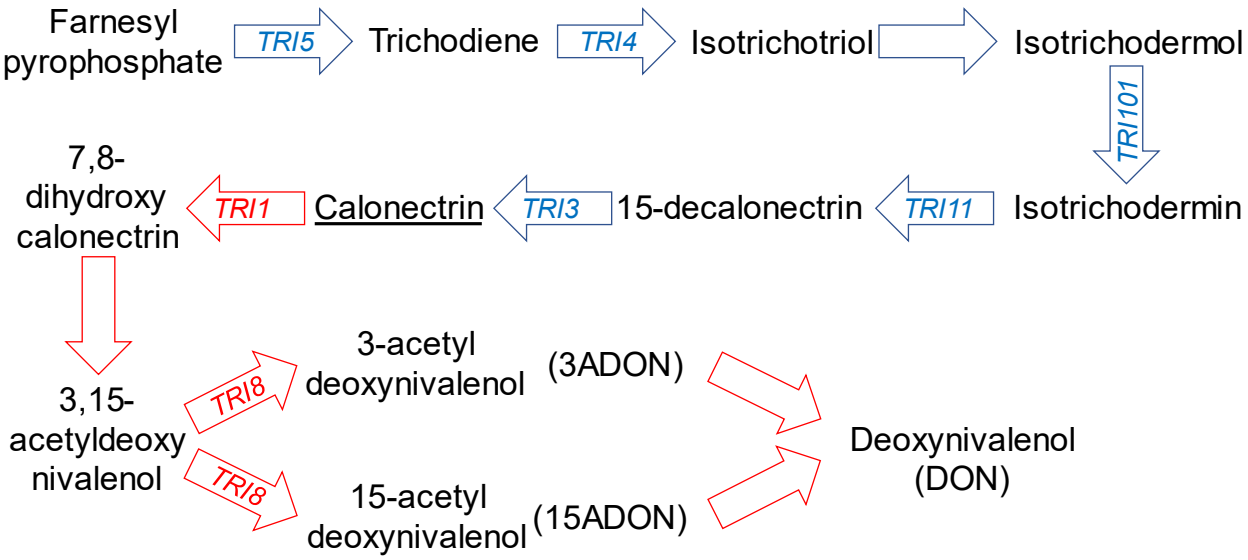

Figure 2.2 A schematic diagram of the biosynthesis pathway of deoxynivalenol with several important *Trichothecene* (*TRI*) genes in *F. graminearum* (adapted from McCormick et al 2011).

Table 2.1 Location and function of all *Trichothecene* (*TRI*) genes involved in the deoxynivalenol (DON) biosynthesis pathway in *Fusarium* genome. Data were obtained and modified from multiple sources (Brown et al. 2002; McCormick et al. 2004; Gale et al. 2005; Kulik 2008; Lee et al. 2008; Foroud et al. 2019).

***TRI* gene**	**Chromosome**	**Gene description in *F. graminearum* strains producing DON**
TRI1	Chr1[1]	C-7 and C-8 hydroxylation by cytochrome P450 monooxygenase
TRI2	N/A[2]	Very little information (only found in *F. tricinctum*)
TRI3	Chr2	C-15 acetylation by acetyltransferase
TRI4	Chr2	Four oxygenations from trichodiene to isotrichotriol by cytochrome P450 monooxygenase
TRI5	Chr2	Farnesyl pyrophosphate cyclized to produce trichodiene by sesquiterpene cyclase
TRI6	Chr2	Transcription factor (Zinc-finger DNA binding protein)
TRI7	Chr2	*Dysfunction of C-4 acetylation due to mutations and an insertion
TRI8	Chr2	C-3 or C-15 deacetylation by esterase/deacetylase
TRI9	Chr2	Unknown
TRI10	Chr2	Transcription factor
TRI11	Chr2	C-15 hydroxylation by cytochrome P450 monooxygenase
TRI12	Chr2	MFS transporter for toxin efflux
TRI13	Chr2	*Dysfunction of C-4 oxygenation due to substitution, insertions, and deletions
TRI14	Chr2	Unknown
TRI15	Chr3	Transcription factor (Zinc-finger DNA binding protein)
TRI16	Chr1	*Dysfunction of C-8 acetylation due to stop codons and frame shift
TRI101	Chr4	C-3 acetylation by acetyltransferase

[1]Chr Chromosome; [2]N/A Not applicable

*The DON producing strains have non-functional *TRI7* and *TRI13* genes, while NIV strains have functional *TRI7* and *TRI13* genes. Type B trichothecene chemotypes had non-functional *TRI16* gene, compared with Type A trichothecene chemotypes.

2.3.3 Toxicity of deoxynivalenol and its role in pathogenicity

The structure of DON imparts toxicity by enabling it to bind to the ribosome, thus, impeding protein synthesis (Garreau De Loubresse et al. 2014). Specifically, studies in yeast and animal cell lines demonstrated that the 12,13-epoxy ring binds to the magnesium ion (Mg^{2+}) in the aminoacyl-transfer RNA site of the peptidyl transferase center within the 60S ribosomal subunit, inducing a conformational change in the complex which inhibits the elongation of the nascent polypeptide

(**Figure 2.1**) (McLaughlin et al. 2009; Garreau De Loubresse et al. 2014; Foroud et al. 2016; Mayer et al. 2017). Alternatively, the toxicity of trichothecene has been suggested to result from the disruption of both mitochondrial structure and function through a yeast study (McLaughlin et al. 2009).

In the *Fusarium*-wheat pathosystem, DON functions as an important virulence factor and elevated DON concentrations are often seen directly beneath the penetration pegs and ahead of the movement of mycelia (Kang and Buchenauer 1999). Disease spread from spikelet to spikelet can be facilitated by the presence of DON, although the mycotoxin is not required for initial infection (Proctor et al. 1995; Bai et al. 2002; Langevin et al. 2004). Studies using a *Fg* mutant deficient in trichothecene production demonstrated that the pathogen was confined to the rachis of the inoculated floret due to the plant defense response of thickening the cell wall in the rachis node; this resulted in limiting the spread of the pathogen into neighboring spikelets. Conversely, when the wildtype trichothecene-producing *Fg* was used, the host plant failed to develop a thicken cell wall and the pathogen was able to invade neighboring florets, suggesting DON functioned to repress the host defense response in this pathosystem (Jansen et al. 2005). Chemical modification to DON such as acetylation and biological conjugation of DON (i.e., glucoside, glutathione and sulfate) can reduce the toxicity to *Fg* itself or host plants and results in less disease severity than unmodified DON (Okubara et al. 2002; Berthiller et al. 2005; Kluger et al. 2013; Warth et al. 2015).

2.4 Management of Fusarium head blight

2.4.1 Cultural practices

Use of resistant cultivars and fungicides, as well as cultural practices including crop rotation and tillage are common FHB management tools used in Canada (Gilbert and Fernando 2004; McMullen et al. 2012; Gilbert and Haber 2013; Chen et al. 2019; Aboukhaddour et al. 2020). The use of genetic resistance in wheat is discussed in section 2.5 and fungicide application is briefly mentioned in section 2.4.2. In Manitoba, even after two years, both soil buried and unburied FDK could produce perithecia, but only unburied FDK successfully produced ascospores which act as the primary inoculum responsible for natural FHB infections. This suggests that at a least two years without an FHB susceptible crop and tillage should be recommended as cultural practices to control FHB in Canada (Inch and Gilbert 2003). Maize grown one to two years prior to wheat was strongly discouraged due to high FHB infection and substantial DON content (Dill-Macky and Jones 2000; Blandino et al. 2012; Vogelgsang et al. 2019). Canola-wheat and flax-wheat rotations accumulated the same amount of *F. graminearum* colonies on crop residues as wheat-wheat rotation, thus such crop rotation patterns should not be promoted in Manitoba (Guo et al. 2010). Soybean-wheat and pea-wheat as two year rotations had lower FHB disease incidence, disease severity and DON contamination as well as higher wheat yield than wheat-wheat or maize-wheat rotations (Dill-Macky and Jones 2000; Guo et al. 2010). Ideally, more than two year rotation periods were the best way to reduce primary ascospore inoculum and should be strongly recommended to wheat farmers in Canada (Inch and Gilbert 2003).

Zero or minimum tillage systems were not enough to reduce the colonization of *F. graminearum* on crop stubble, but conventional tillage was able to decrease fungal colonies based on a four year field study in Manitoba (Guo et al. 2010). Another field study in Minnesota demonstrated that conventional tillage (e.g. moldboard plow) dramatically reduced previous crop residues left on the soil surface compared to conservation tillage (e.g. chisel plow) and no-till, resulting in statistically different, but relative small decreases in FHB disease incidence, disease severity and DON accumulation along with slightly increased wheat yield (Dill-Macky and Jones 2000; Gilbert and Fernando 2004). A six site-year study in Europe also showed that ploughing in conventional tillage consistently reduced DON content compared with no-till system (Blandino et al. 2012). In conclusion, it was believed that good crop rotations had much larger impact on FHB management than different tillage methods (Gilbert and Fernando 2004).

2.4.2 Chemical control

In addition to the use of resistant wheat cultivars and the proper cultural practices, fungicide applications are common FHB management tools in Canada, United States and Europe (Gilbert and Fernando 2004; Blandino et al. 2012; McMullen et al. 2012; Gilbert and Haber 2013; Chen et al. 2019; Vogelgsang et al. 2019; Aboukhaddour et al. 2020). To maximize fungicide coverage in FHB management, the best spray technique was to deliver droplets within 300 to 350 µm size by flat fan spray nozzles angled at 30 degrees from horizontal (McMullen et al. 2012). The optimal spray timing for most fungicides (except strobilurin fungicides) was just before the beginning of the anthesis stage up to seven days after anthesis (McMullen et al. 2012; Gilbert and Haber 2013). There is a concern that strobilurin fungicides increase DON accumulation when FHB infection

occurs before the fungicide application, thus it was strongly suggested to apply strobilurin type fungicides at the stem elongation stage (Gilbert and Haber 2013).

Triazole-based fungicides belonging to demethylation inhibitor (DMI) fungicides were able to reduce FHB visual rating index and DON content on both spring and winter wheat. As a result, they were recommended as one of the most effective fungicides in FHB disease control in North America and Europe (Paul et al. 2008; Blandino et al. 2012; Gilbert and Haber 2013; Torres et al. 2019; Vogelgsang et al. 2019). Common triazole-based fungicides are tebuconazole, prothioconazole, metconazole, propiconazole and the combination of tebuconazole and prothioconazole (Paul et al. 2007, 2008; McMullen et al. 2012). The mode-of-action of azole fungicide is to damage the integrity of fungal cell membranes through the change of ergosterol biosynthesis pathway by elevating expression of three *Cyp51* genes (cytochrome P450 sterol 14α-demethylase) (Becher et al. 2011). After the tebuconazole treatment, the ergosterol content in *F. graminearum* was reduced (Liu et al. 2011). Further, it was found that different DMI fungicides preferentially target different Cyp51 proteins in *F. graminearum* This explained why various *F. graminearum* strains showed different sensitivities to different types of DMI fungicides, suggesting that the mixture of different DMI fungicides with synergistic effects had very good control on FHB disease (Liu et al. 2011). This was confirmed by the combination of prothioconazole and tebuconazole which was associated with lower field FHB visual rating index than the other four individual DMI fungicides used individually (Paul et al. 2008). There was a significant reduction of field disease infection and DON content achieved by using the combination of prothioconazole and tebuconazole on different wheat cultivars with various resistant levels (Willyerd et al. 2012). However, this beneficial synergistic effect might not always

apply to the reduction of mycotoxin accumulation, since one study found that metconazole alone had higher field FHB visual rating index, but slightly lower DON content than the combination of prothioconazole and tebuconazole (Paul et al. 2008).

Strobilurin is another common fungicide class used since the late 1990s and is capable of restricting fungal growth through interference in mitochondrial respiration by blocking electron transport (Gilbert and Haber 2013; Torres et al. 2019). The combination of strobilurin and triazole was commonly used in Switzerland to prevent FHB disease and DON contamination (Vogelgsang et al. 2019). However, in an eight-year winter wheat field survey study conducted in Switzerland, farms relying on strobilurin-based fungicides alone had much higher DON content and FHB disease than farms using triazole alone, or the combination of triazole and strobilurin (Vogelgsang et al. 2019). Thus, strobilurin fungicides alone have been considered as the least effective fungicides to reduce DON accumulation in FHB management (Gilbert and Haber 2013; Torres et al. 2019).

Fungicide applications alone in susceptible cultivars were insufficient to prevent economic loss in heavy FHB epidemics (Mesterházy et al. 2003). The use of resistant cultivars had a synergistic effect on fungicide efficacy compared to fungicide use on susceptible cultivars (Mesterházy et al. 2003). Moderately resistant cultivars without any fungicide application had similar visual disease symptoms, but much lower DON content than susceptible cultivars treated with a fungicide application (Willyerd et al. 2012). Overall, the best FHB disease management is fungicide application combined resistant cultivars, which gives a strong additive effect for FHB control (Willyerd et al. 2012; Torres et al. 2019).

2.4.3 Biological control

In addition to chemical fungicides, there were several biocontrol agents (BCAs) available for integrated management of FHB: fungi, yeast and bacteria (McMullen et al. 2012; Gilbert and Haber 2013). Some fungal species (like *Clonostachys rosea*) were found to repress Fusarium growth. A strain of *C. rosea* consistently repressed mycelial growth and conidial germination *in vitro*, but inconsistently reduced FHB infection in field trials (Xue et al. 2009). Another test of the same strain of *C. rosea* as a bio-fungicide found it did not successfully reduced FHB infection or DON content in two field trials (Nowakowski 2018). A few yeast strains (*Cryptococcus spp.*) acting as antagonists could compete for nutrients with Fusarium were shown to reduce disease severity in greenhouse, but insignificantly decreased FHB symptoms in the field (Schisler et al. 2011; McMullen et al. 2012; Gilbert and Haber 2013). Treatment with the gram negative bacteria *Lysobacter enzymogenes* prior to Fusarium infection induced host resistance and limited disease severity in greenhouse tests, but could not effectively control FHB infection in field experiments (Jochum et al. 2006; Li et al. 2008b). Gram positive bacteria *Bacillus subtilis* is one BCA that produced antimicrobial components (like fengycin and bacillomycin D) to restrict *Fusarium* growth in wheat spikes in a indoor study (Ramarathnam et al. 2007; Chan et al. 2009). Two *Bacillus* spp., *B. subtilis* and *B. velezensis*, reduced FHB infection in field tests (Zhao et al. 2014; Palazzini et al. 2016). Use of biocontrol agents may be an alternate management tool for controlling FHB resistance, especially for organic growers, however, requires more research and evaluations specific to improving their effectiveness in field applications is required (McMullen et al. 2012).

2.5 FHB disease resistance breeding in wheat

2.5.1 Active host defense mechanisms of FHB resistance

2.5.1.1 Five types of FHB resistance

In wheat breeding, the development of FHB resistant cultivars is typically focused on mitigating yield loss and minimizing mycotoxin contamination in the grain. Host genetic resistance to FHB is divided into active and passive mechanisms. Active response mechanisms relate to the direct response to the pathogen, while passive mechanisms usually relate to morphological traits that indirectly contribute to resistance (Mesterházy 1995). Five types of active host resistance are described in the *Fusarium*-wheat pathosystem: Type I resistance describes the decrease of initial FHB infection; Type II describes the restriction of the fungus inside infected spikes; Type III resistance describes the reduction of FDK; Type IV describes the prevention of yield loss under disease pressure; and Type V describes the reduced accumulation of mycotoxin in infected grains (Mesterházy 1995).

2.5.1.2 Sources of genetic resistance to FHB

Currently most sources of FHB resistance come from spring wheat, but these alleles are also functional in winter wheat (Buerstmayr et al. 2009, 2019). Although QTL for FHB resistance have been identified on each chromosome, no single QTL grants total resistance to the disease. Sources of FHB resistance can be found in cultivars, landraces, and wild cereal relatives. Since 1999, the

Chinese spring wheat cultivar, Sumai 3, has been the most important source of FHB resistance (Waldron et al. 1999; Anderson et al. 2001; Cuthbert et al. 2006, 2007; Ma et al. 2006b, a). A Sumai 3-derived cultivar, Ning 7840, has been also a good candidate for FHB resistance (Bai et al. 1999; Zhou et al. 2002; Guo et al. 2003; Somers et al. 2005; Kang et al. 2011). Another Sumai 3-derivative, CM-82036, was found to carry a Type II resistance gene *Fhb1* and a Type I resistance QTL *Qfhs.ifa-5A*, both of which have been transferred to European winter wheat (Buerstmayr et al. 2002, 2003; Salameh et al. 2011). CM-82036 was also used in other studies related to FHB resistance, including the study of the *Fhb1* gene and resistance of toxicity of DON and T-2 toxin (Lemmens et al. 2005; Nathanail et al. 2015; Schweiger et al. 2016). FHB resistance derived from Sumai 3 and its derivates have repeatably reported on the five chromosomes (2D, 3B, 4B, 5A and 6B), which are allelic or identical to *Qfhs.nau-2DL*, *Fhb1*, *Rht-B1a*, *Qfhs.ifa-5A* and *Fhb2*, respectively (Buerstmayr et al. 2009, 2019).

The Chinese wheat landrace, Wangshuibai, is another important FHB resistance source from Asian and recently reviewed by Jia et al. (2018). Notably, this landrace had been repeatedly found to carry four *Fhb* genes (*Fhb1*, *Fhb2*, *Fhb4* and *Fhb5*) (Buerstmayr et al. 2009, 2019; Jia et al. 2018). Also, the FHB resistance of Nyubai with unknown pedigree has been studied in several QTL mapping populations and three transcriptional profiling studies with microarray or RNA sequencing technology (Somers et al. 2005; Cuthbert et al. 2006; McCartney et al. 2007; Tamburic-Ilincic et al. 2009; Pan et al. 2018; Brauer et al. 2019; Fauteux et al. 2019). Two regions allelic to *Fhb1* and *Qfhs.ifa-5A* were repeatedly reported with FHB resistance in Nyubai (Buerstmayr et al. 2009, 2019).

In addition to the Asian resistance sources, a spring wheat Brazilian cultivar, Frontana, is a good alternative resistance source (Steiner et al. 2004; Mardi et al. 2006; Srinivasachary et al. 2008b; Yabwalo et al. 2011; Szabó-Hevér et al. 2012; Mesterhazy 2020). Type I resistance on chromosome 3A in Frontana was consistently reported. A review written by Zhu et al. (2019) mentioned the good impact of Frontana to United States spring wheat germplasm pedigrees. However, introgression of this Frontana-derived 3A resistance into Canadian winter wheat germplasms could be a concern due to association with low protein content (Tamburic-Ilincic 2012).

Several QTL studies on European winter wheat cultivars (e.g. Arina, Dream, Patterson) were review by Buerstmayr et al (2009). Several regions in eight chromosomes in Arina were associated with Type II resistance, where QTL for anther retention and Type II resistance were co-localized on chromosomes 4A and 6B (Paillard et al. 2004; Draeger et al. 2007; Semagn et al. 2007; Buerstmayr and Buerstmayr 2015). Also, the presence of wildtype allele *Rht-D1a* in the dwarfing gene *Rht-D1* locus in Arina increased height and FHB resistance (Draeger et al. 2007). Three winter wheat populations were found to carry QTL for FHB resistance in fourteen chromosomes, where chromosomes 1B and 4D were common regions among three linkage maps and a common dwarf gene *Rht-D1* was co-localized with the 4D QTL (Holzapfel et al. 2008). According to a review paper written by Buerstmayr et al (2019), major FHB resistance QTL published in 2009-2019 were located on ten chromosomes (1A, 1B, 2A, 4A, 4D, 5A, 6B, 7A and 7B) for European winter wheat, two chromosomes (3B and 7D) for Asian winter wheat, and fifteen chromosomes (1A, 1B, 2A, 2B, 2D, 3A, 3B, 3D, 4A, 4B, 4D, 5A, 5B, 6A and 6B) for North America winter wheat. Many other QTL for FHB resistance have been detected in diploid and tetraploid wheat

and wild relatives (such as *T. macha*, *Thinopyrum elongatum*, *Th. ponticum*, *Leymus racemosus*) and mentioned in review articles (Gilbert and Tekauz 2000; Buerstmayr et al. 2009; Gilbert and Haber 2013; Ma et al. 2020).

2.5.1.3 Common QTL for Type I, II and V resistance

Several reviews have shown that numerous FHB QTL have been identified and many of them have been validated (Liu et al. 2009; Buerstmayr et al. 2009, 2019). Reviews of reported major QTL for FHB resistance in **Table 2.2** showed that the largest number of major FHB QTL detected were associated with reducing disease severity, while the number of major QTL for decreasing disease incidence and DON content was similar for both types of resistances and much lower than for reducing disease severity (**Table 2.2**) (Buerstmayr et al. 2009, 2019). Numbers of QTL for disease severity included QTL identified in both spray inoculation methods from field trials and point inoculation methods from greenhouse experiments, while numbers of QTL for disease incidence and DON content were obtained from inoculated field trails and measurement of DON content. Seven chromosomes (2B, 2D, 3A, 3B, 4B, 4D and 5A) were commonly reported to contain major QTL for disease incidence, while major QTL for disease severity were often detected on chromosomes 1B, 2A, 2D, 3B, 4B, 5A, 6B. Two chromosomes (3B and 5A) commonly had the highest number of QTL associated with DON content. Markers closely linked to common FHB resistance QTL and genes on seven chromosomes (2D, 3A, 3B, 4B, 5A, 6A, 6B and 7B) were recommended by Buerstmayr et al (2009) for marker assisted selection.

Table 2.2 Summary of previously reported major QTL for Fusarium head blight (FHB) resistance and morphological traits associated with these major FHB resistance in 21 wheat chromosomes based on information adapted from the two reviews (Buerstmayr et al. 2009, 2019).

	(Buerstmayr et al. 2009)[1]					(Buerstmayr et al. 2019)[2]					
LG[3]	**Inc[4]**	**Sev[5]**	**DON[6]**	**Ht[7]**	**Anth[8]**	**Inc**	**Sev**	**DON**	**Ht**	**Anth**	**AE[9]/AR[10]**
1A		3	2	1		2	3	2			
2A		7	2	1		1	7	2		1	1
3A	3	8				1	4				
4A	1	1	1			1	3	1			1
5A	3	9	4	2		1	14	6	6		
6A		3				1	3	1	1		
7A		6		1			4	2			
A genome	**7**	**37**	**9**	**5**	**0**	**7**	**38**	**14**	**7**	**1**	**2**
1B	1	10				2	4	2	1		1
2B	3	7		1	1	2	5		1		
3B	3	32	6			2	16	5	1		
4B	1	6				3	8	2	7		3
5B		5				1	3	1	1		
6B	2	10				1	8		1		1
7B	1	5		1			3		1	1	
B genome	**11**	**75**	**6**	**2**	**1**	**11**	**47**	**10**	**13**	**1**	**5**
1D		2									
2D	2	8	3	1	1	4	7	2	5	3	1
3D		4						2			
4D	1	3		2		3	7	1	7		2
5D	1	1	1								
6D		1		1							
7D						2	4				
D genome	**4**	**19**	**4**	**4**	**1**	**9**	**18**	**5**	**12**	**3**	**3**
Total	**22**	**131**	**19**	**11**	**2**	**27**	**103**	**29**	**32**	**5**	**10**

[1]Fifty-two QTL studies for FHB resistance and morphological traits associating FHB resistance in 2001-2009 were reviewed by Buerstmayr et al (2009); [2]Another fifty-two QTL studies in 2009-2019 were summarized by Buerstmayr et al (2019); [3]LG represents Linkage group; [4]Inc disease incidence; [5]Sev disease severity; [6]DON deoxynivalenol content; [7]Ht plant height; [8]Anth anthesis date; [9]AE anther extrusion; [10]AR anther retention

*Major QTL for three FHB traits (Inc, Sev and DON) are shown, while morphological QTL for Ht, Anth, AE and AR co-localized with major QTL for the three FHB traits were also listed in this table.

2.5.1.4 Common *Fhb* genes

To date, seven *Fhb* genes have been discovered from wheat and its related species (**Table 2.3**) (Liu et al. 2006; Cuthbert et al. 2007; Qi et al. 2008; Xue et al. 2010a, 2011; Cainong et al. 2015; Guo et al. 2015; Rawat et al. 2016). The *Fhb1* gene was first fine mapped in Sumai 3 and Nyubai in 2006 (Cuthbert et al. 2006; Liu et al. 2006) (**Table 2.3**). Several potential functional genes in this locus/region have been proposed to confer Type II resistance: a pore-forming toxin-like gene (Rawat et al. 2016), a start codon deletion of a gene encoding a putative histidine-rich calcium-binding (His) protein (Su et al. 2019), and a rare deletion in the 3' exon of the same *His* gene (Li et al. 2019). Notably, Su et al (2019) hypothesized that a His^S allele as a susceptibility factor was disrupted by the deletion of the start codon in Ning 7480, resulting in a loss-of-function mutation conferring the *Fhb1* resistance, while Li et al (2019) suspected a rare deletion created an alternative splicing for the open reading frame in a His^R allele in Wangshuibai, resulting in a gain-of-function mutation for the *Fhb1* resistance. Lagudah and Krattinger (2019) suggested a dominant-negative effect theory that either the deletion of the His^S allele in Ning 7480, or the altered variation of the His^R allele in Wangshuibai, might change formations of multimers from normal His proteins, leading to reduce the FHB infection. More future studies are required to understand and validate the exact mechanism of the resistance of *Fhb1* gene. Beside the *Fhb1* gene, other four *Fhb* genes (*Fhb2*, *Fhb3*, *Fhb6* and *Fhb7*) also improve Type II resistance and reduce disease severity, where *Fhb2* was derived from Sumai 3 and the other three *Fhb* genes from close relative grass species (**Table 2.3**). Two *Fhb* genes (*Fhb4* and *Fhb5*) were derived from Wangshuibai and decrease disease incidence.

Table 2.3 Current *Fhb* genes in characterized in wheat or wheat relatives, their chromosomal location, type of resistance and source.

Name	Chromosome	Resistance	Source	References
Fhb1	3B	Type II[1]	Sumai 3[3]	(Liu et al. 2006; Rawat et al. 2016)
Fhb2	6B	Type II	Sumai 3	(Cuthbert et al. 2007)
Fhb3	T7AL·7Lr#1S (7A)	Type II	*Leymus racemosus*	(Qi et al. 2008)
Fhb4	4B	Type I[2]	Wangshuibai[4]	(Xue et al. 2010a)
Fhb5	5A	Type I	Wangshuibai	(Xue et al. 2011)
Fhb6	1Ets#1S (1A)	Type II	*Elymus tsukushiensis*	(Cainong et al. 2015)
Fhb7	7DS.7el2L (7D)	Type II	*Thinopyrum ponticum*	(Guo et al. 2015)

[1]Type I resistance reduces disease incidence; [2]Type II resistance decreases disease severity
[3]Chinese wheat cultivar, Sumai 3, belongs to hexaploid wheat *Triticum aestivum*; [4]Chinese wheat landrace, Wangshuibai, also belongs to hexaploid wheat *Triticum aestivum*

2.5.1.5 The association of FHB susceptibility

An alternate approach to improve FHB resistance is the identification and removal of the regions associated with FHB susceptibility as summarized by Fabre et al. (2020). Deletion of a few regions on chromosomes 3B, 4D, 6A, 6B, 7A and 7B reduced disease severity and DON content (Ma et al. 2006a). A susceptible tetraploid *T. turgidum* genotype had less FHB infections in three greenhouse tests after substituting its chromosome 2A with a tetraploid wild emmer wheat *T. dicoccoides*, suggesting the presence of susceptibility determinants in that chromosome (Garvin et al. 2009). A region located on the short arm of chromosome 2D in Sumai 3 was suspected to associate with FHB susceptibility and increased FDK (Basnet et al. 2012). A deletion of the long arm of chromosome 3D in a susceptible spring wheat cultivar, USU-Apogee, decreased FHB infection and DON content (Garvin et al. 2015). Moreover, other traits could also associate with high FHB infection. The presence of *Rht-B1b* or *Rht-D1b* alleles often associated with higher FHB infection and DON content (Buerstmayr and Buerstmayr 2016; Tamburic-Ilincic and Rosa 2017). Also, the presence of vernalization genes *Vrn-A1a* or *Vrn-B1a* alleles was also associated with

increasing FHB infection. In total, Fabre et al. (2020) summarized the existence of FHB susceptibility determinants in fourteen wheat chromosomes.

2.5.2 Morphological traits affecting FHB

Several QTL for morphological traits including plant height, anthesis date and spike characteristics (awns and compactness) have been associated QTL for FHB resistance (Mesterházy 1995; Buerstmayr et al. 2009, 2019). More recently, an understanding of the role of anther extrusion/retention in FHB resistance has risen and led to the detection of numbers of QTL related to this trait. **Table 2.2** shows that QTL for plant height, anthesis date and anther extrusion/retention co-localized with QTL for FHB resistance.

2.5.2.1 Association between plant height and FHB

In the host-pathogen pathosystem, wheat genotypes do not only use their resistance genes against FHB infection, but they also rely on several passive mechanisms to limit the initial *Fg* invasion. As an important agronomic trait, plant height plays an important role in passive resistance to FHB (Mesterházy 1995; Buerstmayr et al. 2009, 2019; Yan et al. 2011; Saville et al. 2012). Three hypotheses have been developed to explain the association between the two traits. The first theory postulates that tall plants have an increased distance between the spikes and the primary inoculum source on the ground, which reduces the chance of natural infection (Mesterhazy 1995). The second hypothesis suggests that height alters the micro-environment around the spikes, thus contributing to lower FHB infection. In this scenario, short plants have higher local humidity

around the spikes compared to tall plants, which can create favorable conditions for *Fg* development (Yan et al. 2011). The third hypothesis proposes that the association between height and FHB resistance is due to the pleiotropic effect of the dwarfing genes on hormone crosstalk (Saville et al. 2012; Buerstmayr and Buerstmayr 2016). To date, none of above hypotheses proven to be the sole mechanism by which increased height enhances FHB resistance, while decreased height promotes susceptibility to the disease.

Taller plant height has been associated with better FHB resistance (Mesterházy 1995; Buerstmayr et al. 2009; Yan et al. 2011; Saville et al. 2012). In particular, the *Rht-B1a* and *Rht-D1a* alleles were associated with increases in height and FHB resistance in several QTL studies (Lu et al. 2013; He et al. 2016; Xu et al. 2020). However, the gibberellic acid (GA)-insensitive dwarfing alleles *Rht-B1b* and *Rht-D1b* reduce plant height, which allows wheat growers to increase fertilizer use to achieve high yield without the risk of lodging under high input agriculture (Hedden 2003). The introduction of dwarf alleles *Rht-B1b* or *Rht-D1b* has increased grain yield and lodging resistance but is associated with FHB susceptibility. Many other agronomic traits were improved by using either of the two semi-dwarfing alleles (Lanning et al. 2012). The presence of the dwarf allele *Rht-B1b* or *Rht-D1b* in near isogenic lines (NIL) reduced plant height and produced more tillers and higher seeds per spike than the NILs with the tall allele types, *Rht-B1a* or *Rht-D1a* (Lanning et al. 2012; Chen et al. 2016). Although the semi-dwarf plants carrying either the *Rht-B1b* or *Rht-D1b* allele had slightly lower thousand kernel weight, test weight and grain protein, and slightly delayed maturity compared to the tall plants carrying either the *Rht-B1a* or *Rht-D1a* allele, the two dwarf alleles have been widely used in spring and winter wheat cultivars in North America (Guedira et al. 2010; Lanning et al. 2012; Chen et al. 2016). Thus, the use of wildtype *Rht-B1a* or *Rht-D1a*

allele for improving FHB resistance has been discouraged due to the associated height increase leading to lodging and yield reduction (Verma et al. 2005; Voss et al. 2008; Guedira et al. 2010; Lanning et al. 2012; Chen et al. 2016).

In the early 2000s, the frequency of the *Rht-B1b* allele in US soft winter wheat cultivars and hard winter wheat cultivars was 28% and 77%, respectively (Guedira et al. 2010). The distribution of the *Rht-D1b* allele was 45% and 8% in US soft winter wheat cultivars and hard winter wheat cultivars, respectively (Guedira et al. 2010). The two dwarf alleles have been introduced and widely used in western Canada since the 1990s (Chen et al. 2016). Balancing optimal height and strong FHB resistance is one of current breeding challenges.

2.5.2.2 Association between anther retention and FHB

In additional to height, other morphological traits such as anther extrusion/retention have been found to be associated with FHB (Skinnes et al. 2010). In wheat, anther morphology ranges from being completely enclosed in cleistogamous florets to being completely extended beyond the floret; both situations are unfavorable for *Fg* to infect and/or colonize wheat spikes. Intermediate anther morphology, where the anther is retained (anther retention) in the open floret, has been correlated with FHB susceptibility. Although the exact mechanism underlying this association remains unknown, one hypothesis is that anthers trapped between the lemma and palea in wheat florets provides favorable conditions for initial mycelial growth and colonization (Buerstmayr and Buerstmayr 2016). Specifically, mycelia might be able to grow within the filaments which provides an expedited pathway to the rachis from which it invades neighboring spikelets.

Several QTL for anther retention have been identified across the genome through genetic mapping studies (Lu et al. 2013; He et al. 2016; Xu et al. 2020). Coincidentally, these QTL often co-localize with QTL for FHB resistance and plant height (Lu et al. 2013; He et al. 2016; Xu et al. 2020). In particular, QTL for FHB resistance, anther retention and plant height all overlapped such that they all contained the *Rht-B1* gene (Lu et al. 2013; He et al. 2016; Xu et al. 2020). Based on the additive effect, the *Rht-B1a* allele was associated with increased height, anther extrusion and FHB resistance. Conversely, the *Rht-B1b* allele was associated with decreased height, and increased anther retention and FHB occurrence (Lu et al. 2013; Buerstmayr and Buerstmayr 2016; He et al. 2016; Xu et al. 2020).

2.6 Cross talk among different phytohormones during host defense

2.6.1 The regulation of gibberellin on plant height and the gibberellin-dependent dwarfing

Plant growth can be regulated with different hormones, including auxins, brassinosteroid, cytokinins and gibberellin. The interactions among those hormoneses have been reviewed by several authors (Wang et al. 2017b; Liu and Timko 2021). The *Rht-B1a* allele in wheat affects plant height through a GA-dependent mechanism, which was first well understood in *Arabidopsis* and rice (Xu et al. 2014; Nelson and Steber 2016). More than one hundred GAs have been discovered in plants, but only six are bioactive forms (Murase et al. 2008; Xu et al. 2014). In *Arabidopsis*, a GA receptor GA-insensitive dwarf1 (GID1) first uses its N-terminal extension to recognize a lactone ring in a bioactive GA molecule through several hydrophobic interactions

(Murase et al. 2008; Shimada et al. 2008) (**Figure 2.3 a**). Then, a pocket-like core domain in the GID1 forms hydrogen bonds with the C3 hydroxyl group and the C6 carboxylate group in the GA molecule to further embed the GA inside the GID1, which results in a stable GA-GID1 complex (Murase et al. 2008; Shimada et al. 2008). The change from a C2 non-hydroxyl group to a C2 hydroxyl in a GA molecule switches a bioactive form to a non-activated form by disturbing the hydrophobic interactions between GA and GID1, which causes a conformational change in the GID1, resulting in failure to bind with the non-bioactive GA molecule (Murase et al. 2008). All three wheat homoeologous *TaGID1* genes (*TaGID1-A1*, *TaGID1-B1* and *TaGID1-D1*) producing functional GA receptors have been found in the long arms of the three group 1 wheat chromosomes (1A, 1B and 1D, respectively) (Li et al. 2013).

In *Arabidopsis*, DELLA protein, which is named based on its N-terminal conserved amino acid sequence (Asp-Glu-Leu-Leu-Ala; D-E-L-L-A), consists of a N-terminal DELLA domain and a C-terminal domain. The C-terminal domain was also named as GRAS functional domain containing three genes (GA insensitive, Repressor of GA1 and SARECROW) (**Figure 2.3 b**) (Hauvermale et al. 2012; Thomas et al. 2016). Several reviews focused on how the C-terminal GRAS domain of the DELLA protein interacts with different transcriptional factors (TFs) to suppress GA-dependent plant growth in *Arabidopsis* (Hauvermale et al. 2012; Thomas et al. 2016). DELLA protein uses its N-terminal DELLA domain to interact with the N-terminal extension of GA-GID1 complex to further form a GA-GID1-DELLA complex (Silverstone et al. 2001; Griffiths et al. 2006; Murase et al. 2008; Shimada et al. 2008). After binding with the GA-GID1 complex, the C-terminal GRAS domain of the DELLA protein is further interacted with a $SCF^{SLY1(SLEEPY1)}$ (Skp1, Cullin, F-box) E3 ubiquitin ligase complex via multiple processes, which leads to the polyubiquitination of the

DELLA (Hedden and Sponsel 2015; Nelson and Steber 2016). The polyubiquitinated DELLA protein carrying an ubiquitin chain can be recognized by 26S proteasome, which results in the destruction of DELLA protein complex and release of DELLA-suppressed TFs to promote the growth of plant height (Hedden and Sponsel 2015; Nelson and Steber 2016).

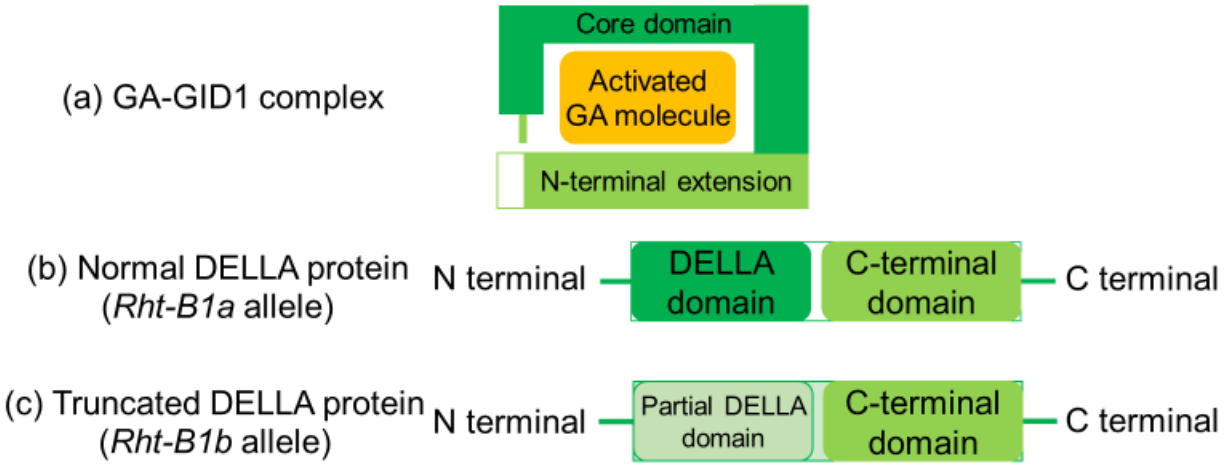

Figure 2.3 A schematic diagram of the formation of GA (gibberellic acid)-GID1 (GA-insensitive dwarf1)-DELLA (D-E-L-L-A; Asp-Glu-Leu-Leu-Ala) complex for the regulation of gibberellin on plant height, which was adapted from Nelson and Steber (2016) and Hedden and Sponsel (2015). (a) A GID1 protein binds a bioactive GA molecule by using its N-terminal extension and the pocket-like core domain, which forms a GA-GID1 complex. (b) A wildtype allele *Rht-B1a* produces a normal DELLA protein with an intact DELLA domain and a C-terminal GRAS functional domain, which enables interaction with GA-GID1 complex to form a GA-GID1-DELLA complex. (c) A dwarf allele *Rht-B1b* encodes a truncated DELLA protein, which the partial DELLA domain cannot bind with GA-GID1 complex.

In wheat, *Rht-B1a* in chromosome 4B encode DELLA proteins like *Arabidopsis* (Peng et al. 1999; Pearce et al. 2011) (**Figure 2.3 b**). Compared with wildtype *Rht-B1a*, semi-dwarf allele *Rht-B1b* replaces a cytosine by a thymine in the LExLE motif of the N-terminal DELLA domain and causes a change from a Q64 codon (CGA) to a translational stop codon (TGA), resulting in a truncated DELLA protein (**Figure 2.3 c**) (Peng et al. 1999; Pearce et al. 2011). Truncated DELLA protein has an incomplete N-terminal DELLA domain preventing binding of the GA-GID1 complex and remains a C-terminal GRAS functional domain, which results in failure to be degraded by 26S

proteasome and continually binds with TFs to suppress plant growth, thus the *Rht-B1b* allele in wheat produces semi-dwarf plants (Pearce et al. 2011).

2.6.2 Role of jasmonic acid signalling in wheat FHB resistance

Jasmonic acid (JA) is involved in host plant-pathogen interactions (Glazebrook 2005; Koornneef and Pieterse 2008; Shigenaga and Argueso 2016). The JA biosynthesis and signalling pathways in *Arabidopsis* have been reviewed in detail (Zhai et al. 2017; Ruan et al. 2019). In *Arabidopsis*, the jasmonate ZIM-domain (JAZ) protein family is the most important negative regulator in the JA signaling pathway, where the ZIM domain is named from zinc-finger protein expressed in inflorescence meristem (Chini et al. 2007; Thines et al. 2007). Typically, a JAZ1 protein has three important domains, N-terminal (NT), ZIM and JA-associated (Jas), located in the N-terminal, center, and C-terminal of the protein, respectively (Hou et al. 2010). In the absence of a bioactive JA jasmonoyl-isoleucine (JA-Ile), both ZIM and Jas domain of JAZ proteins suppress JA-related disease resistance by interacting with an important TF *myelocytomatosis oncogenes* (*MYC2*) that responds to bind G-box motifs (where G-Box motif is a DNA sequence having the core motif CACGTG) in promoter regions of JA response genes (Meier and Gruissem 1994; Chini et al. 2007; Thines et al. 2007; Hou et al. 2010). In the presence of JA-Ile, an F-box protein coronatine insensitive (COI1) recognizes and binds the JA-Ile molecule to form a JA-COI1 complex (Sheard et al. 2010; Zhai et al. 2017; Ruan et al. 2019). The JA-COI1 complex further physically interacts with a JAZ1 protein to form a JA-COI1-JAZ1 complex. Later, the ubiquitination of JAZ1 occurs in the JA-COI1-JAZ1 complex, which leads to the degradation of JAZ1 by 26S proteasome resulting in release of *MYC2* to trigger downstream JA response genes (Xie et al. 1998; Thines et

al. 2007; Chini et al. 2009). Similarly, in wheat, the protein TaJAZ1 enables binding with the transcriptional factor *TaMYC4* to suppress the JA pathway (Jing et al. 2019).

During wheat-*Fg* interaction, the JA signalling pathway plays an important role in FHB resistance (Ding et al. 2011; Qi et al. 2016; Buhrow et al. 2016; Pan et al. 2018; Brauer et al. 2019). The direct application of JA into fungal growth media is able to reduce *Fg* spore viability and mycelial growth *in vitro* (Qi et al. 2016). After FHB infection, a resistant cultivar, Wangshuibai, had higher endogenous JA content and stronger expression of JA-response genes than a susceptible line (Ding et al. 2011). Similar observations have been found in two hormonal profiling studies where the levels of JA and/or SA increased after FHB infection (Buhrow et al. 2016; Brauer et al. 2019). Several real time polymerase chain reaction studies have confirmed that transcripts of JA-response genes are up-regulated during FHB infection (Qi et al. 2016, 2019; Brauer et al. 2019). Moreover, recent microarray studies suggest that the JA signalling pathway is able to be up-regulated in both resistant and susceptible cultivars, which suggests it may be involved in several defense processes, such as DON detoxification, glutathione conjugation, and thickened cell walls (Brauer et al. 2019; Qi et al. 2019). In an RNA sequencing (RNA-seq) study, many differentially expressed genes (DEGs) related to JA pathways were trigged after the FHB infection (Pan et al. 2018).

Resistant wheat had earlier and stronger expression of JA response genes than susceptible wheat in one RNA-seq study (Wang et al. 2018). A similar result was found in one wheat microarray study that showed that resistant wheat had more up-regulated genes specifically related to the JA pathway than susceptible wheat, even though susceptible wheat had more total DEGs than resistant wheat (Sun et al. 2016). In contrast, a few other experiments have observed a different expression

pattern related to the JA signaling pathway between resistance and susceptible wheat (Pan et al. 2018; Brauer et al. 2019; Qi et al. 2019). An RNA-seq study discovered that FHB susceptible wheat had more gene expression involved with the JA pathway than FHB resistant wheat (Pan et al. 2018). A microarray study showed that a susceptible wheat cultivar, Roblin, had very few SA-related DEGs and high amounts of JA-related DEGs four days post inoculation (Qi et al. 2019). Another microarray study found that expression of disease response genes in susceptible wheat was higher than that in resistant wheat (Brauer et al. 2019). Overall, it has been well recognized that JA related defense responses are involved in FHB resistance and inconsistency among different studies could be related with other factors (such as sampling timing and genotype) that play important roles during the FHB infection in wheat.

2.6.3 Crosstalk between GA and JA pathways affecting wheat FHB resistance

The host-pathogen interaction relying on the JA pathway can be affected by crosstalk with other phytohormones. In *Arabidopsis*, DELLA protein enhances the JA pathway and its related resistance against necrotrophic pathogens, while inducing host susceptibility toward biotrophic pathogens by suppressing the SA pathway (Navarro et al. 2008). The mechanism for such phenomenon can be explained by understanding the interaction of DELLA and JAZ1 during crosstalk between the GA and JA pathways. DELLA protein uses its C-terminal GRAS domain to physically interact with NT and Jas domains in a JA negative regulator JAZ1 protein and releases the TF *MYC2* that previously bound with the Jas domain, resulting in the increase of the JA signaling pathway and expression of JA response genes (Hou et al. 2010). Hou *et al.* (2010) also discovered that the N-terminal side of the C-terminal GRAS domain in DELLA protein was the

key binding site for the DELLA-JAZ1 interaction. Even deletion of the entire N-terminal DELLA domain in truncated DELLA protein resulted in partial interaction between truncated DELLA and JAZ1 proteins.

In wheat, a similar pattern to *Arabidopsis* has been found between the *Rht-B1a* NIL producing normal DELLA and the *Rht-B1b* NIL producing truncated DELLA after testing several biotrophic, hemi-biotrophic and necrotrophic pathogens (Saville et al. 2012) (**Figure 2.3 b and c**). Plants carrying either the *Rht-B1a* or *Rht-B1b* allele produce bioactive JA (JA-Ile) to degrade JAZ protein to release TF *MYC2* and initiates JA-related defense response, while truncated DELLA proteins produced by the *Rht-B1b* allele can further bind with additional JAZ proteins to free more *MYC2* and provide a stronger JA-related disease resistance than normal DELLA proteins produced by the *Rht-B1a* allele that cannot interact with JAZ protein due to the degradation of the GA-GID1-DELLA complex.

On the other hand, through the same hormonal crosstalk, the JA pathway is able to affect GA-related growth (Hou et al. 2010; Yang et al. 2012). Exogenous methyl jasmonate can reduce shoot length in rice seedlings (Yang et al. 2012). Exogenous JA also can reduce root length in *Arabidopsis* seedlings while increasing DELLA protein levels (Hou et al. 2010; Yang et al. 2012). The dysfunction of the important JA receptor COI1 significantly increases cell lengths and internode lengths (Yang et al. 2012). Overexpression of JAZ protein increases the lengths of the petiole and hypocotyl, and induces early flowering (Yang et al. 2012). All these phenomena result in JAZ proteins in the JA signaling pathway that compete with GA-related growth TFs such as *PIF4* to bind with the C-terminal GRAS domain in DELLA protein leading to suppression of plant

growth (Yang et al. 2012). Therefore, the JA and GA signaling pathways have antagonistic effects to each other in disease resistance and plant growth (Yang et al. 2012; Qi et al. 2014; Liu and Timko 2021).

CHAPTER 3

QTL MAPPING OF FUSARIUM HEAD BLIGHT RESISTANCE IN AN ELITE DOUBLED HAPLOID WINTER WHEAT CROSS 32C*17/PEREGRINE AND EVALUATION OF MARKER ASSISTED SELECTION EFFICIENCY OF DETECTED QTL IN THE RECIPROCAL CROSS

3.1 Abstract

Resistance to Fusarium head blight (FHB) is complex and involves multiple genes with relatively small effects. The breeding line 32c*17 showed strong FHB resistance under severe disease pressure in both Canada and Germany. A doubled haploid (DH) population (3CPR) was generated from the cross between 32c*17 and the cultivar, Peregrine, with intermediate FHB resistance. Another DH population (PR3C) was created from the reciprocal cross. The objectives of this study were to identify quantitative trait loci (QTL) for FHB resistance and other agronomic traits associated with FHB resistance. The efficiency of marker assisted selection (MAS) based on the detected strong FHB QTL in the 3CPR population was estimated in its reciprocal population PR3C. Transgressive segregation in the 3CPR population was observed for all traits measured in field and greenhouse tests. Three main QTL were detected across a combination of FHB traits (especially for deoxynivalenol (DON) content) on chromosomes 4D, 6A and 6D with resistance derived from 32c*17 in the 3CPR population. Several other FHB QTL on chromosomes 1A, 1B, 2A, 2D, 3A, 4A, 5D, 6B, 7A and 7B were inconsistently detected in different individual environments. *QFhb/QFdk/QDon.umb-4D* were not associated with plant height. Unlike previously published

QTL on chromosome 6D that were associated with disease severity, the current *QFhb/QFdk/QDon.umb-6D* strongly associated with Type I and DON resistance, which provided a new insight on FHB QTL on chromosome 6D. Markers within QTL on chromosomes 4D, 6B and 6D consistently predicted FHB resistance in the reciprocal cross PR3C across the two site years tested, which suggests that they may be good candidate markers for future MAS.

3.2 Introduction

One of the most serious diseases of wheat (*Triticum aestivum*) worldwide is Fusarium head blight (FHB), caused by fungal pathogens *Fusarium spp.*, resulting in yield and end-use quality losses (McMullen et al. 1997). *Fusarium graminearum sensu stricto* Schwabe (teleomorph: *Gibberella zeae* (Schwein.) Petch) (*Fg*) is the most predominant causal agent of FHB in North America (Gilbert and Tekauz 2000). Fusarium head blight disease symptoms and historical FHB epidemics with economic loss were reported in several review papers (McMullen et al. 1997; Gilbert and Tekauz 2000; Bai and Shaner 2004; Trail 2009). Deoxynivalenol (DON) released by *F. graminearu*m is an important virulence factor for disease spread among spikelets in infected spikes and is toxic to human and animal cells (Proctor et al. 1995; Bai et al. 2002; Jansen et al. 2005; Sobrova et al. 2010; Mayer et al. 2017). Mesterhazy (1995) introduced five types of active FHB resistance; Type I resistance reduces numbers of infected spikes, while Type II resistance decreases numbers of infected spikelets within infected spikes. Type III resistance indicates low Fusarium damaged kernels (FDK). Type IV resistance is a general overall tolerance to FHB infection. Type V resistance results in low DON content in infected grains.

In addition to the five types of active resistance, several morphological traits, especially anther extrusion and plant height, play important roles in FHB resistance (Mesterházy 1995; Buerstmayr et al. 2009; Skinnes et al. 2010; He et al. 2016). Anther extrusion is associated with FHB resistance and anther retention links with FHB susceptibility (Skinnes et al. 2010; Lu et al. 2013; He et al. 2016; Xu et al. 2020). The two most common semi-dwarfing genes *Rht-B1* and *Rht-D1* used in wheat were originally introduced from a Japanese dwarf wheat line Norin 10. The semi-dwarfing

alleles increase grain yield by reducing height and lodging, and increasing harvest index under intensive management (Hedden 2003). Current spring and winter cultivars in North America commonly carry one, or both, of the dwarfing alleles *Rht-B1b* or *Rht-D1b* (Guedira et al. 2010; Chen et al. 2016). However, it has been found that both *Rht-B1b* and *Rht-D1b* decrease Type I resistance and anther extrusion, leading to FHB susceptibility (Srinivasachary et al. 2009; He et al. 2016). Another dwarfing gene named *Rht8* located on chromosome 2D has been commonly used in European wheats varieties and is also associated with FHB (Worland et al. 1998b; Mao et al. 2010; McCartney et al. 2016). The relationship between anther extrusion/retention and *Rht8* gene remains unknown. Thus, FHB resistance that is associated with increased plant height might increase risk of lodging, resulting in limited application of tall plant height for FHB resistance. It is important for wheat breeding programs to improve FHB resistance without increasing height and anther retention, or to use dwarfing genes that are not associated with FHB susceptibility (e.g., *Rht24*) (Tian et al. 2017; Herter et al. 2018; Miedaner et al. 2022).

Numerous QTL for FHB resistance had been found and are distributed across all 21 chromosomes in wheat (Buerstmayr et al. 2009, 2019). The Chinese spring wheat cultivar, Sumai 3, is one of the most important FHB resistance source and has been widely used in breeding programs worldwide (Gilbert and Tekauz 2000; Bai and Shaner 2004; Buerstmayr et al. 2009, 2019; Zhu et al. 2019). After reviewing many United States and Canadian spring and winter wheat pedigrees, Zhu *et al.* (2019) demonstrated that Sumai 3 has played an important role in North American wheat cultivar development. To date, FHB resistance from Sumai 3, and its derivatives, has been repeatedly found in four chromosomes (2D, 3B, 5A and 6B) (Liu et al. 2009; Löffler et al. 2009; Buerstmayr et al. 2009). The 2D QTL for Type II resistance derived from Sumai 3 and Sumai 3-derivates (CJ9306,

CS-SM3-7ADS and DH181) was located in the long arm of the chromosome, which is in a different region from the dwarfing gene *Rht8* (Liu et al. 2009; Buerstmayr et al. 2009). The recently cloned *Fhb1* gene contributing Type II resistance was first widely reported in the Sumai 3 genetic background and mapped in chromosome 3B (Liu et al. 2006; Buerstmayr et al. 2009; Rawat et al. 2016; Steiner et al. 2017). Several potential functional genes (a pore-forming toxin-like gene, a histidine-rich calcium-binding gene or a putative membrane gene) in the *Fhb1* region have been suggested to confer FHB and DON resistance (Rawat et al. 2016; Li et al. 2019; Su et al. 2019; Paudel et al. 2020). The 5A QTL for Type I resistance derived from Sumai 3 has been fine mapped into one QTL with a major effect and one QTL with a minor effect, which were located across the centromere (*Qfhs.ifa-5Ac*) and a distal region of the short arm (*Qfhs.ifa-5AS*) of chromosome 5A, respectively (Steiner et al. 2019). A superfamily of transcript factor (named as NAC) consists of no apical meristem, *Arabidopsis* transcription activation factor and cup-shaped cotyledon and involved with different stress response signaling pathways (Puranik et al. 2012). Recently, it was hypothesized that *Qfhs.ifa-5Ac* encodes a NAC secondary wall thickening promoting factor1-like protein, which might be associated with increased FHB resistance and anther extrusion (Steiner et al. 2019). Another common Sumai 3 QTL for Type II resistance was fine mapped in chromosome 6B and renamed as *Fhb2* gene (Cuthbert et al. 2007). In addition to the previously mentioned four QTL, many other QTL and genes for FHB resistance have been reported in Sumai 3 (Buerstmayr et al. 2009, 2019, 2021; Zhao et al. 2018a; Zhu et al. 2019; Berraies et al. 2020).

Based on the summary of previously reported major QTL for FHB resistance in the **Table 2.2** in the previous section 2.5.1.3, major QTL for disease incidence were identified on seven chromosomes (2B, 2D, 3A, 3B, 4B, 4D and 5A), while major QTL for disease severity were

frequently reported on another seven chromosomes (1B, 2A, 2D, 3B, 4B, 5A, 6B) (Buerstmayr et al. 2009, 2019). Chromosomes 3B and 5A had the highest number of major QTL for DON content. There have been much higher number of identified major QTL for disease severity compared to the number of major QTL for incidence and DON content. The complexity of FHB resistance means that optimal resistance levels require multiple genes with relatively small effects, rather than only a few resistant genes with big effects. Thus, the identification of new major QTL for Type I and DON resistance to pyramid with the previously reported major QTL for Type II resistance could benefit FHB resistance breeding in wheat.

An elite winter wheat breeding line (named 32c*17) was developed by the University of Manitoba, Canada breeding program and demonstrated strong FHB and DON resistance under severe disease pressure in both Canada and Germany. Based on a haplotyping study (unpublished data), this line does not carry any common Sumai 3 Type I and Type II FHB resistance (*Fhb1, Qfhs.ifa-5AS* and *Fhb2*), which indicated that this line has inherited non-common useful FHB resistance from either of its parental line (Sumai 3 or a winter wheat cultivar, McClintock) and possesses a potential breeding value for FHB resistance. To better understand the resistance carried by 32c*17, a QTL mapping study was conducted in one elite winter wheat doubled haploid (DH) population (named as 3CPR) generated from a cross between 32c*17 and a winter wheat cultivar, Peregrine. The objective of this study was to: 1) identify QTL of FHB resistance and other agronomic traits associated with FHB resistance in the 3CPR population and 2) estimate the efficiency of markers closely linked with 3CPR FHB QTL to predict resistant lines in the reciprocal population (PR3C) for marker-assisted selection (MAS).

3.3 Materials and Methods

3.3.1 Plant material

The 3CPR population consisted of 122 DH lines, generated from a cross where 32c*17 was the maternal parent and Peregrine was the paternal parent. The winter wheat breeding line, 32c*17, was generated from a cross between susceptible female parent McClintock and resistant male parent Sumai 3. Peregrine, which was generated from a cross between McClintock and S86-808, is a FHB intermediate cultivar released by the Crop Development Centre, University of Saskatchewan and is in the Canadian Western Special Purpose wheat class (Fowler 2010). All field and greenhouse tests related to the 3CPR population included DH lines, parental lines and six checks. The six check lines were Caledonia, Emerson, FHB148, Freedom, Hanover and 43I*18. Caledonia is a FHB susceptible soft white winter wheat developed and released by Cornell Agricultural Experiment Station in 1998 (Sorrells et al. 2004). Emerson is a FHB resistant hard red winter wheat developed by the Lethbridge Research and Development Centre of Agriculture and Agri-Food Canada (AAFC) in Lethbridge, AB (Graf et al. 2013). FHB148 is a FHB resistant winter wheat line developed by the Ottawa Research and Development Centre, AAFC in Ottawa, ON. Freedom is a FHB intermediate soft red winter wheat released and developed by the Ohio State University, Ohio Agricultural Research and Development Centre in 1991 (Gooding et al. 1997). Hanover is a FHB susceptible line (pers. comm. A. Brûlé-Babel., 2015) and 43I*18 is an intermediate resistant winter wheat breeding line.

3.3.2 Inoculum preparation

Four *F. graminearum* isolates obtained from Dr. Jeannie Gilbert at the Cereal Research Centre, AAFC in Winnipeg, Manitoba were used in this study. Two isolates were the 3-acetyl-deoxynivalenol (3ADON) chemotype: M7-07-1 and M9-07-1. Two isolates were the 15-acetyl-deoxynivalenol (15ADON) chemotype: M1-07-2 and M3-07-2. All macroconidia suspensions were prepared based on a modified protocol originally developed by Dr. Jeannie Gilbert and described in McCallum *et al.* (2004). For each isolate, a single conidium was first isolated from a previous sporodochia colony and then grown on a potato dextrose agar (PDA) plate. After mycelia colonized the whole plate (four to seven days), a portion of mycelia and the PDA agar were selected and transferred into a sterile Spezieller Nährstoffarmer agar (SNA) media plate (20 milliliter (ml) media/plate). After culturing seven days in light at room temperature, the contents of several SNA plates (eight to twelve plates) were added into a 1.5-liter liquid carboxymethyl cellulose (CMC) media. Then, CMC media flasks were aerated for seven days in light at room temperature. Macroconidia were then harvested from each flask by filtration through sterile cheesecloth. A haemocytometer under a 10x magnification microscope was used to determine conidia numbers in order to obtain the accurate concentration of the different macroconidia suspensions. The inoculum suspensions used in both field and greenhouse tests were a mixture of equal proportions of the four isolates. The total concentration of inoculum was 50,000 macroconidal per ml. Four ml of Tween 20 (Uniqema Americas LLC) were added to each two-liter mixture suspension to increase conidia adhesion prior to the inoculation.

3.3.3 Field experiments for the 3CPR population

All DH lines in the 3CPR population, parental lines and six checks were evaluated in a total six field trials conducted at two field research stations in the University of Manitoba (The Point Field Research Laboratory, Winnipeg, MB and Ian N. Morrison Research Farm, Carman, MB) from summer 2015 to 2017. Each field trial was a randomized complete block design with three replicates. Each plot was a one-meter row and rows were spaced 30 cm apart. Seventy seeds were planted in each one-meter plot. When 50 percent of spikes in the same plot were flowering (record as anthesis date (Anth) based on Julian calendar), approximately 50 ml of the inoculum were applied to both sides of the spikes in each plot. The same amount of inoculum was applied again to each plot two or three days after the first inoculation. A CO_2 backpack sprayer operated at 30 psi was used to spray the inoculum. An overhead misting system was run for ten minutes every hour for ten to twelve hours immediately following the inoculations to maintain high humidity for optimal disease development.

Eighteen to 21 days after the first inoculation, disease incidence (Inc) and severity (Sev) were visually estimated for each plot, when plots were at the maximum disease development stage and before the disease symptoms became indistinguishable from symptoms caused by natural senescence. Incidence was the percentage of infected spikes for each plot and Sev represented the mean percentages of infected spikelets in infected spikes for each plot. FHB visual rating index (VRI) was calculated by multiplying Inc and Sev and dividing by 100. When plants were fully mature, a final plant height (Ht), excluding awns, was determined by taking the average of three measurements for each plot. Each plot was hand cut with a sickle and threshed using a low wind

speed stationary combine, which prevented the loss of shriveled kernels. Seeds from the same genotype in three replicates at each site year were pooled together before sending out to SGS Canada Inc, Mississauga, ON, Canada (former BioVision Seed Labs, Winnipeg, MB) for post-harvest analyses. Fusarium damaged kernel were identified based on typical shrunken chalk-like or pink colored appearance and were represented as a percentage by weight of a 50 g sample. For DON measurement, 10 g sub-samples take from the 50 g sample were ground into fine powder, which enabled the sample to pass through a 20-mesh sieve. Each of the 10 g samples was first dissolved into 100ml distilled water follow by filtering through a Neogen filter syringe. The filtrate from the syringe was collected for measurement using a standardized Enzyme-linked immunosorbent assay (ELISA) kit Veratox® DON 5/5 quantitative test kit (Neogen Corporation, Lansing, MI). To accurately measure DON content within the accuracy range of the kit, additional distilled water dilutions were conducted where necessary.

3.3.4 Greenhouse experiment for the 3CPR population

To specifically estimate FHB Type II resistance, all 3CPR DH lines, parental lines and the six checks were tested in a greenhouse located at the University of Manitoba, Winnipeg, MB in 2015. All genotypes were first sown in root trainers (root trainer cell size: 3.5 cm x 2.5 cm x 14 cm) and grown for two to three weeks in a growth chamber with 16 hours of light at 22 °C followed by 8 hours of dark at 18 °C until they reached the three-leaf stage. Each root trainer consists of seventy cells and one seed was planted per cell. All plants were then moved to a cool room set with 16 hours light and 8 hours dark at 4 °C and vernalized for nine to ten weeks. After vernalization, plants were placed in a growth chamber set at 10-15 °C with 16 hours of light and 8 hours of dark

for one week of acclimation before transplanting into 2-liter pots in a greenhouse (16 hours light with 22±6 °C and 8 hours dark with 18±2 °C). The experimental design was a completely randomized design with five replicates. Each replicate contained one plant per genotype and was seeded within a two- to three-week interval between each replicate to manage workload and prevent all plants flowering together. The ideal stage for inoculation was when spikes were at the 30-50% anthesis stage. Since this greenhouse test was conducted between December 2015 to April 2016, the greenhouse anthesis dates (GAnth) were calculated as the number of days from transplanting into pots after vernalization and the date of the 30-50% anthesis stage, rather than using the Julian calendar date. The first five flowering spikes on each plant were dual floret inoculated with the same macroconidal mixture suspension as used in the field trials. Two adjacent florets with a spikelet located at the top third of each flowering spike were injected with 10ul inoculum through a pipette. After inoculation, the spike was covered with a glassine crossing bag for 48 hours to provide a high humidity micro-environment. The number of infected spikelets below the inoculated points in each inoculated spike were counted and calculated to determine greenhouse disease severity (GSev). The first disease rating (GSev1) was conducted when susceptible checks reached 80 to 95 percent GSev. The second disease rating (GSev2) was recorded three days after the first rating time. Depending on fluctuations of temperatures from early winter to early spring in the greenhouse, most of the disease rating periods on inoculated spikes were conducted 17 days to 22 days after inoculation (dai).

3.3.5 Linkage and QTL mapping in the 3CPR population

Five to seven seeds of each genotype were grown together on a wetted cotton ball in a plastic container/well. Cotton balls were maintained moisture under 16-hour light and 8-hour dark at room temperature for one week. After one week, two centimeters lengths of two healthy coleoptiles were selected for each genotype and harvested with forceps into a collection tube, immersed in liquid nitrogen, and stored at -20 °C. Later, all samples were freeze dried for two or three days. In total, freeze dried leaf samples of 122 3CPR DH lines and the two parents were sent to National Research Council Canada (NRC) at Saskatoon, Saskatchewan and genotyped by 90K wheat Illumina Infinium iSelect SNP array (Illumina, San Diego, CA) (Wang et al. 2014). In addition, markers closely linked with three semi-dwarf genes (*Rht-B1*, *Rht-D1* and *Rht8*) and four common FHB genes/QTL (*Fhb1*, *Fhb2*, *Fhb5* and *Qfhs.ifaSA*) were tested on parental lines (**Appendix 3.1**) and those that were polymorphic on the parental lines were further screened with all 3CPR DH lines.

Single nucleotide polymorphism (SNP) calling on raw data was conducted with GenomeStudio V2011.1 software (Illumina, San Diego, CA) by a technical officer Kerry Boyle from NRC-Saskatoon. Markers with too much missing data (>10%) or high segregation distortion were removed. A function named "Binning of Redundant Markers" with its default setting in QTL IciMapping version 4.1.0.0 (available from http://www.isbreeding.net) software was used to group different co-segregating SNP markers into different bins (Meng et al. 2015). Only one marker from each bin was selected for generating a linkage map in MapDisto v.1.7.7 (Lorieux 2012) software. The protocol for using MapDisto to generate an accurate linkage map was obtained from McCartney *et al.* (2016). Marker distances (centimorgan (cM)) were calculated using the Kosambi

mapping function (Kosambi 1943). The default parameters for the "AutoMap" function to create linkage groups were used to set a minimum logarithm of the odds (LOD) score of 3 and a maximum recombination frequency of 0.3 (the distance between two markers must be less than 30 cM). A function called "Color Genotypes" was used to check double recombinants. After creating a linkage map in MapDisto, previously excluded co-segregating markers were added back to the map based on their corresponding bin number. Each linkage group was assigned to a wheat chromosome based on the majority of markers located in a common consensus map published by Wang *et al.* (2014). The physical positions of SNP markers were obtained by using the updated wheat reference genome of Chinese Spring (IWGSC RefSeq v2.1) (Zhu et al. 2021). To further increase the accuracy of the current linkage map, the marker order was adjusted according to the physical positions of SNP markers.

QTL mapping was conducted using QTL IciMapping version 4.1.0.0 and QGene v4.3.10 software (Joehanes and Nelson 2008; Li et al. 2008a; Meng et al. 2015). The interval mapping (IM) and inclusive composite interval mapping (ICIM) methods were used in QTL IciMapping. The protocol for using QTL IciMapping to conduct QTL mapping and generate an accurate linkage map was obtained from McCartney *et al.* (2016). Either IM or ICIM method was first run with the mapping parameters of 5 cM steps and 10,000 permutations to estimate the LOD threshold. Then, IM and ICIM methods were rerun with the mapping parameters of 0.1 cM steps and the previously obtained permutation values to calculate positions, LOD values and additive effects of QTL (pers. comm. C. McCartney., 2018). The single interval mapping (SIM) and the single-trait composite interval mapping (CIM) based on maximum-likelihood estimation were the two methods used in QGene. In the CIM method, a stepwise cofactor selection was chosen with the recommended

setting, which was the maximum number of five cofactors and the F to add/drop = 0.05 (pers. comm. C. McCartney., 2018). A permutation test with 10,000 iterations ($P < 0.05$) was conducted to determine a significance threshold for each trait. Physical locations of markers below peaks of 3CPR QTL and previously identified QTL were compared to study the relationship between 3CPR QTL and previously identified QTL. Sequences of markers below peaks of QTL were found in a public online database for *Triticeae* and *Avena* (GrainGenes: https://wheat.pw.usda.gov/GG3/) and blasted against the updated wheat reference genome of Chinese Spring (IWGSC RefSeq v2.1) to obtain physical locations (Zhu et al. 2021).

3.3.6 Statistical analyses

A completely random model was used to analyze all traits measured in field trials and a greenhouse experiment. For the five traits (Anth, Ht, Inc, Sev and VRI) measured in field trials, all phenotypic data from DHs, parental and checks were first analyzed in individual site years by the PROC Mixed procedure in SAS® Studio (Enterprise Edition 3.8) (SAS Institute Inc., Cary, NC, USA) (**Appendix 3.2**). Normality and homogeneity of variance were checked to determine whether the data could be combined for analysis. The data for the five traits were then combined and analyzed together (**Tables 3.1** and **3.2**). The two post-harvest traits (FDK and DON) and the three greenhouse traits (GAnth, GSev1 and GSev2) were analyzed similarly (**Tables 3.1** and **3.2**).

Broad sense heritability (h^2) for multiple site years on Anth, Ht, Inc, Sev and VRI measured in field trials was calculated by the formula ($h^2 = \sigma^2_G/(\sigma^2_G + \sigma^2_{G*SY}/SY + \sigma^2_e/R*SY)$), where σ^2_G represented genetic variance, σ^2_{G*SY} was the variance of interaction between genotype and site year,

σ^2_e was the residual variance, SY was the number of site years and R was the number of replicates. For FDK and DON measured on composited samples from three replicates in each site year the formula for heritability was $h^2= \sigma^2_G/(\sigma^2_G + \sigma^2_e/SY$. The three greenhouse traits only had five replicates and heritability was calculated as $h^2= \sigma^2_G/(\sigma^2_G + \sigma^2_e/R)$. The Proc Corr procedure computed Pearson correlation coefficients among means of all traits of all 3CPR DHs in all site years.

3.3.7 Estimation of prediction accuracy of resistant PR3C DHs by using the markers located within the putative 3CPR QTL

Another DH population (named as PR3C) containing 190 DHs were generated from the 3CPR reciprocal cross to evaluate the stability and consistency of the detected 32c*17-derived FHB QTL obtained from the 3CPR population. In 2015, sixty-six PR3C DH lines were tested in a field test in the Ian N. Morrison Research Farm, Carman, MB and the remaining PR3C DH lines were evaluated in 2016. The same field disease inoculation procedures as used in the replicated field trials for the 3CPR population were used. Incidence and Sev were recorded and used to calculate VRI. The same procedure described previously was used to collect the freeze-dried leaf samples for this population. All samples of 190 PR3C DH lines were sent to NRC at Saskatoon, Saskatchewan for the same 90K array genotyping. The same markers, which were in a 10 cM interval flanking the QTL peaks in the 3CPR population, were selected in the PR3C population. In single marker analysis, T-tests were conducted by using PR3C phenotypic data and the selected markers. The markers having significant *P*-values (<0.05) in the T-tests were reported. Additive effect of each significant marker in the PR3C population was calculated by taking the mean of

phenotypic data of PR3C DH lines carrying the 32c*17 allele minus the mean of phenotypic data of PR3C DH lines carrying the Peregrine allele and then dividing by two.

3.4 Results

3.4.1 Phenotyping for the 3CPR population, parental lines and checks

Four 3CPR DH lines were excluded from phenotypic data analysis due to lack of seed or abnormal growth. Individual site year analyses (**Appendix 3.2**), showed that genotype was consistently significant for all five field traits (Anth, Ht, Inc, Sev and VRI) in each of the six site years. According to the distributions of residuals and the plots for normal quantiles, all five traits were approximately fitted to normal distributions and the six site years were able to be pooled together for a combined analysis. In the combined analyses, all sources of variation were significant for all traits in both the field and greenhouse tests (**Table 3.1**).

All six checks in field trials and the greenhouse experiment behaved according to the expectation, and the results were shown in **Appendix 3.3**. Based on the results in **Table 3.2** and **Appendix 3.3**, a wide range of disease symptoms in genotypes tested were shown, and differences among lines could be differentiated, indicating sufficient disease pressure was applied in this study. The two parental lines had a small Ht difference (3.82 cm) and significantly different responses to FHB infection in both field and greenhouse tests where 32c*17 was more resistant to FHB than Peregrine (**Table 3.2**). 32c*17 had the same level of field FHB resistance and lower FDK, DON and GSev than the two resistant checks (**Table 3.2** and **Appendix 3.3**). Peregrine showed an

intermediate level of FHB resistance in field tests and a susceptible level in the greenhouse test (**Table 3.2**). The frequency distributions of the 3CPR DH population are shown for all traits in **Figure 3.1**. There was transgressive segregation in the 3CPR population for all the traits (**Figure 3.1** and **Table 3.2**). Heritability estimates ranged from a low of 62.01% for VRI to a high of 85.32% for Ht (**Table 3.2**).

Based on the results of Pearson correlation (**Appendix 3.4**), Anth in the 3CPR population correlated with Ht (r=0.31), DON content (r=0.22) and GAnth (0.35), while Ht correlated with Inc (r=0.19) and DON content (r=0.22) and GAnth (r=0.27). Incidence was strongly correlated with FDK (r=0.79) and DON (r=0.87), but not correlated with Sev. Severity was only correlated with FDK (r=0.19) and GSev (r=0.36 and 0.40), however, GSev was negatively correlated with GAnth (r=-0.25 and -0.27). There was a strong correlation between FDK and DON (r=0.88).

Table 3.1 Combined analysis of variance for anthesis date (Anth), height (Ht), incidence (Inc), severity (Sev), visual rating index (VRI), Fusarium damaged kernel (FDK) and deoxynivalenol (DON) for the 3CPR population tested in field experiments conducted in six site years in Manitoba and analysis of variance for greenhouse anthesis (GAnth) and greenhouse severity (GSev1 and GSev2) conduced in a greenhouse trial in 2015. Replicate nested within each site year for the combined field analysis.

Source of	Anth		Ht		Inc		Sev		VRI	
Variation	DF[1]	MS[2]	DF	MS	DF	MS	DF	MS	DF	MS
Genotype (G)	125	18.73****	125	441.62****	125	999.90****	125	1022.75****	125	584.41****
Site year (SY)	5	3956.36****	5	38731.00****	5	127189.00****	5	18172.00****	5	9553.70****
Replicate (SY)[3]	12	49.65****	12	1137.65****	12	2574.51****	12	993.98****	12	555.88****
G*SY	549	3.04***	549	32.22****	549	169.59****	549	167.71****	549	51.17****
Residual	1336	2.47	1331	18.75	1326	123.52	1326	110.04	1326	28.43

Source of	FDK		DON	
Variation	DF	MS	DF	MS
Genotype (G)	125	47.44****	125	127.93****
Site year (SY)	5	4101.76****	5	6623.72****
Residual	589	7.69	589	18.73

Source of	GAnth		GSev1		GSev2	
Variation	DF	MS	DF	MS	DF	MS
Genotype (G)	106	261.17****	106	699.46****	106	1146.15****
Replicate	4	2092.48****	4	1131.48****	4	1269.72***
Residual	404	97.81	396	161.10	397	278.59

[1]DF Degrees of freedom; [2]MS Mean squares; [3]Replicate nested within individual site year
****P value< 0.0001; ***P value< 0.001; **P value < 0.01; *P value < 0.05

Table 3.2 Broad sense heritability and descriptive statistics of parental lines and the 3CPR doubled haploid (DH) population for traits measured in the combined six site year field trials and one greenhouse test. Traits include anthesis date (Anth), height (Ht), incidence (Inc), severity (Sev), visual rating index (VRI), Fusarium damaged kernel (FDK), deoxynivalenol (DON), greenhouse anthesis date (GAnth) and greenhouse severity (GSev1 and GSev2).

Trait	32c*17 (P1)[1]	Peregrine (P2)[2]	Mid-parent point	DH			Heritability (%)
				Mean	Min	Max	
Anth (Julian)[3]	167.51	168.89	168.20	168.38	165.20	171.17	82.92
Ht (cm)	105.15	101.33	103.24	103.08	93.40	111.53	85.32
Inc (%)	18.29	39.44	28.87	27.80	8.50	44.89	66.45
Sev (%)	20.18	32.28	26.23	25.87	11.12	46.60	67.78
VRI (%)	3.64	13.08	8.36	7.55	2.03	16.13	62.01
FDK (%)	4.17	10.60	7.39	6.29	0.67	14.19	74.60
DON (ppm[3])	6.11	15.09	10.60	8.21	1.70	17.57	72.73
GAnth (days)[4]	80.32	62.32	71.32	74.06	59.08	92.08	70.66
GSev1 (%)	22.10	58.66	40.38	33.24	12.53	74.13	80.74
GSev2 (%)	27.35	78.20	52.78	44.21	14.41	87.30	79.54

[1]32c*17 (Parent 1) was the maternal parent; [2]Peregrine (Parent 2) was the paternal parent; [3]Anthesis date in field tests were calculated based on Julian calendar; [4]ppm parts per million; [5]Greenhouse anthesis date was calculated as the time between date of transplanting into pots and the date at 30-50% anthesis stage

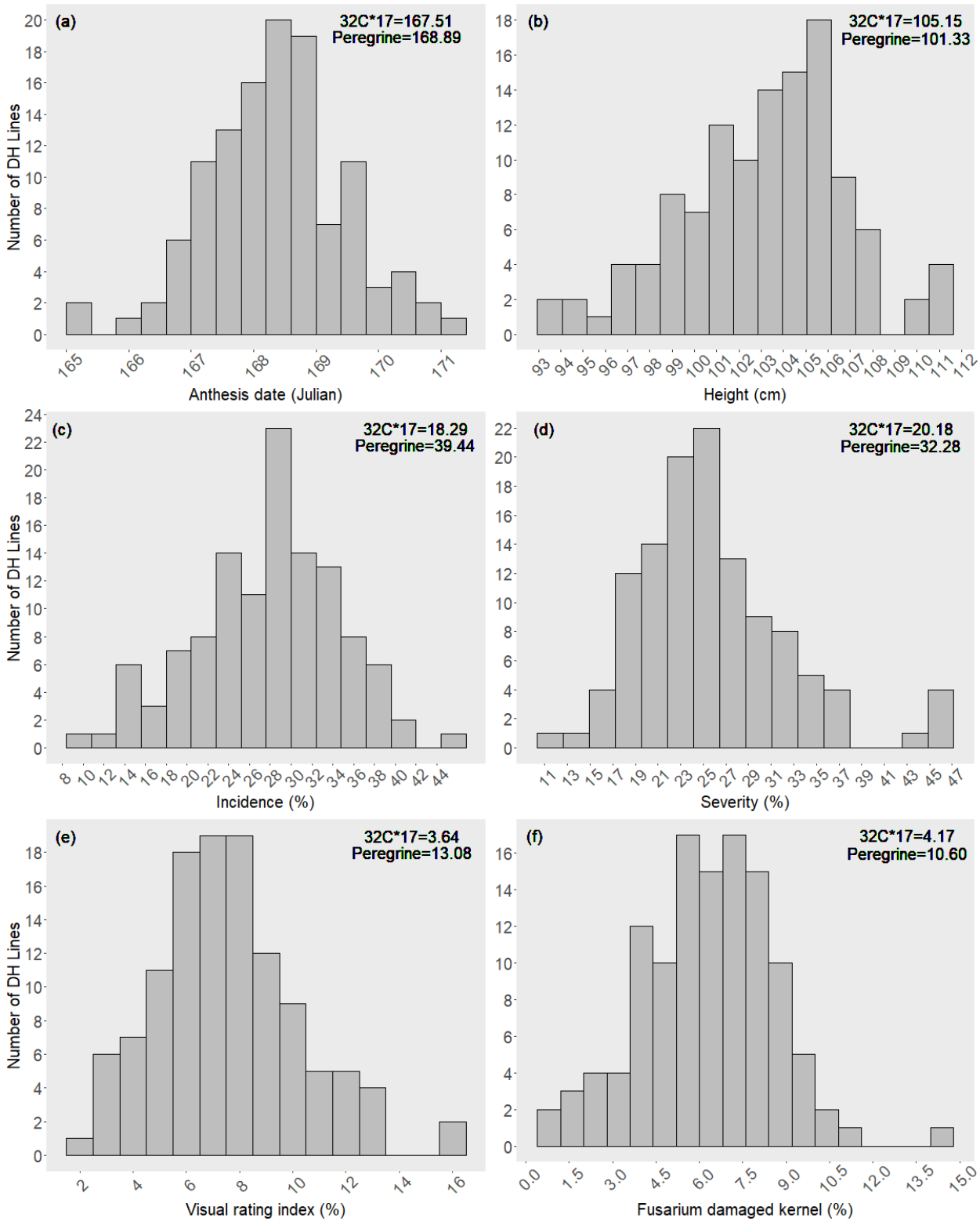
(a)
32C*17=167.51
Peregrine=168.89
Number of DH Lines
Anthesis date (Julian)
(b)
32C*17=105.15
Peregrine=101.33
Height (cm)
(c)
32C*17=18.29
Peregrine=39.44
Number of DH Lines
Incidence (%)
(d)
32C*17=20.18
Peregrine=32.28
Severity (%)
(e)
32C*17=3.64
Peregrine=13.08
Number of DH Lines
Visual rating index (%)
(f)
32C*17=4.17
Peregrine=10.60
Fusarium damaged kernel (%)

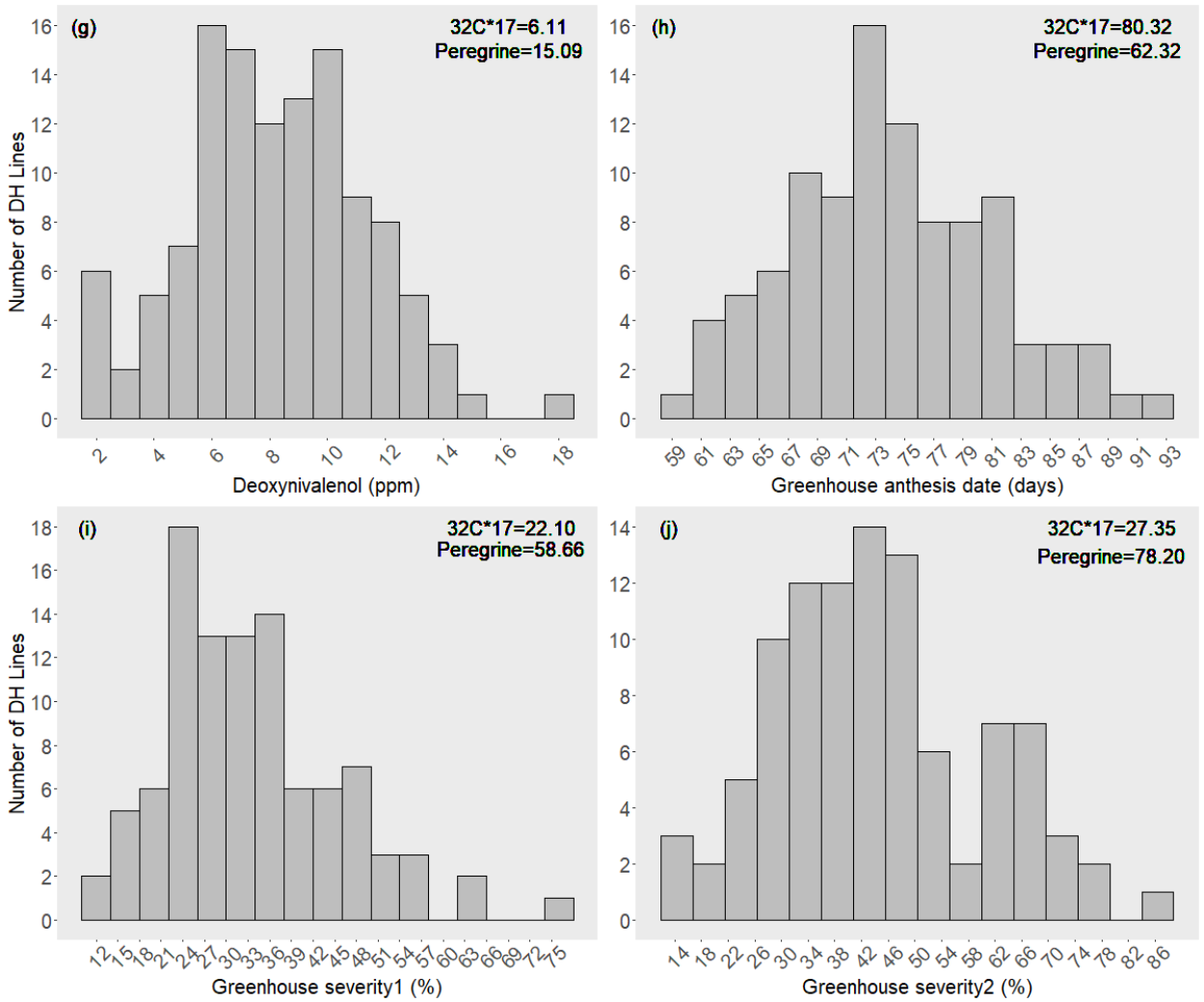

Figure 3.1 Frequency distributions of measured traits for the 3CPR doubled haploid (DH) lines based on means from six site year field trials and one year greenhouse test: anthesis date (a), height (b), incidence (c), severity (d), visual rating index (e), Fusarium damaged kernel (f), deoxynivalenol (g), greenhouse anthesis (h), greenhouse severity1 (i) and greenhouse severity2 (j). Means of parental lines for these traits were included. Anthesis date in field tests were calculated based on Julian calendar, while greenhouse anthesis date was calculated as the number of days between the date of transplanting into pots and the date at 30-50% anthesis stage.

3.4.2 Linkage mapping

The two parental lines were monomorphic for *Rht-B1*, *Rht-D1*, *Rht8* and *Fhb1*, and polymorphic for *Fhb2*, *Fhb5* and *Qfhs.ifaSA* (**Appendix 3.1**), thus markers close to the three loci were included in linkage mapping. Three 3CPR DHs were excluded from linkage mapping, due to either more

than 25% missing genotypic data, poor SNP clustering, or a low SNP call rate and one line was removed due to unusual phenotype suggesting an error in line identity. Thus, 118 3CPR DH lines were used in linkage mapping. In total, 8,103 SNP markers were used to generate thirty-four linkage groups for the 3CPR population with a total map length of 1635.63 cM (**Table 3.3**). Detailed information for each linkage group is shown in **Table 3.3**. After aligning the 8,103 SNP markers with their physical positions in the Chinese Spring reference genome (IWGSC RefSeq 2.1), the genome coverage of this map was 11.89 giga base pairs (Gbp) (International Wheat Genome Sequencing Consortium (IWGSC) 2018) (**Table 3.3**).

3.4.3 QTL mapping

Four QTL mapping methods (IM and ICIM in QTL IciMapping, and SIM and CIM in QGene) were used in this study to locate positions of QTL related to Anth, GAnth, Ht and multiple FHB resistance traits (visual FHB traits, FDK and DON content) based on each of six site years, the combined data of all site years, and one greenhouse test. Ten thousand permutations generated a LOD threshold for both IM and ICIM of 2.90, while SIM and CIM gave different LOD thresholds depending on the traits and ranged from 2.79 to 3.10. Comparing different QTL mapping methods, some QTL were detected by multiple methods and other QTL were unique to a specific mapping method (**Table 3.4**). All QTL reported in the 3CPR population were either detected by more than one mapping method, or were associated with more than one trait (**Table 3.4**). Major QTL in this study were QTL reported in more than one environment, while minor QTL were QTL reported only in a single environment.

3.4.3.1 QTL for anthesis date

Based on field and greenhouse tests, three major QTL for Anth were identified on chromosomes 2A, 4A (LG: 4A.1) and 7B (LG: 7B.2), which were named *QAnth.umb-2A*, *QAnth.umb-4A* and *QAnth.umb-7B* (**Table 3.4**). The 32c*17 allele delayed the flowering date at *QAnth.umb-2A* and shortened Anth at *QAnth.umb-4A* and *QAnth.umb-7B*. The phenotypic variation explained by *QAnth.umb-2A*, *QAnth.umb-4A* and *QAnth.umb-7B* was 9.2-14.4%, 11.7-20.3% and 8.5-20.8%, respectively, for the individual environments. *QAnth.umb-4A* explained phenotypic variation of 13.3-16.2% across combined environments. *QAnth.umb-2A* was the only QTL for Anth detected in both field and greenhouse tests, with a genetic distance of approximately 17 cM between the peaks of *QAnth.umb-2A*detected in the field and greenhouse tests using ICIM. Also, one minor QTL *QAnth.umb-1B* was discovered on chromosome 1B (LG: 1B.2) that explained a relatively large amount of phenotypic variation (27.3-32.9%) in the greenhouse environment (**Table 3.4**). Phenotypically, flowering of 32c*17 (Anth = 167.51 and GAnth = 80.32) was one day earlier in the field and eighteen days later in the greenhouse than Peregrine (Anth = 168.89 and GAnth = 62.32). However, in the DH population the additive effect of the 32c*17 allele was 0.5 in the field and 2.1 in the greenhouse (**Tables 3.2** and **3.4**).

3.4.3.2 QTL for plant height

There were two major Ht QTL (named *QHt.umb-6A* and *QHt.umb-7A*) detected on chromosomes 6A (LG: 6A.3) and 7A, which explained 12.1-17.9% and 11.6-14.5% of the phenotypic variation, respectively, across individual site years (**Table 3.4**). The phenotypic variation explained by

QHt.umb-6A was 13.5-13.8%, across combined environments. Position locations of *QHt.umb-7A* in two individual site years were approximately 24 cM away from each other. The 32c*17 allele increased Ht at both QTL. A minor QTL *QHt.umb-4A* explained 11.0% of the phenotypic variation in a single site-year and mapped within 22.0-28.0 cM of *QAnth.umb-4A* on the same linkage group 4A.1 (**Table 3.4**). The Peregrine allele increased Ht at *QHt.umb-4A* and delayed flowering at *QAnth.umb-4A*. Phenotypically, the maternal line 32c*17 (Ht = 105.15 cm) was only 3.82 cm taller than the paternal line Peregrine (Ht = 101.33 cm) (**Table 3.2**). Several markers tightly linked with three common wheat dwarf loci (*Rht-B1*, *Rht-D1* and *Rht8*) were monomorphic between the parental lines (**Appendix 3.1**).

3.4.3.3 QTL for FHB resistance

For ease of presentation, QTL for FHB resistance were categorized by trait with *QFhb* used to designate QTL related to the visual FHB parameters (Inc, Sev and VRI), while QTL for FDK and DON content were designated as *QFdk* and *QDon*, respectively (**Table 3.4**). Field severity was distinguished from GSev1 or GSev 2 under the site year column in **Table 3.4**.

3.4.3.3.1 Visual FHB traits (Inc, Sev, VRI)

Five major QTL for FHB resistance were identified across a combination of visual FHB traits on chromosomes 2A, 4A (LG: 4A.1), 5D (LG: 5D.1), 6B and 6D (**Table 3.4**). The 32c*17 allele contributed resistance based on *QFhb.umb-6B* and *QFhb.umb-6D*, while the Peregrine allele contributed resistance on *QFhb.umb-2A*, *QFhb.umb-4A* and *QFhb.umb-5D*. Among the five major

QTL, *QFhb.umb-6D* was the most frequently detected across individual site years, which explained 2.2-14.5%, 10.7% and 12.1-14.3% of the phenotypic variation for Inc, Sev and VRI, respectively. *QFhb.umb-6B* explained 11.5% of the phenotypic variation for Sev in a single environment and 11.8-13.7% of the phenotypic variance for VRI in the combined environment. Four markers linked with one Type II resistance gene *Fhb2* located on chromosome 6B were tested in this project (**Appendix 3.1**). Parental lines showed polymorphism at all four markers linked with the *Fhb2* locus (**Appendix 3.1**), where the three markers (Wmc398, Gwm644 and Wmc397) were located at 56.90 cM, 62.20 cM and 65.71 cM, respectively in the chromosome 6B linkage group and the marker Gwm133 was unlinked with the current 6B linkage group in the 3CPR population. Thus, the estimated position of *Fhb2* locus was 56.90-65.71 cM, which was 6.4-15.71 cM from *QFhb.umb-6B* (50.0-50.5 cM). *QFhb.umb-2A* explained 10.6-12.7% and 10.2% of the phenotypic variation for Inc and VRI across individual environments and was within 8.5-29.1 cM of *QAnth.umb-2A*. The Peregrine allele shortened time to anthesis and decreased Inc and VRI. *QFhb.umb-4A* explained 14.6-18.1% and 10.7% of the phenotypic variation for Inc and VRI, respectively, across individual environments. *QFhb.umb-5D* explained 11.5-12.0%, 14.9-18.7% and 19.6% of the phenotypic variation for Inc, Sev and VRI, respectively, across individual environments. Among these five major QTL, it was more common to find QTL associated with both VRI and Inc than for VRI and Sev.

Two additional major QTL specific for Inc were reported on chromosomes 2D and 4D (LG: 4D.1) that explained phenotypic variation of 2.8-13.2%, 3.4-17.8%, respectively, across individual environments (**Table 3.4**). The phenotypic variation explained by *QFhb.umb-2D* and *QFhb.umb-4D* across combined environments were approximately 12.0% and 12.4%, respectively. Two

minor QTL was discovered on chromosomes 1B (LG: 1B.2) and 7B (LG: 7B.2) in individual environments, which contributed 2.8% and 12.2%, respectively, of phenotypic variation for Inc (**Table 3.4**). *QFhb.umb-7B* overlapped with *QAnth.umb-7B* in the same region of chromosome 7B.

QFhb.umb-3A was specific for Sev on chromosome 3A (LG: 3A.2), and explained 13.8-22.1% and 10.8-12.9% of the phenotypic variation across field and greenhouse environments, respectively (**Table 3.4**). The Peregrine allele contributed to Type II resistance at this QTL. Furthermore, four minor QTL related to Sev, *QFhb.umb-1A.1*, *QFhb.umb-1A.2*, *QFhb.umb-1B.2* and *QFhb.umb-7A*, explained 17.3-22.8%, 10.8-14.0%, 12.4-15.4% and 10.6-11.0% of the phenotypic variation, respectively, across single environments (**Table 3.4**). *QFhb.umb-1A.1* and *QFhb.umb-1B.2* were detected in the greenhouse test, while *QFhb.umb-1A.2* and *QFhb.umb-7A* were expressed in field trials. The 32c*17 allele reduced Sev at all four minor QTL. The peak position of *QFhb.umb-1A.1* was approximately at 13.5 cM on the short arm of chromosome 1A, while the peak of *QFhb.umb-1A.2* was located at approximately 45.0 cM on the long arm of chromosome 1A. Since the distance between the two peaks of QTL was more than 30 cM and located at different arms of the chromosome, the two QTL are not considered to be the same QTL. *QFhb.umb-7A* was localized on the same linkage group 7A with *QHt.umb-7A* within 31.8-56.0 cM, where the 32c*17 allele increased Ht and reduced Sev. Phenotypically, the difference of Sev between 32c*17 (Sev = 20.18%) and Peregrine (Sev = 32.28%) was smaller than the difference of GSev between 32c*17 (GSev1 = 22.10% and GSev2 = 27.35%) and Peregrine (GSev1 = 58.66% and GSev2 = 78.20%). In summary of all QTL related to field and greenhouse Sev, only *QFhb.umb-3A* was detected in both field and greenhouse and received its Type II resistance from the Peregrine allele. The 32c*17 allele contributed Type II resistance for the six QTL, *QFhb.umb-*

1A.1, *QFhb.umb-1A.2*, *QFhb.umb-1B.2*, *QFhb.umb-6B*, *QFhb.umb-6D* and *QFhb.umb-7A*, which were detected only in single environments.

In addition, three markers in **Appendix 3.1** closely linked with *Qfhs.ifa-5AS* (a common Sumai 3 QTL for Type I resistance) were polymorphic between the parental lines and mapped together at position 47.58 cM on chromosome 5A.1. However, no QTL in this chromosome was detected in the 3CPR map (**Table 3.4**). Moreover, markers linked with one Type II resistance gene, *Fhb1*, were monomorphic between the parental lines (**Appendix 3.1**).

3.4.3.3.2 FDK and DON content

One major and four minor QTL for FDK were detected on chromosomes 6D, 4A (LG: 4A.1), 4D (LG: 4D.1), 6A (LG: 6A.3) and 6B, respectively and named as *QFdk.umb-6D*, *QFdk.umb-4A*, *QFdk.umb-4D*, *QFdk.umb-6A* and *QFdk.umb-6B*, respectively (**Table 3.4**). The 32c*17 allele reduced FDK at one major and three minor *QFdk*, while the Peregrine allele reduced FDK at only one QTL, *QFdk.umb-4A*. *QFdk.umb-4A*, explained 10.4-15.2% of the phenotypic variation in a single environment, but overlapped with *QFhb.umb-4A* in the same region and co-localized with *QHt.umb-4A* and *QAnth.umb-4A* within 16.5-16.7 cM and 5.3-11.5 cM, respectively, indicating that the Peregrine allele at this locus for reduced FHB visual symptoms and FDK, increased Ht and delayed Anth. *QFdk.umb-4D*, *QFdk.umb-6A* and *QFdk.umb-6D* explained 11.8-14.9%, 13.7-18.9% and 9.9-11.0%, respectively, of phenotypic variation across one or two individual environments. *QFdk.umb-6B* explained 13.0-15.4% of the phenotypic variation across combined environments and shared the same position as *QFhb.umb-6B.*

Three major QTL for DON were found on chromosomes 4D (LG: 4D.1), 6A (LG: 6A.3) and 6D, where the 32c*17 allele reduced DON content at all three *QDon*. This agreed with results in **Table 3.2** and **Appendix 3.3** that showed that 32c*17 had the lowest DON content among all checks and parental lines. *QDon.umb-6D* explained 10.1-14.1% of the phenotypic variation across four individual environments. Also, *QFhb.umb-6D* and *QFdk.umb-6D* were located at the exact region as *QDon.umb-6D*. *QDon.umb-4D* explained 12.9-19.5% and 12.6-12.7% of phenotypic variation across three individual and combined environments, respectively (**Table 3.4**). *QDon.umb-4D*, *QFdk.umb-4D* and *QFhb.umb-4D* were co-localized in the same region of chromosome 4D. *QDon.umb-6A* explained 10.8-19.1% of phenotypic variation across two individual environments and shared the same position as *QFdk.umb-6A*, where both QTL co-localized with *QHt.umb-6A* within 0.4-1.4 cM and 1.4-1.9 cM, respectively. All three *QDon* were mostly co-localized with *QFhb* related to Inc.

The QTL pyramiding effects for VRI and DON were analyzed using the two most consistent QTL on chromosomes 4D and 6D (**Appendix 4.5**). The 32c*17 allele reduced VRI and DON at both QTL. The average VRI without the two 32c*17 alleles at either QTL was 9.08 %, while the presence of a single 32c*17 allele at either QTL reduced VRI by 1.71-1.86 % relative to the presence of both major susceptible cumulative QTL allele combinations (S-4B/S-6D). The cumulative pyramiding effect of the two 32c*17 alleles at both QTL further decreased VRI by 2.46 % relative to the presence of both major susceptible cumulative QTL allele combination (S-4B/S-6D) (**Appendix 4.5**). Average DON without the two 32c*17 alleles at either QTL was 9.86 ppm (parts per million). The presence of the 32c*17 allele at the 4D QTL (7.72 ppm) reduce DON content more than the presence of the 32c*17 allele at the 6D QTL (8.50 ppm), while the

cumulative pyramiding effect of two 32c*17 alleles at both QTL (6.73 ppm) decreased DON the most (**Appendix 4.5**).

Table 3.3 Summary of linkage map for the 3CPR population including numbers of markers, genetic and physical distance, and average spacing between markers for genetic and physical map

LG[1]	SNP number	Genetic map (cM)[2]	Physical map (Mbp)[3]	Genetic map average spacing (cM)[4]	Physical map average spacing (Mbp)[5]
1A	523	52.01	530.19	0.10	1.01
2A	971	103.34	786.24	0.11	0.81
3A.1	46	25.86	25.32	0.56	0.55
3A.2	252	101.16	639.97	0.40	2.54
4A.1	412	91.49	674.44	0.22	1.64
4A.2	236	5.98	35.28	0.03	0.15
5A.1	373	78.29	549.02	0.21	1.47
5A.2	68	28.94	36.90	0.43	0.54
6A.1	72	2.54	7.90	0.04	0.11
6A.2	5	4.40	1.18	0.88	0.24
6A.3	341	5.16	506.99	0.02	1.49
6A.4	177	24.95	21.84	0.14	0.12
7A	246	102.23	661.65	0.42	2.69
A genome	**3,722**	**626.35**	**4,476.92**	**0.27**	**1.03**
1B.1	268	71.04	542.10	0.27	2.02
1B.2	46	5.94	18.83	0.13	0.41
2B	632	65.70	634.29	0.10	1.00
3B	767	145.17	839.25	0.19	1.09
4B.1	190	50.47	606.97	0.27	3.19
4B.2	30	36.00	17.23	1.20	0.57
5B	398	117.14	673.82	0.29	1.69
6B	679	65.71	557.99	0.10	0.82
7B.1	11	0.85	1.15	0.08	0.10
7B.2	562	80.72	687.85	0.14	1.22
B genome	**3,583**	**638.75**	**4,579.48**	**0.28**	**1.21**
1D	237	104.67	473.78	0.44	2.00
2D	302	45.19	564.26	0.15	1.87
3D.1	61	1.76	4.01	0.03	0.07
3D.2	10	34.71	526.59	3.47	52.66
4D.1	17	14.38	459.68	0.85	27.04
4D.2	3	24.24	9.83	8.08	3.28
5D.1	13	5.11	316.35	0.39	24.33
5D.2	4	7.75	5.44	1.94	1.36
6D	111	69.20	424.86	0.62	3.83
7D.1	37	36.62	30.13	0.99	0.81
7D.2	3	26.90	22.56	8.97	7.52
D genome	**798**	**370.53**	**2,837.49**	**2.36**	**11.34**
Total	**8,103**	**1,635.63**	**11,893.89**	**0.95**[6]	**4.42**[7]

[1]LG Linkage group; [2]cM Centimorgan; [3]Mbp Million base pairs; [4]Genetic map average spacing = linkage map length / its corresponding SNP number; [5]Physical map average spacing = Physical

map length / its corresponding SNP number; [6]Mean of all chromosomes for genetic map average spacing; [7] Mean of all chromosomes for physical map average spacing

Table 3.4 Summary of 3CPR QTL detected for all traits measured in field and greenhouse experiments using the following four methods: interval mapping (IM), inclusive composite interval mapping (ICIM), simple interval mapping (SIM) and composite interval mapping (CIM).

QTL name[1]	Site year[2]	Chr[3]	IM				ICIM				SIM				CIM			
			Pos[4]	LOD	PVE[5]	Add[6]	Pos	LOD	PVE	Add	Pos	LOD	PVE	Add	Pos	LOD	PVE	Add
Anthesis date (Anth)																		
QAnth.umb-1B	GH15	1B.2	4.4	8.9	29.8	4.1	4.3	9.0	32.4	3.9	5.0	8.6	32.9	4.0	4.0	8.4	27.3	3.2
QAnth.umb-2A	GH15	2A	23.9	3.2	11.8	2.6	23.9	3.0	9.2	2.1	24.0	3.2	13.7	2.6	24.0	3.0	10.7	1.8
QAnth.umb-2A	Wpg15	2A					41.0	5.2	14.4	0.5								
QAnth.umb-4A	Wpg15	4A.1					52.4	4.3	11.7	-0.5								
QAnth.umb-4A	Wpg16	4A.1	55.8	4.7	19.7	-0.5	54.9	4.7	19.8	-0.5	56.0	4.7	11.9	-0.5	54.0	4.3	14.9	-0.4
QAnth.umb-4A	Wpg17	4A.1	50.3	5.8	20.3	-0.6	50.3	5.8	20.3	-0.6	50.0	5.6	19.7	-0.6	50.0	5.5	18.7	-0.6
QAnth.umb-4A	Comb	4A.1	50.4	4.1	16.2	-0.4	50.6	5.1	16.2	-0.4	50.5	3.7	19.5	-0.4	50.0	3.8	13.3	-0.4
QAnth.umb-7B	Crm15	7B.2	6.0	3.7	16.0	-0.5	5.9	8.2	20.8	-0.6	6.0	3.7	13.4	-0.5				
QAnth.umb-7B	Wpg15	7B.2					11.9	3.3	8.5	-0.4								
Plant height (Ht)																		
QHt.umb-4A	Crm17	4A.1													28.0	3.1	11.0	-1.5
QHt.umb-6A	Wpg17	6A.3	1.3	3.4	12.1	1.7	2.6	4.4	13.2	1.7	2.5	3.5	12.5	1.6	2.5	5.2	17.9	1.8
QHt.umb-6A	Comb	6A.3									2.0	3.7	13.5	1.4	0.0	3.9	13.8	1.3
QHt.umb-7A	Crm16	7A	0.0	3.3	14.5	1.5	0.0	3.3	14.5	1.5	0.0	3.3	11.6	1.3	0.0	3.3	11.6	1.3
QHt.umb-7A	Wpg17	7A					24.2	3.7	10.9	1.6					24.0	4.2	14.8	1.6
Visual FHB traits (Inc, Sev, VRI)																		
QFhb.umb-1A.1	GH15(GSev1)	1A	13.7	6.2	19.3	-6.1	13.7	5.6	22.8	-5.4	13.5	5.9	20.1	-4.9	13.5	6.1	20.4	-4.6
QFhb.umb-1A.1	GH15(GSev2)	1A	13.7	5.6	17.3	-7.3	13.7	5.1	20.4	-6.3	13.5	5.4	18.4	-5.9	13.5	5.6	18.9	-5.5
QFhb.umb-1A.2	Wpg15(Sev)	1A	45.2	3.1	13.4	-2.3	45.2	3.8	14.0	-2.4	45.0	3.0	10.8	-1.9	45.0	3.7	12.9	-2.0
QFhb.umb-1B.1	Wpg15(Inc)	1B.2					5.9	3.9	2.8	3.2								
QFhb.umb-1B.2	GH15(GSev1)	1B.2	5.1	3.8	12.6	-4.9	5.0	3.2	12.4	-3.9	5.0	3.7	13.2	-4.0	5.0	3.9	13.6	-3.6
QFhb.umb-1B.2	GH15(GSev2)	1B.2	5.1	4.4	13.9	-6.5	5.0	3.8	14.9	-5.4	5.0	4.3	14.9	-5.3	5.0	4.4	15.4	-4.8
QFhb.umb-2A	Crm17(Inc)	2A					52.9	3.0	11.4	1.9	53.0	3.6	12.7	2.0	52.5	3.5	12.3	2.0
QFhb.umb-2A	Wpg17(Inc)	2A	49.6	3.0	11.2	2.1	49.5	3.6	11.0	2.1	49.5	3.0	10.6	2.0	49.5	3.3	11.6	1.9
QFhb.umb-2A	Wpg17(VRI)	2A					49.5	3.0	10.2	1.2								
QFhb.umb-2D	Wpg15(Inc)	2D					0.8	3.8	2.8	-3.2								
QFhb.umb-2D	Wpg16(Inc)	2D					0.8	3.0	13.2	-2.0	1.0	2.9	10.4	-1.6	0.5	2.9	10.3	-1.6

QFhb.umb-2D	Comb(Inc)	2D									0.0	3.4	12.0	-2.4	0.0	3.5	12.3	-2.4
QFhb.umb-3A	Crm16(Sev)	3A.2	0.9	5.4	22.1	3.3					1.0	5.2	17.8	2.7	1.5	5.0	17.1	2.4
QFhb.umb-3A	Comb(Sev)	3A.2									16.0	4.0	14.4	2.6	16.0	3.9	13.8	2.5
QFhb.umb-3A	GH15(GSev1)	3A.2	5.1	3.2	10.8	4.6					5.0	3.2	11.3	3.7				
QFhb.umb-3A	GH15(GSev2)	3A.2	5.1	3.7	12.0	6.1					5.0	3.6	12.9	5.0				
QFhb.umb-4A	Wpg17(Inc)	4A.1	31.4	4.6	17.0	2.6	30.7	5.4	17.3	2.7	31.5	4.2	14.6	2.4	30.0	5.3	18.1	2.5
QFhb.umb-4A	Wpg17(VRI)	4A.1					44.7	3.1	10.7	1.2								
QFhb.umb-4D	Crm16(Inc)	4D.1	14.3	3.3	14.4	-2.3	14.3	3.1	14.4	-2.1	14.0	3.2	11.3	-1.9	14.0	3.3	11.7	-1.8
QFhb.umb-4D	Wpg15(Inc)	4D.1	3.4	4.1	17.8	-4.6	2.6	4.7	3.4	-3.5	3.5	4.0	14.0	-3.7	3.0	4.0	14.0	-3.7
QFhb.umb-4D	Wpg16(Inc)	4D.1													2.5	2.8	10.2	-3.7
QFhb.umb-4D	Comb(Inc)	4D.1									14.0	3.4	12.4	-2.4				
QFhb.umb-5D	Crm16(Inc)	5D.1									3.0	3.2	11.5	1.9	3.5	3.4	12.0	1.8
QFhb.umb-5D	Crm16(Sev)	5D.1					0.0	4.4	18.7	2.6	3.0	4.7	16.3	2.5	0.0	4.3	14.9	2.2
QFhb.umb-5D	Crm16(VRI)	5D.1									3.0	5.8	19.6	1.0	3.0	5.8	19.6	1.0
QFhb.umb-6B	Crm15(Sev)	6B													50.5	3.2	11.5	-2.2
QFhb.umb-6B	Comb(VRI)	6B									50.0	3.2	11.8	-0.9	50.0	3.9	13.7	-0.9
QFhb.umb-6D	Crm15(Inc)	6D	3.4	3.3	14.3	-5.2	3.4	3.6	14.5	-5.1	3.5	3.2	11.2	-4.1	3.0	3.3	11.7	-4.0
QFhb.umb-6D	Wpg15(Inc)	6D					3.4	3.2	2.2	-2.9								
QFhb.umb-6D	Crm15(Sev)	6D													3.0	3.0	10.7	-2.1
QFhb.umb-6D	Wpg15(VRI)	6D					3.4	2.9	12.1	-1.7								
QFhb.umb-6D	Comb(VRI)	6D									8.0	3.4	12.6	-1.0	6.0	4.1	14.3	-1.0
QFhb.umb-7A	Wpg15(Sev)	7A					56.6	3.1	11.0	-2.2					56.0	3.0	10.6	-1.8
QFhb.umb-7B	Crm15(Inc)	7B.2					5.9	3.1	12.2	-4.6								
Fusarium damaged kernel (FDK)																		
QFdk.umb-4A	Wpg17	4A.1	44.7	3.0	13.3	0.5	44.7	11.9	15.2	1.0	44.5	2.9	10.4	0.5				
QFdk.umb-4D	Wpg16	4D.1	14.3	3.5	14.9	-0.7	14.3	3.5	14.9	-0.7	14.0	3.3	11.8	-0.6	14.0	3.3	11.8	-0.6
QFdk.umb-6A	Crm16	6A.3	4.3	4.2	18.4	-1.0	4.3	5.4	18.9	-1.1	4.5	3.9	13.7	-0.8	4.0	3.9	13.7	-0.8
QFdk.umb-6B	Comb	6B									50.0	3.6	13.0	-0.9	50.0	4.4	15.4	-2.3
QFdk.umb-6D	Crm16	6D					4.4	3.0	9.9	-0.8								
QFdk.umb-6D	Crm17	6D	6.1	3.0	11.0	-0.7	6.1	3.0	11.0	-0.7								
Deoxynivalenol content (DON)																		
QDon.umb-4D	Crm16	4D.1	14.3	3.9	14.7	-1.5	14.3	3.4	13.0	-1.3	14.0	3.7	13.1	-1.2	14.0	3.8	13.5	-1.1
QDon.umb-4D	Wpg15	4D.1	3.4	2.9	12.9	-1.2	3.3	3.0	13.8	-1.2								

QDon.umb-4D	Wpg16	4D.1	11.8	4.4	19.5	-1.1	11.8	4.4	19.5	-1.1	12.0	4.2	14.8	-0.8	14.0	4.8	16.5	-0.8
QDon.umb-4D	Comb	4D.1									14.0	3.5	12.6	-1.2	14.0	3.6	12.7	-1.2
QDon.umb-6A	Wpg16	6A.3													4.0	3.0	10.8	-0.6
QDon.umb-6A	Wpg17	6A.3	4.3	4.3	15.5	-0.7	4.3	5.0	17.0	-0.7	4.0	3.9	13.7	-0.6	3.0	5.6	19.1	-0.7
QDon.umb-6D	Crm15	6D	3.4	3.1	13.7	-3.5	3.4	3.1	13.7	-3.5	3.0	4.0	14.1	-3.2	3.0	3.0	10.8	-2.8
QDon.umb-6D	Crm16	6D	0.1	3.0	11.4	-1.4	2.2	3.4	13.1	-1.3								
QDon.umb-6D	Wpg15	6D					3.4	3.0	13.6	-1.2	3.0	3.0	10.7	-1.0				
QDon.umb-6D	Wpg17	6D					6.1	3.1	10.1	-0.5					6.0	3.4	12.1	-0.5

[1]The specific agronomic traits associated with QTL *QAnth* and *QHt* were field and greenhouse anthesis date and plant height, while the traits associated with QTL for FHB resistance *QFhb*, *QFdk* and *QDon* were incidence (Inc), field and greenhouse severity (Sev, GSev1 and GSev2), visual rating index (VRI), Fusarium damaged kernel (FDK) and deoxynivalenol (DON), which are indicated in brackets after site year; [2]Site year (Crm = Carman, Wpg = Winnipeg, GH= greenhouse, 15 = year 2015, 16 = year 2016, 17 = year 2017, Comb = the combination of six site years); [3]Chr = chromosome (the decimal designation was used when more than one linkage group was present in the same chromosome. *E.g.* 1B.2); [4]Pos = the genetic position of peak of QTL in centimorgan; [5]PVE = phenotypic variation explained (R^2 in percentage); [6]Add = additive effect of allele substitution (a positive additive effective means that 32c*17 increased the value of the trait, and vice-versa)

*LOD threshold for both IM and ICIM was 2.90, while SIM and CIM had the thresholds ranging from 2.79 to 3.10 for different traits.

3.4.4 Marker prediction of 3CPR QTL in the reciprocal population PR3C

A total 1884 SNP markers, which were in a 10 cM interval flanking the peaks of all *QFhb, QFdk* and *QDon* in the 3CPR population previously shown in **Table 3.4**, were used to conduct T-tests in the reciprocal PR3C population. Phenotypic data from the PR3C population were obtained from breeding trials conducted in the Carman winter wheat Fusarium head blight screening nursery over two years. The results for the markers within the peaks of all detected 3CPR QTL are shown in **Table 3.5**. The majority of the markers within *QFhb/QFdk/QDon.umb-6D* consistently and accurately predicted resistance to all three FHB traits (Inc, Sev and VRI) in the PR3C lines across two site years (**Table 3.5**). *QFhb.umb-4D* markers that were specific for Inc across individual and combined environments in the 3CPR population (**Table 3.4**) consistently and accurately predicted the Inc in the PR3C lines across both site years. *QFhb.umb-6B* for Sev and VRI was detected in the 3CPR population and many of the markers within the same region also accurately predicted Sev in the PR3C lines in both site years. Moreover, the majority of the markers within *QFhb.umb-2D, QFhb.umb-3A, QFdk/QDon.umb-6A* and *QFhb.umb-7B* predicted FHB resistance in the PR3C lines in a single site year. Few markers within *QFhb.umb-1A.1, QFhb.umb-1A.2, QFhb.umb-1B.1/1B.2* and *QFhb.umb-2A* predicted FHB resistance in the PR3C lines. No markers within *QFhb/QFdk.umb-4A, QFhb.umb-5D* and *QFhb.umb-7A* predicted FHB resistance in the PR3C lines.

Table 3.5 Validation of markers under peaks of 3CRP QTL in the reciprocal population PR3C for field FHB incidence (Inc), field FHB severity (Sev) and FHB visual rating index (VRI) in 2015 and 2016 by using single marker analyses (T-test) between PR3C phenotypic data and the selected markers.

3CPR population		**PR3C population**											
QTL name[1]	**No. of Mrk[2]**	**2015**						**2016**					
		Inc		**Sev**		**VRI**		**Inc**		**Sev**		**VRI**	
		Mrk[3]	**Add[4]**	**Mrk**	**Add**	**Mrk**	**Add**	**Mrk**	**Add**	**Mrk**	**Add**	**Mrk**	**Add**
QFhb.umb-1A.1	25			1	-5.5					1	-2.7		
QFhb.umb-1A.2	172	1	-4.7					35	2.3~2.6	1	2.9	1	1.4
QFhb.umb-1B.1/1B.2	34					2	4.5~4.6						
QFhb.umb-2A	412	49	4.4~4.8										
QFhb.umb-2D	43									42	-3.1~-2.5	39	-1.5~-1.3
QFhb.umb-3A	133							114	2.8~3.7	106	2.4~2.8	114	1.5~2.0
QFhb/QFdk.umb-4A	28												
QFhb/QFdk/QDon.umb-4D	13	12	-6.4~-5.1			3	-4.0~-3.8	13	-3.9~-3.1			9	-1.6~-1.3
QFhb.umb-5D	10												
QFdk/QDon.umb-6A	275							275	-3.8~-2.9	275	-3.6~-3.0	275	-2.1~-1.8
QFhb/QFdk.umb-6B	428	4	-5.3~-4.7	399	-6.0~-4.3	187	-4.7~-3.8	1	-2.5	401	-4.1~-2.4	52	-2.0~-1.3
QFhb/QFdk/QDon.umb-6D	6	5	-6.9~-6.3	5	-7.3~-6.8	5	-7.0~-6.7	5	-3.4~-3.0	4	-2.8~-2.6	5	-1.6~-1.4
QFhb.umb-7A	9												
QFhb.umb-7B	296	296	-7.1~-5.4	296	-8.4~-6.7	296	-7.8~-5.9						

[1]QTL for FHB resistance previously detected in the 3CPR population; [2]number of markers selected in a 10 cM interval flanking the QTL peaks in the 3CPR population; [3]the number of markers selected that were significant in the PR3C population in single marker analyses; [4]the range of additive effects of the significant markers in the PR3C population

3.5 Discussion

The estimated wheat genome size is around 16 Gbp (Walkowiak et al. 2020). Lengths of some common consensus maps range from 2,569 to 3,800 cM (Somers et al. 2004; Cavanagh et al. 2013; Wang et al. 2014). The 3CPR map (11.89 Gbp & 1635.63 cM) had relatively good wheat genome coverage for the QTL mapping procedure (**Table 3.3**). The parental lines had a common parent, McClintock, which reduced polymorphism between the two parents and affected the 3CPR linkage map length and size. QTL were identified for all traits measured in both field and greenhouse environments (**Table 3.4**).

Four QTL *QAnth* for anthesis data were detected on chromosomes 1B (LG: 1B.2), 2A, 4A (LG: 4A.1) and 7B (LG: 7B.2). *QAnth.umb-4A* (physical position: 629.41~640.83 Mbp (million base pairs)) was the most consistent across three individual environments and the combined environment and shared the same region with *QHt.umb-4A* (physical position: 610.95~611.26 Mbp), *QFhb.umb-4A* (physical position: 629.41 Mbp) and *QFdk.umb-4A* (physical position: 623.60 Mbp), where the Peregrine allele delayed Anth, increased Ht and reduced Inc, VRI and FDK in this region. McCartney et al. (2016) reported *QAnth.crc-4A* (physical position: 624.83~666.06 Mbp), *QFhb.crc-4A.1* (physical position: 529.91~584.12 Mbp) and *QFhb.crc-4A.2* (physical position: 618.03~724.17 Mbp) in the Kenyon/86ISMN 2137 population, where the current 3CPR *QAnth/QHt/QFhb/QFdk.umb-4A* share the same region as *QAnth.crc-4A* and *QFhb.crc-4A.2* based on the overlapping physical positions. Thambugala et al. (2020) also found *QAnth.mcb-4A.1* (physical position: 68.55~68.56 Mbp), *QAnth.mcb-4A.2* (physical position: 677.45~683.21 Mbp) and *QFhb.mcb-4A* (physical position: 37.02~68.56 Mbp) were located on

chromosome 4A in the Cutler/AC Barrie population, which the current 3CPR *QAnth/QHt/QFhb/QFdk.umb-4A* was 36.62 Mbp away from *QAnth.mcb-4A.2* in chromosome 4A. Interestingly, *QAnth.umb-1B* shared the same region with *QFhb.umb-1B.1* contributed from the Peregrine allele for decreasing Inc and *QFhb.umb-1B.2* derived from the 32c*17 allele for reducing GSev. The relationship among three QTL on the linkage group 1B.2 could be studied in the future. *QAnth.umb-7B* shared the same region with *QFhb.umb-7B*, while *QAnth.umb-2A* was co-localized with *QFhb.umb-2A* within 8.5-29.1 cM on chromosomes 2A. All four *QAnth* detected in this study were associated with FHB resistance by sharing the same region or co-localized with *QFhb*.

There were three *QHt* reported on chromosomes 4A (LG:4A.1), 6A (LG:6A.3) and 7A in the 3CPR population in only one of six site-years (**Table 3.4**). Little Ht difference (3.82 cm) between parents and monomorphism for common dwarfing loci are consistent with the findings that no major or consistent Ht QTL exist in the 3CPR population (**Table 3.2** and **Appendix 3.1**). The population mean was intermediate between the two parents, but there was transgressive segregation among the DH lines with a range of 93.40 to 111.53 cm for Ht. Despite the range in Ht, all lines would generally be considered as tall, which could explain why there were fewer and less consistent Ht QTL detected in the 3CPR population. Based on linkage positions (**Table 3.4**), *QHt.umb-6A* shared the same region with *QFdk.umb-6A* and *QDon.umb-6A*. Physical positions of *QHt.umb-7A* detected were located at 82.08 Mbp in 2016 and 673.73-676.60 Mbp in 2017, while *QFhb.umb-7A* was found at 701.92-704.33 Mbp in 2015. The linkage distance between *QHt.umb-7A* and *QFhb.umb-7A* was 31.8-56.0 cM, which would require further study to determine the relationship between two QTL.

Several *QFhb* related to visual FHB parameters (Inc, Sev and VRI) and *QFdk* and *QDon* associating with post-harvesting FHB parameters (FDK and DON content) in both field and greenhouse tests were detected in the 3CPR population, but they were not consistently shown through all site years. QTL *QFhb* specifically related to visual FHB parameters were detected on five chromosomes 1A, 2D, 3A (LG: 3A.2) and 5D (LG: 5D.1) across individual and/or the combined environments in the 3CPR population. All QTL *QFdk* and *QDon* were often co-localized with other QTL (i.e., *QAnth*, *QHt* and/or *QFhb*).

Among the five *QFhb* across a combination of visual FHB traits detected on chromosomes 2A, 4A (LG: 4A.1), 5D (LG: 5D.1), 6B and 6D, it was more common to find QTL associated with both VRI and Inc (i.e., *QFhb.umb-2A*, *QFhb.umb-4A*, *QFhb.umb-6D*) than for VRI and Sev (*QFhb.umb-6B*), implying that Inc could play a more important role in differentiating VRI among DH lines than Sev in the 3CPR population (**Table 3.4**). Since Inc for 32c*17 (Inc = 18.29%) was half of the Inc for Peregrine (Inc = 39.44%) (**Table 3.2**), it was not surprising that the 32c*17 allele reduced incidence within the most commonly detected QTL *QFhb* specific to Inc (*QFhb.umb-2D*, *QFhb.umb-4D*, *QFhb.umb-6D* and *QFhb.umb-7B*), while the Peregrine allele contributed to reduced Inc on four QTL (*QFhb.umb-1B.*1, *QFhb.umb-2A*, *QFhb.umb-4A* and *QFhb.umb-5D*). Since 32c*17 (FDK = 4.17) had less FDK than Peregrine (FDK = 10.60) (**Table 3.2**), it was consistent with the findings that the 32c*17 allele contributed the resistance of the majority of *QFdk.* Also, *QFdk* were more co-localized with *QFhb* related to Inc than *QFhb* related to Sev, suggesting that Inc had strong influence on FDK in the 3CPR population. All three QTL *QDon* were mostly co-localized with *QFhb* related to Inc, indicating that Inc had strong influence on DON content in the 3CPR population.

The *QDon* QTL on chromosomes 4D (LG: 4D.1), 6A (LG: 6A.3) and 6D were detected in more environments than most QTL for other traits measured in this study (**Table 3.4**). Also, the majority of the markers within QTL located on chromosomes 4D and 6D consistently and accurately predicted the FHB resistance in the PR3C lines across both site years.

Many previous studies found a strong association between increased Ht and FHB resistance controlled by loci on chromosome 4D, especially in the dwarfing *Rht-D1* locus, where height was increased by the *Rht-D1a* allele leading to reduced Inc (Srinivasachary et al. 2008a, 2009; Voss et al. 2008; Löffler et al. 2009; Buerstmayr et al. 2009; Buerstmayr and Buerstmayr 2016; He et al. 2016). In the current study, no Ht QTL were identified on chromosome 4D, but QTL for field FHB traits, FDK and DON (QTL peak linkage position: 2.55~14.38 cM; physical position: 50.67~485.73 Mbp) were identified on this chromosome (**Table 3.4**). To study the relationship of *QFhb/QFdk/QDon.umb-4D* and the dwarfing gene *Rht-D1*, two Kompetitive allele-specific PCR (KASP) markers for *Rht-D1* locus were tested in the two parental lines (**Appendix 3.1**); the result showed monomorphism between 32c*17 and Peregrine. The estimated physical location of the *Rht-D1* locus (19.19 Mbp) was predicted to be at least 30 Mbp away from *QFhb/QFdk/QDon.umb-4D*, indicating the FHB resistance on chromosome 4D in the 3CPR population was not directly derived from the *Rht-D1* locus. Based on parental and grandparental allele types, FHB resistance of *QFhb/QFdk/QDon.umb-4D* were derived from 32c*17, which had been inherited from Sumai 3.

Along with the current study, other studies reported QTL for FHB resistance without linking with Ht on chromosome 4D, which are different from the *Rht-D1* locus and also located within, or

overlapped with, the current 3CPR *QFhb/QFdk/QDon.umb-4D* (**Table 3.6**) (Yang et al. 2005; Ma et al. 2006b; McCartney et al. 2016; Berraies et al. 2020). These findings implied that Sumai 3 and its derivatives might carry one region associated with FHB resistance without altering Ht, which is truly different from the *Rht-D1* locus (Yang et al. 2005; Ma et al. 2006b; Berraies et al. 2020). In a proteomic study, one region of chromosome 4D (GDEEGVY02IBJ9C and F1BEJMU01CRWY4; linkage position: 52~82 cM; physical position: 62.58~466.13 Mbp) was found to accumulate high amounts of specific proteins only expressed in the resistant cultivar, Xinong 538, where this location was within the current 3CPR 4D QTL for FHB resistance (Yang et al. 2021). Therefore, there are some FHB resistance genes on chromosome 4D that are not associated with Ht and the negative agronomic impacts from increased Ht. These could be used for FHB resistance breeding in wheat. With current genetic and genomic information, the influence of *Rht-D1* gene to this 3CPR 4D.1 QTL remains unknown. Further genomic and genetic research around the 4D centromere region will help to study the relationship between this QTL and the *Rht-D1* locus.

Unlike FHB resistance in chromosome 4D, chromosome 6D had not been widely found to carry repeatable QTL for FHB resistance prior to 2009 (Liu et al. 2009; Löffler et al. 2009; Buerstmayr et al. 2009). All the previously reported 6D QTL were only estimated for disease severity (**Table 3.6**) (Gervais et al. 2003; Paillard et al. 2004; Holzapfel et al. 2008; Cai and Bai 2014; Eckard et al. 2015; Cai et al. 2019). Thus, the current study provided a new insight that *QFhb/QFdk/QDon.umb-6D* was strongly associated with Type I and DON resistance and located in the centromere region of chromosome 6D (QTL peak linkage position: 3-6.13 cM; physical position: 153.17~443.67 Mbp), which overlapped with most of the previously published

chromosome 6D QTL (**Tables 3.4** and **3.6**). No QTL for Ht were detected in that region. The relationships between previously identified 6D QTL and the current 3CPR QTL remain unknown. Heterogeneity was observed in this 6D region for both McClintock and Sumai 3 after genotyping multiple times (unpublished data), thus it remains unknown which parental line contributed which 6D QTL allele to 32c*17.

In a proteomic study, one main region of chromosome 6D (GA8KES402JPXUA and GCE8AKX01A3U59; linkage position: 61.19~104.39 cM; physical position: 69.38~443.12 Mbp) was found to accumulate high amounts of specific proteins which were only expressed in the resistant cultivar, Xinong 538 (Yang et al. 2021). This result matched with the current 3CPR 6D QTL findings. Furthermore, a leucine rich repeat receptor like kinase (LRR-RLK) gene *TaLRRK-6D* (GenBank: GU084176.1; the estimated physical position: 313.61 Mbp), which was associated with Type II resistance and salicylic signaling pathway, was also found in the same region as the 6D FHB QTL in this study (Thapa et al. 2018). The relationship between *TaLRRK-6D* and 6D QTL needs to be studied in detail in the future.

Many papers have reported 6A QTL for Type II resistance in spring, winter and durum wheat germplasm from Europe, North America and Asia (**Table 3.6**) (Anderson et al. 2001; Paillard et al. 2004; Schmolke et al. 2005; Ma et al. 2006a; Häberle et al. 2007; Srinivasachary et al. 2008a; Voss et al. 2008; Buerstmayr et al. 2012a; Liu et al. 2012; Eckard et al. 2015; Petersen et al. 2017, 2016; Malihipour et al. 2017; Sari et al. 2018; Zhao et al. 2018b; Aviles et al. 2020). In the current study, *QFdk/QDon.umb-6A* located near the centromere region of chromosome 6A (QTL peak linkage position: 3-4.5 cM; physical position: 65.94~573.15 Mbp) which overlapped with

previously reported 6A QTL (**Tables 3.4** and **3.6**). *QHt.umb-6A* was also detected in the same region (QTL peak linkage position: 1.3-2.6 cM; physical position: 63.85~457.05 Mbp). Based on parental and grandparental allele types, FHB resistance of chromosome 6A QTL was derived from 32c*17, which was inherited from Sumai 3 (unpublished data).

European winter wheat germplasm has been most frequently reported to carry QTL for FHB resistance on chromosome 6A, which has been inconsistently associated with QTL for Ht (Paillard et al. 2004; Schmolke et al. 2005; Häberle et al. 2007; Srinivasachary et al. 2008a; Voss et al. 2008). In chromosome 6A, a dwarfing gene *Rht24* (Barc103 and Wmc256; physical position: 179.05~551.93 Mbp) commonly used in Europe was physically linked with a SNP marker Excalibur_rep_c69275_346 (physical position: 501,31 Mbp) (Tian et al. 2017; Würschum et al. 2017; Herter et al. 2018). It was confirmed that this *Rht24* gene could affect Ht without influencing FHB resistance (Herter et al. 2018). In the current 3CPR population, the same SNP marker showed monomorphism in both parental lines, 32c*17 and Peregrine, as well as Sumai 3 (unpublished data), therefore, the allele type for *Rht24* in the 3CPR population is still unknown. In a proteomic study, one region of chromosome 6A (wsnp_BE490604A_Ta_2_1 and wsnp_Ex_c26147_35395059_6A; linkage position: 89.32~160.48 cM; physical position: 55.28~576.25 Mbp) was found to accumulate high amounts of specific proteins which were only expressed in the resistant cultivar, Xinong 538, which overlapped with *QFdk/QDon.umb-6A* (Yang et al. 2021). To summarize, all FHB resistance (including the current 3CPR chromosome 6A QTL) reported in chromosome 6A in germplasm from different geographical areas can be used and pyramided with the dwarfing gene *Rht24* to benefit both agronomy and FHB disease breeding in both hexaploid and tetraploid wheat.

In **Appendix 3.1**, *Qfhs.ifa-5AS* (a common Sumai 3 QTL for Type I resistance) and *Fhb2* (a common Type II resistance gene) were polymorphic between the parental lines. No detection of FHB QTL in chromosome 5A in the 3CPR map indicated that this region of *Qfhs.ifa-5AS* does not play an important role in FHB resistance in the 3CPR population (**Table 3.4**). The chromosome 6B QTL, *QFhb/QFdk.umb-6B*, detected in the current study showed that the 32c*17 allele reduced Sev and FDK (**Table 3.4**). In a previous fine mapping study on a common Type II resistance gene *Fhb2*, two markers (Wmc398 and Gwm133) were reported to be located at one side of the *Fhb2* locus and the two markers (Wmc397 and Gwm644) were located at the other side of the *Fhb2* locus (Cuthbert et al. 2007). Based on linkage positions of all three flanking markers of the *Fhb2* locus (except Gwm133), the estimated position of the *Fhb2* locus was mapped from 56.9 cM to 65.71 cM in the 3CPR 6B linkage group, which was close to 1-LOD interval of *QFhb/QFdk.umb-6B* (linkage map position: 41-51 cM). The parent 32c*17 does not carry the *Fhb2* resistance allele based on the previous haplotype study (unpublished data), but it contributed FHB resistance at *QFhb/QFdk.umb-6B*. The relationship between the *Fhb2* gene and *QFhb/QFdk.umb-6B* remains uncertain. Regardless, *QFhb.umb-6B* reduced Sev in single field environment and not in the greenhouse test, suggesting that this region was not important in the 3CPR population for FHB resistance.

The prediction efficiency of markers closely linked with 3CPR QTL *QFhb* for resistant lines in the reciprocal population (PR3C) for marker-assisted selection showed that three QTL *QFhb.umb-4D*, *QFhb.umb-6B* and *QFhb/QFdk/QDon.umb-6D* consistently and accurately predicted FHB resistance in the PR3C lines across both site years (**Table 3.5**). Therefore, markers developed from QTL based on multiple site year data ensure prediction accuracy in MAS. Markers within QTL on

chromosome 4D, 6B and 6D consistently predicted FHB resistance and might be considered as potential markers for MAS in future.

Table 3.6 A summary of QTL for FHB resistance previously reported in bi-parental QTL studies in other studies using the different FHB parameters, including incidence (Inc), greenhouse or field severity (Sev), visual rating index (VRI), Fusarium damaged kernel (FDK) and deoxynivalenol (DON) content.

Donor for resistance allele	FHB parameter	Markers within QTL[1]	Physical position[2] (Mbp[3])	Reference
4D QTL for FHB resistance				
ND3085, ND744 (Sumai 3's derivates)	Inc, Sev, VRI, FDK	Wmc48	67.62	(Berraies et al. 2020)
86ISMN 2137	Inc, Sev, VRI	Wmc720, wsnp_BE497160D_Ta_2_1	74.59~455.69	(McCartney et al. 2016)
DH181 (Sumai 3's derivate)	Inc, FDK	Wmc473, Wmc331	227.39~453.54	(Yang et al. 2005)
Sumai 3 chromosome 7A disomic substitution line	Sev	Wmc331, Cfd84	453.54~498.7	(Ma et al. 2006)
6D QTL for FHB resistance				
Overland and a backcross-derived line Wesley-*Fhb1*-BC56	Sev	wsnp_Ex_c18664_27540364, wsnp_CAP12_c720_382116	1.76~3.44	(Eckard et al. 2015)
Renan	Sev	Cfd42	23.52	(Gervais et al. 2003)
Arina	Sev	Cfd19, Cfd47	341.26~398.31	(Paillard et al. 2004)
Jagger	Sev	Barc175, Cfd76	383.68~433.17	(Cai and Bai 2014; Cai et al. 2019)
Romanus	Sev	Barc96	439.75	(Holzapfel et al. 2008)
6A QTL for FHB resistance in winter wheat				
a backcross line Wesley-*Fhb1*-BC56	Sev	Xiwa1282, Xiwa2812	26.58~500.89	(Eckard et al. 2015)
Spark	Sev	wPt-8833	33.61	(Srinivasachary et al. 2008a)
VA00W-38	FDK	wPt730772, wPt0902	124.02	(Liu et al. 2012)
Apache	Sev	Gwm82	437.46	(Holzapfel et al. 2008)
Dream	Sev	Gwm82	437.46	(Schmolke et al. 2005; Häberle et al. 2007)
NC-Neuse	Inc, Sev, FDK, DON	wsnp_Ex_c34545_42833327, wsnp_Ex_c36801_44683992	499.13~571.9	(Petersen et al. 2016, 2017)
Neuse	DON	wsnp_CAP11_c1137_6650, CAP11_c7092_120	542.2~603.1	(Aviles et al. 2020)
AC Brio	Inc, Sev	Gwm132.1, Wmc621	574.78~614.67	(Malihipour et al. 2017)

Forno	Sev	Gwm169	598.22	(Paillard et al. 2004)
6A QTL for FHB resistance in spring wheat				
Sumai 3 and its derivate ND2603	Sev	XksuH4	unknown	(Anderson et al. 2001)
a disomic substitution of chromosome 7A from Sumai 3 into Chinese Spring	Sev	Wmc256, Wmc553	551.93~577.02	(Ma et al. 2006b)
ND2710 (Sumai 3's derivates)	Sev, DON	tplb0037a05_913	610,98	(Zhao et al. 2018b)
6A QTL for FHB resistance in tetraploid wheat				
Td161 (*T. dicoccum*)	Sev	Gwm356, Gwm132	469.44~574.78	(Buerstmayr et al. 2012b)
Strongfield (*T. turgidum*)	Sev, VRI	Tdurum_contig27441_373, BobWhite_c4255_127	213.54~456.33	(Sari et al. 2018)

[1]Markers below or close to peaks QTL were obtained from the original paper; [2]Sequences of the markers were found in a public online database for *Triticeae* and *Avena* (GrainGenes: https://wheat.pw.usda.gov/GG3/) and blasted against the updated wheat reference genome of Chinese Spring (IWGSC RefSeq v2.1) to obtain their estimated physical locations;Mbp million base pairs

3.6 Conclusions

This study demonstrated that spring wheat Sumai 3 could pass on strong Type I and DON resistance to the Canadian winter wheat line 32c*17 without relying on strong Type II resistance genes (i.e. *Fhb1* and *Fhb2*). The line 32c*17 would be a valuable parent for future breeding since this line showed strong FHB and DON resistance in both field and greenhouse tests. Some DHs from the 3CPR population surpassed the resistance of parental lines due to transgressive segregation, which may be useful for future breeding. Previously discovered QTL for Type II resistance have been reported five times more frequently than either QTL for Type I or DON resistance (Liu et al. 2009), thus the three main QTL (*QFhb/QFdk/QDon.umb-4D*, *QHt/QFdk/QDon.umb-6A* and *QFhb/QFdk/QDon.umb-6D*) carrying good Type I and DON resistance might be valuable to wheat breeders to utilize without association with Ht. Since the allele type *Rht-D1a* increases FHB resistance, but also increases Ht and the risk of lodging, the current *QFhb/QFdk/QDon.umb-4D* for FHB resistance that is not associated with Ht could be a good alternative FHB resistance source. Most previously reported 6D QTL were associated with disease severity, while *QFhb/QFdk/QDon.umb-6D* mainly reduced Inc, FDK and DON, providing a new insight on FHB 6D QTL on chromosome 6D. Multiple QTL for FHB resistance in chromosome 6A have been reported. *QHt/QFdk/QDon.umb-6A* could be one of the previously published QTL. Based on the marker validation in the PR3C population, FHB resistance from chromosomes 4D and 6D was more promising than the resistance from chromosome 6A (LG: 6A.3). The desirable alleles for *QFhb/QFdk/QDon.umb-4D* and *QHt/QFdk/QDon.umb-6A* were originally inherited from Sumai 3 and the desirable alleles for *QFhb/QFdk/QDon.umb-6D* could be inherited from either Sumai 3 or McClintock. Further genetic and genomic studies on

chromosome 6D will help to understand whether Sumai 3 contributed resistance on the chromosome 6D FHB QTL. Markers below peaks of *QFhb/QFdk/QDon.umb-4D* and *QFhb/QFdk/QDon.umb-6D* can be applied in future marker-assisted breeding. The presence of the 32c*17 allele at either QTL reduced VRI and the combination of the 32c*17 allele at both QTL had cumulative effects on decreasing DON content. With the rising concern of food safety over mycotoxin in export markets, mechanisms associated with DON resistance in *QFhb/QFdk/QDon.umb-4D* and *QFhb/QFdk/QDon.umb-6D* could be further studied and characterized. Future studies related to additive effects of pyramiding the chromosome 4D and 6D QTL with other common FHB resistance QTL/genes would be useful for wheat breeders.

CHAPTER 4

CHARACTERIZATION AND VALIDATION OF FUSARIUM HEAD BLIGHT RESISTANCE QTL IN AN ELITE DOUBLED HAPLOID WINTER WHEAT CROSS 18I*45/32C*17

4.1 Abstract

In Canada, *Fusarium graminearum* is the primary causal agent of Fusarium head blight (FHB) in wheat, resulting in yield and end-use quality losses. The breeding line 32c*17 showed strong FHB resistance under severe disease pressure in both Canada and Germany. To characterize FHB resistance in 32c*17, a doubled haploid (DH) population (8I3C) was generated from the cross between a breeding line 18*45 with moderate FHB resistance and the resistant 32c*17 line. Transgressive segregation was observed for all traits measured in several field and greenhouse tests. Three main quantitative trait loci (QTL) for anthesis date and plant height that were not associated with FHB resistance were identified across multiple individual environments on chromosomes 1D, 2B and 7B. Three major QTL for FHB resistance were detected across a combination of FHB traits (especially for deoxynivalenol (DON) content) and environments on chromosomes 4B, 6D and 7A with resistance derived from 32c*17. The *Rht-B1a* allele at *QHt/QFhb/QFdk/QDon.umb-4B* consistently increased height, reduced anther retention, and was associated with Type I and DON resistance. The *QFhb/QFdk/QDon.umb-6D* was consistently detected and was mainly associated with disease incidence and DON content. In another QTL mapping study where 32c*17 was the common parental line, several FHB QTL were detected and

also derived from 32c*17. The same 6D QTL for Type I and DON resistance was also found. The repeated detection of this QTL after crossing 32c*17 with different genotypic backgrounds showed that 32c*17 is a good source of FHB resistance for winter wheat breeding.

4.2 Introduction

Wheat (*Triticum aestivum* L.) is one of the most important crops in Canadian agriculture. *Fusarium graminearum sensu stricto* Schwabe (teleomorph: *Gibberella zeae* (Schwein.) Petch) (*Fg*) infects wheat spikes, causing bleaching of the spike and producing mycotoxin deoxynivalenol (DON) in infected grains. This results in yield loss, poor grain quality and reduced grain price (Windels 2000; Bai and Shaner 2004). Major Fusarium head blight (FHB) disease outbreaks in wheat occurred in 1980 in the eastern Canada and in 1993 in western Canada (Gilbert and Tekauz 2000; Aboukhaddour et al. 2020). Fusarium head blight has become a common wheat disease in western Canada since 1990s. In a review by Aboukhaddour *et al.* (2020), it was hypothesized that the increase in FHB was associated with the switch from conventional tillage to conservation tillage in the three prairie provinces between 1990 and 2010.

Mesterházy (1995) named five types of active FHB resistance in wheat; Type I resistance reduces numbers of infected spikes, while Type II resistance decreases the number of infected spikelets within infected spikes. Type III resistance is associated with low Fusarium damaged kernels (FDK). Type IV resistance is a general overall tolerance to FHB infection. Type V resistance results in low DON content in infected grains.

To date, many quantitative trait loci (QTL) for different types of FHB resistance have been found and are distributed across all 21 chromosomes in wheat (Liu et al. 2009; Buerstmayr et al. 2009, 2019). Seven *Fhb* genes (*Fhb1-7*) have been documented from wheat and its related species (Liu et al. 2006; Cuthbert et al. 2007; Qi et al. 2008; Xue et al. 2010a, 2011; Cainong et al. 2015; Guo et al. 2015; Rawat et al. 2016). The **Table 2.2** in the previous section 2.5.1.3 showed a summary of the previously reported major QTL for disease incidence, severity and DON content on chromosomes (1B, 2A, 2B, 2D, 3A, 3B, 4B, 4D, 5A and 6B) over two decades (Buerstmayr et al. 2009, 2019). The number of major QTL for disease severity was much higher than the number of major QTL for incidence and DON content. The complexity of FHB resistance means that optimal resistance levels require multiple genes with relatively small effects, rather than only a few resistant genes with big effects. Thus, the identification of new major QTL for Type I and DON resistance to pyramid with the previously reported major QTL for Type II resistance could benefit FHB resistance breeding in wheat.

Currently, the most important FHB resistance source worldwide is the Chinese spring wheat cultivar, Sumai 3 (Gilbert and Tekauz 2000; Bai and Shaner 2004; Buerstmayr et al. 2009, 2019; Zhu et al. 2019). This cultivar has been widely included in pedigrees of many United States and Canadian spring and winter wheat cultivars to improve FHB resistance (Zhu et al. 2019). Common Sumai 3-derived FHB QTL have been frequently identified in four chromosomes (2D, 3B, 5A and 6B) (Liu et al. 2009; Löffler et al. 2009; Buerstmayr et al. 2009).

In addition to the five types of active resistance, Mesterházy (1995) reported that several morphological traits, especially plant height, were associated with FHB resistance. Several FHB

QTL mapping studies validated that height QTL were closely located with FHB QTL in some chromosomes (Gervais et al. 2003; Draeger et al. 2007; Häberle et al. 2009; Buerstmayr et al. 2011, 2012b; Lu et al. 2013). Two important semi-dwarfing genes *Rht-B1* and *Rht-D1* were originally introduced from a Japanese dwarf wheat line Norin 10 to increase grain yield by reducing height (Hedden 2003). In western Canada, the two genes have been commonly used in spring wheat varieties (Chen et al. 2016). Canadian cultivars carrying either the *Rht-B1b* or *Rht-D1b* alleles had ten percent height reduction and ten percent higher yield, but slightly reduced protein content, thousand kernel weight and test weight, and minor delays in heading and maturity (Chen et al. 2016). The wild type *Rht-B1a* or *Rht-D1a* alleles increased height and decreased disease incidence and DON contamination, showing that FHB QTL co-localized with the *Rht-B1* or *Rht-D1* loci (McCartney et al. 2007; Liu et al. 2009; Srinivasachary et al. 2009; Xue et al. 2010b; Mao et al. 2010; Yan et al. 2011; Suzuki et al. 2012; Saville et al. 2012; Buerstmayr et al. 2012b; Lu et al. 2013; Lv et al. 2014; Eckard et al. 2015; Buerstmayr and Buerstmayr 2016; He et al. 2016; Tamburic-Ilincic and Rosa 2017; Xu et al. 2020). Therefore, wheat breeders have encountered a dilemma between the use of the wild type alleles for FHB resistance and the application of the semi-dwarf alleles for yield increase and lodging resistance (Miedaner and Voss 2008; Steiner et al. 2017).

Recently, anther extrusion (AE) has been associated with FHB resistance, while anther retention (AR) was associated with FHB susceptibility (Steiner et al. 2017).The locations of QTL for AE were close to, or overlapped with, FHB and DON resistance in three wheat chromosomes (1A, 1B and 7A) (Skinnes et al. 2010). Other FHB QTL were identified to associate with height and/or AE QTL (Lu et al. 2013). For example, the *Rht-B1a* allele did not only increase height and FHB

resistance, it also increased anther extrusion (Lu et al. 2013). Through additional mapping populations, it was validated that the two semi-dwarf alleles (*Rht-B1b* or *Rht-D1b*) contributed to FHB susceptibility along with decreased plant height and increased anther retention (opposite as anther extrusion) (He et al. 2016; Xu et al. 2020). It was hypothesized that anthers trapped between the lemma and palea in wheat florets provide favorable conditions for initial mycelial growth and colonization of the florets, resulting in the strong association between anther retention and FHB susceptibility (Buerstmayr and Buerstmayr 2016).

An elite winter wheat breeding line (named 32c*17) was developed by the University of Manitoba, Canada breeding program and demonstrated strong FHB and DON resistance under severe disease pressure in both Canada and Germany. Based on a haplotyping study (unpublished data), this line does not carry any common Sumai 3 Type I and Type II FHB resistance (*Fhb1*, *Qfhs.ifa-5AS* and *Fhb2*), which indicated that this line possesses a potential breeding value for FHB resistance. In the previous chapter, three main QTL were detected across a combination of FHB traits (especially for DON content) and environments on chromosomes 4D (LG: 4D.1), 6A (LG: 6A.3) and 6D with resistance derived from 32c*17 in the 3CPR population, where QTL for height were not associated with these three regions. In the reciprocal population PR3C in Chapter 3, the majority of the markers within a 10 centimorgan (cM) interval flanking the peaks of 3CPR *QFhb/QFdk/QDon.umb-4D* and *QFhb/QFdk/QDon.umb-6D* consistently and accurately predicted FHB resistance in the PR3C lines across two site years. Since Peregrine and 32c*17 shared the common parental line McClintock, it is important to estimate FHB resistance in 32c*17 under a different genetic background. To better characterize and validate 32c*17-derived QTL for FHB resistance, another QTL mapping study was conducted. The objective of this study was to: 1)

identify QTL of FHB resistance and other agronomic traits associated with FHB resistance in a doubled haploid (DH) population derived from the cross 18i*45/32c*17 (8I3C) and 2) compare the 8I3C QTL with the 3CPR QTL to estimate how FHB resistance derived from 32c*17 would be transferred to progeny after crossing with a moderate FHB resistant line 18i*45.

4.3 Materials and Methods

4.3.1 Plant material

One DH population, named as 8I3C, consisting of 200 DH lines was generated from the cross between a breeding line 18i*45 as the maternal line and 32c*17 as the paternal line. The winter wheat breeding line, 32c*17, was generated from a cross between susceptible female parent McClintock and resistant male parent Sumai 3. The winter wheat breeding line, 18i*45, was generated from a cross between UM6233 and UM1174. All field and greenhouse tests related to the 8I3C population included DH lines, parental lines and six checks. The six check lines were Caledonia, Emerson, FHB148, Freedom, Hanover and 43I*18. Caledonia is a FHB susceptible soft white winter wheat developed and released by Cornell Agricultural Experiment Station in 1998 (Sorrells et al. 2004). Emerson is a FHB resistant hard red winter wheat developed by the Lethbridge Research and Development Centre of Agriculture and Agri-Food Canada (AAFC) in Lethbridge, AB (Graf et al. 2013). FHB148 is a FHB resistant winter wheat line developed by the Ottawa Research and Development Centre, AAFC in Ottawa, ON. Freedom is a FHB intermediate soft red winter wheat released and developed by the Ohio State University, Ohio Agricultural Research and Development Centre in 1991 (Gooding et al. 1997). Hanover is a FHB susceptible

line (pers. comm. A. Brûlé-Babel., 2015) and 43I*18 is an intermediate resistant winter wheat breeding line.

4.3.2 Inoculum preparation

Four different *F. graminearum* isolates obtained from Dr. Jeannie Gilbert at the Cereal Research Centre, AAFC in Winnipeg, Manitoba were used in this study. Two isolates were the 3-acetyl-deoxynivalenol (3ADON) chemotype: M7-07-1 and M9-07-1. Two isolates were the 15-acetyl-deoxynivalenol (15ADON) chemotype: M1-07-2 and M3-07-2. All macroconidia suspensions were prepared based on a modified protocol originally developed by Dr. Jeannie Gilbert and described in McCallum *et al.* (2004). For each isolate, a single conidium was first isolated from a previous sporodochia colony and then grown on a potato dextrose agar (PDA) plate. After mycelia colonized the whole plate (four to seven days), a portion of mycelia and the PDA agar were selected and transferred into a sterile Spezieller Nährstoffarmer agar (SNA) media plate (20 milliliter (ml) media/plate). After culturing seven days in light at room temperature, the contents of several SNA plates (eight to twelve plates) were transferred to a 1.5-liter liquid carboxymethyl cellulose (CMC) media. The CMC media flasks were aerated for seven days in light at room temperature. Macroconidia spores were then harvested from each flask by filtration through sterile cheesecloth. A haemocytometer under a 10x magnification microscope was used to determine conidia numbers in order to obtain the accurate concentration of the different macroconidia suspensions. The inoculum suspensions used in both field and greenhouse tests were a mixture of equal proportions of the four isolates. The total concentration of inoculum was 50,000

macroconidal per ml. Four ml of Tween 20 (Uniqema Americas LLC) were added to each two-liter macroconidal mixture prior to the inoculation to increase conidia adhesion.

4.3.3 Field experiments for the 8I3C population

All DH lines in the 8I3C population, parental lines and six checks were evaluated in a total six field trials conducted at two field research stations at the University of Manitoba (The Point Field Research Laboratory, Winnipeg, MB and Ian N. Morrison Research Farm, Carman, MB) from summer 2015 to 2017. Each field trial was a randomized complete block design with three replicates. Each plot was a one-meter row and rows were spaced 30 cm apart. Seventy seeds were planted in each one-meter plot. When 50 percent of spikes in the same plot were flowering (recorded as anthesis date (Anth) based on Julian calendar), approximately 50 ml of the inoculum was applied to both sides of the spikes in each plot. The same amount of inoculum was applied again to each plot two or three days after the first inoculation. A CO_2 backpack sprayer operated at 30 psi was used to spray the inoculum. An overhead misting system was run for ten minutes every hour for ten to twelve hours immediately following the inoculations to maintain high humidity for optimal disease development.

Eighteen to 21 days after the first inoculation, disease incidence (Inc) and severity (Sev) were visually estimated for each plot, when plots were at the maximum disease development stage and before disease symptoms became indistinguishable from symptoms caused by natural senescence. Incidence was the percentage of infected spikes for each plot and Sev represented the mean percentages of infected spikelets in infected spikes for each plot. Visual rating index (VRI) was

calculated by multiplying Inc and Sev and dividing by 100. When plants were fully mature, plant height (Ht), excluding awns was determined by taking the average of three height measurements for each plot. Each plot was hand cut with a sickle and threshed using a low wind speed stationary combine, which prevented the loss of shriveled kernels. Seeds from the same genotype in three replicates at each site year were pooled together before sending out to SGS Canada Inc, Mississauga, ON, Canada (former BioVision Seed Labs, Winnipeg, MB) for post-harvest analyses. Fusarium damaged kernel were identified based on typical shrunken chalk-like or pink colored appearance and were represented as a percentage by weight of a 50 g sample. For DON measurement, 10 g sub-samples take from the 50 g sample were ground into fine powder, which enabled the sample to pass through a 20-mesh sieve. Each of the 10 g samples was first dissolved into 100ml distilled water follow by filtering through a Neogen filter syringe. The filtrate from the syringe was collected for measurement using a standardized Enzyme-linked immunosorbent assay (ELISA) kit Veratox® DON 5/5 quantitative test kit (Neogen Corporation, Lansing, MI). To accurately measure DON content within the accuracy range of the kit, additional distilled water dilutions were conducted where necessary.

4.3.4 Greenhouse experiment for FHB resistance for the 8I3C population

To specifically estimate FHB Type II resistance, all 8I3C DH lines, parental lines and the six checks were tested in a greenhouse located at the University of Manitoba, Winnipeg, MB in 2016. All genotypes were first sown in root trainers (root trainer cell size: 3.5 cm x 2.5 cm x 14 cm) and grown for two to three weeks until they reached the three-leaf stage. Each root trainer consisted of seventy cells and one seed was planted per cell. All plants were then moved to a cool room set

with 16 hours light and 8 hours dark at 4 °C and vernalized for nine to ten weeks. After vernalization, plants were placed in a growth chamber set at 10-15 °C with 16 hours of light and 8 hours of dark for one week of acclimation before transplanting into 2-liter pots in a greenhouse (16 hours light with 22±6 °C and 8 hours dark with 18±2 °C).

The experimental design was a completely randomized design with five replicates. Each replicate contained one plant per genotype and was seeded within a two- to three-week interval to prevent all plants flowering together and spread out the workload. The ideal stage for inoculation was when spikes were at the 30-50% anthesis stage. Since this greenhouse test was conducted between December 2016 to April 2017, the greenhouse anthesis dates (GAnth) were calculated as the number of days from transplanting into pots after vernalization and the date of the 30-50% anthesis stage, rather than using the Julian calendar date.

The first five flowering spikes on each plant were dual floret inoculated with the same macroconidal mixture suspension as used in the field trials. Two adjacent florets with a spikelet located at the top third of each flowering spike were injected with 10ul inoculum through a pipette. After inoculation, the spike was covered with a glassine crossing bag for 48 hours to provide a high humidity micro-environment. The number of infected spikelets below the inoculated points in each inoculated spike were counted and calculated to determine greenhouse disease severity (GSev). The first disease rating (GSev1) was conducted when susceptible checks reached 80 to 95 percent GSev. The second disease rating (GSev2) was recorded three days after the first rating time. Depending on fluctuations of temperatures from early winter to early spring in the

greenhouse, most of the disease rating periods on inoculated spikes were conducted 17 days to 22 days after inoculation (dai).

4.3.5 Greenhouse experiment for anther retention for the 8I3C population

To specifically estimate AR, all 8I3C DH lines, parental lines and the six checks were tested in a greenhouse located at the University of Manitoba, Winnipeg, MB in 2019. All genotypes were planted similar to the 2016 greenhouse experiment. The experimental design was a completely randomized design with two replicates, with each replicate consisting of two pots (one plant per pot) per genotype. To be consistent with the 2016 GAnth method of measurement, the 2019 greenhouse anthesis dates (GAnth2) were calculated as the number of days from transplanting into pots after vernalization and the date of the 30-50% anthesis stage, rather than using the Julian calendar date. The first five flowering spikes on each plant were tagged to estimate anther retention. Plant height in greenhouse (GHt) was measured from the tip of each spike (excluding the length of awns) to the soil surface prior to spike collection. Collected spikes were immediately stored at -20 °C until anthers could be counted. The method for counting AR was modified from the protocol published by Buerstmayr and Buerstmayr (2016). Primary and secondary florets of four alternate spikelets located in the center of a spike were opened to count the number of anthers remaining inside the florets. In total, eight florets were examined in each spike. The proportion of greenhouse anther retention (GAR) was calculated for each spike by dividing the number of retained anthers inside the eight florets by the total number of expected anthers (24 anthers = 3 anthers per floret x 8 florets).

4.3.6 Linkage and QTL mapping in the 8I3C population

Five to seven seeds of each genotype were grown together on a wetted cotton ball in a plastic container/well. Cotton balls were maintained moisture under 16-hour light and 8-hour dark at room temperature for one week. After a week, 2 centimeters lengths from each of two healthy coleoptiles for each genotype were selected and harvested with forceps into a collection tube, immersed in liquid nitrogen, and stored at -20 °C. Later, all samples were freeze dried for two or three days. In total, freeze dried leaf samples of 200 8I3C DH lines and the two parents were sent to National Research Council Canada (NRC) at Saskatoon, Saskatchewan and genotyped by 90K wheat Illumina Infinium iSelect SNP array (Illumina, San Diego, CA) (Wang et al. 2014).

In addition, markers closely linked with three semi-dwarf genes (*Rht-B1*, *Rht-D1* and *Rht8*) and four common FHB genes/QTL (*Fhb1*, *Fhb2*, *Fhb5* and *Qfhs.ifaSA*) were tested on parental lines (**Appendix 4.1**) and those that were polymorphic on the parental lines were further screened with all 8I3C DH lines. Single nucleotide polymorphism (SNP) calling on raw data was conducted with GenomeStudio V2011.1 software (Illumina, San Diego, CA) by a technical officer, Kerry Boyle, from NRC-Saskatoon. Markers with too much missing data (>10%) or high segregation distortion were removed. A function named "Binning of Redundant Markers" with its default setting in QTL IciMapping version 4.1.0.0 (available from http://www.isbreeding.net) software was used to group different co-segregating SNP markers into different bins (Meng et al. 2015). Only one marker from each bin was selected for generating a linkage map in MapDisto v.1.7.7 (Lorieux 2012) software.

The protocol for using MapDisto to generate an accurate linkage map was obtained from McCartney *et al.* (2016). Marker distances (cM) were calculated using the Kosambi mapping function (Kosambi 1943). The default parameters for the "AutoMap" function to create linkage groups were used to set a minimum logarithm of the odds (LOD) score of 3 and a maximum recombination frequency of 0.3 (the distance between two markers must be less than 30 cM). A function called "Color Genotypes" was used to check double recombinants. After creating a linkage map in MapDisto, previously excluded co-segregating markers were added back to the map based on their corresponding bin number. Each linkage group was assigned to a wheat chromosome based on the majority of markers located in a common consensus map published by Wang *et al.* (2014). The physical positions of SNP markers were obtained by using the updated wheat reference genome of Chinese Spring (IWGSC RefSeq v2.1) (Zhu et al. 2021). To further increase the accuracy of the current linkage map, the marker order was adjusted according to the physical positions of SNP markers.

QTL mapping was conducted using QTL IciMapping version 4.1.0.0 and QGene v4.3.10 software (Joehanes and Nelson 2008; Li et al. 2008a; Meng et al. 2015). The interval mapping (IM) and inclusive composite interval mapping (ICIM) were the two methods used in QTL IciMapping. The protocol for using QTL IciMapping to conduct QTL mapping and generate an accurate linkage map was obtained from McCartney *et al.* (2016). The IM or ICIM methods were first run with the mapping parameters of 5 cM steps and 10,000 permutations to estimate the LOD threshold. Then, IM and ICIM methods were rerun with the mapping parameters of 0.1 cM steps and the previously obtained permutation values to calculate positions, LOD values and additive effects of QTL (pers. comm. C. McCartney., 2018). The single interval mapping (SIM) and the single-trait composite

interval mapping (CIM) based on maximum-likelihood estimation were the two methods used in QGene. In the CIM method, a stepwise cofactor selection was chosen with the recommended setting, which was the maximum number of five cofactors and the F to add/drop = 0.05 (pers. comm. C. McCartney., 2018). A permutation test with 10,000 iterations ($P < 0.05$) was conducted to determine a significance threshold for each trait. Physical locations of markers below peaks of 8I3C QTL and previously identified QTL were compared to study the relationship between 8I3C QTL and the previously identified QTL. Sequences of markers below peaks of QTL were found in a public online database for *Triticeae* and *Avena* (GrainGenes: https://wheat.pw.usda.gov/GG3/) and blasted against the updated wheat reference genome of Chinese Spring (IWGSC RefSeq v2.1) to obtain physical locations (Zhu et al. 2021), shown in **Table 4.5**.

4.3.7 Statistical analyses

A completely random model was used to analyze all traits measured in field trials and the greenhouse experiments. For the five traits (Anth, Ht, Inc, Sev and VRI) measured in field trials, all phenotypic data from DHs, parents and checks were first analyzed as individual site years by the PROC Mixed procedure in SAS® Studio (Enterprise Edition 3.8) (SAS Institute Inc., Cary, NC, USA) (**Appendix 4.2**). Normality and homogeneity of variance were checked before the combined analysis. Data for the five traits were combined and analyzed. The two post-harvest traits (FDK and DON), the 2016 three greenhouse traits (GAnth, GSev1 and GSev2) and the 2019 three greenhouse traits (GAnth2, GHt and GAR) measured were analyzed similarly.

Broad sense heritability (h^2) for multiple site years on each of the five traits measured in field trials was calculated by the formula ($h^2= \sigma^2_G/(\sigma^2_G + \sigma^2_{G*SY}/SY + \sigma^2_e/R*SY)$), where σ^2_G represented genetic variance, σ^2_{G*SY} was the variance of interaction between genotype and site year, σ^2_e was the residual variance, SY was the number of site years and R was the number of replicates. For FDK and DON measured on composited samples from three replicates in each site year, the formula for heritability was $h^2= \sigma^2_G/(\sigma^2_G + \sigma^2_e/SY)$. The 2016 three greenhouse traits only had five replicates and heritability was calculated as $h^2= \sigma^2_G/(\sigma^2_G + \sigma^2_e/R)$, while the 2019 three greenhouse traits only had two replicates and heritability was calculated as $h^2= \sigma^2_G/(\sigma^2_G + \sigma^2_e/R)$. The Proc Corr procedure was used to compute Pearson correlation coefficients among means of all traits of all 8I3C DHs in all site years.

4.4 Results

4.4.1 Phenotyping for the 8I3C population, parental lines and checks

Individual site year analyses (**Appendix 4.2**), showed that genotype was consistently significant for all five field traits Anth, Ht, Inc, Sev and VRI in each of the six site years. According to the distributions of residuals and the plots for normal quantiles, all five traits were approximately fitted to normal distributions and the six site years were able to be pooled together for a combined analysis. All sources of variation were significant for all traits in the combined field analyses and the greenhouse tests (**Table 4.1**). Malfunctions of the greenhouse system in Summer 2019 resulted in higher than expected temperatures and powdery mildew infections. As a result, some genotypes

were lost in this experiment and the high temperatures may have affected anthesis date, anther retention and height for some genotypes.

The two parental lines had similar anthesis dates in field tests with 32c*17 being 1.43 days earlier than 18i*45, while 18i*45 (50.43 days) had an earlier anthesis date than 32c*17 (64.38 days) in the 2016 greenhouse experiment. In the 2019 greenhouse experiment, flowering of 18i*45 (101.48 days) was severely delayed, which may have been caused by reversal of vernalization under high temperatures or inadequate vernalization prior to transplanting to the greenhouse. 32c*17 had lower anther retention than 18i*45 (**Table 4.2**). Means of field tests and the 2019 greenhouse test showed that 32c*17 was taller than 18i*45 (**Table 4.2**). The two parental lines differed in response to FHB infection in field tests where 32c*17 was more resistant to FHB than 18i*45 (**Table 4.2**).

In the 2016 greenhouse experiment, the two parental lines had similar disease severity (**Table 4.2**). Compared to the checks, 32c*17 had FHB reactions in the field that were similar to, or slightly lower than, the resistant checks (Emerson and FHB 148) and FDK, DON were lower than the checks. Greenhouse severity of 32c*17 was lower than the two resistant checks (**Table 4.2** and **Appendix 4.3**). In the 2019 greenhouse study, 32c*17 had lower anther retention than all six checks (**Table 4.2** and **Appendix 4.3**). Compared with the checks, the FHB reaction of 18i*45 was higher than the resistance checks (Emerson and FHB 148), but lower than the intermediate checks (Freedom and 43I*18) for most FHB traits measures in field and greenhouse tests (**Table 4.2** and **Appendix 4.3**). The frequency distributions of the 8I3C DH population are shown for all traits in **Figure 4.1**. There was transgressive segregation in the 8I3C doubled haploid population for all the traits (**Figure 4.1** and **Table 4.2**).

Based on the results of Pearson correlation in **Appendix 4.4**, the correlation between Anth and 2016 GAnth (r=0.66) was stronger than the correlations of 2019 GAnth2 with Anth (r=0.33) and GAnth (r=0.36). Field anthesis date in the 8I3C population also positively correlated with Ht (r=0.45), 2019 GAR (r=0.15) and most of field FHB parameters (i.e., Inc (r=0.18), Sev (r=0.31), VRI (r=0.27), DON (r=0.15)) and only negatively correlated with 2016 GSev1 (r=-0.15). Greenhouse anther retention in 2019 negatively correlated with Ht (r=-0.24) and 2019 GHt (r=-0.29) and positively correlated with all five field FHB parameters (i.e., Inc (r=0.57), Sev (r=0.34), VRI (r=0.51), FDK (r=0.54) and DON (r=0.54)). A very strong correlation (r=0.82) was found between Ht and GHt, while Ht was also positively correlated with 2016 GSev2 (r=0.17) and negatively correlated with most of the FHB parameters except Sev (i.e., Inc (r=-0.54), VRI (r=-0.37), FDK (r=-0.53) and DON (r=-0.46)) (**Appendix 4.4**). Like Ht, greenhouse height in 2019 was consistently negatively correlated with most of FHB parameters except Sev (i.e., Inc (r=-0.53), VRI (r=-0.41), FDK (r=-0.53) and DON (r=-0.43)). Field incidence positively correlated with all other FHB parameters (Sev (r=0.70), VRI (r=0.92), FDK (r=0.89) and DON (r=0.89)). Field severity was positively correlated with VRI (r=0.87), FDK (r=0.71), DON (r=0.70), GSev1 (r=0.38) and GSev2 (r=0.43), while GSev1 was positively correlated with VRI (r=0.17) and FDK (r=0.15) and GSev2 only correlated with VRI (r=0.17). There was a strong correlation between FDK and DON (r=0.92).

Table 4.1 Analysis of variance for anthesis date (Anth), height (Ht), incidence (Inc), severity (Sev), visual rating index (VRI), Fusarium damaged kernel (FDK) and deoxynivalenol (DON) for the 8I3C population based on the combination of all six site years in Manitoba, analysis of variance for greenhouse anthesis (GAnth) and greenhouse severity (GSev1 and GSev2) in 2016, and analysis of variance for greenhouse anthesis (GAnth2), greenhouse height (GHt) and greenhouse anther retention (GAR) in 2019. Replicate nested within each site year was analyzed when all site years were combined.

Source of	Anth		Ht		Inc		FSev		VRI	
Variation	DF[1]	MS[2]	DF	MS	DF	MS	DF	MS	DF	MS
Genotype (G)	207	7894.39	207	2033.82	207	2009.62	207	1216.42	207	758.90
Site year (SY)	5	8566.64	5	51648.00	5	235675.00	5	26104.00	5	26563.00
Replicate (SY)[3]	12	96.02	12	493.75	12	2571.44	12	860.85	12	506.38
G*SY	1036	3.26	1035	52.64	1035	300.15	1035	154.04	1035	93.26
Residual	2453	2.64	2440	20.14	2429	124.98	2429	95.18	2429	28.20

Source of	FDK		DON	
Variation	DF	MS	DF	MS
Genotype (G)	207	80.74	207	161.89
Site year (SY)	5	9224.38	5	10322.00
Residual	1035	12.77	1035	22.25

Source of	GAnth		GSev1		GSev2		GAnth2		GHt		GAR	
Variation	DF	MS	DF	MS	DF	MS	DF	MS	DF	MS	DF	MS
Genotype (G)	207	379.81	207	707.01	207	1181.22	191	1483.87	191	661.65	191	542.38
Replicate	4	25009.00	4	1594.83	4	7250.18	1	7402.82	1	621.84	1	942.71
Residual	813	126.53	802	168.31	812	232.07	542	192.68	426	43.48	426	75.08

[1]DF Degrees of freedom; [2]MS Mean squares; [3]Replicate nested within individual site year
*P value for all factors in this table are less than 0.0005.

Table 4.2 Broad sense heritability and descriptive statistics of parental lines and the 8I3C doubled haploid (DH) population for traits measured in combined six site year field trials and two greenhouse tests. Traits include anthesis date (Anth), height (Ht), incidence (Inc), severity (Sev), visual rating index (VRI), Fusarium damaged kernel (FDK), deoxynivalenol (DON), 2016 greenhouse anthesis date (GAnth), 2016 greenhouse severity (GSev1 and GSev2), 2019 greenhouse anthesis date (GAnth2), 2019 greenhouse height (GHt) and anther retention (GAR).

Trait	18i*45 (P1)[1]	32c*17 (P2)[2]	Mid-parent point	DH			Heritability (%)
				Mean	Min	Max	
Anth (Julian)[3]	169.96	168.53	169.25	168.89	164.78	173.44	96.38
Ht (cm)	93.22	103.87	98.55	100.34	78.19	124.40	97.36
Inc (%)	33.89	17.20	25.55	28.64	11.17	61.89	81.75
Sev (%)	24.01	20.92	22.47	21.87	9.17	47.17	82.13
VRI (%)	10.14	3.64	6.89	7.74	1.43	31.75	80.34
FDK (%)	9.57	6.74	8.16	6.71	2.06	18.64	82.13
DON (ppm[4])	12.17	6.63	9.40	9.14	2.67	27.95	84.49
GAnth (days)[5]	50.43	64.38	57.41	59.20	39.52	85.96	74.48
GSev1 (%)	33.17	35.07	34.12	36.59	18.33	72.37	80.13
GSev2 (%)	45.90	44.38	45.14	47.27	19.19	86.26	82.98
GAnth2 (days)[6]	101.48	82.25	91.87	80.50	43.85	120.40	89.11
GHt (cm)	79.13	84.00	81.57	88.84	58.27	118.04	94.28
GAR (%)	31.88	17.50	24.69	33.54	10.00	66.94	85.33

[1]18i*45 (Parent 1) was the maternal parent; [2]32c*17 (Parent 2) was the paternal parent; [3]Anthesis date in field tests were calculated based on Julian calendar; [4]ppm part per million; [5]Greenhouse anthesis date was calculated as the time between date of transplanting into pots and the date at 30-50% anthesis stage in 2016; [6]Greenhouse anthesis date was calculated as the time between date of transplanting into pots and the date at 30-50% anthesis stage in 2019;

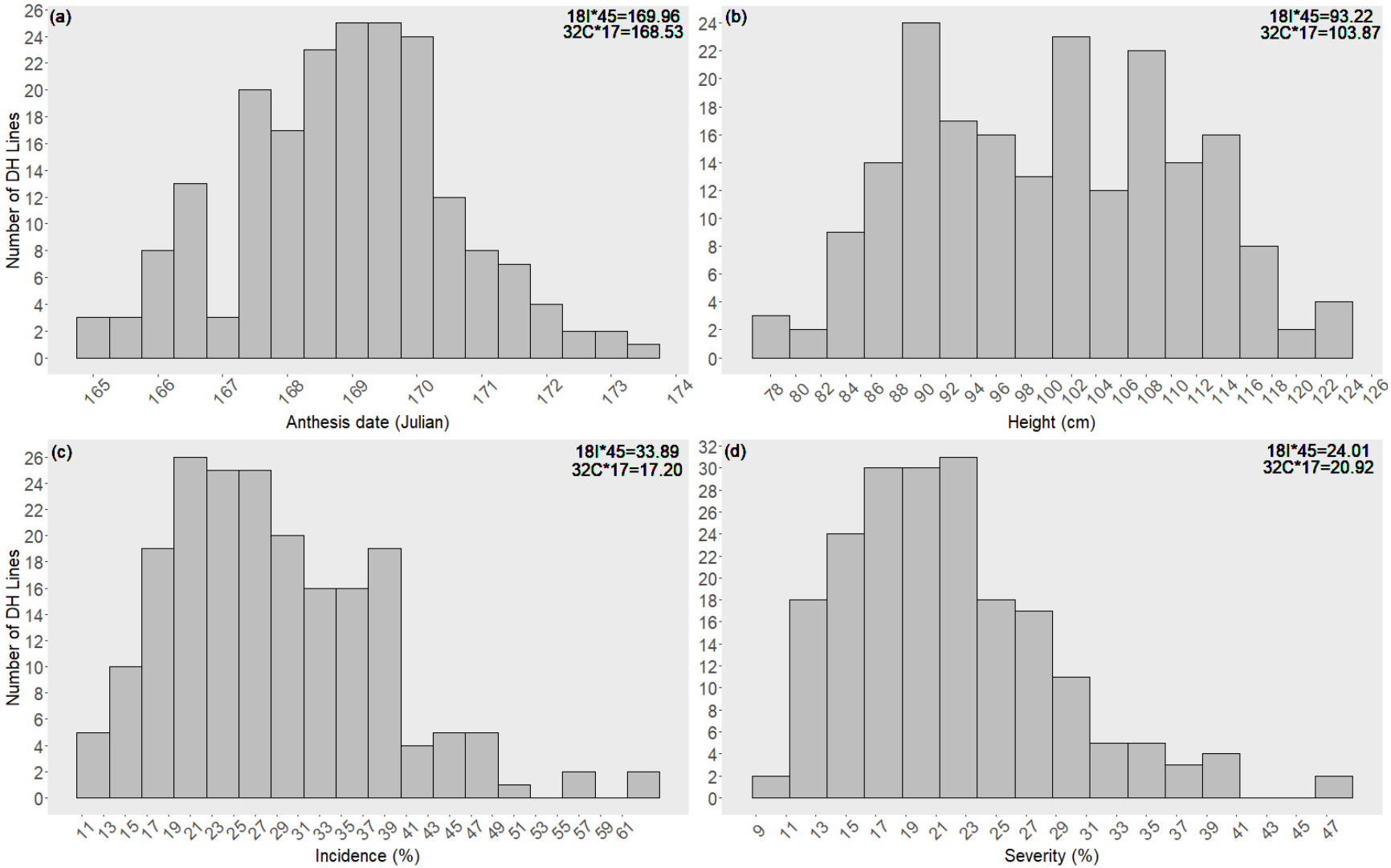
(a)
18I*45=169.96
32C*17=168.53
Number of DH Lines
Anthesis date (Julian)
(b)
18I*45=93.22
32C*17=103.87
Height (cm)
(c)
18I*45=33.89
32C*17=17.20
Number of DH Lines
Incidence (%)
(d)
18I*45=24.01
32C*17=20.92
Severity (%)

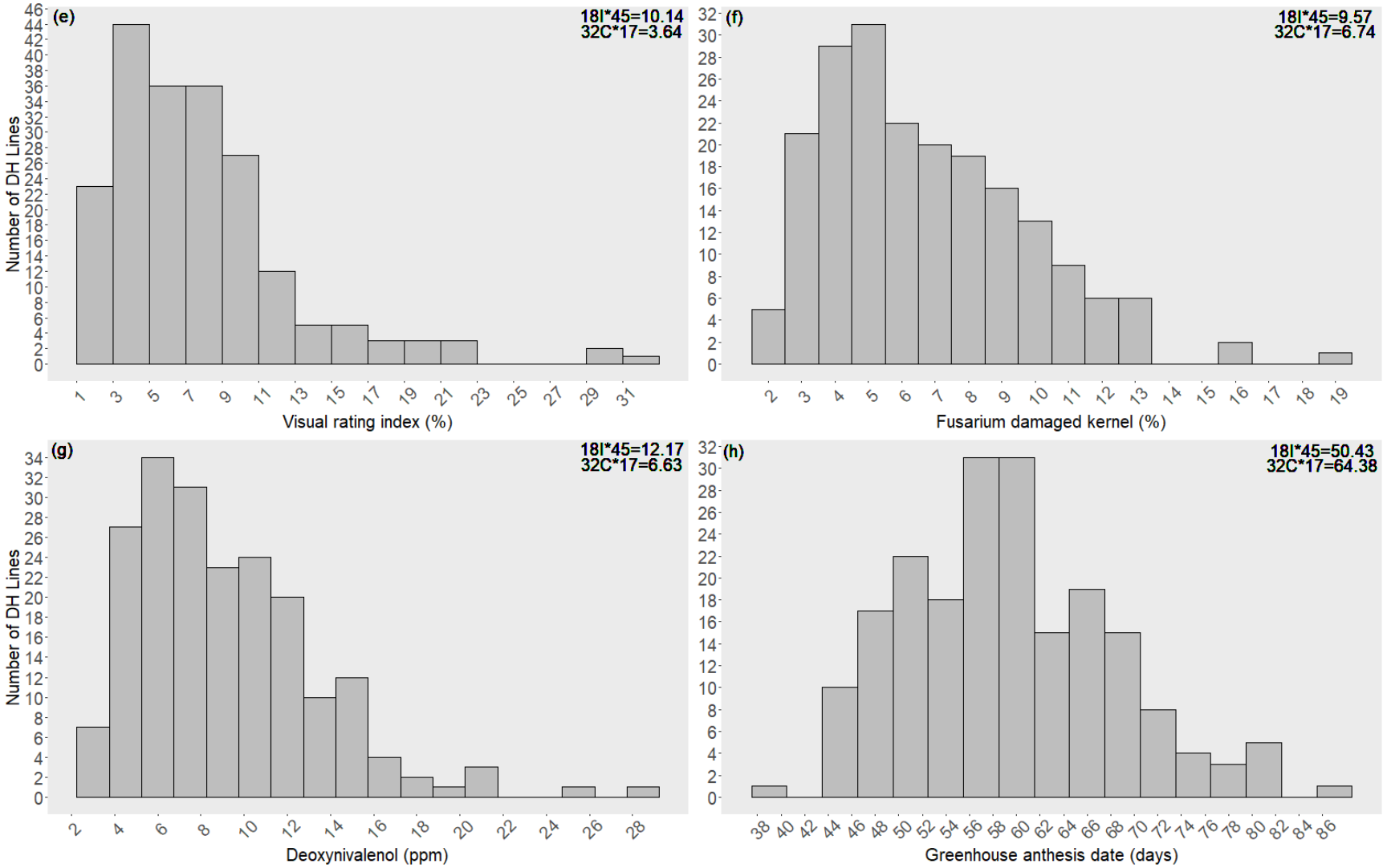
(e)
18I*45=10.14
32C*17=3.64
Number of DH Lines
Visual rating index (%)
(f)
18I*45=9.57
32C*17=6.74
Fusarium damaged kernel (%)
(g)
18I*45=12.17
32C*17=6.63
Number of DH Lines
Deoxynivalenol (ppm)
(h)
18I*45=50.43
32C*17=64.38
Greenhouse anthesis date (days)

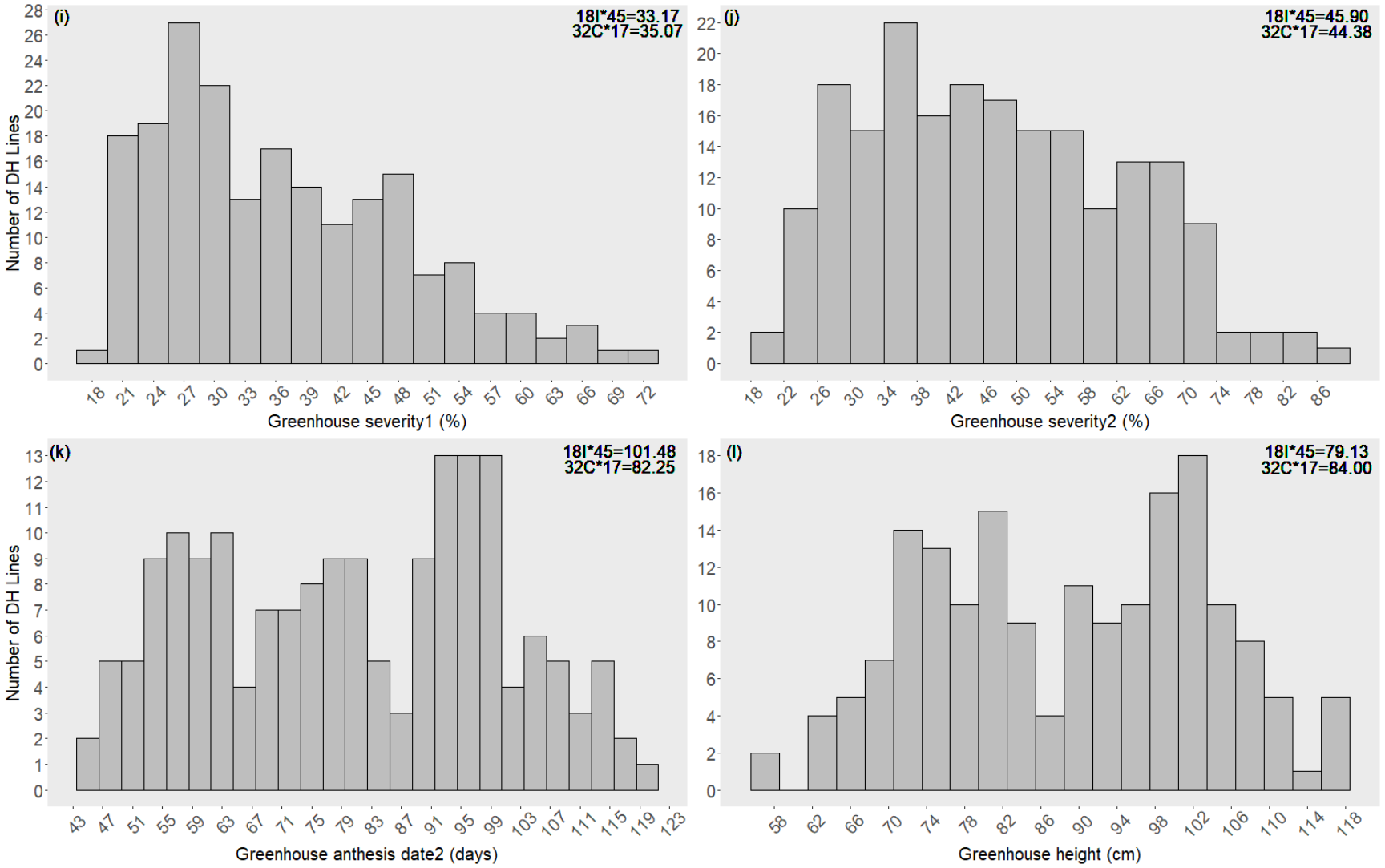
(i)
18I*45=33.17
32C*17=35.07
Number of DH Lines
Greenhouse severity1 (%)
(j)
18I*45=45.90
32C*17=44.38
Greenhouse severity2 (%)
(k)
18I*45=101.48
32C*17=82.25
Number of DH Lines
Greenhouse anthesis date2 (days)
(l)
18I*45=79.13
32C*17=84.00
Greenhouse height (cm)

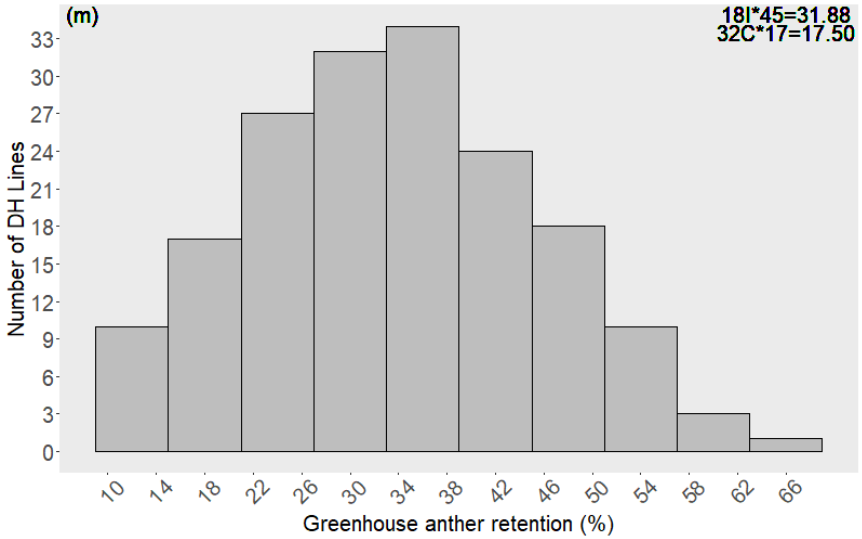

Figure 4.1 Frequency distributions of measured traits for the 8I3C doubled haploid (DH) lines based on means from six site year field trials and greenhouse tests conducted in 2016 and 219: anthesis date (a), height (b), incidence (c), severity (d), visual rating index (e), Fusarium damaged kernel (f), deoxynivalenol (g), 2016 greenhouse anthesis (h), 2016 greenhouse severity1 (i), 2016 greenhouse severity2 (j), 2019 greenhouse anthesis (k), 2019 greenhouse height (l), and 2019 greenhouse anther retention (m). Means of parental lines for these traits were included. Anthesis date in field tests were calculated based on Julian calendar, while greenhouse anthesis date in 2016 and 2019 were calculated as the number of days between the date of transplanting into pots and the date at 30-50% anthesis stage.

4.4.2 Linkage mapping

The two parental lines were monomorphic for *Rht-D1*, *Rht8* and *Fhb1*, and polymorphic for *Rht-B1*, *Fhb2*, *Fhb5* and *Qfhs.ifa-5AS* (**Appendix 4.1**), thus markers close to the four polymorphic loci were included in linkage mapping. Eight 8I3C DHs were excluded from linkage mapping, due to either more than 25% missing genotypic data, poor SNP clustering, a low SNP call rate, or too many false double recombinants. Therefore, one hundred ninety-two 8I3C DH lines were used to develop the linkage map. In total, 10,144 SNP markers were used to generate twenty-eight linkage groups for the 8I3C population with a total map length of 2434.97 cM (**Table 4.3**). Detailed information for all linkage groups is shown in **Table 4.3**. After aligning the 10,144 SNP markers with their physical positions in the Chinese Spring reference genome (IWGSC RefSeq v1.0), the genome coverage of this map was 13.34 giga base pairs (Gbp) (International Wheat Genome Sequencing Consortium (IWGSC) 2018) (**Table 4.3**).

4.4.3 QTL mapping

Four QTL mapping methods (IM and ICIM in QTL IciMapping, and SIM and CIM in QGene) were used in this study to locate positions of QTL related to anthesis date (field and greenhouse), height and multiple FHB resistance traits (visual FHB traits, FDK and DON content) based on each of six site year, the combined data of all site years, and each of the two greenhouse tests. Ten thousand permutations generated a LOD threshold for both IM and ICIM of 3.00, while SIM and CIM gave different LOD thresholds depending on the traits and ranged from 2.85 to 3.25. Comparing different QTL mapping methods, some QTL were detected by multiple methods and

other QTL were unique to a specific mapping method (**Table 4.4**). All QTL reported in the 8I3C population were either detected by more than one mapping method, or were associated with more than one trait (**Table 4.4**). In this study, a QTL was considered to be major when the QTL was reported in more than one individual environment, while minor QTL were QTL reported only in single environment.

4.4.3.1 QTL for anthesis date

Based on field and greenhouse tests, four major QTL for anthesis date were identified on chromosomes 1D, 2B, 5D (LG: 5D.3) and 7B, which were named *QAnth.umb-1D, QAnth.umb-2B, QAnth.umb-5D* and *QAnth.umb-7B*, respectively (**Table 4.4**). The 32c*17 allele delayed the flowering date at *QAnth.umb-1D, QAnth.umb-2B* and *QAnth.umb-5D* and shortened the anthesis date at *QAnth.umb-7B*. The phenotypic variation explained by *QAnth.umb-1D, QAnth.umb*-2B, QAnth.*umb-5D* and *QAnth.umb-7B* was 5.6-7.7%, 6.7-19.2%, 5.5-7.4% and 5.9-9.8%, respectively, for the individual environments and 6.0%, 8.4-16.6%, 6.2% and 5.6-9.1%, respectively, across combined environments. *QAnth.umb-2B* was the only QTL for anthesis date detected in both field and 2016 greenhouse tests. Also, two minor QTL *QAnth.umb-1B* and *QAnth.umb-5A* were discovered on chromosome 1B and 5A that explained phenotypic variation 8.2-10.1% in the 2019 greenhouse environment and 8.3-8.5% in the 2016 greenhouse environment, respectively (**Table 4.4**). The 32c*17 allele shortened the anthesis date at both minor QTL for anthesis date *QAnth*. Phenotypically, flowering of 32c*17 (Anth = 168.53 and GAnth = 64.38) was one day earlier in the field and fourteen days later in the 2016 greenhouse than 18i*45 (Anth = 169.96 and GAnth = 50.43) (**Table 4.2**). As previously mentioned, the 2019 greenhouse suffered

unexpected high indoor temperatures and extremely high humidity, which may have affected the results due to loss of 32c*17 plants and inadequate vernalization of 18i*45. In contrast, flowering of 32c*17 (GAnth2 = 82.25) was nineteen days earlier in the 2019 greenhouse than 18i*45 (GAnth2 = 101.48) (**Table 4.2**).

4.4.3.2 QTL for anther retention

There were only two minor QTL *QAR.umb-4B* and *QAR.umb-6D* detected on chromosomes 4B and 6D in the 2019 greenhouse test, which explained phenotypic variation of 7.1-8.7% and 7.8-8.8%, respectively (**Table 4.4**). The 32c*17 allele reduced anther retention at both minor QTL *QAR*, which agreed with the results that 32c*17 (GAR = 17.5%) had lower anther retention than 18i*45 (GAR = 31.88%) (**Table 4.2**).

4.4.3.3 QTL for plant height

There were five major height QTL (named *QHt.umb-1D, QHt.umb-2B, QHt.umb-4B, QHt.umb-4D* and *QHt.umb-7B*) detected on chromosomes 1D, 2B, 4B (LG: 4B.2), 4D and 7B, which explained 6.2-8.6%, 5.2-10.9%, 19.3-36.6%, 5.1-8.0% and 5.1-8.5% of the phenotypic variation, respectively, across individual site years (**Table 4.4**). The phenotypic variation explained by *QHt.umb-1D*, *QHt.umb-2B*, *QHt.umb-4B* and *QHt.umb-7B* were 6.4-7.8%, 6.5-10.0%, 28.1-33.0% and 7.7%, respectively, across combined environments. Importantly, *QHt.umb-2B* and *QHt.umb-4B* were consistently detected in all six site-years and the combined environment, and *QHt.umb-4B* was also identified in the 2019 greenhouse. The 32c*17 allele increased height at all four major

QTL *QHt*, except at *QHt.umb-7B*. 32c*17 (Ht = 103.87 cm and GHt = 84 cm) was taller than 18i*45 (Ht = 93.22 cm and GHt = 79.13 cm) in both field and 2019 greenhouse tests (**Table 4.2**)

QHt.umb-2B shared the same position as *QAnth.umb-2B*, while *QHt.umb-1D* and *QHt.umb-7B* co-localized with *QAnth.umb-1D* and *QAnth.umb-7B* which mapped within 24.5 cM and 31.5-45.4 cM, respectively, of each other on chromosomes 1D and 7B (**Table 4.4**). The 32c*17 allele increased height and delayed the flowering on chromosomes 1D and 2B and reduced height and shortened the anthesis date on chromosome 7B (**Table 4.4**). *QHt.umb-4B* co-localized with *QAR.umb-4B* within 0.0-18.6 cM on chromosome 4B, suggesting that the 32c*17 allele increased height and reduced anther retention on the chromosome 4B (**Table 4.4**). Several markers tightly linked with three common wheat dwarf loci (*Rht-B1*, *Rht-D1* and *Rht8*) were tested between the parental lines (**Appendix 4.1**), and the results indicated that the parents were polymorphic at the *Rht-B1* locus on chromosome 4B and monomorphic at *Rht8* on chromosome 2D and *Rht-D1* on chromosome 4D. After screening all 8I3C DH lines, it was confirmed that the wildtype allele *Rht-B1a* in 32c*17 was located at 12.02 cM on the linkage group 4B.2 and shared the same position as *QHt.umb-4B* (**Table 4.4**). Monomorphism for the *Rht-D1* locus indicated that *QHt.umb-4D* was not derived from the *Rht-D1* locus.

4.4.3.4 QTL for FHB resistance

For ease of presentation, QTL for FHB resistance were categorized by trait with *QFhb* used to designate QTL related to the visual FHB parameters (Inc, Sev and VRI), while QTL for FDK and DON content were designated as *QFdk* and *QDon*, respectively (**Table 4.4**). Field severity was

distinguished from greenhouse severity (GSev1 or GSev 2) under the site year column in **Table 4.4**. Moreover, an overall summary of all QTL detected in both 8I3C population and 3CPR population is listed in **Table 4.5**, which 32c*17 was the common parental line. The comparison of 32c*17-derived QTL detected in the two populations will be discussed in section 4.5.

4.4.3.4.1 Visual FHB traits (Inc, Sev, VRI)

Four major QTL for FHB resistance were identified across a combination of visual FHB traits on chromosomes 4B (LG: 4B.2), 6A, 6D (LG: 6D.1) and 7A (**Table 4.4**). The 32c*17 allele contributed resistance on all four QTL (*QFhb.umb-4B*, *QFhb.umb-6A*, *QFhb.umb-6D* and *QFhb.umb-7A*). Among the four major QTL, *QFhb.umb-4B* explained 5.0-16.3%, 6.7-8.3% and 7.0-15.8% of the phenotypic variation for Inc, Sev and VRI across individual environments and 14.8-15.6% and 10.0-11.2% of the phenotypic variance for Inc and VRI in the combined environment. This QTL was the most frequently detected QTL across all site years for Inc and shared the same position as the *Rht-B1* locus and *QAR/QHt.umb-4B. QFhb.umb-6A* explained 8.4-10.0% and 6.5% of the phenotypic variation for Inc and VRI, respectively, across individual environments, while *QFhb.umb-6D* explained 5.8-6.5% and 7.3% of the phenotypic variation for Inc and VRI, respectively, across individual environments. *QFhb.umb-6D* co-localized within 0.0-5.3 cM of *QAR.umb-6D* on chromosome 6D, and the 32c*17 allele reduced anther retention and increased FHB resistance at these QTL. Unlike the previous three QTL, *QFhb.umb-7A* was mainly related to Inc and VRI, and explained 7.0-11.9% and 8.9-9.4% of the phenotypic variation for Sev across four site years and the combined environment, respectively, while the phenotypic variations for GSev1 and GSev2 explained by *QFhb.umb-7A* were 9.9-14.7% and 10.0-14.4% in the 2016

greenhouse, respectively. This QTL also explained 7.6-8.7% of the phenotypic variance for VRI in a single site year.

One minor QTL *QFhb.umb-1A* specific for Sev explained phenotypic variation of 6.7% across the combined environment, while another minor QTL *QFhb.umb-6B* explained 6.9% and 6.2-7.0% of the phenotypic variation for GSev1 and GSev2, respectively (**Table 4.4**). The 32c*17 allele contributed resistance on both minor QTL. Four markers linked with one Type II resistance gene, *Fhb2* located on chromosome 6B, were tested in this project (**Appendix 4.1**). Parental lines showed polymorphism at all four markers linked with the *Fhb2* locus (**Appendix 4.1**), where the three markers (Wmc398, Gwm644 and Wmc397) were located at 65.57 cM, 75.16 cM and 75.68 cM, respectively in the chromosome 6B linkage group and one marker Gwm133 was unlinked with the current 6B linkage group. Thus, the estimated position of *Fhb2* locus might be from 65.57-75.68 cM, which was 3.32-25.57 cM from *QFhb.umb-6B* (40.0-79.0 cM). In addition, three markers in **Appendix 4.1** that are closely linked with *Qfhs.ifa-5AS* (a common Sumai3 QTL for Type I resistance) were polymorphic between the parental lines and mapped together at position 54.25 cM on chromosome 5A. However, no QTL in this chromosome was detected in the 8I3C map (**Table 4.4**). Moreover, markers linked with one Type II resistance gene, *Fhb1*, were monomorphic between the parental lines (**Appendix 4.1**).

Phenotypically, the difference of Inc between 32c*17 (Inc = 17.2%) and 18i*45 (Inc = 33.89%) was bigger than the difference of Sev and GSev between 32c*17 (Sev = 20.92%, GSev1 = 35.07% and GSev2 = 44.38%) and 18i*45 (Sev = 24.01%, GSev1 = 33.17% and GSev2 = 45.90%). Thus, of all QTL related to visual FHB traits, most of the major *QFhb* QTL were detected for Inc and

the 32c*17 allele contributed Type I resistance. The 32c*17 allele also contributed Type II resistance for one major and two minor QTL *QFhb*. Alleles from the moderately resistant maternal line 18i*45 did not contribute to FHB resistance for any of the visual FHB traits tested.

4.4.3.4.2 FDK and DON content

Three major and one minor QTL for FDK were detected on chromosomes 4B (LG: 4B.2), 6D (LG: 6D.1), 7A and 1B, and named as *QFdk.umb-4B, QFdk.umb-6D*, *QFdk.umb-7A* and *QFdk.umb-1B*, respectively (**Table 4.4**). The 32c*17 allele reduced FDK at all major and minor QTL. *QFdk. QFdk.umb-4B* explained 7.2-21.0% and 18.8-20.8% of the phenotypic variation in all six site years and the combined environment, respectively, which shared the same position as the *Rht-B1* locus and *QAR/QHt/QFhb.umb-4B. QFdk.umb-6D* explained 6.6-9.0% and 6.8-8.9% of the phenotypic variation in two individual environments and the combined environment, respectively, and shared the same position as *QAR/QFhb.umb-6D*. *QFdk.umb-7A* explained 6.6-7.4% and 7.0% of the phenotypic variation in a single environment and the combined environment, respectively, and co-localized with *QFhb.umb-7A* within 0.2-10.3 cM on chromosome 7A. The minor QTL *QFdk.umb-1B* explained 5.7-6.6% of the phenotypic variation in a single environment, which was 91.5-91.7 cM away from *QAnth.umb-1B*.

Two major and two minor QTL for DON were found on chromosomes 4B (LG: 4B.2), 6D (LG: 6D.1), 3A and 7A, respectively, where the 32c*17 allele reduced DON content at all major and minor *QDon. QDon.umb-4B* explained 7.4-17.1% and 14.4-16.2% of the phenotypic variation in all six site years and the combined environment, respectively, which shared the same position as

the *Rht-B1* locus and *QAR/QHt/QFhb/QFdk.umb-4B*. *QDon.umb-6D* explained 5.9-8.0% and 6.2-10.0% of the phenotypic variation in three individual environments and the combined environment, respectively, which shared the same position as *QAR/QFhb/QFdk.umb-6D*. The phenotypic variation explained by two minor QTL *QDon.umb-3A* and *QDon.umb-7A* were 6.4-7.3% and 7.0%, respectively, across single environments, where *QDon.umb-7A* shared the same position as *QFdk.umb-7A* and co-localized within 1.8-10.3 cM of *QFhb.umb-7A* on chromosome 7A. The results for FDK and DON content agreed with results in **Table 4.2** and **Appendix 4.3** that showed that 32c*17 had the lowest FDK and DON content among all checks and parental lines. The moderate resistant maternal line 18i*45 allele did not contribute resistance alleles for FDK and DON.

The QTL pyramiding effects for GAR, Ht, VRI, FDK and DON were analyzed according to major QTL on each trait (**Appendix 4.5**). For GAR, a single 32c*17 allele at either QTL (*QAR.umb-4B* or *QAR.umb-6D*) reduced GAR by 4 %, while the cumulative pyramiding effect of the two 32c*17 alleles at both QTL further decreased GAR by 13.35 % (**Appendix 4.5**). For VRI, a single 32c*17 allele at either *QFhb.umb-4B* or *QFhb.umb-6D* reduced VRI by 7.94-8.18% relative to the presence of the four major susceptible cumulative QTL allele combination (S-4B/S-6A/S-6D/S-7A), while the two 32c*17 alleles together reduced VRI the most among all two resistant QTL allele combinations. The cumulative pyramiding effect of 32c*17 alleles at four *QFhb* QTL further decreased VRI by 11.67 % relative to the presence of the four major susceptible cumulative QTL allele combination (S-4B/S-6A/S-6D/S-7A) (**Appendix 4.5**). For FDK, a single 32c*17 allele at either *QFdk.umb-4B, QFdk.umb-6D* or *QFdk.umb-7A* reduced FDK by 3.48-4.37% relative to the presence of the three major susceptible cumulative QTL allele combination (S-4B/S-6D/S-7A),

while the two 32c*17 alleles together at *QFdk.umb-4B* and *QFdk.umb-6D* reduced FDK by 5.92 % relative to the presence of the three major susceptible cumulative QTL allele combination (S-4B/S-6D/S-7A), which is similar to the pyramiding effects of 32c*17 alleles at all three *QFdk* (**Appendix 4.5**). For DON, the single 32c*17 allele at either *QDon.umb-4B* or *QDon.umb-6D* reduced DON by 2.72-3.79% compared to the presence of both major susceptible cumulative QTL allele combination (S-4B/S-6D), while the cumulative pyramiding effect of the 32c*17 alleles at both QTL further decreased DON by 5.67 % relative to the presence of both major susceptible cumulative QTL allele combination (S-4B/S-6D) (**Appendix 4.5**).

Table 4.3 Summary of linkage map for the 8I3C population including numbers of markers, genetic and physical distance, and average spacing between markers for genetic and physical map.

LG[1]	SNP number	Genetic map (cM)[2]	Physical map (Mbp)[3]	Genetic map average spacing (cM)[4]	Physical map average spacing (Mbp)[5]
1A.1	348	68.25	544.65	0.20	1.57
1A.2	83	11.00	19.14	0.13	0.23
2A	580	106.20	780.41	0.18	1.35
3A	514	174.95	739.23	0.34	1.44
4A	626	147.90	734.35	0.24	1.17
5A	663	200.05	710.82	0.30	1.07
6A	716	108.38	617.04	0.15	0.86
7A	627	196.42	743.20	0.31	1.19
A genome	**4,157**	**1,013.15**	**4,888.84**	**0.23**	**1.11**
1B	1279	104.30	700.36	0.08	0.55
2B	933	130.31	805.64	0.14	0.86
3B.1	572	107.12	787.19	0.19	1.38
3B.2	58	39.39	39.39	0.68	0.68
4B.1	5	5.23	1.12	1.05	0.22
4B.2	230	78.05	659.20	0.34	2.87
5B	726	168.00	708.93	0.23	0.98
6B	695	132.69	727.67	0.19	1.05
7B	589	158.80	762.75	0.27	1.29
B genome	**5,087**	**923.87**	**5,192.25**	**0.35**	**1.10**
1D	174	87.84	435.82	0.50	2.50
2D	300	29.92	575.39	0.10	1.92
3D.1	8	26.45	467.40	3.31	58.43
3D.2	62	1.05	7.27	0.02	0.12
4D	21	79.26	494.80	3.77	23.56
5D.1	15	11.62	289.07	0.77	19.27
5D.2	3	19.12	24.89	6.37	8.30
5D.3	63	31.33	27.91	0.50	0.44
6D.1	8	19.74	301.35	2.47	37.67
6D.2	161	12.44	16.78	0.08	0.10
7D	85	179.18	614.48	2.11	7.23
D genome	**900**	**497.95**	**3,255.16**	**1.82**	**14.50**
Total	**10,144**	**2,434.97**	**13,336.25**	**0.89[6]**	**6.37[7]**

[1]LG Linkage group; [2]cM Centimorgan; [3]Mbp Million base paris; [4]Genetic map average spacing = Linkage map length / its corresponding SNP number; [5]Physical map average spacing = Physical map length / its corresponding SNP number; [6]Mean of all chromosomes for genetic map average spacing; [7] Mean of all chromosomes for physical map average spacing

Table 4.4 Summary of 8I3C QTL detected for all traits measured in field and greenhouse experiments using the following four methods: interval mapping (IM), inclusive composite interval mapping (ICIM), simple interval mapping (SIM) and composite interval mapping (CIM).

QTL name[1]	Site year[2]	Chr[3]	IM				ICIM				SIM				CIM			
			Pos[4]	LOD	PVE[5]	Add[6]	Pos	LOD	PVE	Add	Pos	LOD	PVE	Add	Pos	LOD	PVE	Add
Anthesis date (Anth)																		
QAnth.umb-1B	GH19	1B	0.0	3.5	10.1	-5.8					0.0	3.7	9.2	-6.0	0.0	3.7	8.2	-5.3
QAnth.umb-1D	Comb	1D					59.6	3.7	6.0	0.4								
QAnth.umb-1D	Crm15	1D					59.6	4.1	6.6	0.5								
QAnth.umb-1D	Crm16	1D					59.6	3.6	5.6	0.4					59.5	3.5	7.7	0.4
QAnth.umb-2B	Comb	2B	49.3	6.4	8.4	0.6	49.3	9.2	15.9	0.7	49.0	6.5	13.9	0.6	49.0	7.9	16.6	0.7
QAnth.umb-2B	Crm15	2B	51.4	5.8	8.5	0.7	49.3	6.6	11.1	0.6	51.0	6.0	13.0	0.7	49.5	8.2	17.2	0.8
QAnth.umb-2B	Crm16	2B	49.3	5.7	12.6	0.6	49.3	8.2	13.4	0.7	49.0	5.6	12.0	0.6	49.0	7.6	16.0	0.6
QAnth.umb-2B	Crm17	2B	49.3	3.5	7.7	0.7	49.3	3.9	7.7	0.7	49.0	3.4	7.5	0.7	49.0	3.6	8.0	0.7
QAnth.umb-2B	Wpg15	2B	53.7	4.3	7.2	0.6	54.1	4.3	10.2	0.6	53.5	4.7	10.2	0.6	54.0	4.5	9.8	0.6
QAnth.umb-2B	Wpg16	2B	49.3	7.1	11.2	0.7	49.3	7.8	15.2	0.7	49.0	7.2	15.2	0.8	49.0	8.0	16.8	0.8
QAnth.umb-2B	Wpg17	2B	49.3	4.0	6.7	0.6	49.3	4.6	9.0	0.6	49.0	4.1	8.9	0.6	49.0	4.8	10.4	0.6
QAnth.umb-2B	GH16	2B	54.0	8.6	15.2	3.8	54.6	10.4	19.2	3.7	55.0	8.4	17.6	3.8	54.0	8.7	18.1	3.9
QAnth.umb-5A	GH16	5A									197.0	3.8	8.3	-2.6	198.0	3.9	8.5	-2.4
QAnth.umb-5D	Comb	5D.3					31.3	3.8	6.2	0.4								
QAnth.umb-5D	Crm15	5D.3					31.3	3.9	6.3	0.5								
QAnth.umb-5D	Crm16	5D.3					31.3	3.6	5.5	0.4					31.0	3.3	7.4	0.4
QAnth.umb-7B	Comb	7B	56.4	4.1	5.6	-0.5	56.3	3.6	5.9	-0.4	52.5	4.2	9.1	-0.5				
QAnth.umb-7B	Crm15	7B	53.2	4.4	6.4	-0.6	53.2	4.5	7.3	-0.5	52.5	4.5	9.8	-0.6	49.0	3.3	7.3	-0.5
QAnth.umb-7B	Wpg15	7B	56.4	3.6	5.9	-0.5	56.3	3.7	8.6	-0.5	56.5	3.5	7.8	-0.5	56.0	3.2	7.2	-0.5
QAnth.umb-7B	Wpg17	7B	53.5	3.6	6.1	-0.6					53.5	3.9	8.6	-0.6				
Anther retention (AR)																		
QAR.umb-4B	GH19	4B.2	12.9	3.0	8.7	-3.3									32.0	3.2	7.1	-2.9
QAR.umb-6D	GH19	6D.1	19.7	3.1	8.8	-3.2	19.7	4.4	7.8	-3.7								
Plant height (Ht)																		
QHt.umb-1D	Comb	1D	35.0	3.3	6.4	2.9					35.0	3.5	7.8	3.0				
QHt.umb-1D	Crm17	1D	35.0	3.7	6.2	2.8					35.0	3.9	8.6	2.9				
QHt.umb-1D	Wpg16	1D	35.0	3.4	6.4	2.7					35.0	3.6	8.0	2.8				

QHt.umb-1D	Wpg17	1D	35.0	3.3	6.4	3.0					35.0	3.5	7.8	3.1				
QHt.umb-2B	Comb	2B					54.6	4.2	6.5	2.6	57.5	4.5	9.9	3.5	54.5	4.6	10.0	2.8
QHt.umb-2B	Crm15	2B					54.6	4.3	6.2	3.4	57.5	4.6	9.9	4.7	54.5	4.8	10.4	3.7
QHt.umb-2B	Crm16	2B					49.3	4.1	7.1	2.1	49.0	3.4	7.6	2.3				
QHt.umb-2B	Crm17	2B	56.3	4.7	8.1	3.2	54.6	4.3	7.9	2.5	57.5	5.0	10.8	3.4	54.5	4.7	10.2	2.7
QHt.umb-2B	Wpg15	2B					54.6	3.7	5.2	3.1	57.0	3.9	8.6	4.3	54.5	4.0	8.7	3.3
QHt.umb-2B	Wpg16	2B									66.0	3.1	6.9	2.6				
QHt.umb-2B	Wpg17	2B					54.6	5.3	8.5	3.0	57.5	4.9	10.8	3.7	54.5	5.0	10.9	3.0
QHt.umb-4B	Comb	4B.2	12.0	16.8	28.1	6.0	12.0	17.7	32.0	5.8	12.0	16.1	30.9	6.0	12.0	17.4	33.0	5.8
QHt.umb-4B	Crm15	4B.2	12.0	18.9	35.4	8.4	12.0	20.0	35.1	8.1	12.0	18.2	34.2	8.4	12.0	19.8	36.6	8.1
QHt.umb-4B	Crm16	4B.2	12.0	10.9	22.4	3.8	12.0	10.4	19.3	3.4	12.0	10.3	21.2	3.8	12.0	9.9	20.4	3.6
QHt.umb-4B	Crm17	4B.2	13.1	13.4	20.4	5.0	12.5	12.8	25.9	4.5	13.0	12.9	25.6	5.0	12.5	12.9	25.7	4.7
QHt.umb-4B	Wpg15	4B.2	12.0	18.8	35.2	8.3	12.0	19.7	33.8	7.9	12.0	18.0	33.9	8.2	12.0	19.3	35.9	7.9
QHt.umb-4B	Wpg16	4B.2	12.0	14.6	24.7	5.1	12.0	15.5	29.0	4.9	12.0	13.7	27.0	5.0	12.0	14.5	28.4	5.0
QHt.umb-4B	Wpg17	4B.2	12.0	12.4	22.0	5.4	12.0	13.4	23.7	5.0	12.0	11.8	23.8	5.4	12.0	13.4	26.5	5.1
QHt.umb-4B	GH19	4B.2	13.4	14.7	31.1	8.5					13.0	13.8	30.3	8.3	12.0	12.9	25.8	7.0
QHt.umb-4D	Crm16	4D					1.0	3.4	5.8	1.9								
QHt.umb-4D	Wpg16	4D					7.8	3.2	5.1	2.1					7.5	3.6	8.0	2.4
QHt.umb-7B	Comb	7B													14.0	3.5	7.7	-2.6
QHt.umb-7B	Crm15	7B													14.0	3.7	8.1	-3.5
QHt.umb-7B	Wpg15	7B					11.1	3.2	5.4	-3.2					12.0	3.9	8.5	-3.6
QHt.umb-7B	Wpg17	7B					16.7	3.0	5.1	-2.3					17.5	3.6	7.9	-2.6
Visual FHB traits (Inc, Sev, VRI)																		
QFhb.umb-1A	Comb(Sev)	1A.1	52.0	3.1	6.7	-1.9	51.9	3.5	6.7	-1.8								
QFhb.umb-4B	Comb(Inc)	4B.2	12.0	7.3	15.6	-3.8	12.0	7.4	15.6	-3.7	12.0	6.9	14.8	-3.8	12.0	6.9	14.8	-3.8
QFhb.umb-4B	Crm15(Inc)	4B.2	6.9	4.7	10.2	-6.8	5.7	4.6	10.2	-6.6	3.0	4.8	10.5	-6.9	3.0	4.8	10.5	-6.9
QFhb.umb-4B	Crm16(Inc)	4B.2	12.0	3.4	7.9	-1.8	12.1	4.1	7.8	-1.7	12.0	3.2	7.2	-1.8	12.0	3.2	7.2	-1.7
QFhb.umb-4B	Crm17(Inc)	4B.2	12.1	3.5	7.8	-2.1	12.1	3.5	7.8	-2.1	12.0	3.3	7.2	-2.1	12.5	3.1	6.8	-2.0
QFhb.umb-4B	Wpg15(Inc)	4B.2	12.0	7.7	16.3	-7.4	12.0	7.8	16.3	-7.3	12.0	7.2	15.2	-7.2	12.0	7.2	15.2	-7.2
QFhb.umb-4B	Wpg16(Inc)	4B.2	12.6	3.4	5.0	-3.0					12.0	3.5	7.7	-3.1	12.5	3.5	7.8	-3.1
QFhb.umb-4B	Wpg17(Inc)	4B.2	12.0	4.0	5.9	-2.6					12.0	3.6	8.1	-2.5	12.0	4.3	9.5	-2.6
QFhb.umb-4B	Wpg15(Sev)	4B.2	12.0	3.3	7.7	-2.4	12.0	3.6	8.3	-2.3	12.0	3.0	6.7	-2.3	12.0	3.3	7.3	-2.4
QFhb.umb-4B	Comb(VRI)	4B.2	12.0	4.9	11.2	-1.7	12.0	5.0	11.2	-1.6	12.0	4.6	10.0	-1.6	12.0	5.0	10.9	-1.7

QFhb.umb-4B	Crm15(VRI)	4B.2					5.7	3.5	9.5	-3.7	3.0	3.4	7.5	-3.8	1.5	4.4	9.6	12.5
QFhb.umb-4B	Wpg15(VRI)	4B.2	12.0	6.7	15.8	-3.4	12.0	6.9	15.8	-3.2	12.0	6.2	13.4	-3.3	12.0	6.2	13.4	-3.3
QFhb.umb-4B	Wpg17(VRI)	4B.2					12.0	3.2	7.0	-1.2								
QFhb.umb-6A	Crm16(Inc)	6A	41.2	4.4	10.0	-2.0	41.2	4.4	8.4	-1.8	41.0	4.4	9.7	-2.0	41.0	4.4	9.7	-2.0
QFhb.umb-6A	Wpg17(Inc)	6A									41.0	4.3	9.4	-2.8	41.0	4.1	9.0	-2.5
QFhb.umb-6A	Crm16(VRI)	6A									41.0	2.9	6.5	-0.5				
QFhb.umb-6B	GH16(GSev1)	6B									40.0	3.1	6.9	-3.2				
QFhb.umb-6B	GH16(GSev2)	6B									79.0	3.1	7.0	-4.1	79.0	3.1	7.0	-4.1
QFhb.umb-6D	Crm16(Inc)	6D.1					14.4	3.1	5.8	-1.5								
QFhb.umb-6D	Wpg17(Inc)	6D.1					19.7	3.5	6.4	-2.2					19.5	2.9	6.5	-2.1
QFhb.umb-6D	Wpg17(VRI)	6D.1					17.9	3.2	7.3	-1.2								
QFhb.umb-7A	Comb(Sev)	7A	100.4	4.5	9.4	-2.2	100.4	4.9	9.4	-2.1	100.5	4.2	9.1	-2.2	100.0	4.1	8.9	-2.2
QFhb.umb-7A	Crm16(Sev)	7A	100.4	4.9	10.8	-1.9	100.4	4.9	10.8	-1.9	100.5	5.1	11.0	-2.0	100.0	4.9	10.8	-2.0
QFhb.umb-7A	Wpg15(Sev)	7A	96.2	3.1	7.3	-2.3									96.0	3.2	7.1	-2.3
QFhb.umb-7A	Wpg16(Sev)	7A									104.5	3.1	7.0	-1.9				
QFhb.umb-7A	Wpg17(Sev)	7A	99.9	4.8	10.4	-4.2	99.8	6.1	11.9	-4.5	102.0	4.3	9.4	-4.2	99.5	4.9	10.6	-4.3
QFhb.umb-7A	GH16(GSev1)	7A	100.4	6.5	9.9	-4.4	100.4	5.9	14.3	-4.1	101.0	6.9	14.7	-4.7	100.0	6.5	14.0	-4.5
QFhb.umb-7A	GH16(GSev2)	7A	100.5	6.2	10.0	-5.6	100.4	5.6	13.8	-5.1	101.0	6.8	14.4	-6.0	100.0	6.5	13.9	-5.8
QFhb.umb-7A	Crm16(VRI)	7A					100.4	4.2	8.7	-0.6	100.5	3.5	7.8	-0.6	100.0	3.4	7.6	-0.6
Fusarium damaged kernel (FDK)																		
QFdk.umb-1B	Wpg16	1B					91.7	3.0	5.7	-0.6					91.5	3.0	6.6	-0.6
QFdk.umb-4B	Comb	4B.2	12.0	9.8	19.6	-1.4	12.0	11.8	20.5	-1.4	12.0	9.0	18.8	-1.3	12.0	10.1	20.8	-1.4
QFdk.umb-4B	Crm15	4B.2	12.0	5.8	13.0	-3.0	12.0	6.0	13.0	-2.9	12.0	5.2	11.4	-2.9	12.0	5.2	11.4	-2.9
QFdk.umb-4B	Crm16	4B.2	12.0	6.0	12.9	-1.0	12.0	6.0	12.9	-1.0	12.0	5.5	11.9	-1.0	12.0	5.5	11.9	-1.0
QFdk.umb-4B	Crm17	4B.2	12.0	4.8	10.0	-0.8	12.0	5.0	10.4	-0.8	12.0	4.3	9.4	-0.8	12.0	4.6	10.1	-0.8
QFdk.umb-4B	Wpg15	4B.2	11.4	10.1	21.0	-2.1	11.4	10.1	21.0	-2.1	11.5	9.4	19.4	-2.1	11.5	9.4	19.4	-2.1
QFdk.umb-4B	Wpg16	4B.2	12.0	3.6	8.4	-0.7	12.5	4.0	7.5	-0.7	12.0	3.3	7.2	-0.7	12.5	3.6	7.9	-0.7
QFdk.umb-4B	Wpg17	4B.2	12.0	4.5	11.2	-0.6	12.0	5.5	11.2	-0.6	12.0	4.3	9.3	-0.6	12.0	5.3	11.5	-0.6
QFdk.umb-6D	Comb	6D.1									16.0	3.1	6.8	-0.8	15.5	4.1	8.9	-0.8
QFdk.umb-6D	Wpg16	6D.1					15.9	3.8	7.3	-0.7	16.0	3.0	6.6	-0.6	15.5	4.1	9.0	-0.7
QFdk.umb-6D	Wpg17	6D.1													19.5	3.2	7.1	-0.5
QFdk.umb-7A	Comb	7A	94.7	3.3	7.0	-0.8												
QFdk.umb-7A	Crm17	7A	94.2	3.5	7.4	-0.7	95.8	3.5	7.2	-0.7	94.5	3.0	6.6	-0.7	95.5	3.1	6.9	-0.7

Deoxynivalenol content (DON)																	
QDon.umb-3A	Wpg15	3A					120.2	3.1	6.4	-1.3	112.5	3.1	6.8	-1.3	116.0	3.3	7.3	-1.3
QDon.umb-4B	Comb	4B.2	12.0	7.2	15.3	-1.7	11.9	8.3	15.8	-1.7	12.0	6.8	14.4	-1.6	12.0	7.7	16.2	-1.6
QDon.umb-4B	Crm15	4B.2	12.5	3.4	7.6	-2.8	12.5	4.1	8.0	-3.0	11.5	3.4	7.4	-2.9	12.5	4.0	8.8	-3.0
QDon.umb-4B	Crm16	4B.2	11.6	4.4	9.8	-2.2	11.6	4.4	9.8	-2.2	11.5	4.0	8.8	-2.1	11.5	4.0	8.8	-2.1
QDon.umb-4B	Crm17	4B.2	12.0	5.3	11.1	-1.0	12.0	6.2	12.0	-1.0	12.0	4.8	10.5	-1.0	12.0	5.4	11.7	-1.0
QDon.umb-4B	Wpg15	4B.2	12.0	7.0	14.9	-1.9	12.0	7.6	14.5	-1.9	12.0	6.5	13.9	-1.9	12.0	6.6	14.1	-1.8
QDon.umb-4B	Wpg16	4B.2	10.4	3.6	8.1	-1.0	11.9	3.8	8.0	-1.0	10.5	3.5	7.6	-1.0	12.0	3.6	7.9	-1.0
QDon.umb-4B	Wpg17	4B.2	12.0	7.5	16.0	-1.0	12.0	8.6	16.2	-1.0	12.0	6.9	14.7	-1.0	12.0	8.1	17.1	-1.0
QDon.umb-6D	Comb	6D.1					19.7	3.5	6.2	-1.1					15.5	4.6	10.0	-1.3
QDon.umb-6D	Crm15	6D.1					19.7	3.1	5.9	-2.6					14.5	3.6	7.9	-2.8
QDon.umb-6D	Crm17	6D.1													15.5	3.4	7.6	-0.8
QDon.umb-6D	Wpg17	6D.1					19.7	3.5	6.2	-0.6					19.5	3.6	8.0	-0.7
QDon.umb-7A	Crm17	7A	94.2	3.3	7.0	-0.8												

[1]The specific agronomic traits associated with QTL *QAnth*, *QHt* and *QAR* were field and greenhouse anthesis date, field and greenhouse plant height and greenhouse anther retention, while the traits associated with QTL for FHB resistance *QFhb*, *QFdk* and *QDon* were incidence (Inc), field and greenhouse severity (Sev, GSev1 and GSev2), visual rating index (VRI), Fusarium damaged kernel (FDK) and deoxynivalenol (DON), which are indicated in brackets after site year; [2]Site year (Crm = Carman, Wpg = Winnipeg, GH= greenhouse, 15 = year 2015, 16 = year 2016, 17 = year 2017, 19 =year 2019, Comb = the combination of six site years); [3]Chr = chromosome (the decimal designation was used when more than one linkage group presented in the same chromosome. *E.g.* 5D.3); [4]Pos = the genetic position of peak of QTL in centimorgans; [5]PVE = phenotypic variation explained (R^2 in percentage); [6]Add = additive effect of allele substitution (a positive additive effective means that 32c*17 increased the value of the trait, and vice-versa).

*LOD threshold for both IM and ICIM was 3.00, while SIM and CIM had the thresholds ranging from 2.85 to 3.25 for different traits.

4.5 Discussion

The estimated wheat genome size is approximately 16 Gbp (Walkowiak et al. 2020). Length of common consensus maps have ranged from 2,569 to 3,800 cM (Somers et al. 2004; Cavanagh et al. 2013; Wang et al. 2014). The 8I3C map (13.34 Gbp & 2434.97 cM) provided good wheat genome coverage for QTL mapping (**Table 4.3**). In the previous QTL mapping study from the 32c*17/Peregrine cross (named 3CPR) in Chapter 3, 8,103 SNP markers generated a total map length of 1635.63 cM (unpublished data). The current 8I3C map had more SNP markers and longer map length than the previous 3CPR map, because 32c*17 and 18i*45 did not share common parents, while McClintock was a common parent between 32c*17 and Peregrine in the 3CPR population. Also, the 8I3C population was almost two times larger than the 3CPR population. Population size and the higher number of polymorphic markers in the 8I3C population contributed to the longer linkage map compared to the 3CPR population.

In the 8I3C population, QTL were identified for all traits measured in both field and greenhouse environments (**Table 4.4**). Comparisons of QTL identified in the 8I3C population and the 3CPR populations are represented in **Table 4.5**. Several common QTL were observed between the two populations and the contributions of the 32c*17 alleles are indicated (**Table 4.5**). Common QTL between the two populations were found on chromosomes 1A, 1B, 6A, 6B and 6D for several FHB traits, FDK and DON. In all cases the 32c*17 allele decreased disease. This demonstrates the usefulness of 32c*17 as a source of FHB resistance.

4.5.1 QTL for agronomic traits (Anth, GAnth and Ht)

In the 8I3C population, four major *QAnth* QTL were detected on chromosomes 1D, 2B, 5D (LG: 5D.3) and 7B and five major *QHt* QTL were found on chromosomes 1D, 2B, 4B (LG: 4B.2), 4D and 7B (**Tables 4.4** and **4.5**). Except for *QAnth.umb-5D*, all major 8I3C *QAnth* QTL co-localized with, or were on the same linkage groups as, 8I3C *QHt* QTL (**Table 4.5**). Without improving FHB resistance, the 18i*45 allele shortened Anth and GAnth and decreased Ht at *QAnth.umb-1D*, *QHt.umb-1D* and *QAnth/QHt.umb-2B*, while the 32c*17 allele shortened Anth and decreased Ht at *QAnth.umb-7B* and *QHt.umb-7B* (**Table 4.5**). Since the reduction of plant height is preferred for agronomic traits (like lodging resistance), but is often associated with increased FHB infection, it is important to decrease height without influencing FHB resistance.

QHt.umb-4D (physical position: 26.05~380.19 Mbp (million base pairs)) in the 8I3C population was identified across two individual site years, where the 32c*17 allele contributed to increased Ht (**Tables 4.4** and **4.5**). No QTL for FHB were identified in this region in the 8I3C population, however, major QTL *QFhb/QFdk/QDon.umb-4D* (physical position: 50.67~485.73 Mbp) were detected in this region in the 3CPR population, where the 32c*17 allele mostly contributed Type I and DON resistance. Many previous studies found a strong association between increased height and FHB resistance at a common dwarf *Rht-D1* locus in chromosome 4D, where the *Rht-D1a* allele increased height and reduced FHB incidence (Srinivasachary et al. 2008a, 2009; Voss et al. 2008; Löffler et al. 2009; Buerstmayr et al. 2009; Buerstmayr and Buerstmayr 2016; He et al. 2016). Two kompetitive allele-specific PCR (KASP) markers for the *Rht-D1* locus were tested in the two parental lines (**Appendix 4.1**); the result showed monomorphism in both 8I3C and 3CPR

populations. Based on the wheat reference genome (IWGSC RefSeq v2.1), the estimated physical location of the *Rht-D1* locus was 19.19 Mbp, which is estimated to be 6.86~361 Mbp away from 8I3C *QHt.umb-4D* and 31.48~466.54 Mbp away from 3CPR *QFhb/QFdk/QDon.umb-4D*. Further genomic and genetic research will help to study the relationship among 8I3C *QHt*, 3CPR *QFhb* and the *Rht-D1* locus.

The most consistent QTL for Anth *QAnth.umb-2B* (physical position: 61.92~65.19 Mbp) was identified across all six site years, the combined environment, and one greenhouse environment, and shared the same region with one of the most consistent QTL for Ht *QHt.umb-2B* (physical position: 61.92~105.51 Mbp) (**Tables 4.4** and **4.5**). A whole genome association mapping study for plant height in a European winter wheat cultivar collection reported that one SSR marker (Wmc154; physical position: 41.23 Mbp) was strongly associated with height on chromosome 2B, which is 20.69 Mbp away from the current 813C *QHt.umb-2B* (Zanke et al. 2014). A Ht QTL, *QPLH-2B*, was found to locate at 154.20 Mbp in a genome-wide association study in US winter wheats, which is at least 50 Mbp away from the current 8I3C *QAnth/QHt.umb-2B* (Daba et al. 2020). A dwarf gene *Rht4* (Wmc317; physical position: 794.37 Mbp) was reported at the long arm of chromosome 2B, but this gene was far away from *QHt.umb-2B* according to physical positions (Ellis et al. 2005; Zanke et al. 2014). A photoperiod gene *Ppd2/Ppd-B1a* on chromosome 2B had been previous reported to shorten heading and flowering date and reduce height, tiller number, spikelet number (Worland et al. 1998a; Díaz et al. 2012). Based on data published by Díaz et al. (2012), the *Ppd-B1* locus (the estimated physical position: 63.36~63.47 Mbp) appears to be in the same region as the current 8I3C *QAnth/QHt.umb-2B*. Although several QLT for FHB resistance

were previously reported on chromosome 2B, some of which were associated with QTL for Anth and/or Ht, no segregation of FHB traits was found on chromosome 2B in the 8I3C population (Gervais et al. 2003; Holzapfel et al. 2008; Liu et al. 2009; Buerstmayr et al. 2009, 2011; Xue et al. 2010b; Wang et al. 2017a; Zhao et al. 2018a; Aviles et al. 2020; Zhang et al. 2020; Yang et al. 2021).

QAnth.umb-1D (physical position: 52.81 Mbp) co-localized with *QHt.umb-1D* (physical position: 19.45~19.46 Mbp) within 24.5 cM on chromosome 1D (**Tables 4.4** and **4.5**). Zanke et al. (2014) reported two SNP markers (tplb0025b13_2687 and wsnp_Ex_c1358_2602235; physical position: 2.66 and 9.02 Mbp) were associated with plant height on chromosome 1D in a whole genome wide study for plant height in winter wheat, where the two SNP markers are 10.44~16.79 Mbp away from the current 8I3C *QHt.umb-1D*. Interestingly, a *TaGID1-D1* (gibberellin-insensitive dwarf1) gene (physical position: 348.97 Mbp) was also identified on chromosome 1D and 296.16 Mbp away from the 8I3C *QHt.umb-1D* (Li et al. 2013). The influence of the *TaGID1-D1* gene to the 8I3C *QHt.umb-1D* remains unknown. Although other studies reported an association between plant height and FHB resistance on chromosome 1D, no associations between these traits were identified in the 8I3C population, indicating that the parents did not differ in FHB resistance alleles on this chromosome (Ma et al. 2006b; Holzapfel et al. 2008; Liu et al. 2009; Buerstmayr et al. 2009; Arruda et al. 2016; Petersen et al. 2016; Zhu et al. 2016; Aviles et al. 2020)

QAnth.umb-7B (physical position: 1.27~6.71 Mbp) mapped within 31.5-45.4 cM of *QHt.umb-7B* (physical position: 67.68~132.60 Mbp) on chromosome 7B in the 8I3C population (**Tables 4.4** and **4.5**). In the 3CPR population, *QAnth/QFhb.umb-7B* (physical position: 594.42~646.93 Mbp)

was detected on chromosome 7B, but based on the physical positions, *QAnth.umb-7B* and *QHt.umb-7B* in the 8I3C population are not considered to be the same QTL as 3CPR *QAnth/QFhb.umb-7B*. Zanke et al. (2014) reported two SSR markers (Gwm400 and Barc267; physical position: 36.55 and 381.39 Mbp) and four SNP markers (Ex_c101666_634, wsnp_Ex_c24376_33618864, S00024215_51 and Tdurum_contig42584_1190; physical position: 26.39, 36.16, 85.70 and 755.55 Mbp, respectively) were associated with plant height. The plant height marker at the 85.70 Mbp position was within the region of *QHt.umb-7B* in the 8I3C population. Similar to the 8I3C population, Mao et al. (2010) found a 7B QTL for Ht (Xcdo595 and Xfbb343; unknown physical positions) that did not associate with QTL for FHB resistance. Similarly, He et al. (He et al. 2016) also identified a 7B QTL (unknown physical positions) for Ht without FHB resistance in a bi-parental QTL study.

In addition to the four major QTL *QAnth*, a minor QTL *QAnth.umb-1B* in the 8I3C population was found in the 2019 greenhouse test, while one QTL *QAnth.umb-1B* was reported in a greenhouse environment in the 3CPR population (**Tables 4.4** and **4.5**). However, these two QTL are not considered to be the same QTL due to the 32c*17 allele decreasing GAnth2 at the 8I3C *QAnth.umb-1B* and increasing GAnth at 3CPR *QAnth.umb-1B*. Interestingly, none of the *QAnth* in the 8I3C population associated with FHB resistance, while all *QAnth* in the 3CPR population associated with FHB resistance (**Table 4.5**). The three Ht QTL (*QHt.umb-1D*, *QAnth/QHt.umb-2B* and *QHt.umb-7B*) in the 8I3C that are not directly associated with FHB resistance, indicate that it should be possible to achieve optimal semi-dwarf height without negative impacts on FHB resistance.

4.5.2 QTL for FHB resistance

Several *QFhb* related to visual FHB parameters (Inc, Sev and VRI) and *QFdk* and *QDon* associated with post-harvesting FHB parameters (FDK and DON content) in both field and greenhouse tests were detected in the 8I3C population (**Tables 4.4** and **4.5**). The QTL on chromosome 4B were consistently detected for Ht in all field and greenhouse tests and were the most consistently detected among all QTL for Inc, FDK and DON through all site years in this study (**Tables 4.4** and **4.5**). Many studies have reported the co-localization of QTL for height, Type I and DON resistance and anther extrusion with the *Rht-B1* locus. The *Rht-B1a* allele increases height and anther extrusion and decreases disease incidence and DON contamination, while the *Rht-B1b* allele reduces height, lodging and anther extrusion, and increases yield, FHB and DON (McCartney et al. 2007; Liu et al. 2009; Srinivasachary et al. 2009; Xue et al. 2010b; Mao et al. 2010; Yan et al. 2011; Suzuki et al. 2012; Saville et al. 2012; Buerstmayr et al. 2012b; Lu et al. 2013; Lv et al. 2014; Eckard et al. 2015; Buerstmayr and Buerstmayr 2016; He et al. 2016; Tamburic-Ilincic and Rosa 2017; Xu et al. 2020). Similarly, *QHt.umb-4B* which was confirmed to contain the *Rht-B1* locus in the 8I3C population co-localized with *QFhb.umb-4B* (physical position: 18.81~41.75 Mbp), *QFdk/QDon.umb-4B* (physical position: 29.26~41.75 Mbp) and *QAR.umb-4B* (physical position: 40.76~637.03 Mbp) (**Tables 4.4**, **4.5** and **Appendix 4.1**). This differed from the 3CPR population where no QTL for FHB resistance were detected on chromosome 4B and the population was monomorphic for the *Rht-B1* locus (**Table 4.5**).

Two other QTL, *QFhb.umb-6D* and *QFhb.umb-7A*, were commonly found across individual and/or the combined environments in the 8I3C population and shared the same regions with *QFdk/QDon.umb-6D* and *QFdk/QDon.umb-7A*, respectively (**Tables 4.4** and **4.5**). *QAR/QFhb/QFdk/QDon.umb-6D* (physical position: 153.17~443.67 Mbp) were commonly reported in the 8I3C population, where the 32c*17 allele reduced GAR, Inc, VRI, FDK and DON (**Tables 4.2**, **4.4** and **4.5**).

In the 3CPR population, *QFhb/QFdk/QDon.umb-6D* (physical position: 69.82~443.67 Mbp) were also identified in the same region across several individual and the combined environments, suggesting that the 6D QTL is the same in both populations (**Table 4.5**). No QTL for Ht were detected in that region in either population. Chromosome 6D has not been widely found to carry repeatable QTL for FHB resistance (Liu et al. 2009; Löffler et al. 2009; Buerstmayr et al. 2009, 2019). All previously reported QTL on chromosome 6D were associated with disease severity in different winter wheat germplasm (Gervais et al. 2003; Paillard et al. 2004; Holzapfel et al. 2008; Cai and Bai 2014; Eckard et al. 2015; Cai et al. 2019). Notably, this study differed from other studies that only measured disease severity and provided a new insight of FHB QTL on chromosome 6D (**Table 4.5**). In the 8I3C population, the 32c*17 allele for *QAR.umb-6D* also studies in that the 32c*17 allele contributed Type I and DON resistance at *QFhb/QFdk/QDon.umb-6D* in both 8I3C and 3CPR populations reduced anther retention (**Tables 4.4** and **4.5**). Additional field and greenhouse studies will be required to validate the role of the 32c*17 allele on anther retention at this QTL in both 8I3C and 3CPR populations. Further genomic and genetic research will help to determine whether the current 32c*17-derived alleles for *QAR/QFhb/QFdk/QDon* are novel and the relationship with other previous 6D QTL for Type II resistance. Unfortunately,

heterogeneity was observed in this 6D region for both McClintock and Sumai3 after genotyping multiple times (unpublished data), thus it remains unknown which parental line contributed the 6D QTL allele to 32c*17.

In a proteomic study, one main region of chromosome 6D (physical position: 69.38~443.12 Mbp) was found to accumulate high amounts of specific proteins which were only expressed in the resistant cultivar, Xinong 538 (Yang et al. 2021). This location was within the current 6D QTL found in both populations derived from crosses with 32c*17 in this study (**Table 4.5**). Furthermore, a leucine rich repeat receptor like kinase (LRR-RLK) gene *TaLRRK-6D* (GenBank: GU084176.1; the estimated physical position: 313.61 Mbp), which was associated with Type II resistance and salicylic signaling pathway, was found in the same region as the 6D FHB QTL in this study (Thapa et al. 2018). More work needs to be done to determine the relationship between this gene and the current 32c*17-derived 6D QTL for Type I and DON resistance.

One major QTL *QFhb.umb-7A* (physical position: 131.40~518.92 Mbp) specific to Type II resistance was identified across four field site years, the combined environment and one greenhouse environment in the 8I3C population (**Tables 4.4** and **4.5**). In the same region, *QFdk/QDon.umb-7A* (physical position: 121.81~131.47 Mbp) was identified across one or two individual environments, where the 32c*17 allele contributed Type II and DON resistance. In the 3CPR map, the 32c*17 allele contributed Type II resistance at one minor QTL *QFhb.umb-7A* (physical position: 701.92~704.33 Mbp) and increased plant height at *QHt.umb-7A* (physical position: 82.08 Mbp and 673.73~676.60 Mbp) (**Table 4.5**). Based on the comparison of linkage map positions through common markers in both 8I3C and 3CPR maps, it is considered that 8I3C

QFhb/QFdk/QDon.umb-7A (8I3C QTL peak linkage position in the 8I3C map: 94.15-100.42 cM) might not be the same as 3CPR *QFhb.umb-7A* (the estimated 3CPR QTL peak linkage position in the 8I3C map: 145.73-147.31 cM). The Type II resistance gene, *Fhb3* (BE585744-STS; physical position: 237.93 Mbp), reported on chromosome 7A, was within the same region as 8I3C *QFhb/QFdk/QDon.umb-7A* (**Table 4.5**). Another study found that the CDC Buteo allele reduced Sev, VRI, FDK and DON at a 7A FHB QTL (IAAV6131 and wsnp_JD_c38071_27729378; physical position: 28.23~233.83 Mbp) in a QTL mapping study for the cross 22A*13/CDC Buteo, which overlapped with the 8I3C 7A QTL based on physical positions (Mwaniki 2017). A 7A QTL for Inc, Sev and VRI (physical position: 102.00~113.00 Mbp) was identified in a durum wheat study, which is 8.81 Mbp away from the 8I3C QTL (Ruan et al. 2020). Further research is required to evaluate the relationship between the 8I3C *QFhb/QFdk/QDon.umb-7A* and *Fhb3.*

In addition to the FHB QTL identified on chromosomes 4B, 6D and 7A, two major QTL *QFhb.umb-6A* and *QFhb.umb-6B* specific to FHB visual traits were detected, where the 32c*17 allele reduced Inc at *QFhb.umb-6A* and GSev at *QFhb.umb-6B* (**Tables 4.4** and **4.5**). The 32c*17 allele contributed Type I resistance at *QFhb.umb-6A* in the 8I3C population and increased height and reduced FDK and DON content at *QHt/QFdk/QDon.umb-6A* in the 3CPR population. Based on linkage and physical positions, 8I3C *QFhb.umb-6A* is considered to be the same QTL as 3CPR *QHt/QFdk/QDon.umb-6A* (**Table 4.5**). Based on parental and grandparental allele types, FHB resistance on chromosome 6A QTL was derived from 32c*17, which was inherited from Sumai3 (unpublished data). In chromosome 6A, a dwarfing gene *Rht24* (Barc103 and Wmc256; physical position: 179.05~551.93 Mbp) which is commonly used in Europe was physically linked with a SNP marker Excalibur_rep_c69275_346 (physical position: 501.31 Mbp), and is within the region

of the chromosome 6A QTL for FHB resistance and height in the 8I3C and 3CPR populations (Tian et al. 2017; Würschum et al. 2017; Herter et al. 2018) (**Table 4.5**). Many other 6A QTL for FHB resistance were inconsistently associated with QTL for Ht within the same region (Anderson et al. 2001; Paillard et al. 2004; Schmolke et al. 2005; Ma et al. 2006b; Häberle et al. 2007; Srinivasachary et al. 2008a; Holzapfel et al. 2008; Liu et al. 2012; Eckard et al. 2015; Petersen et al. 2016, 2017; Malihipour et al. 2017; Zhao et al. 2018b).

In **Appendix 4.1**, *Qfhs.ifa-5AS* (a common Sumai3 QTL for Type I resistance) and *Fhb2* (a common Type II resistance gene) were polymorphic between the parental lines. No QTL were detected on chromosome 5A in the 8I3C map indicating that this region of *Qfhs.ifa-5AS* does not play an important role in FHB resistance in the 8I3C population (**Table 4.4**). Type II resistance at *QFhb.umb-6B* was detected in the greenhouse environment for the 8I3C population, while the 32c*17 allele in the 3CPR population reduced Sev, VRI and FDK at *QFhb/QFdk.umb-6B* (**Table 4.5**). Based on physical positions, 8I3C *QFhb.umb-6B* is considered to be the same QTL as 3CPR *QFhb/QFdk.umb-6B* (**Table 4.5**). In a previous fine mapping study on a common Type II resistance gene *Fhb2*, markers Wmc398 and Gwm133 and markers Wmc397 and Gwm644 flanked the *Fhb2* locus (Cuthbert et al. 2007). The four markers tested in both 8I3C and 3CRP populations, revealed that three of the flanking markers of *Fhb2* locus (except Gwm133) mapped on chromosome 6B. The estimated position of the *Fhb2* locus was 65.57-75.68 cM in the 8I3C map and 56.9-65.71 cM in the 3CPR map, which was located within the 1-LOD interval of 8I3C *QFhb.umb-6B* (linkage map position: 38-87 cM) and close to the 1-LOD interval of 3CPR *QFhb/QFdk.umb-6B* (linkage map position: 41-51 cM) (**Tables 4.4** and **4.5**). The parent 32c*17 does not carry the Sumai 3 *Fhb2* resistance allele based on the previous haplotype study

(unpublished data), but it contributed FHB resistance at *QFhb/QFdk.umb-6B*. The relationship between *Fhb2* and *QFhb/QFdk.umb-6B* remains uncertain. Regardless, the chromosome 6B QTL for Type II resistance was inconsistently detected in both 8I3C and 3CPR populations, suggesting that this region was not important for FHB resistance. Moreover, a minor QTL *QFhb.umb-1A* in the 8I3C population was considered to be the same as the 3CPR *QFhb.umb-1A.2* (**Tables 4.4** and **4.5**). A minor QTL *QFdk.umb-1B* in the 8I3C population was also considered to be the same as the 3CPR *QFhb.umb-1B.2* (**Tables 4.4** and **4.5**).

Table 4.5 Comparison of QTL detected in the two populations 8I3C (18I*45/32c*17) and 3CPR (32c*17/Peregrine) and the effect of the 32c*17 allele for specific traits associated with the QTL.

8I3C population			**3CPR population**		
QTL name[1]	**Physical pos (Mbp[2])**	**32c*17 allele[3]**	**QTL name**	**Physical pos (Mbp)**	**32c*17 allele**
			QFhb.umb-1A.1	23.27~23.65	↓ GSev
QFhb.umb-1A	505.76~510.53	↓ Sev	*QFhb.umb-1A.2*	499.68~524.21	↓ Sev
QAnth.umb-1B	1.20~690.58*	↓ GAnth2			
			QAnth.umb-1B	679.34~681.73	↑ GAnth
			QFhb.umb-1B.1	698.17	↑ Inc
QFdk.umb-1B	682.40	↓ FDK	*QFhb.umb-1B.2*	695.78~700.53	↓ GSev
QHt.umb-1D	19.45~19.46	↑ Ht			
QAnth.umb-1D	52.81	↑ Anth			
			QAnth.umb-2A	47.07~83.04	↑ Anth, GAnth
			QFhb.umb-2A	696.84~718.11	↑ Inc, VRI
QAnth/QHt.umb-2B	61.92~105.51	↑ Anth, GAnth, Ht			
			QFhb.umb-2D	78.41~397.06	↓ Inc
			QFhb.umb-3A	180.36~639.50	↑ Sev, GSev
QDon.umb-3A	697.31	↓ DON			
			QAnth/QHt/QFhb/ QFdk.umb-4A	610.95~640.83	↓ Anth, Ht; ↑ Inc, VRI, FDK
QAR.umb-4B	40.76~637.03	↓ GAR			
QHt/QFhb/QFdk/ QDon.umb-4B	18.81~41.75	↑ Ht, GHt; ↓ Inc, Sev, VRI, FDK, DON			
QHt.umb-4D	26.05~380.19	↑ Ht			
			QFhb/QFdk/ QDon.umb-4D	50.67~485.73	↓ Inc, FDK, DON
QAnth.umb-5A	707.23~709.77	↓ GAnth			
			QFhb.umb-5D	76.06~370.14	↑ Inc, Sev, VRI
QAnth.umb-5D	567.23	↑ Anth			
QFhb.umb-6A	51.46	↓ Inc, VRI	*QHt/QFdk/ QDon.umb-6A*	63.85~573.15	↑ Ht; ↓ FDK, DON
QFhb.umb-6B	30.11~659.31	↓ GSev	*QFhb/QFhb.umb-6B*	51.32~52.95	↓ Sev, VRI, FDK

QAR/QFhb/QFdk/ QDon.umb-6D	153.17~443.67	↓ GAR, Inc, VRI, FDK, DON	*QFhb/QFdk/ QDon.umb-6D*	69.82~443.67	↓ Inc, Sev, VRI, FDK, DON
QFhb/QFdk/ QDon.umb-7A	121.81~518.92	↓ Sev, GSev, VRI, FDK, DON			
			QHt.umb-7A	82.08; 673.73~676.60	↑ Ht
			QFhb.umb-7A	701.92~704.33	↓ Sev
QHt.umb-7B	1.27~6.71	↓ Ht			
QAnth.umb-7B	67.68~132.60	↓ Anth			
			QAnth/QFhb.umb-7B	594.42~646.93	↓ Anth, Inc

[1]The specific agronomic traits associated with QTL *QAnth*, *QHt* and *QAR* were field and greenhouse anthesis date, field and greenhouse plant height and greenhouse anther retention, while the traits associated with QTL for FHB resistance *QFhb*, *QFdk* and *QDon* were incidence (Inc), field and greenhouse severity (Sev, GSev1 and GSev2), visual rating index (VRI), Fusarium damaged kernel (FDK) and deoxynivalenol (DON); [2]Physical positions of markers below peaks of 8I3C and 3CPR QTL are shown in million base pairs (Mbp); [3]The presence of the 32c*17 at each QTL increase (↑) or decrease (↓) the agronomic and/or FHB traits measured.
*The same QTL reported in both two populations are highlighted.

4.6 Conclusions

This study demonstrated that spring wheat 32c*17 could pass on strong Type I and DON resistance to the Canadian winter wheat line without relying on strong Type II resistance genes (i.e. *Fhb1* and *Fhb2*). The line 32c*17 would be a valuable parent for future breeding since this line showed strong FHB and DON resistance in both field and greenhouse tests. Some DHs from the 8I3C population surpassed the resistance of parental lines due to transgressive segregation, which may be useful for future breeding. Previously, discovered QTL for Type II resistance have been reported five times more frequently than either QTL for Type I or DON resistance (Liu et al. 2009), thus the two main QTL (*QHt/QFhb/QFdk/QDon.umb-4B* and *QAR/QFhb/QFdk/QDon.umb-6D*) associated with good Type I and DON resistance and one main QTL *QFhb/QFdk/QDon.umb-7A* associated with good Type II and DON resistance might be valuable to wheat breeders to utilize, especially the QTL on chromosomes 6D and 7A that were not associated with Ht. The allele type *Rht-B1a* is known to increase FHB resistance and reduce anther retention, but also increases Ht and the risk of lodging, which might not be the ideal for breeding agronomic traits in wheat. The 32c*17 allele at the 8I3C *QHt.umb-4D* and 3CPR *QFhb/QFdk/QDon.umb-4D* could reduce height without influencing FHB resistance or be a good alternative FHB resistance source without worrying association with Ht.

Most previously identified QTL on chromosome 6D were associated with disease severity, while the current 32c*17-derived *QFhb/QFdk/QDon.umb-6D* mainly reduced Inc, FDK and DON in both 8I3C and 3CPR populations, providing a new insight of FHB QTL on chromosome 6D. The current 6D QTL can be consistently detected after crossing 32c*17 with different genotypic

backgrounds in that region. As reported in Chapter 3 marker validation, the majority of the markers within a 10 cM interval flanking the peaks of 3CPR *QFhb/QFdk/QDon.umb-6D* consistently and accurately predicted resistance to all three FHB traits (Inc, Sev and VRI) in the PR3C lines across two site years. Based on the two QTL mapping populations (8I3C and 3CPR) and the marker validation in the PR3C population, FHB resistance from chromosome 6D in 32c*17 shows promise for future FHB resistance breeding in wheat. The origin of resistance controlled by the chromosome 6D QTL could be derived from either Sumai3 or McClintock. The 8I3C 7A QTL for Type II resistance was frequently identified in both field and greenhouse, which previously was not detected in the 3CPR population. This 7A QTL had been previously reported by other researchers. *QHt/QFdk/QDon.umb-6A* identified in both populations could be one of the previously published QTL. With the rising concern of food safety over mycotoxins in export markets, mechanisms associated with DON resistance contributed by 32c*17 in *QFhb/QFdk/QDon.umb-4D* and *QFhb/QFdk/QDon.umb-6D* could be further studied and characterized. Future studies related to additive effects of pyramiding the chromosome 4D and 6D QTL with other common FHB resistance QTL/genes would be useful for wheat breeders. The ideal breeding goal is to maintain optimal height and improve FHB resistance. The relationship between the three major Ht QTL (*QHt.umb-1D*, *QAnth/QHt.umb-2B* and *QHt.umb-7B*) that are not directly associated with FHB resistance could be used to optimize semi-dwarf height without negative impacts on FHB resistance.

CHAPTER 5

GENE EXPRESSION ANALYSIS OF PUTATIVE GENES RELATED TO THE HOST-PATHOGEN INTERACTION

5.1 Abstract

The dwarfing allele *Rht-B1b* benefits wheat growers by reducing plant height and lodging and increasing grain yield. On the other hand, multiple studies suggested that the wildtype allele *Rht-B1a* increases FHB resistance, anther extrusion and plant height. Previous research implied that the semi-dwarf allele *Rht-B1b* increased disease incidence and reduced disease spread and deoxynivalenol (DON). The objectives of this study were to evaluate disease severity and relative gene expression of pathogen and plant defense genes in two near isogenic lines (NILs) carrying either the *Rht-B1a* or *Rht-B1b* allele under different inoculation treatments, spray *Fusarium graminearum* (*Fg*) (sF), point inoculated *Fg* (iF) and point injected DON (iD) and Mock (water) at four time points (1.5, 3, 7 and 14 days after inoculation (dai)). Three checks (Caledonia, Sumai 3 and 32c*17) with different genetic backgrounds and known FHB reactions were also tested in the iF and sF treatments. The *Rht-B1b* NIL had significantly less disease severity than the *Rht-B1a* NIL only in the iF treatment. The resistant check Sumai 3 had the highest disease severity among the checks at 3 dai and the lowest at 14 dai, while the susceptible check Caledonia had the reverse pattern as Sumai 3. For the pathogen genes (*Trichothecene* (*TRI5*, *TRI6*, *TRI12* and *TRI101*) examined, inoculated spikelets in the iF treatment and infected spikes in the late time point of the sF treatment often had lower *TRI* gene expression in genotypes with high disease severity. In

contrast, spikelets that were not directly inoculated in the iF treatment and infected spikes in the early time point in the sF treatment often had lower *TRI* gene expression in genotypes with less disease severity. For host genes (*ABCC6, NFXL1, AOS, JAZ1, PR1b, PR4* and *PDF1.2*) examined, the timing of gene expression may play an important role in FHB resistance. The *Rht-B1a* NIL and Caledonia had generally higher expression levels of *ABCC6, AOS* and *PR4* in the late time point (14 dai) in all three inoculation treatments, implying that late expression of these genes might be insufficient to reduce disease severity. Higher expression of the three genes (*ABCC6, AOS* and *PR4*) at earlier time points (3 dai) and a lower expression level of *NFXL1* at the late time point may be associated with FHB resistance. There were no disease symptoms in the resistant genotype 32c*17 at 3 dai in the sF treatment and no increase of severity in Sumai 3 from 7 dai to 14 dai in both the iF and sF treatments. The FHB resistance in 32c*17 and Sumai 3 could not be fully explained with the limited genes tested in this study. Future studies with more genes and other disease resistant pathways are required to reveal their role in FHB resistance.

5.2 Introduction

Fusarium head blight (FHB) is one of most common fungal diseases of wheat (*Triticum aestivum* L.) worldwide and can be caused by multiple *Fusarium spp.*, resulting in yield and end-use quality losses (McMullen et al. 1997)(McMullen et al. 1997). In North America, *Fusarium graminearum sensu stricto* Schwabe (teleomorph: *Gibberella zeae* (Schwein.) Petch) (*Fg*) is the predominant causal species of FHB in wheat. The mycotoxin deoxynivalenol (DON) released by *Fg* is toxic to human and animal cells and poses a threat to food and feed safety (Proctor et al. 1995; Bai et al. 2002; Jansen et al. 2005; Sobrova et al. 2010; Buhrow et al. 2016; Mayer et al. 2017). Resistance to FHB is complex and involves multiple genes with relatively small effects. In one of the naming systems, five types of active FHB resistance in wheat were categorized (Mesterházy 1995); Type I resistance reduces numbers of infected spikes, while Type II resistance decreases numbers of infected spikelets within infected spikes. Type III resistance reduces Fusarium damaged kernels (FDK). Type IV resistance is a general overall tolerance to FHB infection. Type V resistance results in low DON content in infected grains.

Taller plant height has been associated with better FHB resistance (Mesterházy 1995; Buerstmayr et al. 2009; Yan et al. 2011; Saville et al. 2012). Several studies have shown that some height QTL co-localize with QTL for FHB resistance and anther extrusion. In particular, QTL for FHB resistance, anther retention and plant height overlapped such that they all contained the gibberellic acid (GA)-insensitive dwarfing *Rht-B1* gene (Lu et al. 2013; Buerstmayr and Buerstmayr 2016; He et al. 2016; Xu et al. 2020). Based on the additive effect, the wildtype *Rht-B1a* allele was associated with increases in height, anther extrusion and FHB resistance. Conversely, the dwarfing

Rht-B1b allele was associated with decreases in height and increases in both anther retention and FHB occurrence.

The dwarfing *Rht-B1b* allele also played an important role in the "Green revolution" due to reductions in plant height, that allowed wheat growers to increase fertilizer use to achieve high yields without the risk of lodging (Hedden 2003). The introduction of the dwarf allele *Rht-B1b* increased grain yield and lodging resistance, but was associated with FHB susceptibility. Thus, the use of the wildtype *Rht-B1a* allele for improving FHB resistance has been discouraged due to the associated height increase leading to lodging and yield reduction (Verma et al. 2005; Voss et al. 2008; Guedira et al. 2010; Lanning et al. 2012; Chen et al. 2016).

One study found that the *Rht-B1b* allele was present in 28% and 77% of estimated soft and hard winter wheat varieties, respectively, grown in the United States (Guedira et al. 2010). In addition to reducing plant height, many other agronomic traits can be affected by the *Rht-B1b* allele (Lanning et al. 2012). A comparison of semi-dwarf near isogenic lines (NILs) with their wild-type lines in four different genetic backgrounds, demonstrated that the NILs with the *Rht-B1b* allele had higher grain yield, more tillers, higher seed numbers per spike, bigger harvest index and thicker stems than their wild-types. Lines with the wild-type *Rht-B1a* allele had higher kernel weight, higher test weight, higher grain protein and earlier heading date than the semi-dwarf NILs (Lanning et al. 2012).

The height variation between the wildtype *Rht-B1a* and the semi-dwarf type *Rht-B1b* alleles is a direct result of whether DELLA protein (which is named based on its N-terminal conserved amino acid sequence (Asp-Glu-Leu-Leu-Ala; D-E-L-L-A)) is degraded in the GA pathway or not (Nelson and Steber 2016). Plants carrying the wildtype *Rht-B1a* allele are able to encode an intact DELLA protein. The bioactive GAs bind to the GA-insensitive dwarf1 (GID) receptor forming a complex which interacts with DELLA to release the repression of the transcriptional factors (TFs); the free TFs enable the expression of genes related to height, ultimately resulting in tall wheat plants. Compared with the *Rht-B1a* allele, the *Rht-B1b* allele encodes a truncated DELLA protein that is unable to interact with the GA-GID complex; consequently, plant height fails to increase leading to a semi-dwarf phenotype (Nelson and Steber 2016; Thomas 2017).

Unlike the traditional understanding of the association of FHB susceptibility and the *Rht-B1b* allele, Saville et al. (2012) reported that a Maris Huntsman NIL carrying the *Rht-B1b* allele had less FHB symptoms than its NIL carrying the *Rht-B1a* allele in both indoor point inoculation and direct mycotoxin DON injection tests. Meanwhile, the study also found that the *Rht-B1a* NIL had less bleached spikelets than the *Rht-B1b* NIL in a field spray experiment. The authors hypothesized that the *Rht-B1b* allele reduced Type I resistance and increased Type II and DON resistance.

In the life cycle of *Fusarium*, mycotoxins play an important role during colonization. Mycotoxins in *Fusarium* belong to a class of compounds called trichothecenes, where DON is Type B trichothecene (Foroud et al. 2019). The DON biosynthesis pathway has been thoroughly reviewed (a graphical summary is presented in **Figure 2.2**) and a summary of all known *Trichothecene* (*TRI*) biosynthesis genes is presented in **Table 2.1** (Foroud and Eudes 2009; McCormick et al. 2011;

Foroud et al. 2019). The biosynthesis pathway begins with the conversion of farnesyl pyrophosphate to trichodiene, where *TRI5* plays an important role in this initial stage of the biosynthesis pathway (Cane et al. 1985; Hohn and Beremand 1989; McCormick et al. 2011). It was found that approximately 200 *TRI6* binding sites existed in *F. graminearum* genome. In *F. graminearum*, promotor regions of eleven *TRI* genes (*TRI1*, *TRI3*, *TRI4*, *TRI5*, *TRI6*, *TRI8*, *TRI9*, *TRI11*, *TRI12*, *TRI14* and *TRI101*) had the *TRI6* binding sites (Seong et al. 2009). *TRI6* positively regulated many *TRI* genes (Seong et al. 2009; Nasmith et al. 2011). This gene not only controlled toxin synthesis as a pathway-specific transcription factor, but was also involved with the isoprenoid biosynthetic pathway, ABC-transporters, cellular metabolisms (such as carbon, lipid and nitrogen metabolism), growth regulation and glucose signal transduction as a global transcription regulator (Seong et al. 2009; Nasmith et al. 2011).

The *TRI12* was one of the important *TRI* genes located on chromosome 2 and encoded the major facilitator superfamily protein mainly responsible to toxin efflux and self-protection (Alexander et al. 1999; Menke et al. 2012). In the middle of the biosynthesis pathway, *TRI101* converted isotrichodermol to isotrichodermin by adding an acetyl group at the C-3 position (McCormick et al. 1999). Disruption of this gene in *F. sporotrichioides* (*Fs*) resulted in the accumulation of isotrichodermol and the absence of T-2 toxin (Type A trichothecene) (McCormick et al. 1999). Two real time polymerase chain reaction (qRT-PCR) studies related to *TRI101* in infected wheat spikes showed 3ADON producing isolates generally had higher *TRI101* transcripts than 15ADON producing isolates through the most of the time-course (Lee et al. 2014; Amarasinghe and Fernando 2016). It is hypothesized that *TRI101* acetylates at the C-3 position to protect fungus itself from the toxicity of trichothecene during the trichothecene biosynthesis progress (Kimura et

al. 1998). Later, it was confirmed that *TRI101* actually improves tolerance to the toxin, but did not act in as a critical role on for self-protection as *TRI12* (McCormick et al. 1999). Furthermore, it was demonstrated that transgenic wheat cultivar, Bobwhite, with *FsTRI101* had less disease severity and less DON accumulation than the wildtype (Okubara et al. 2002; Alexander 2008).

The regulatory function of jasmonic acid (JA) on FHB resistance has been previously studied in wheat (Xiao et al. 2013; Kazan and Gardiner 2018). Details of the JA pathway and the cross talk with other hormones were reviewed (Berens et al. 2017; Yang et al. 2019; Liu and Timko 2021). DELLA protein is able to bind with a key JA-repressor JASMONATE ZIM (zinc-finger inflorescence meristem)-DOMAIN (JAZ) protein, resulting in enhancing the JA signaling pathway. Qi et al. (2016) showed JA-related genes (*allene oxide synthase* (*AOS*), *pathogenesis-related* (*PR1b*), *PR4* and *plant defensin* (*PDF1.2*)) were involved in FHB resistance in wheat. Thus, Saville et al. (2012) hypothesized, and later confirmed, that the *Rht-B1b* allele might promote the JA signalling pathway and inhibit the salicylic acid (SA) signalling pathway, resulting in susceptibility to biotrophic pathogens and resistance to necrotrophic pathogens. Furthermore, *ABCC6* (*ATP-binding cassette sub-family C member*) encoding ATP-binding cassette transporter proteins were involved with DON resistance (Chetouhi et al. 2016; Pierron et al. 2016; Gunupuru et al. 2017; Kazan and Gardiner 2018; Foroud et al. 2019; Brauer et al. 2020). *NFXL1* (*nuclear transcription factor, X-box binding like 1*) gene encoding the NF-X1-type zinc finger protein was inducted by FHB infection and DON injection, which was associated with FHB susceptibility (Pan et al. 2018; Brauer et al. 2020; Haldar et al. 2021).

In order to further understand how the truncated DELLA protein encoded by the *Rht-B1b* allele plays a role in the JA pathway with the *Fg*-wheat pathosystem, a gene-expression study on various genotypes (two NILs and three wheat checks) was conducted. The objectives of the project were: 1) to estimate the disease responses in different genotypes under different indoor inoculation methods and 2) to study expression of important DON biosynthesis *TRI* genes (*TRI5, TRI6, TRI12* and *TRI101*) using different inoculation methods and 3) determine expression levels of selected genes (*ABCC6, NFXL1, AOS, JAZ1, PR1b, PR4* and *PDF1.2*) by time series.

5.2 Materials and Methods

5.2.1 Plant material

The winter cultivar, Maris Huntsman, carrying the wildtype allele *Rht-B1a* (tall plant) and its two NILs carrying either the *Rht-B1b* allele (semi-dwarf) or the *Rht-B1c* allele (super dwarf) were generously provided by Dr. Paul Nicholson, John Innes Centre, UK. These had been used in the previously mentioned study conducted by Saville *et al.* (2012). Five FHB checks 18I*45, 32c*17 (32c), Emerson, Caledonia (Cal) and Sumai 3 (Su3) were included in this study as well. With the exception of Sumai 3, all wheat checks were winter wheat. Due to high powdery mildew infection caused by *Blumeria graminis* on the NIL *Rht-B1c* and Emerson, and inadequate vernalization of 18I*45, these lines were later excluded from the study. Sumai 3 is a Chinese spring wheat cultivar that has been used as the most important genetic source of FHB resistance (Buerstmayr et al. 2009). Caledonia is a highly FHB susceptible soft white winter wheat developed and released by Cornell Agricultural Experiment Station in 1998 (Sorrells et al. 2004). 32c*17 is an elite breeding line

developed by the University of Manitoba, Canada breeding program that has Sumai 3 in its lineage and strong FHB and DON resistance under severe disease pressure in Canada, but does not carry the common Sumai3 alleles for FHB and DON resistance. Liquid sulphur was applied weekly to control powdery mildew. Previous work (unpublished data) has shown that liquid sulphur did not interfere with FHB reaction. Only plant materials with minimal powdery mildew were retained for further study.

5.2.2 Fusarium inoculum and deoxynivalenol solution

Two *Fg* isolates obtained from Dr. Jeannie Gilbert at the Cereal Research Centre, AAFC in Winnipeg, Manitoba were used in this study. Both isolates were 3-acetyl deoxynivalenol (3ADON) producers: M7-07-1 and M9-07-1. All macroconidia suspensions were prepared based on a modified protocol originally developed by Dr. Jeannie Gilbert as mentioned in McCallum *et al.* (2004). For each isolate, a single conidium was first isolated from a previous sporodochia colony and then grown on a potato dextrose agar (PDA) plate. After mycelia colonized the whole plate (four to seven days), a portion of mycelia and the PDA agar were selected and transferred to a sterile Spezieller Nährstoffarmer agar (SNA) media plate (20 milliliter (ml) media/plate). After seven days in light at room temperature, the contents of several SNA plates (eight to twelve plates) were added to 1.5-liter liquid carboxy methyl cellulose (CMC) media. The CMC media flasks were aerated for seven days in light at room temperature. Macroconidia were then harvested from each flask. A haemocytometer under a 10x magnification microscope was used to determine the number of macroconidia and develop the desired concentration in the macroconidia suspensions. To

increase solution adhesion prior to the inoculation, 0.3 ml of Tween 20 (Uniqema Americas LLC) was added to each 100 ml solution in each treatment.

In order to obtain enough *Fg* RNA from infected spikes for gene expression analysis, the total concentration of inoculum was 100,000 macroconidia per ml composed of equal proportions of each of the two isolates. This was twice the normal concentration used in other FHB studies for wheat (Saville et al. 2012; Amarasinghe et al. 2016). To maintain the optimal disease development and viability of macroconidia, inoculum was freshly made from SNA plates every two weeks. Pure DON powder was purchased from TripleBond (Guelph, Ontario). The powder was dissolved into distilled water to obtain a final concentration of 15 microgram (ug) per microliter (ul) and stored at 4 °C for up to six days.

5.2.3 Experiment design for four different inoculation methods

Soilless mix (Sunshine® Mix #4 Aggregate Plus) was purchased from Sun Gro® Horticulture. With the exception of spring wheat Sumai 3, all other genotypes were first sown in root trainers (root trainer cell size: 3.5 cm x 2.5 cm x 14 cm) and grown in a growth chamber with 16 hours of light at 22 °C followed by 8 hours of dark at 18 °C until reaching the two to three leaf stage. Each root trainer consists of seventy cells and one seed was planted per cell. All plants were then moved to a cool room set with 16 hours light and 8 hours dark at 4 °C and vernalized for at least eight weeks. After vernalization, plants were placed in a growth chamber set at 10-15 °C with 16 hours of light and 8 hours of dark for one week of acclimation before transplanting into 2-liter pots in a growth chamber with 16 hours light with 22 °C and 8 hours dark with 18 °C. When winter wheat

plants were out of vernalization, Sumai 3 plants were directly seeded into 2-liter pots to synchronize the flowering period between spring and winter wheat genotypes.

The entire experiment was conducted in the same growth chamber with 16 hours of light at 22 °C followed by 8 hours of dark at 18 °C. Fifteen ml of a water-soluble fertilizer (Plant-Prod 20-20-20 Classic) (Master Plant-Prod Inc., Brampton) was dissolved into 4 liters of water and applied before and after the vernalization period. One tablespoon (approximately 18 g) of controlled-release fertilizer (ACERnt 13-12-12 Hanging Basket) (Master Plant-Prod Inc., Brampton) was added to each 2-liter pot.

Four inoculation treatments (Trt) were used: point inoculation of *Fg* (iF), point inoculation of DON (iD), spray inoculation of *Fg* (sF) and a Mock water control (**Figure 5.1** and **Table 5.1**). The Mock treatment contained five time points (0, 1.5, 3, 7 and 14 days after inoculation (dai)) and the other treatments consisted of four time points (1.5, 3, 7 and14 dai) (**Table 5.1**). Five genotypes (G) were used: Maris Huntsman *Rht-B1a* NIL and *Rht-B1b* NIL, 32c, Cal and Su3. The experimental design was a split plot with four replicates. Each replicate contained one pot per genotype per time point per treatment for a total of sixty-four pots in each replicate. The inoculation treatments were considered as main plots, while G were the sub plot treatments and different time points (T) of spike collection were subsamples (**Table 5.1**). Each pot was only used for one collection time point. The first five flowering spikes in each pot were selected to inoculate with the same method. All pots (one plant per time point per genotype) within the same treatment in each replicate were randomized. Plants were checked every other day to obtain the optimal timing for inoculation. The ideal stage for inoculation was when spikes were at the 30-50% anthesis stage.

In the iF treatment, the primary and secondary florets of two alternate spikelets located at the top third of each flowering spike were marked and injected with 10 ul *Fg* spore suspension per floret with a pipette placed between the palea and lemma (**Figure 5.1**). In total, four florets (two per spikelet) per spike were inoculated in the iF treatment (**Table 5.1**). In order to provide a high humidity micro-environment, inoculated spikes were sprayed with distilled water and covered with a glassine crossing bag. The glassine crossing bag was removed after two days. In the DON treatment, a 10 ul solution of DON was applied to each floret with the same procedure as the iF treatment (**Figure 5.1**). Due to the high cost of pure DON, only the *Rht-B1a* and *Rht-B1b* NILs were included in the DON treatment (**Table 5.1**). In the sF treatment, all flowering spikelets in the inoculated spikes were labelled with a permanent marker prior to spray inoculation (**Table 5.1**). A spray bottle was used to apply a total of 1.5 milliliter (ml) of the same suspension to both sides of a whole spike (**Figure 5.1**). A glassine crossing bag was immediately placed over the spike without spraying additional distilled water, to maintain high humidity. The glassine bag was removed after two days. In the Mock treatment, four spikelets were injected with distilled water using the same procedure as the iF treatment. The four spikelets were inoculated in the Mock treatment to guarantee enough plant tissue for RNA extraction (**Figure 5.1** and **Table 5.1**).

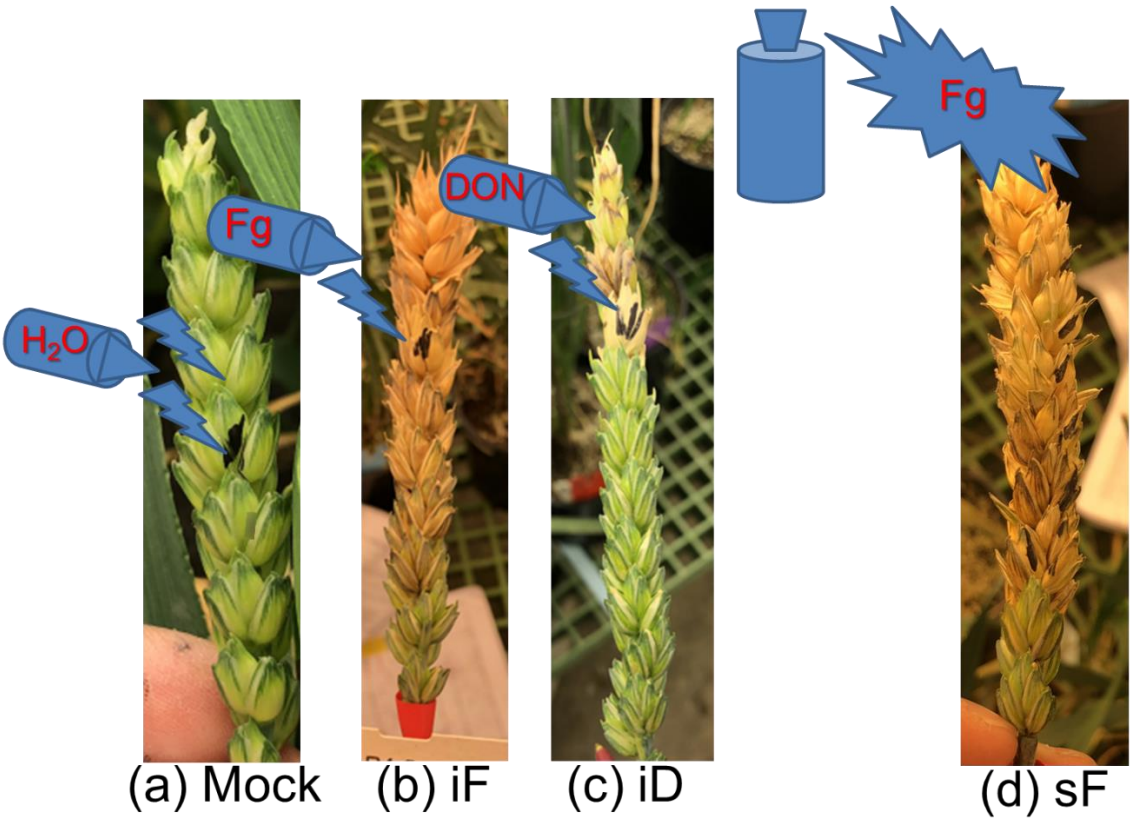

Figure 5.1 A schematic diagram of the *Rht-B1b* NIL under the following four inoculation methods. (a) the spikelet labelled with the black mark, the spikelet above and the alternate spikelets on the other side of the picture were the four inoculated spikelets in the Mock treatment 0 days after inoculation (dai); (b, c) the spikelet labelled with black mark and the alternate spikelet were the two inoculated spikelets in the point inoculated *Fusarium* treatment (iF) or the point injected DON treatment (iD) 14 dai; (d) the spikelets labelled with black marks were the flowering spikelets in the spray inoculated *Fusarium* treatment (sF) 14 dai.

Table 5.1 The detailed information for the collection time points for different genotypes in different treatments in this experiment.

Treatment	NIL[1]	Check[2]	Solution[3]	Inoculated spikelets[4]
sF	1.5d, 3d, 7d, 14d	3d, 7d, 14d	*Fg*	flowering spikelets
iF	1.5d, 3d, 7d, 14d	3d, 7d, 14d	*Fg*	2
iD	1.5d, 3d, 7d, 14d	/	DON	2
Mock	0h, 1.5d, 3d, 7d, 14d	0h, 3d, 7d, 14d	Water	4

[1]Two near isogenic lines (NIL) of cultivar, Maris Huntsman, carrying either the allele type *Rht-B1a or Rht-B1b*; [2]Three checks were Caledonia, 32c*17 and Sumai 3; [3]Macroconidia suspension of *Fusarium graminearum* (*Fg*) was used in iF and sF treatments, while DON solution was applied in iD treatment and distilled water was used in the Mock treatment. Tween 20 was added into all treatment; [4]Two florets (primary and secondary) per each of two spikelets were point inoculated in iF and iD treatments, while four spikelets were inoculated with distilled water in the Mock treatment. The sF treatment sprayed whole spikes and with flowering spikelets recorded in each spike prior to spray application.

5.2.4 Measurement of phenotypic data and spike sampling

Each plant was grown and discarded after the sampling time point. Due to growth chamber space limitations, only the two NILs had an additional time point (1.5 dai) in the iF, sF and Mock treatment, while the three checks did not have the 1.5 dai time point (**Table 5.1**). Disease severity (Sev) and plant height (Ht) for each treated spike were measured prior to spike collection. Plant height was measured from the tip of each spike (excluding the length of awns) to the soil surface. In the iF and iD treatments, the number of infected spikelets below the inoculation points in each inoculated spike was counted and calculated to determine Sev (= infected spikelets / total spikelets x 100%). Due to the potential of infection interfering with nutrient flow to the upper portion of the spike, the total spikelets in the iF and iD treatments were the total numbers of spikelets from the inoculated florets to the basal florets, not the whole spike. In the sF treatment, the number of infected spikelets of the whole spike was counted for the calculation of Sev and the total spikelets were the total numbers of spikelets of the whole spike. In the Mock treatment, the water-injected spikes were collected with the same procedure as the iF and iD treatments. In additional, plants in the Mock treatment were regularly monitored during the experiment to ensure no inoculum drift from the other inoculation methods. Collected spikes were wrapped with aluminum foil, immediately immersed in liquid nitrogen and later stored in a bag in a -80 °C freezer until RNA extraction.

5.2.5 RNA purification and quantitative reverse transcription PCR

To better understand the disease progress and host response, the labelled spikelets in the inoculated five spikes from the same pot were pooled together as the inoculated spikelet part (IS part) and ground by mortar and pestle under liquid nitrogen for the iF, iD and Mock treatments (**Figure 5.1**). The four spikelets below the inoculation point in the same pot were pooled together as the below inoculated spikelet part (BIS part). In the sF treatment, the center eight spikelets of all five spikes from the same pot were selected. The labelled spikelets with florets at anthesis stage and unlabeled spikelets with no florets at anthesis stage were separately ground as IS and BIS parts, respectively **Figure 5.1**).

All samples were first extracted with Invitrogen™ PureLink™ Plant RNA Reagent (PPR) (Thermo Fisher Scientific Inc., Waltham, MA, USA) using the recommended product protocol with a few modifications. To minimize RNA degradation, 700 ml of PPR solution was used for each sample, instead of 500 ml. There were two washing stages with 600 ml of 75% ethanol at 4 °C rather than one washing with 1000 ml of 75% ethanol at room temperature. Extracted RNA was diluted with Invitrogen™ The RNA Storage Solution (Thermo Fisher Scientific Inc., Waltham, MA, USA) and stored at -80 °C. Many samples collected 7 and 14 dai in the three treatments (except Mock) had little fresh tissue left and also contained high starch and fungal RNase, resulting in technical difficulties to yield good quality fungal and wheat RNA by using the PPR method. Thus, the TRIzol™ Plus RNA Purification Kit (Thermo Fisher Scientific Inc., Waltham, MA, USA) was used with the recommended protocol and minor modification (additional two washing steps with 500 ul of Wash Buffer II) to extract RNA from the inoculated samples that were unable to yield

good quality RNA from the PPR method previously. All centrifuge steps were operated in a 4 °C centrifuge to reduce enzyme degradation activities. Samples which did not yield good quality RNA after three extraction attempts from both methods were considered as missing data.

Integrity and quantity of extracted RNA were analyzed using Thermo Scientific™ NanoDrop™ 3300 Fluorospectrometer (Thermo Fisher Scientific Inc., Waltham, MA, USA) and 1% agarose gel electrophoresis. Genomic DNA in RNA samples was removed with the TURBO DNA-*free*™ Kit using the recommended protocol (Thermo Fisher Scientific Inc., Waltham, MA, USA). The first strand cDNA was synthesized from 1ug mRNA using the Thermo Scientific RevertAid RT Kit recommended protocol (Thermo Fisher Scientific Inc., Waltham, MA, USA) and oligo(dT)18 primers (Integrated DNA Technologies, Inc., Coralville, IA, USA).

qRT-PCR was conducted with a CFX96 Touch Real-Time PCR Detection System (Bio-Rad Laboratories Ltd., Hercules, CA, USA). The thermocycle program was 50 °C for 2 min, followed by 95 °C for 2 min, 45 cycles of 95 °C for 15 second and 60 °C for 30 second. The melt curve steps (95 °C for 1 min, 60 °C for 2 min, followed by 0.5 °C increase every 5 second from 60 °C to 95 °C) were added after the PCR cycles to check formations of primer dimers and specificity of amplified PCR products. According to the standard protocol (Xiao et al. 2013; Henriquez et al. 2016; Zou et al. 2021), all data having quantification cycle (Cq) values more than 40 were removed. All *Fusarium* and wheat primers used in this study were obtained from previously published papers and are listed in detail in **Appendix 5.1**Appendix 5.1. One *Fusarium* housekeeping gene (Glyceraldehyde-3-phosphate dehydrogenase (*GAPDH*)) and one wheat internal control (*Elongation factor-1 alpha* (*EF-1α*)) were included. To amplify Fusarium cDNA products, each

10 ul qRT-PCR reaction in a 96 well plate consisted of 4.2 ul of cDNA after one fifth of dilution, 5 ul of PowerUp™ SYBR™ Green Master Mix (Thermo Fisher Scientific Inc., Waltham, MA, USA) and 0.4 ul of each primer with a concentration of 10 micromolar (uM) (Integrated DNA Technologies, Inc., Coralville, IA, USA). For wheat primers, each 10 ul qRT-PCR reaction contained of 4.2 ul of cDNA after 100x dilution, 5 ul of the same master mix and 0.4 ul of each primer with a concentration of 5 uM.

The best three of four biological replicates with less missing data and two technical replicates were included in this study. The terms gene expression and expression level are used in this study to refer to mRNA expression level. The fold changes of mRNA expression level relative to either wheat or Fusarium housekeeping gene were calculated using the $2^{-\Delta\Delta C_T}$ method (Livak and Schmittgen 2001). In this study, up-regulation of a gene was defined when there was more than a two-fold change of expression level (log10 transformed mRNA expression level ≥ 0.3) and down-regulation was defined when there was less than a 0.5-fold change (log10 transformed mRNA expression level ≤ -0.3).

5.2.6 Statistical Analysis

Untransformed data and data with log 10 transformation were both examined in each step of analysis in this study. Normality of residual plots between untransformed data and transformed data from each model for each trait were compared to decide whether to present the results from untransformed or transformed data. Untransformed data for height and severity across all treatments were analyzed by using the PROC GLM procedure in SAS® Studio (Enterprise Edition

3.8) (SAS Institute Inc., Cary, NC, USA). The three main effects for Trt, G, T and the four interactions (Trt*G, Trt*T, G*T and Trt*G*T) were fixed effects and the only random effect was replicate nested within treatment. To estimate genotype variation in each treatment, severity data were further divided by each treatment and analyzed with similar models, where fixed effects were main effects for G and T and the interaction for G*T and the random effect was replicate.

For quantitative polymerase chain reaction (qPCR) data, a similar approach as described for disease severity and plant height was used to analyze expression level of each gene across all treatments (**Appendix 5.3**). Fixed effects were the four main effects (Trt, G, T and Part) and the eleven interactions (Trt*G, Trt*T, Trt*Part, G*T, G*Part, T*Part, Trt*G*T, Trt*G*Part, Trt*T*Part, G*T*Part and Trt*G*T*Part) and the random effect was replicate nested within treatment. The main effect Part consisted of the IS and BIS part. To further examine gene expression in each treatment, transformed qPCR data was further divided by each treatment and analyzed with similar models, where fixed effects were three main effects (G, T and Part) and the four interaction (G*T, G*Part, T*Part and G*T*Part) and the random effect was replicate (**Appendix 5.4** and **Appendix 5.5**). For multiple means comparison tests, Fisher's least significant difference (LSD) method ($P < 0.05$) was used to separate significantly different means obtained from ANOVA in each model.

5.3 Results

5.3.1 Phenotypic data

Based on the combined analysis of variance for height, there were significant differences for the main effects G and T, the interactions G*T, Trt*G and Trt*T*G, and replicate nested within Trt, while the main effect Trt and interaction Trt*T were not significant (**Table 5.2**). Means comparisons for G showed that height of each genotype was significantly different from other genotypes (Su3 = 84.80 cm, 32c = 67.41 cm, *Rht-B1a* = 63.61 cm, Cal = 50.76 cm and *Rht-B1b* = 45.08 cm) (**Appendix 5.2**). Significant differences between time points were mainly due to the inclusion of only two genotypes at 1.5 dai and all five genotypes at other time points. Interactions involving G are mainly due to differences in magnitude between genotypes at different time points, or treatments, with no changes in genotype rank.

Based on the combined analysis of variance for severity, there were significant differences for all three main effects and all two-way interactions (**Table 5.2**). Means comparison tests for the G*T interaction showed that infected spikelets were visible 3 dai for all genotypes and disease severity increased over time (**Figure 5.2**). At the latest time point (14 dai), the iD treatment had the lowest disease severity for the two genotypes tested and the sF treatment had highest disease severity for all genotypes (**Figure 5.2 b** and **c**). Significant differences between genotypes in the iF treatment were only detected 14 dai and in the sF treatment were observed at all time points except 1.5 dai (**Figure 5.2 a** and **c**). In the iD treatment, the two genotypes tested were not significantly different

from each other at any time point, but there were significant differences between the time points (**Figure 5.2 b**).

Disease severity between the two NILs showed that the *Rht-B1a* NIL had significantly higher disease severity than the *Rht-B1b* NIL in the iF treatment 14 dai, but it had similar severity as the *Rht-B1b* NIL in the sF and iD treatments at all time points (**Figure 5.2**). Disease progression differed among the three checks, where Su3 had the highest disease severity among the checks at 3 dai and the lowest at 14 dai (**Figure 5.2 a** and **c**). The susceptible check, Cal, showed the opposite effect of Su3. Disease severity did not increase in Su3 after 7 dai under both treatments (**Figure 5.2 a** and **c**). Since individual spikes were harvested for RNA extraction after disease rating, the apparent declines in disease severity of Sumai 3 between time points were due to variation between pots of the same genotype. Interestingly, the moderate resistant genotype 32c*17 in the sF treatment showed no symptoms at 3 dai, while spikes of the other genotypes at least had some visible discoloration (**Figure 5.2 c**). For the iD treatments, maximum discolouration was reached by 7 dai (**Figure 5.2 b**).

Table 5.2 Analysis of variance of plant height and disease severity under a controlled environment on five genotypes (G) at five time points (T) under four treatments including mock (Trt).

Source of Variation	Height		Severity	
	DF[1]	*P* value[2]	DF	*P* value
Genotype (G)	4	<0.01	4	<0.01
Time point (T)	4	<0.01	3	<0.01
G*T	13	<0.01	9	<0.01
Treatment (Trt)[3]	3	0.28	2	<0.01
Trt*G	9	<0.01	5	<0.01
Trt*T	9	0.20	6	<0.01
Trt*T*G	21	<0.01	12	0.75
Replicate (Trt)[4]	12	<0.01	9	0.83

[1]DF Degrees of freedom; [2]*P* value indicates a probability value; [3]No disease severity measurement was made for the mock treatment; [4]Replicate nested within individual treatment

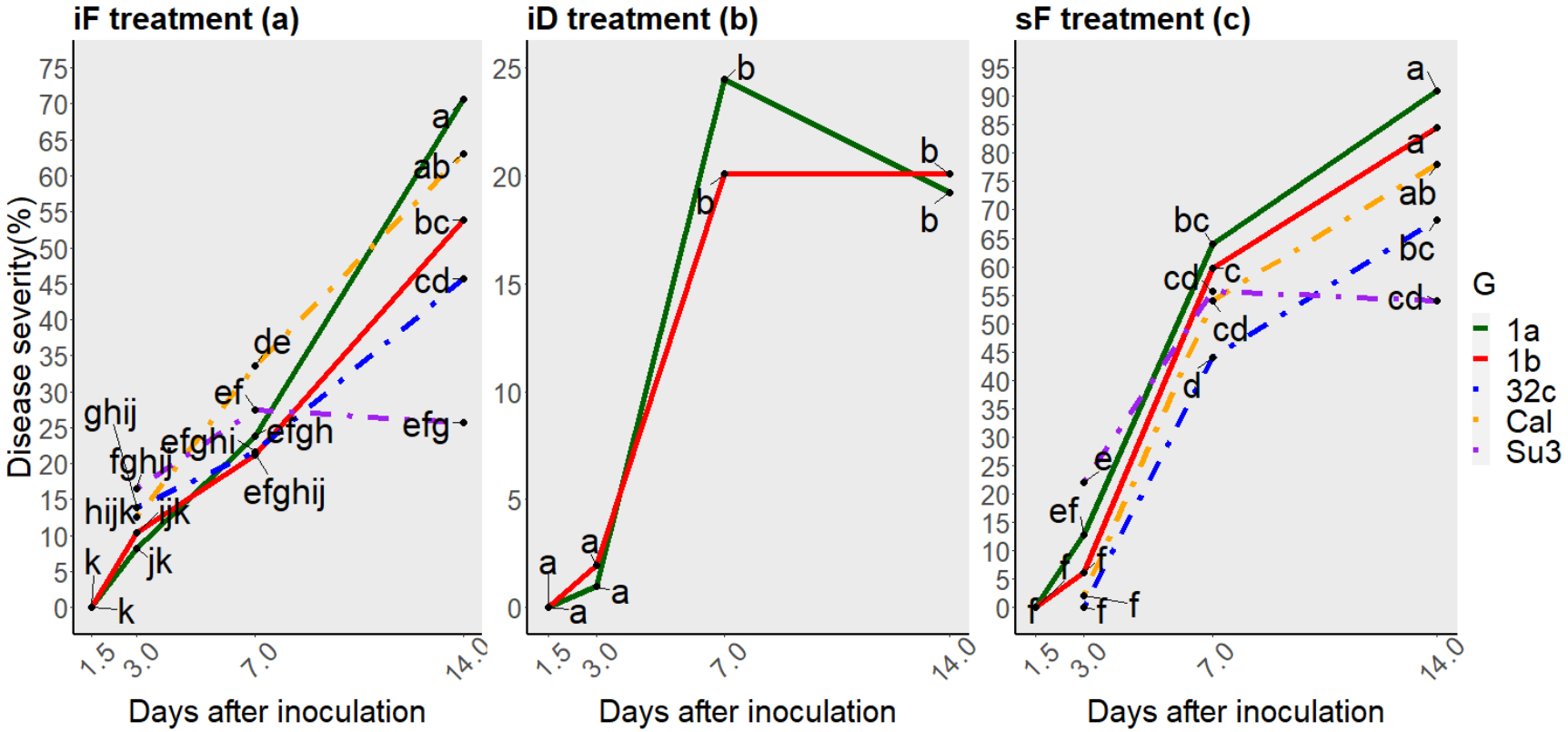

Figure 5.2 Disease severity of infected wheat spikes of five genotypes under the following three inoculation methods: (a) point inoculated with a macroconidal mixture of two 3ADON *F. graminearum* isolates (iF treatment), (b) point injected with a pure deoxynivalenol solution (iD treatment) and (c) spray inoculated with the same mixture (sF treatment). The five genotypes (G) are Maris Huntsman *Rht-B1a* NIL (1a) and *Rht-B1b* NIL (1b), 32c*17(32c), Caledonia (Cal) and Sumai 3 (Su3). The four time points are 1.5, 3, 7, 14 days after inoculation (dai). Letters indicate significant differences ($P < 0.05$) among genotypes across all time points in individual treatments using Fisher's LSD test.

5.3.2 Relative expression of genes in qPCR tests

In this project, expression of *Fusarium* and wheat genes relative to their housekeeping genes were measured from cDNA derived from mRNA in qPCR. Log 10 data transformation of all genes tested provided better normality than untransformed expression data in statistical analyses, thus all the following results and discussion on relative expression of genes in qPCR are based on the transformed data.

5.3.2.1 Four Fusarium *TRI* genes involved in the deoxynivalenol biosynthesis pathway in the iF and sF treatments

Relative expression of four genes (*TRI5*, *TRI6, TRI12* and *TRI101*) involved in the deoxynivalenol biosynthesis pathway were measured in both iF and sF treatments. Based on the combined analysis of variance there were significant differences for the main effect T and the interactions Trt*T and Trt*G*T for relative expression of all *TRI* genes (**Appendix 5.3**). The main effect Trt was significant for all *TRI* genes except *TRI5,* while the G main effect was significant for all *TRI* genes except *TRI6* (**Appendix 5.3**). To better understand the interactions with treatment, the relative expression of all *TRI* genes was separately analyzed across all genotypes and time points under each treatment (**Appendix 5.4)**. Analysis of variance indicated that the two main effects for T and G were significant for all *TRI* gene expression in the iF treatment, but in the sF treatment only the main effect T was significant for all *TRI* genes (**Appendix 5.4**). In the iF treatment, the main effect for part and the interaction G*T was significant for all *TRI* genes except *TRI101*, while the interaction for T*Part was significant for all *TRI* genes except *TRI5*. The interaction G*Part was

significant for *TRI5* and *TRI6*. One three-way interaction for G*T*Part was significant for all *TRI* genes except *TRI12* (**Appendix 5.4**). In the sF treatment, there was one significant interaction, G*T, for all *TRI* genes except *TRI12* (**Appendix 5.4**).

Means comparisons for the significant interaction G*T on all *TRI* genes in individual treatments were conducted (**Figure 5.3**). In general, the expression levels of all four *TRI* genes increased and reached a peak 3 dai and then decreased 7 dai and 14 dai (**Figure 5.3**). All *TRI* genes in all genotypes (except *TRI101* in the BIS part of the *Rht-B1b* NIL in the iF treatment 14 dai) were upregulated in both treatments across all four time points (**Figure 5.3**). For the two NILs, expression of all *TRI* genes for the *Rht-B1a* NIL peaked at 3 dai and then declined in both treatments, while the *Rht-B1b* NIL generally had a decreasing trend for the expression of all *TRI* genes except *TRI6* in the iF treatment and was relatively stable for the expression of all *TRI* genes except *TRI6* in the sF treatment (**Figure 5.3**). Expression of all *TRI* genes for the three checks often followed a decreasing trend for the expression of all *TRI* genes in both treatments, except *TRI5* and *TRI12* in Su3 14 dai in the iF treatment and *TRI101* in 32c 3 dai in the sF treatment (**Figure 5.3 a**, **e** and **h**).

Comparing expression pattern differences between the two-way interaction G*T and the three-way interaction G*T*Part, expression of *TRI5* and *TRI12* for both parts and of *TRI101* for the BIS of the *Rht-B1a* NIL peaked at 3 dai and then declined in the iF treatment (**Figure 5.4 a c** and **d**), which was the same as the trend in **Figure 5.3 a**, **e** and **g**. Both parts of the *Rht-B1b* NIL had a decreasing trend for the expression of all four *TRI* gene (**Figure 5.4**), which was the same as the trend in **Figure 5.3 a**, **e** and **g**. For the three checks, expression of *TRI5* for the IS part of 32c and

Cal declined from 7 dai to 14 dai, while expression of *TRI5* for the IS part of Su3 and the BIS part of all three checks were relative stable (**Figure 5.4a**).

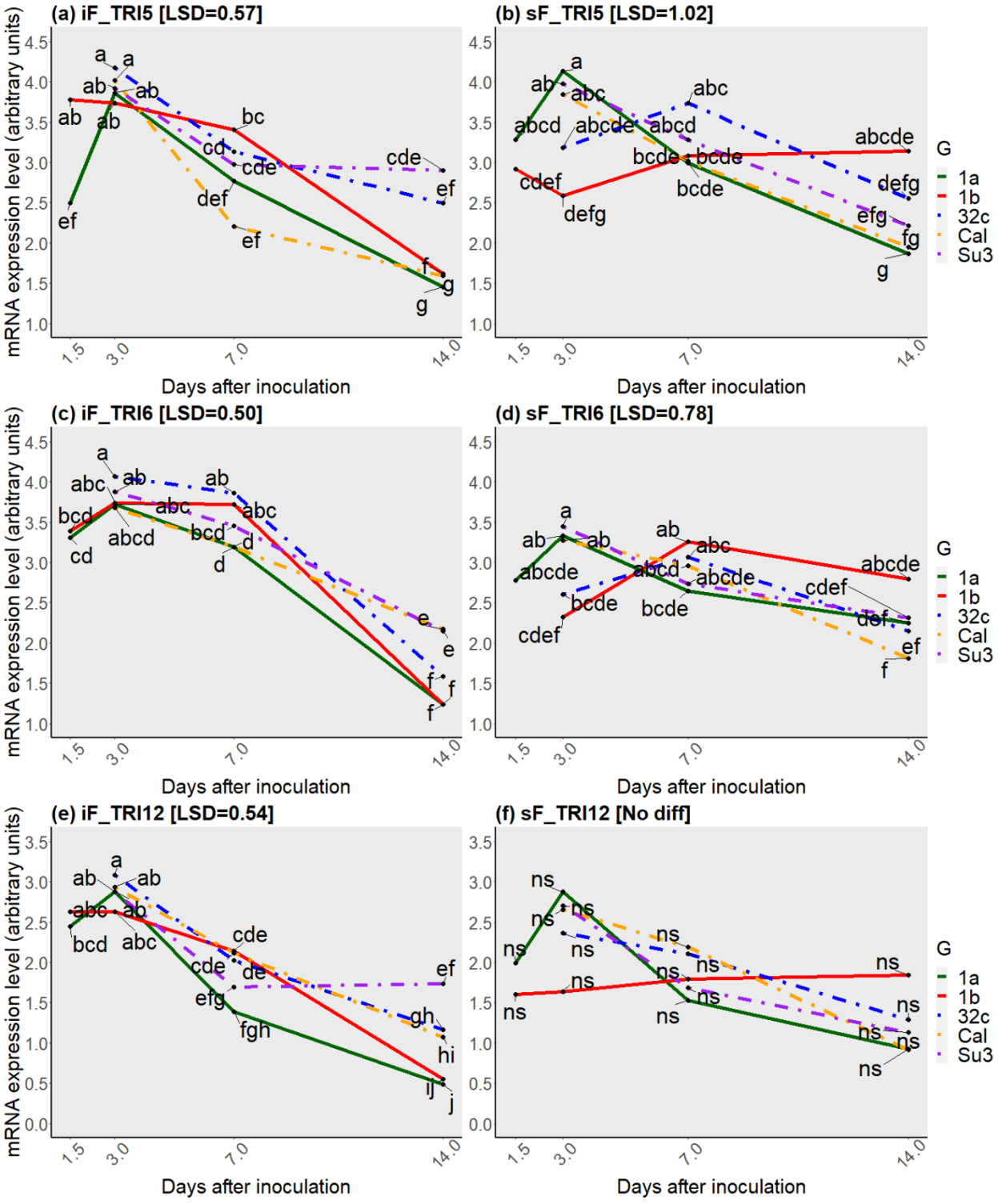

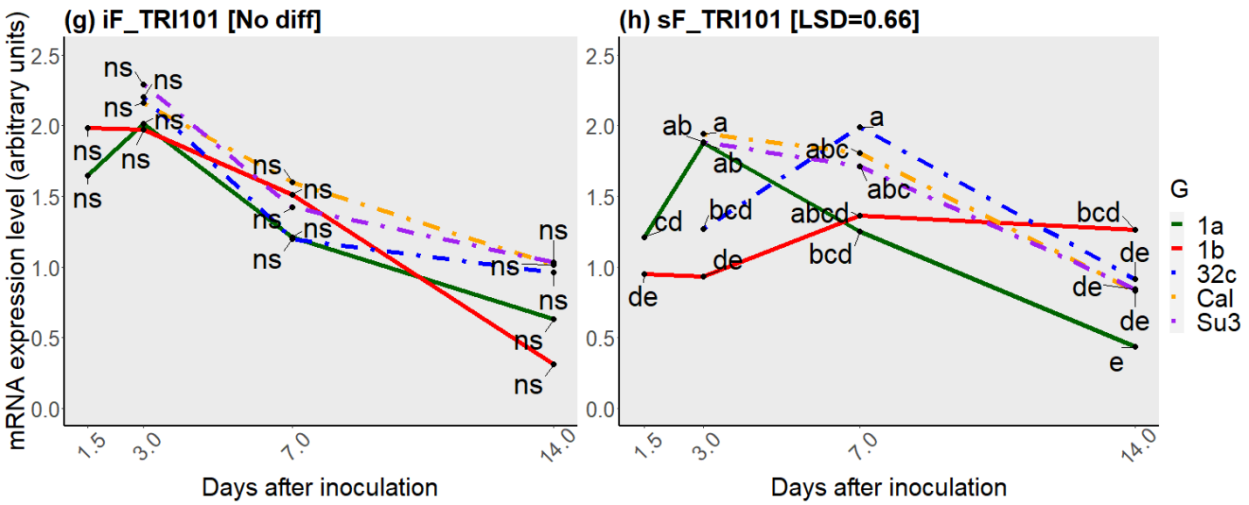

Figure 5.3 Relative expression of four *TRI* genes (*TRI5*, *TRI6*, *TRI12* and *TRI101*) related to DON biosynthesis pathway under a two-way interaction among genotype and time point in the following individual treatments: (a, c, e, g) point inoculated *Fusarium* (iF) and (b, d, f, h) spray inoculated *Fusarium* (sF). No significant expression difference for *TRI12* in the sF treatment and *TRI101* in the iF treatment indicates as "No diff" and "ns" (f and g). The five genotypes (G) are Maris Huntsman *Rht-B1a* NIL (1a) and *Rht-B1b* NIL (1b), 32c*17(32c), Caledonia (Cal) and Sumai 3 (Su3). The four time points are 1.5, 3, 7, 14 days after inoculation (dai). Expression of (a, b) *TRI5* and (g, h) *TRI101* were related to an early and middle stage of the biosynthesis pathway, respectively. Expression of (b, c) *TRI6* and (e, f) *TRI12* were related to a global transcription regulator mediating cellular metabolism and the entire DON biosynthesis pathway and toxin efflux pump, respectively. Mean of relative expression with log10 transformation for each genotype at each time point is shown, and least significant difference (LSD) values are shown. Letters indicate significant differences ($P < 0.05$) among means comparisons of the G*T interaction using Fisher's LSD test in each treatment.

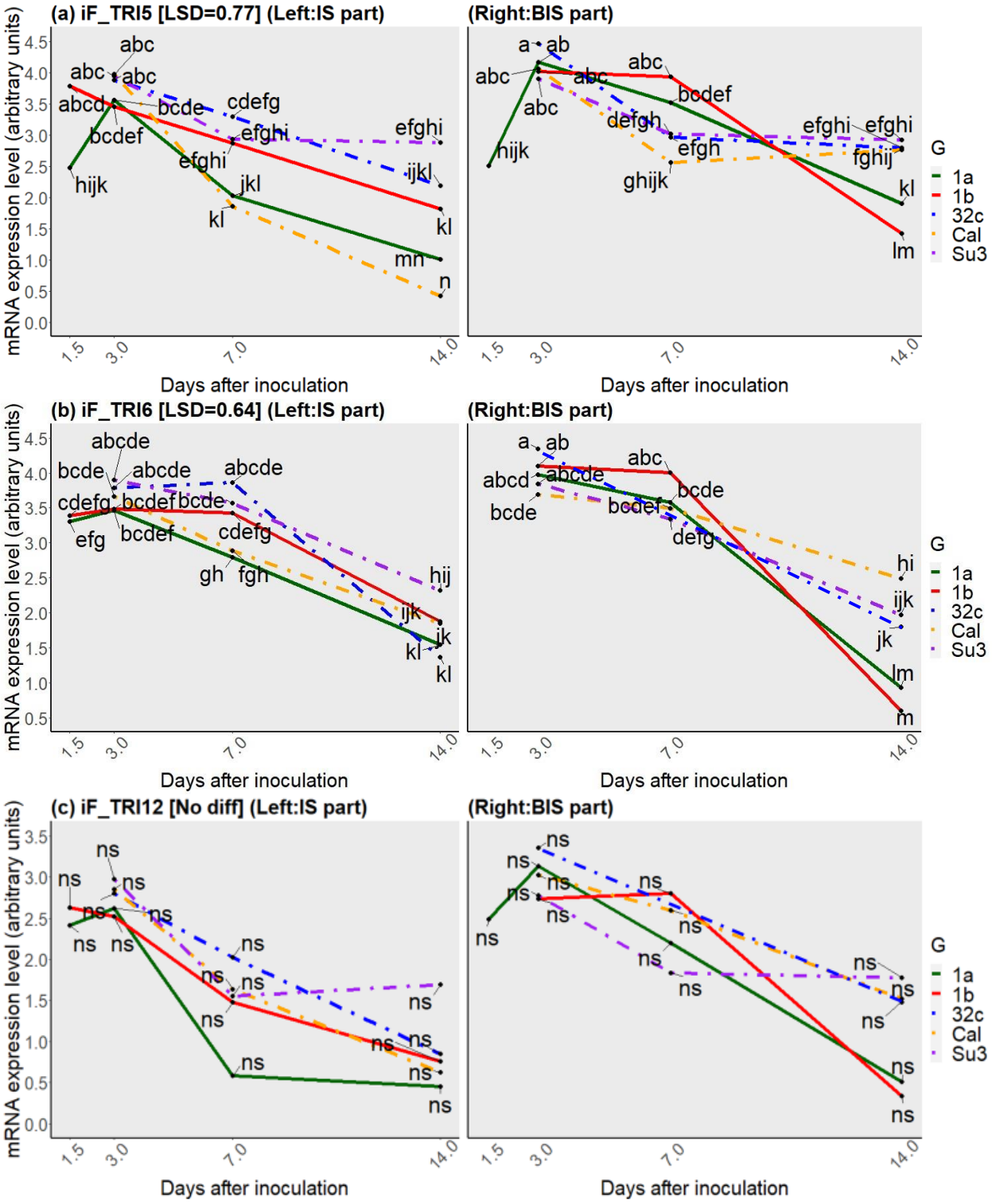
(a) iF_TRI5 [LSD=0.77] (Left:IS part)
(Right:BIS part)
(b) iF_TRI6 [LSD=0.64] (Left:IS part)
(Right:BIS part)
(c) iF_TRI12 [No diff] (Left:IS part)
(Right:BIS part)
mRNA expression level (arbitrary units)
Days after inoculation
1.5
3.0
7.0
14.0
G
1a
1b
32c
Cal
Su3

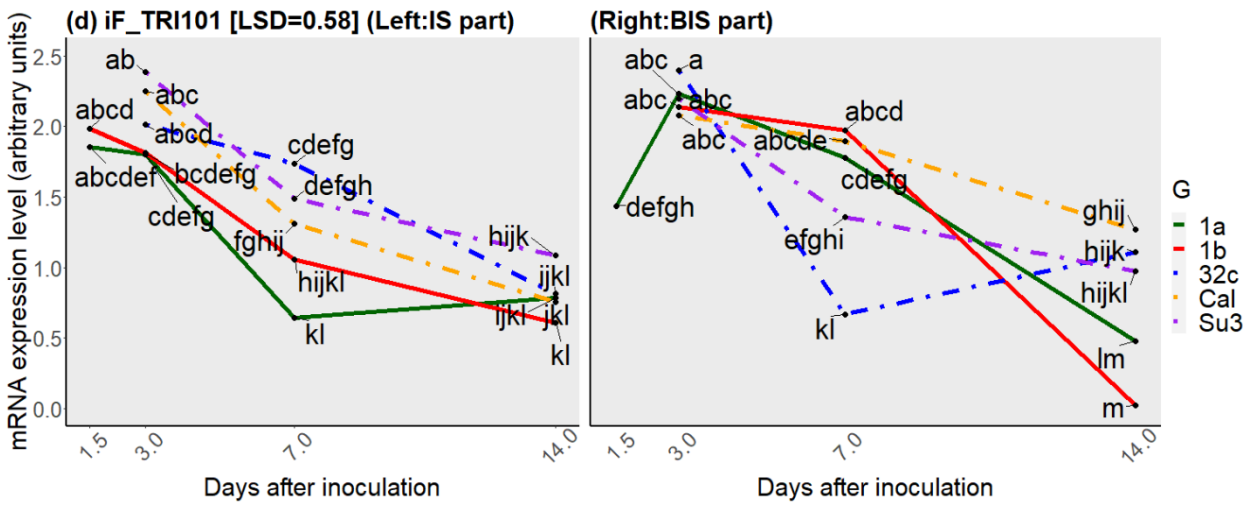

Figure 5.4 Relative expression of all four *TRI* genes (*TRI5*, *TRI6*, *TRI12* and *TRI101*) related to DON biosynthesis pathway under a three-way interaction among part, genotype and time point in the point inoculated *Fusarium* treatments (a-d). No significant expression difference for *TRI12* indicates as "No diff" and "ns" (c). The two parts (IS and BIS part) were the inoculated spikelets and the spikelets below the inoculation points. The five genotypes (G) are Maris Huntsman *Rht-B1a* NIL (1a) and *Rht-B1b* NIL (1b), 32c*17(32c), Caledonia (Cal) and Sumai 3 (Su3). The four time points are 1.5, 3, 7, 14 days after inoculation (dai). Mean of relative expression with log10 transformation for each part of each genotype at each time point is shown, and least significant difference (LSD) values are shown. Letters indicate significant differences ($P < 0.05$) among means comparisons of the G*T*Part interaction using Fisher's LSD test in each treatment. Lines belonging to the IS part are shown in the left side and lines belonging to the BIS part are shown in right side. Y axis labels in the BIS part are the same as y axis in IS part.

5.3.2.2 Response of two wheat genes, *ABCC6* and *NFXL1*, to the iF, sF and iD treatments

Based on the combined analysis of variance for expression of *ABCC6* and *NFXL1*, all main effects were significant (**Appendix 5.3**). The two-way interactions G*T and Trt*Part were significant for both genes and the Trt*G interaction was significant for *NFXL1*, but not *ABCC6*. All three-way interactions and the four-way interaction were significant. To investigate the nature of some of the key interactions, relative expression of both genes was separately analyzed across all genotypes and time points under each treatment (**Appendix 5.5**). The main effect T was significant for both genes in all treatments, and the three-way interaction G*T*Part was not significant for both genes in all treatments (**Appendix 5.5**). In the iF treatment, the two main effects G and Part and the interactions for G*T and T*Part were significant for both genes. In the iD treatment, the main effect for Part and the interactions for T*Part were significant for both genes. The main effect for G was significant for *ABCC6* and the interaction for G*T and the replicate effect were significant for *NFXL1*. In the sF treatment, the main effect for G and the interaction for G*T were significant for both genes.

Means comparisons for the G*T interaction within treatments were conducted (**Figure 5.5**). For the two NILs, expression of *ABCC6* for both NILs peaked at 3 dai or 7 dai and then declined in both iF and sF treatments, where the line of the *Rht-B1a* NIL crossed over with the line of the *Rht-B1b* NIL in the both treatments (**Figure 5.5 a1** and **a3**). Meanwhile, expression of *ABCC6* in both NILs declined in the same pattern in the iD treatment (**Figure 5.5 a2**). Expression of *NFXL1* increased for the *Rht-B1a* NIL over all the time points in both the iF and sF treatments, while expression of this gene for the *Rht-B1b* NIL peaked at 3 or 7 dai and then declined in all three treatments (**Figure 5.5 b1, b2** and **b3**). For the three checks, Su3 and 32c had similar expression

of *ABCC6* and *NFXL1* in the iF treatment (**Figure 5.5 a1** and **b1**), while the three checks had similar expression pattern for *ABCC6* and *NFXL1* in the sF treatment, except Su3 3 dai (**Figure 5.5 a3** and **b3**).

5.3.2.3 Two wheat genes (*AOS* and *JAZ1*) related to jasmonic acid hormone biosynthesis and signaling pathway and three wheat genes (*PR1b, PR4* and *PDF1.2*) involved in defense responses in the iF, sF and iD treatments

Based on the combined analysis of variance, there were significant differences for the two main effects for Trt and T and the interactions Trt*G*T, Trt*T*Part and G*T*Part for expression or all five genes (*AOS, JAZ1*, *PR1b*, *PR4* and *PDF1.2*), while the main effect for Part and the interaction T*Part were not significant for all five genes (**Appendix 5.3**). The main effect for G and the interactions Trt*G were significant for all genes except *PDF1.2*, while the interactions G*T, Trt*Part and G*Part were significant for single genes, *PDF1.2*, *AOS* and *PR1b*, respectively (**Appendix 5.3**).

Due to the significant Trt*G*T interaction, relative expression of the five genes was separately analyzed across all genotypes and time points under each treatment (**Appendix 5.5)**. In the iF treatment, the main effect T was significant for all five genes (**Appendix 5.5**). The main effect for G was significant for all genes except *PR1b* and the main effect Part was significant for all genes except *JAZ1*. There were other significant interactions including G*Part for all genes except *PDF1.2*, G*T for *AOS*, *PR4* and *PDF1.2*, and T*Part for all three host defense response genes

(*PR1b*, *PR4* and *PDF1.2*). The three-way interaction G*T*Part was significant for *PR4* and *PDF1.2* (**Appendix 5.5**).

In the iD treatment, the main effect for part was significant for all genes except JAZ1 and the other main effect T was significant for all three host defense response genes (*PR1b*, *PR4* and *PDF1.2*) (**Appendix 5.5**). No significant difference was found in the main effect G for all genes. There was a significant interaction G*T for all genes except *PR1b*. Other significant interactions included G*Part for *JAZ1*, *PR1b* and *PR4* and T*Part for *PR4*. The three-way interaction G*T*Part was significant for *JAZ1* (**Appendix 5.5**). In the sF treatment, the two main effects G and T were significant for all genes except *PDF1.2* and the interaction for G*T was significant for all genes except *PR1b*. Other significant factors included the main effect Part for *JAZ1*, the three-way interaction G*T*Part for *PR1b*, and replicate for *AOS* (**Appendix 5.5**).

Means comparisons for the G*T interaction within treatments for gene expression of *AOS*, *JAZ1* *PR1b*, *PR4* and *PDF1.2* were conducted (**Figure 5.5**). For the two NILs, expression of *AOS* in the *Rht-B1a* NIL often declined first at 3 dai or 7 dai and then increased in all three treatments (iF, iD and sF), while expression of this gene in the *Rht-B1b* NIL maintained relative stable in the iF treatment, increased first and then declined at 7 dai in the iD treatment, and remained stable and then increased at 7 dai in the sF treatment (**Figure 5.5 c1**-**3**). Expression of *JAZ1* in both NILs generally increased over time in both iF and sF treatments, except the *Rht-B1a* NIL at 14 dai in the sF treatment (**Figure 5.5 d1** and **d3**). Notably, expression of *JAZ1* in both NILs is similar to expression of *AOS* in the iD treatment (**Figure 5.5 c2** and **d2**). Expression of *PR4* in *Rht-B1a* NIL generally increased over time, except at 3 dai in iD treatment, while expression of *PR4* in *Rht-B1b*

NIL increased first and then declined at 3 dai or 7 dai in all the three treatments (**Figure 5.5 f1-3**). For the three checks, Su3 and 32c generally had similar expression patterns for *AOS*, *JAZ1* and *PR4* in both iF and sF treatments, which generally increased from 3 dai to 7 dai (**Figure 5.5 c1**, **c3**, **d1**, **d3**, **f1** and **f3**). Expression of *PDF1.2* for most of five genotypes was down-regulated in most time points in all three treatments (**Figure 5.5 g1-3**).

Means comparison for the significant interactions G*Part were conducted for the iF treatment for *JAZ1* and *PR1b* and the iD treatment for *PR1b* (**Appendix 5.6**). In the iF treatment for the two NILs, the IS part of the *Rht-B1b* NIL had a higher expression level of *PR1b* than that of the *Rht-B1a* NIL, but the BIS part of the *Rht-B1b* NIL had lower expression levels of *JAZ1* and *PR1b* than that of the *Rht-B1a* NIL (**Appendix 5.6 a** and **b**). For the three checks, both parts of Cal generally had higher abundance of *JAZ1* transcripts than those of Su3 and 32c (**Appendix 5.6 a**). In the iD treatment for the two NILs, the IS part of the *Rht-B1a* NIL had a lower expression level of *PR1b* than the BIS part, while there was no significant difference between the IS and BIS parts of the *Rht-B1b* NIL (**Appendix 5.6 c**).

Means comparison for the significant interactions G*T*Part within treatments were conducted (**Figure 5.6**). In the iF treatment, expression of *PR4* in the *Rht-B1a* NIL remained relatively stable in the IS part and increased first and then stabilized at 7 dai in the BIS part, while expression of *PR4* in the *Rht-B1b* NIL generally increased first and then declined in both parts (**Figure 5.6 a**). Expression of *PDF1.2* in the *Rht-B1a* NIL declined first and then increased at 7 dai in the IS part and slowly declined over time in the BIS part, while expression of this gene in the *Rht-B1b* NIL increased first and then decline at 7 dai in the BIS part (**Figure 5.6 b**). In the iD treatment,

expression of JAZ1 in the *Rht-B1a* NIL declined first and then increased in the IS part and remained relative stable in BIS part, while expression of this gene in the *Rht-B1b* NIL increased first and then declined at 7 dai in both parts (**Figure 5.6 c**). In the sF treatment, expression of *PR1b* in the IS part of the *Rht-B1a* NIL is the similar to the BIS part of the *Rht-B1b* NIL, where the gene expression increased first, declined at 3 dai and then increased again at 7 dai. Meanwhile, expression of *PR1b* in the BIS part of the *Rht-B1a* NIL is the similar to the IS part of the *Rht-B1b* NIL, where the expression increased and declined at 7 dai (**Figure 5.6 d**). For the three checks, expression of *PR4* in Cal in the iF treatment increased first and then declined in both parts, while expression of this gene in 32c and Su3 declined over time in the IS part and increased first and then declined in the BIS part (**Figure 5.6 a**). Expression of *PDF1.2* in 32c increased first and then declined at 7 dai in both parts (**Figure 5.6 b**). Due to missing data, expression patterns of *PDF1.2* for the *Rht-B1b* NIL, Cal and Su3 remains unknown (**Figure 5.6 b**).

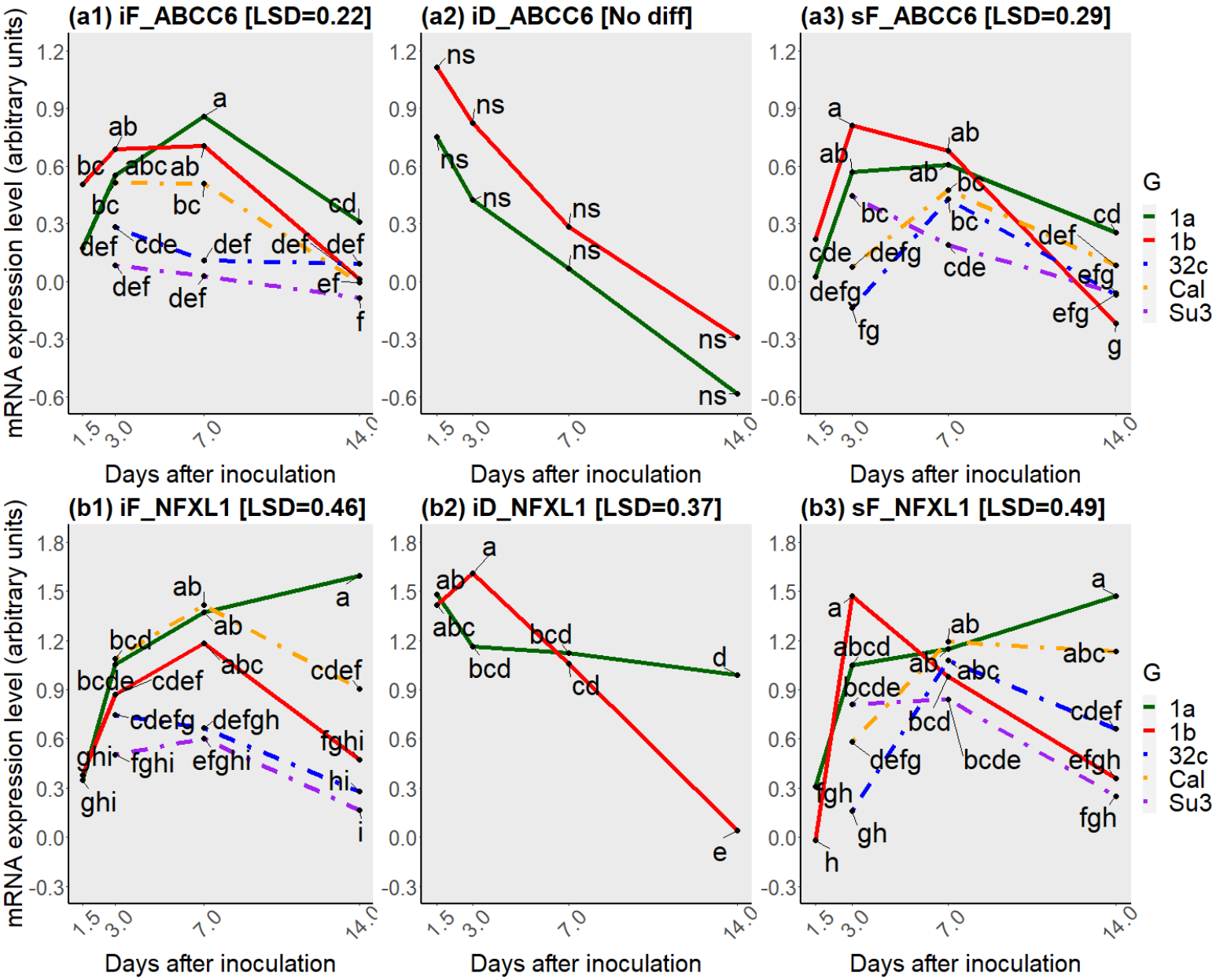
(a1) iF_ABCC6 [LSD=0.22]
(a2) iD_ABCC6 [No diff]
(a3) sF_ABCC6 [LSD=0.29]
(b1) iF_NFXL1 [LSD=0.46]
(b2) iD_NFXL1 [LSD=0.37]
(b3) sF_NFXL1 [LSD=0.49]
mRNA expression level (arbitrary units)
Days after inoculation
1.5
3.0
7.0
14.0
G
1a
1b
32c
Cal
Su3

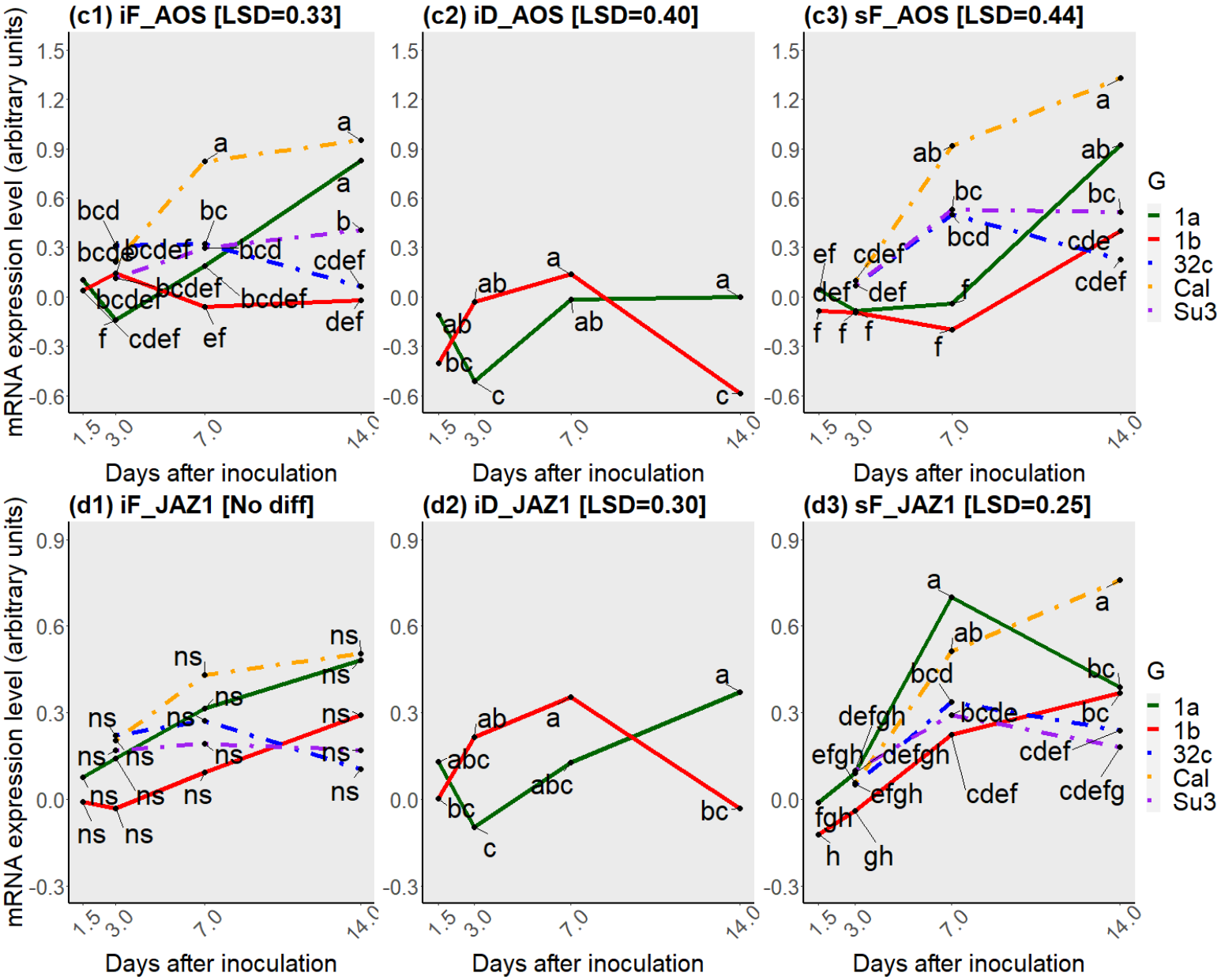
(c1) iF_AOS [LSD=0.33]
(c2) iD_AOS [LSD=0.40]
(c3) sF_AOS [LSD=0.44]
(d1) iF_JAZ1 [No diff]
(d2) iD_JAZ1 [LSD=0.30]
(d3) sF_JAZ1 [LSD=0.25]
mRNA expression level (arbitrary units)
Days after inoculation
1.5
3.0
7.0
14.0
G
1a
1b
32c
Cal
Su3

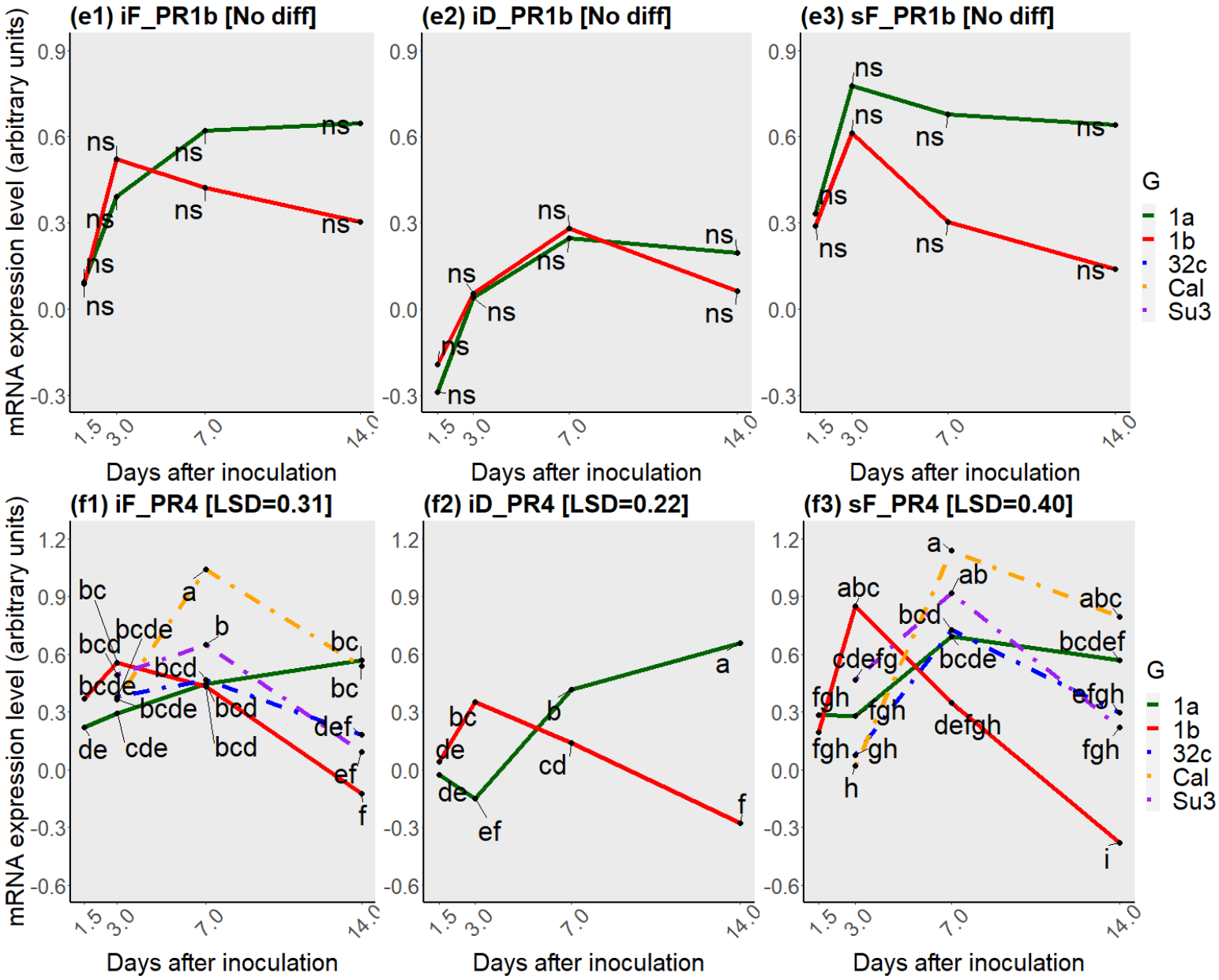
(e1) iF_PR1b [No diff]
(e2) iD_PR1b [No diff]
(e3) sF_PR1b [No diff]
(f1) iF_PR4 [LSD=0.31]
(f2) iD_PR4 [LSD=0.22]
(f3) sF_PR4 [LSD=0.40]
mRNA expression level (arbitrary units)
Days after inoculation
1.5
3.0
7.0
14.0
G
1a
1b
32c
Cal
Su3

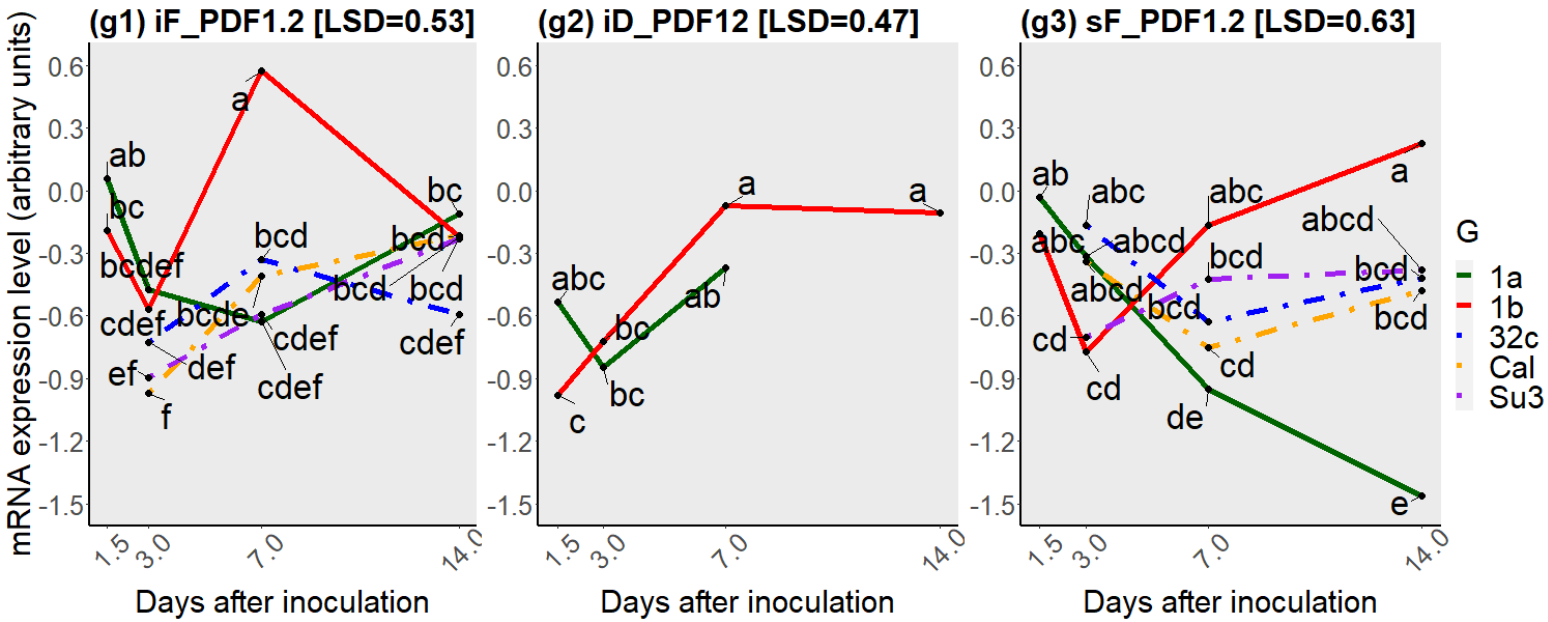

Figure 5.5 Relative expression of seven wheat genes (*ABCC6*, *NFXL1*, *AOS*, *JAZ1*, *PR1b*, *PR4* and *PDF1.2*) under a two-way interaction among genotype and time point in the following individual treatments: (a1-g1) point inoculated *Fusarium* (iF), (a2-g2) point injected DON (iD) and (a3-g3) spray inoculated *Fusarium* (sF). The five genotypes (G) are Maris Huntsman *Rht-B1a* NIL (1a) and *Rht-B1b* NIL (1b), 32c*17 (32c), Caledonia (Cal) and Sumai 3 (Su3). The four time points are 1.5, 3, 7, 14 days after inoculation (dai). Mean of relative expression with log10 transformation for each genotype at each time point is shown, and least significant difference (LSD) values are shown. Letters indicate significant differences ($P < 0.05$) among means comparisons of the G*T interaction using Fisher's LSD test in each treatment. Due to missing data, there was no expression of *PDF1.2* in the *Rht-B1a* NIL at 14 dai in the iD treatment.

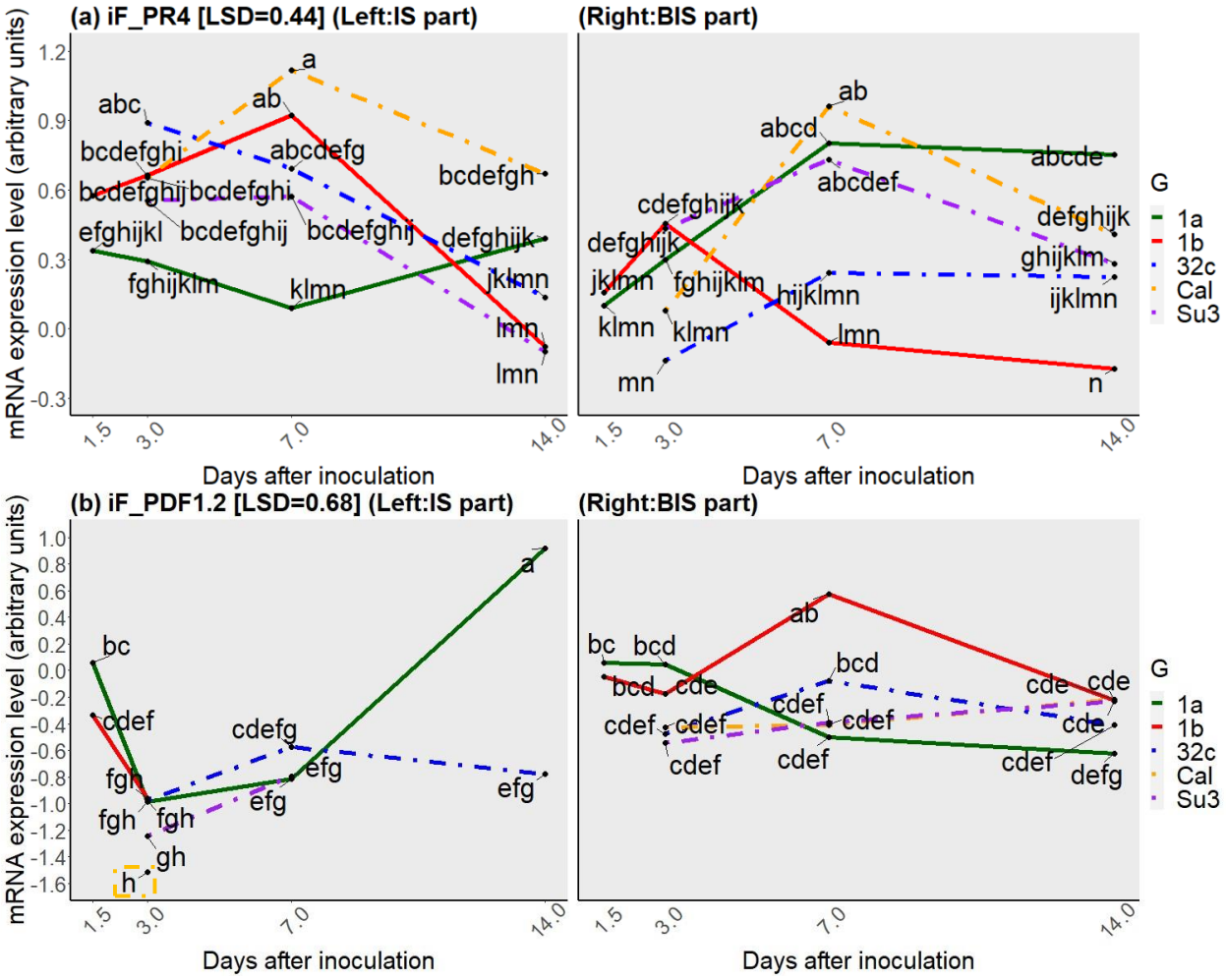
(a) iF_PR4 [LSD=0.44] (Left:IS part)
(Right:BIS part)
mRNA expression level (arbitrary units)
Days after inoculation
(b) iF_PDF1.2 [LSD=0.68] (Left:IS part)
(Right:BIS part)
G
1a
1b
32c
Cal
Su3

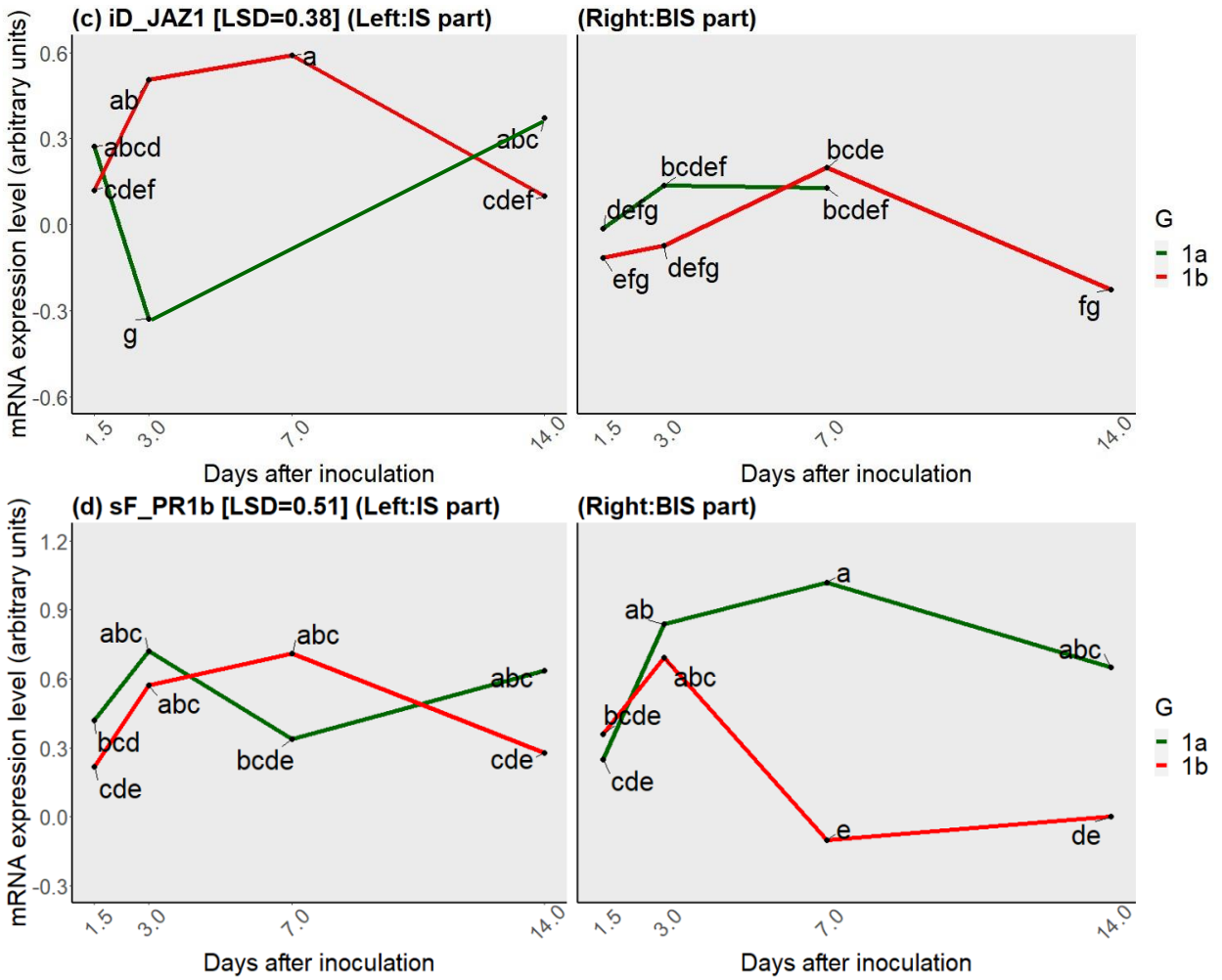

Figure 5.6 Relative expression of four wheat genes (*PR4*, *PDF1.2*, *JAZ1* and *PR1b*) under a three-way interaction among part, genotype and time point in individual treatments: (a) *PR4* and (b) *PDF1.2* in the point inoculated *Fusarium* treatment (iF), (c) *JAZ1* in the point inoculated deoxynivalenol treatment (iD) and (d) *PR1b* in spray inoculated *Fusarium* treatment (sF). The two parts (IS and BIS part) are the inoculated and neighboring spikelets. The four time points are 1.5, 3, 7 and 14 days after inoculation (dai). The five genotypes (G) are Maris Huntsman *Rht-B1a* NIL (1a) and *Rht-B1b* NIL (1b), 32c*17(32c), Caledonia (Cal) and Sumai 3 (Su3). Mean of relative expression with log10 transformation for each part of each genotype at each time point is shown, and least significant difference (LSD) values are shown. Letters indicate significant differences ($P < 0.05$) among means comparisons of the G*T*Part interaction using Fisher's LSD test in each treatment. To improve readability, lines belonging to the IS part are shown in the left side and lines belonging to the BIS part are shown in right side. Due to missing date, lines in certain time points for different genotypes are shortened, especially in the IS part for *PDF1.2*, where Cal only had one time point at 3 dai with a highlighted dotted square and both the *Rht-B1b* NIL and Su3 had shorter lines. Y axis labels in the BIS are the same as y axis in IS part.

5.4 Discussion

FHB caused by *Fg* is one of the most important diseases in wheat. There are five different types of active resistance to reduce disease infection. Studying host-pathogen interactions under three different treatments provided insights into the role of different defense mechanisms on host resistance. The iF treatment injected a high concentration of spore solution inside inoculated spikelets, which is thought to trigger Type II resistance to disease spread in the host. The iD treatment directly injected a high concentration of mycotoxin DON into spikelets and assessed the defense mechanism related to Type V resistance (DON resistance). The sF treatment sprayed the spore solution over the surface of spikelets and the opening area between palea and lemma, triggering Type I resistance to initial disease infection. As expected, plant height was not affected by inoculation methods (**Table 5.2** and **Appendix 5.2**). Plant heights for each genotype matched with the previous knowledge, especially the significant height difference between the two NILs (**Appendix 5.2**).

5.4.1 Expression of *TRI* genes in the five genotypes in the iF treatment

Based on phenotyping between the two NILs in the iF treatment (**Figure 5.2 a**), the semi-dwarf *Rht-B1b* NIL had less severity than the wildtype *Rht-B1a* NIL 14 dai, which suggested that the semi-dwarf allele was associated with higher Type II resistance (Saville et al. 2012). The three checks were significantly different from each other 14 dai (**Figure 5.2 a**), where Cal and Su3 had the highest and lowest severity 14 dai, respectively, and 32c was in the middle. Notably, disease severity did not increase in Su3 after 7 dai under both treatments (**Figure 5.2 a** and **c)** which was

associated with no change of expressional levels of *TRI5* and *TRI12* (**Figure 5.3 a** and **e** and **Figure 5.4 a)**. The total number of the discolored spikelets for Cal, 32c and Su3 was 5.60, 4.53 and 3.00, respectively, 14 dai. When considering the BIS part (the four spikelets below the inoculation points), the number of remaining healthy spikelets for Cal, 32c and Su3 were 0.40, 1.47 and 3.00, respectively, 14 dai.

Initially, the assumption of this experiment was that higher expression levels of *TRI* genes would associate with the genotypes having higher disease symptoms. Based on the phenotypic and genetic results of this study (**Figures 5.2 a** and **5.3 a**, **c** and **e**), among the three checks, Cal generally had lower expression levels of *TRI5* and *TRI6* than that of 32c and Su3 7 dai and lower expression levels of *TRI5* and *TRI12* than that of 32c and Su3 14 dai, which was different from the initial assumption. However, the BIS part of Cal generally had higher expression levels of *TRI6* and *TRI101* than 32c and Su3 7 dai and 14 dai (**Figure 5.4 b** and **d**). This matched with the initial assumption that the BIS part of Cal with only 0.4 remaining healthy spikelets was associated with higher *TRI* gene expression than that of 32c and Su3 with 1.47 and 3.00 remaining healthy spikelets, respectively, 14 dai.

Notably, lower expression of *TRI5* and *TRI6* in Cal than 32c and Su3 (**Figure 5.3 a**, **c** and **e**) was mainly from the IS part, where the IS part of Cal generally had lower expression levels of *TRI5* and *TRI6* than Su3 and 32c 7 dai and 14 dai (**Figure 5.4 a** and **b**). This implied that the IS part of Cal had lower expression levels of *TRI* genes than that of 32c and Su3, which was different from the BIS part of the three checks. One of possible explanation is that disease spread quickly in Cal and there is less need for more DON from the pathogen at the later time points.

For the two NILs, the *Rht-B1a* NIL with higher severity had lower expression levels of *TRI5*, *TRI6* and *TRI12* than the *Rht-B1b* NIL (**Figure 5.2 a** and **Figure 5.3 a**, **c** and **e**), which was also different from the initial assumption that higher expression levels of *TRI* genes would associate with the genotypes having higher disease symptoms. Furthermore, between the two NILs, lower expression levels of *TRI5* were found in the IS part in the *Rht-B1a* NIL compared to *Rht-B1b* NIL at all three time points except 3 dai (**Figure 5.4 a**). Therefore, based on the above mentioned observations in the two NILs and three checks, it was hypothesized that due to the nature of the point inoculation method, the pathogen *Fusarium* might have different *TRI* gene expression inside the inoculated spikelets (as the IS part in this study) and the spikelets below the inoculation points (as the BIS part in this study) in response to different hosts with various resistant levels.

In the iF method, the IS part initially received a high concentration of *Fg* solution, which makes it relatively easy for the pathogen to colonize the inoculated spikelets. *Fusarium* could quickly colonize the IS part of susceptible wheat, and the pathogen may not need to maintain the high production of DON in the IS part. Moreover, *Fg* in the IS part of resistant wheat might encounter stronger host defense than in susceptible wheat, and the pathogen may need to produce higher DON during the colonization of infected spikelets in more resistant wheat genotypes. This might explain the association between higher expression levels of DON biosynthesis genes and stronger host defenses within the inoculated points.

Meanwhile, the BIS part in the point inoculation method initially has no *Fusarium* and later shows discoloration symptoms due to invading mycelia from the inoculated spikelets. *Fusarium* in the BIS part of susceptible wheat might encounter weaker host defense than that in resistant wheat,

and it may be easier for the pathogen to increase *TRI* gene expression and produce higher DON during the colonization of the neighboring spikelets in susceptible wheat than in resistant wheat.

Similar associations between *TRI* gene expression and resistance of genotypes have been reported in another study using a point inoculation method (Amarasinghe and Fernando 2016). In a detailed time series qPCR study with 3ADON isolates point inoculated in wheat, higher expression levels of seven genes (including *TRI5*, *TRI6* and *TRI12*), which are closely involved in the DON biosynthesis pathway, were found in a moderately resistant cultivar, Carberry, than in a susceptible cultivar, Roblin, 2 dai to 14 dai (Amarasinghe and Fernando 2016).

In a study for *TRI5* gene expression by a point inoculation method, both resistant and susceptible lines (Alsen and Wheaten) had lower expression close to inoculation sites and higher expression away from inoculation sites 6 to 21 dai (Hallen-Adams et al. 2011). In a spatial study for expression of five *TRI* genes in a susceptible wheat Bobwhite inoculated by point inoculation, different expression levels of *TRI* genes, including *TRI5* and *TRI6*, were observed in different sequential rachis internodes below the inoculation points, where there was a higher abundance of *TRI* transcripts in tissue without disease symptoms and further away from the inoculation points and lower expression in tissue with symptoms and close to inoculation points (Brown et al. 2011). Matching with the previous two studies, the BIS part in this study also generally had higher expressional levels of *TRI5*, *TRI6* and *TRI101* than the IS part for the five genotypes (**Figure 5.4**).

By studying the inoculated spikelets and the spikelets below the inoculation points in a point inoculation method, this study provided insight into how the pathogen alters its *TRI* gene

expression in spatial and temporal changes. This could explain the association of *TRI* gene expression and resistance of genotypes reported in previous studies (Brown et al. 2011; Hallen-Adams et al. 2011; Amarasinghe and Fernando 2016).

5.4.2 Expression of *TRI* genes in the five genotypes in the sF treatment

Based on phenotyping between the two NILs in the sF treatment (**Figure 5.2 c**), unlike Saville et al (2012), there were few significant differences between the two NILs for disease severity. Additional experiments in both field and indoor tests would be required to examine whether the current indoor spray inoculation tests would provide the same results as field spray inoculation tests. In the three checks, Su3 had higher severity than Cal and 32c in the early time point (3 dai), then had similar severity with the other two checks in the middle time point (7 dai) and finally showed less severity than Cal in the late time point (14 dai) (**Figure 5.2 c**). Average of numbers of spikelets in anthesis stage for each genotype (*Rht-B1a*, *Rht-B1b*, 32c, Cal and Su3) at the inoculation time were 9.09, 8.31, 8.17, 8.14 and 12.20, respectively. Thus, higher severity in Su3 than that in Cal and 32c 3 dai could associate with the higher numbers of spikelets flowering in Su3 than Cal and 32c at the inoculation time.

In the current spray inoculation method, the spikelets with flowering florets were referred as the IS part and the spikelets without anthesis florets were the BIS part. Unlike the iF treatment, there was no significant difference between the IS and BIS part in the sF treatment (**Appendix 5.4**). Comparing the two NILs, expressional levels of all *TRI* genes in the *Rht-B1a NIL* generally peaked 3 dai and then declined, while expression of all *TRI* genes except *TRI6* in the *Rht-B1b* NIL was

generally relatively stable across time points (**Figure 5.3 b**, **d**, **f** and **h**). Reasons for different expression patterns between the two NILs remain unknown. Among the three checks, 32c had lower expression levels of *TRI6* and *TRI101* than Su3 and Cal (**Figure 5.3 d** and **h**), respectively, which corresponded with phenotypic data that showed that 32c had no visible symptoms 3 dai, while all other genotypes had at least some level of discoloration.

Deoxynivalenol production and activation of the detoxification mechanism in a time series could be measured by high performance liquid chromatography or gas chromatography mass spectrometry in future studies in both resistant and susceptible genotypes. This would determine whether DON content in susceptible wheat is higher than in resistant wheat in early time points and whether DON content and/or activation of the detoxification mechanism in resistant wheat is still increasing in late time points.

5.4.3 Expression of seven wheat genes (*ABCC6, NFXL1, AOS, JAZ1, PR1b, PR4* and *PDF1.2*) in the five genotypes in the iF treatment

Several papers and reviews reported that two genes *ABCC3* and *ABCC6*, both encoding ATP-binding cassette transporter proteins, are often induced by *Fg* or DON and contribute DON tolerance (Chetouhi et al. 2016; Pierron et al. 2016; Gunupuru et al. 2017; Kazan and Gardiner 2018; Foroud et al. 2019; Brauer et al. 2020). The *NFXL1* gene encoding the NF-X1-type zinc finger protein was inducted by FHB infection and DON injection and might repress FHB resistance (Pan et al. 2018; Brauer et al. 2020; Haldar et al. 2021). A higher expression of *NFXL1* was found in a susceptible wheat Roblin than in a resistant wheat Wuhan 8 dai with DON (Brauer et al. 2020).

It was well known that *AOS* is associated with the increase of JA biosynthesis pathway in early FHB infection (Li and Yen 2008; Xiao et al. 2013; Ravensdale et al. 2014; Qi et al. 2016; Kazan and Gardiner 2018). *JAZ1* as the key repressor in the JA signaling pathway was also involved in FHB infection (Xiao et al. 2013; Ravensdale et al. 2014). The other three genes tested (*PR1b*, *PR4* and *PDF1.2*) were commonly involved in FHB resistance in wheat (Pritsch et al. 2000; Qi et al. 2012, 2016; Xiao et al. 2013).Up-regulation of *PR1b* and *PR4* genes and down regulation of *PDF1.2* were found four days after either FHB infection or exogenous JA injection (Qi et al. 2016).

In the iF treatment, a higher expression level of *ABCC6* (related to DON resistance) in the *Rht-B1b* NIL was observed in the very early time point (1.5 dai), while the lower expression of *NFXL1* (associated with weaker DON resistance) was found in the same genotype in the late time point (14 dai) (**Figure 5.5 a1** and **b1**). This matched the hypothesis that the *Rht-B1b* NIL has stronger Type II resistance than the *Rht-B1a* NIL. According to the interaction G*Part, a higher expression level of *PR1b* within the inoculated spikelets and a lower expression level of *JAZ1* in the spikelets below the inoculation points could also contribute to stronger Type II resistance of the *Rht-B1b* NIL (**Appendix 5.6 a** and **b**). On the other hand, a higher expression level of *PR1b* in the spikelets below the inoculation points in the *Rht-B1a* NIL also might not be sufficient to restrict the disease spreading among spikelets (**Appendix 5.6 c**). Interestingly, even though there was no difference in overall expression of *PR4* between the two NILs (**Figure 5.5 f1)**, the results in the three-way interaction G*T*Part revealed that the IS and BIS part of the *Rht-B1b* NIL had higher and lower expression of *PR4*, respectively, than that of the *Rht-B1a* NIL 7 dai (**Figure 5.6 a**), implying that different disease progress stages between the IS and BIS part could explain the different *PR4* expression patterns. Furthermore, based on **Figure 5.5 g1**, the *Rht-B1b* NIL up-regulated *PDF1.2*

expression 7 dai, while the *Rht-B1a* NIL down-regulated *PDF1.2* expression. The three-way interaction G*T*Part revealed an up-regulation of *PDF1.2* expression only occurred in the BIS part of the *Rht-B1b* NIL and down-regulations of *PDF1.2* expression were found in both parts of the *Rht-B1a* NIL, which might associate with stronger Type II resistance of the *Rht-B1b* NIL (**Figure 5.6 b**).

Among the three checks in the iF treatment, Cal had higher expression levels of *ABCC6* in two time points (3 dai and 7 dai) than Su3 and 32c, but also had higher expression levels of *NFXL1* in all three time points (**Figure 5.5 a1** and **b1**). Moreover, Cal had higher expression levels of *AOS* and *PR4* than 32c and Su3 7 dai and 14 dai (**Figure 5.5 c1** and **f1**). It may be that higher expression of *NFXL1* related to FHB susceptibility could be one of the reasons that Cal still has high severity, despite its high expression of *ABCC6*, *AOS* and *PR4*. Another hypothesis was that, like the *Rht-B1a* NIL, late expression of *AOS* and *PR4* in Cal might be not sufficient to reduce its severity.

Furthermore, the BIS part of Su3 had a higher expression level of *PR4* than that of 32c in the early time point (3 dai) (**Figure 5.6 a**). This corresponds with phenotypic data at the same time point where the number of discolored spikelets in Su3 was already 2.11, when the numbers of discolored spikelets in the other four genotypes in the early time point (3 dai) were all less than 2. This suggested that the discoloration of spikelets surpassed the initial two inoculated spikelets in Su3 and moved to the neighboring spikelets, which might lead to the increase of *PR4* expression in the BIS part triggered by host defense mechanism.

5.4.4 Expression of seven wheat genes (*ABCC6*, *NFXL1*, *AOS*, *JAZ1*, *PR1b*, *PR4* and *PDF1.2*) in the two genotypes in the iD treatment

In the iD treatment, unlike Saville et al (2012), no significant difference for severity was found between the two NILs (**Figure 5.2 b**). The current study used one-time inoculation per floret, where each floret received 150 ug (=10 ul*15 ug/ul) of DON in total. This differed from the DON inoculation protocols used by Lemmens et al. (2005) and Saville et al. (2012), where florets were injected twice in a 24-hour interval and each floret received 240 ug (=20 ul*10 ug/ul + 20 ul*2 ug/ul) of DON in total. It may be that a higher concentration of DON solution is required to study the DON defense mechanism in the two NILs.

Regardless of the lack of phenotypic differences in this study, differences for gene expression between the two NILs were observed. The study from Saville et al (2012) found that the *Rht-B1b* NIL had less severity than the *Rht-B1a* NIL after the DON injection, which might associate with a trend that the *Rht-B1b* NIL had mathematically higher expression level of *ABCC6* than the *Rht-B1a* NIL in the current study (**Figure 5.5 a2**). The higher abundance of *AOS* and *PR4* transcripts in the early time point (3 dai) and the less abundance of *NFXL1* transcripts in the late time point (14 dai) could associate with DON resistance in the *Rht-B1b* NIL (**Figure 5.5 c2**, **f2** and **b2**). Like the iF treatment, higher expression levels of *AOS* and *PR4* were observed in the *Rht-B1a* NIL in the middle and late time points (7 dai and 14 dai) (**Figure 5.5 c2** and **f2**), implying that the late expression of the two genes might not be sufficient to reduce its severity in the iD treatment.

5.4.5 Expression of seven wheat genes (*ABCC6, NFXL1, AOS, JAZ1, PR1b, PR4* and *PDF1.2*) in the five genotypes in the sF treatment

In the sF treatment, the *Rht-B1b* NIL had a higher expression level of *PR4* in the early time point (3 dai) and a lower expressional level of *NFXL1* in the late time point (14 dai) compared to *Rht-B1a* NIL (**Figure 5.5 f3** and **b3**). This was similar to the iF and iD treatments, implying that the expression of the two genes in different time points could associate with stronger FHB resistance in the *Rht-B1b* NIL (**Figure 5.5 f1, f2, b1** and **b2**). Unique to the sF treatment, the *Rht-B1b* NIL had a higher expressional level than the *Rht-B1a* NIL of *PDF1.2* 7 dai and 14 dai and a lower expressional level of *JAZ1* 7 dai (**Figure 5.5 g3** and **d3**). Like both iF and iD treatments, the *Rht-B1a* NIL had higher expression levels of *ABCC6*, *AOS* and *PR4* in the late time point (14 dai) than the *Rht-B1b* NIL (**Figure 5.5 a3**, **c3** and **f3**), implying that the late expression of these genes might not be sufficient to reduce disease severity in the sF treatment. Among the three checks in the sF treatment, Su3 generally had higher expression levels of *ABCC6* and *PR4* 3 dai and a lower expression level of *NFXL1* 14 dai than 32c and Cal (**Figure 5.5 a3, f3 and b3**), which could associate with its FHB resistance. In both the middle and late time points (7 dai and 14 dai), like the iF treatment, Cal in the sF treatment had a higher expression level of *PR4* than 32c 7 dai and higher expression levels of *AOS, JAZ1* and *PR4* than 32c and Su3 14 dai (**Figure 5.5 f3**, **c3** and **d3**).

The expression patterns of *ABCC6*, *AOS* and *PR4* were generally similar in Cal between the iF and sF treatments (**Figure 5.5 a1**, **a3**, **c1, c3, f1 and f3**), while expression of *ABCC6*, *AOS* and *PR4* in the *Rht-B1a* NIL had similar patterns between the iF and sF treatments (**Figure 5.5 a1**, **a3**, **c1, c3,**

f1 and f3), which could implied that the late expression (7 dai and 14 dai) of these genes might not be sufficient to reduce its severity. Based on the results of the two treatments for the three checks, it is suggested that the two resistant checks 32c and Su3 might use other defense mechanisms than the genes tested in this study to reduce disease progress. The phenomenon of no increase in severity in Su3 from 7 dai to 14 dai in both iF and sF treatments will require further study (**Figure 5.2 a** and **c**).

5.5 Conclusions

Different disease responses between the semi-dwarf and wildtype NILs were found in all three treatments. For pathogen *TRI* genes examined, very different expression patterns of *TRI* genes were found between the inoculation treatments (iF and sF). A similar pattern was found in the IS part in the iF treatment and in the late time point in the sF treatment, where genotypes with high severity often had lower *TRI* gene expression. Another similar pattern was observed in the BIS part in the iF treatment and the early time point in the sF treatment, where genotypes with less severity often had lower *TRI* gene expression. For host genes examined, the timing of gene expression of some wheat genes tested might play an important role in FHB resistance. Consistently, *Rht-B1a* NIL and Cal had higher expression levels of *ABCC6, AOS* and *PR4* in the late time point (14 dai), implying that the late expression of these three genes might not be sufficient to reduce severity. The *Rht-B1b* and Su3 often had higher expression of these three genes (*ABCC6, AOS* and *PR4*) in the early time point (3 dai) and a lower expression level of *NFXL1* in the late time point, implying that the early expression of these three genes and the late low expression of *NFXL1* might contribute/associate to FHB resistance.

Interestingly, the *Rht-B1b* NIL had higher expression of different genes (*PR4* and *PDF1.2*) than the *Rht-B1a* NIL in response to the three different treatments in the middle time point (7 dai). In the iF treatment, the *Rht-B1b NIL* showed increased *PR4* and *PDF1.2* expressions in the IS and BIS part, respectively. In the iD treatment, it generally had higher *ABCC6* expression than the *Rht-B1a* NIL. In the sF treatment, it had higher expression level of *PDF1.2* than the *Rht-B1a* NIL both 7 dai and 14 dai. It was hypothesized that the different inoculation methods cause different disease progress which could affect the rate of mycotoxin challenges to the host and could explain differences in timing of gene expression observed in this study.

Moreover, Cal as a susceptible genotype had higher expression levels of the genes involved with FHB resistance than the resistant check 32c and Su3, meanwhile it also had higher expression levels of the genes involved with repressing FHB resistance than the resistant check 32c and Su3, revealing the complexity of FHB resistance in both resistant and susceptible wheat. In addition, since 32c showed no symptoms 3 dai in the sF treatment and Su3 had no severity increasing after 7 dai in both iF and sF treatments, the limited genes tested in this study could not fully explain FHB resistance in the checks. Future studies which test more genes and other disease resistant pathways (like SA) at more time points will be recommended to reveal their FHB resistance mechanisms. The current qPCR study measured mRNA expressional levels of *Fg* and wheat genes and demonstrated the concept that the stronger FHB resistance (mainly Type II) derived from the *Rht-B1b* allele might involve some DON resistance genes (*ABCC6* and *NXFL1*) and JA signalling pathway. To better represent equivalent changes in gene products in those pathways, future studies on FHB resistance could use a multi-disciplinary approach including transcriptomics, proteomics and metabolomics.

CHAPTER 6

GENERAL DISCUSSION AND CONCLUSION

Fusarium head blight (FHB) is a common diseases of wheat (*Triticum aestivum*)), caused by fungal pathogens *Fusarium spp.*, resulting in high yield loss, poor grain quality, seedling blight, reduced kernel weight, and low germination rates. In North America, *Fusarium graminearum sensu stricto* Schwabe (teleomorph: *Gibberella zeae* (Schwein.) Petch) (*Fg*) is the predominant causal species of FHB in wheat. Deoxynivalenol (DON) released by *F. graminearu*m is an important virulence factor for disease spread among spikelets in infected spikes and poses a threat to food and feed safety. Integrated FHB management in Canada mainly relies on the uses of resistant cultivars and fungicides. Mesterhazy (1995) introduced five types of active FHB resistance; Type I and II resistance reduces numbers of infected spikes and decreases numbers of infected spikelets within infected spikes. Type V resistance results in low DON content in infected grains. Resistance to FHB is complex and involves multiple genes with relatively small effects. No single resistance is efficient enough to completely resist FHB. The current breeding strategy is to combine different types of resistance into a single genotype.

Numerous quantitative trait loci (QTL) for FHB resistance had been found in all 21 chromosomes in wheat (Buerstmayr et al. 2009, 2019). The Chinese spring wheat cultivar, Sumai3, is one of the most important FHB resistance sources and has been widely used in breeding programs worldwide. To date, FHB resistance from Sumai3, and its derivatives, has been repeatedly found in four chromosomes (2D, 3B, 5A and 6B), where QTL on chromosome 2D, 3B and 6B mainly reduce

disease severity and 5A QTL decreases disease incidence (Liu et al. 2009; Löffler et al. 2009; Buerstmayr et al. 2009). An elite winter wheat breeding line (named 32c*17) was developed by the University of Manitoba, Canada breeding program and demonstrated strong FHB and DON resistance under severe disease pressure in both Canada and Germany. Based on a haplotyping study (unpublished data), this line does not carry any common Sumai3 Type I and Type II FHB resistance (*Fhb1*, *Qfhs.ifa-5AS* and *Fhb2*), which indicated that this line has inherited non-common useful FHB resistance from Sumai3 and possesses a potential breeding value for FHB resistance.

To better understand the resistance carried by 32c*17, a doubled haploid (DH) population (3CPR) in Chapter 3 was generated from the cross between 32c*17 and the cultivar, Peregrine, with intermediate FHB resistance. Another DH population (PR3C) was also created from the reciprocal cross. Six site years of field tests and one year of greenhouse testing of the 3CPR population were conducted to collect data for anthesis date (Anth), height (Ht), FHB incidence (Inc), FHB severity (Sev), Fusarium damaged kernels (FDK) and DON. Three main QTL were detected across a combination of FHB traits (especially for DON content) and environments on chromosomes 4D (LG: 4D.1), 6A (LG: 6A.3) and 6D with resistance derived from 32c*17 in the 3CPR population (**Table 3.4**). *QFhb/QFdk/QDon.umb-4D* mostly reduced disease incidence and DON content and was not associated with Ht, suggesting that FHB resistance was not directly imparted by the dwarfing gene *Rht-D1* in this population (**Table 3.6**). Unlike previously published 6D QTL that were associated with disease severity, the current *QFhb/QFdk/QDon.umb-6D* strongly associated with Type I and DON resistance, providing a new insight of FHB QTL on chromosome 6D (**Tables 3.4** and **3.6**). Several other QTL for FHB resistance on ten other wheat chromosomes were inconsistently detected, suggesting strong environmental influence. Buerstmayr et al (2019)

mentioned in a review paper that detections of inconsistent FHB QTL generally are more commonly expected in field trials than detections of few main QTL for FHB resistance.

In Chapter 3, the efficiency of marker assisted selection (MAS) based on the detected strong FHB QTL in the 3CPR population was also estimated in its reciprocal population PR3C. A total 1884 SNP markers, which were in a 10 cM interval flanking the peaks of all 3CPR QTL related to multiple FHB traits (*QFhb*, *QFdk* and *QDon*) previously shown in **Table 3.4**, were used to conduct T-tests with two site years of field data in the reciprocal PR3C population. Markers within QTL on chromosomes 4D (LG: 4D.1), 6B and 6D consistently predicted FHB resistance in the reciprocal cross PR3C across the two site years tested, which suggests that they might be good candidate markers for future MAS.

Since Peregrine and 32c*17 in Chapter 3 for the 3CPR and PR3C populations shared the common parental line McClintock, Chapter 4 focused on FHB resistance of 32c*17 in a different genetic background to further characterize FHB resistance in 32c*17. The DH population (named as 8I3C) was generated from the cross between 32c*17 and a breeding line 18i*45 with moderate FHB resistance. Six site years of field tests and one greenhouse tests of the 8I3C population were conducted to collect the same FHB traits and agronomic traits as the Chapter 3. In addition, since a floral morphological trait anther retention (AR) was associated with FHB susceptibility (Steiner et al. 2017), a greenhouse experiment was also conducted to specifically estimate AR in the 8I3C population. The most consistent QTLs for Ht, Inc, VRI, FDK and DON in the 8I3C population were on chromosome 4B, where the *Rht-B1a* allele at *QHt/QFhb/QFdk/QDon.umb-4B*

consistently increased height, reduced anther retention, and contributed Type I and DON resistance (**Table 4.4**).

Another major QTL *QFhb/QFdk/QDon.umb-6D* was consistently detected and was mainly associated with disease incidence and DON content, while the third major QTL *QFhb.umb-7A* specific to Type II resistance was identified across four field site years, the combined environment and one greenhouse environment in the 8I3C population (**Tables 4.4** and **4.5**). Besides *QHt/QFhb/QFdk/QDon.umb-4B, QAnth/QHt.umb-2B* was another major QTL for Anth and Ht consistently reported, but did not associate with FHB resistance (**Table 4.4**). *QHt.umb-1D* and *QHt.umb-7B* were two major QTL for Ht without association with FHB resistance (**Table 4.4**). Since shorter plant height is preferred for agronomic traits (like lodging resistance), but is often associated with increased FHB infection, it is important to decrease height without influencing FHB resistance. QTL for height on chromosome 1D, 2B and 7B in the 8I3C population could be used in breeding short wheat cultivars.

QTL detected in both 3CPR and 8I3C populations were listed in **Table 4.5**. The 3CPR *QFhb/QFdk/QDon.umb-6D* was one of three main QTL for FHB resistance in Chapter 3, which was also detected in the 8I3C population (**Table 4.5**). The 32c*17 allele reduced AR and decreased Inc, VRI, FDK and DON at the 8I3C *QAR/QFhb/QFdk/QDon.umb-6D* (**Table 4.4**). No QTL for Ht were detected in that region in either population. Both Chapter 3 and Chapter 4 discovered that the 32c*17 allele contributed Type I and DON resistance on chromosome 6D, which differed from other studies (**Tables 3.6** and **4.5)** (Gervais et al. 2003; Paillard et al. 2004; Holzapfel et al. 2008; Cai and Bai 2014; Eckard et al. 2015; Cai et al. 2019). Moreover, based on the physical positions,

it is considered that one main 8I3C QTL *QFhb/QFdk/QDon.umb-7A* might not be the same as 3CPR *QFhb.umb-7A* and *QHt.umb-7A* (**Table 4.5**). The Type II resistance gene, *Fhb3* was also reported on chromosome 7A, which shares the same region as 8I3C *QFhb/QFdk/QDon.umb-7A* (**Table 4.5**). The 3CPR population was monomorphic for the *Rht-B1* locus and no QTL for FHB resistance and height were detected on chromosome 4B in Chapter 3 (**Table 4.5**).

Furthermore, the 3CPR *QFhb/QFdk/QDon.umb-4D* was one of three main QTL for FHB resistance in Chapter 3, however, no FHB QTL were identified in this region in the 8I3C population except a *QHt.umb-4D* for height across two individual site years in Chapter 4, where the 32c*17 allele contributed to increased Ht (**Table 4.5**). Many previous studies found a strong association between increased height and FHB resistance at a common dwarf *Rht-D1* locus in chromosome 4D, where the *Rht-D1a* allele increased height and reduced FHB incidence (Srinivasachary et al. 2008a, 2009; Voss et al. 2008; Löffler et al. 2009; Buerstmayr et al. 2009; Buerstmayr and Buerstmayr 2016; He et al. 2016). Two Kompetitive Allele Specific PCR (KASP) markers for the *Rht-D1* locus were tested in the three parental lines (18i*45, 32c*17 and Peregrine) (**Appendices 3.1** and **4.1**); the result showed monomorphism in both 8I3C and 3CPR populations. The estimated physical location of the *Rht-D1* locus was 19.19 Mbp, which is estimated to be 6.86~361 Mbp away from 8I3C *QHt.umb-4D* and 31.48~466.54 Mbp away from 3CPR *QFhb/QFdk/QDon.umb-4D* (**Table 4.5**). These results suggest that height and FHB resistance are independently controlled, but that loci for these traits are linked. Further genomic and genetic research will help to study the relationship among 8I3C *QHt*, 3CPR *QFhb* and the *Rht-D1* locus. Overall, there were transgressive segregation in the 3CPR and 8I3C populations for FHB traits and

some 3CPR and 8I3C DHs surpassed the resistance of parental lines due to transgressive segregation, which may be useful for future breeding (**Figures 3.1** and **4.1** and **Tables 3.2** and **4.2**).

Taller plant height has been associated with better FHB resistance (Mesterházy 1995; Buerstmayr et al. 2009; Yan et al. 2011; Saville et al. 2012). In particular, several studies have shown that QTL for FHB resistance, anther retention and plant height overlapped such that they all contained the gibberellic acid (GA)-insensitive dwarfing *Rht-B1* gene, including the current 8I3C *QAR/QHt/QFhb/QFdk/QDon.umb-4B* in Chapter 4 (Lu et al. 2013; Buerstmayr and Buerstmayr 2016; He et al. 2016; Xu et al. 2020). Based on the additive effect, the wildtype *Rht-B1a* allele was associated with increased plant height, anther extrusion and FHB resistance. Conversely, the dwarfing *Rht-B1b* allele was associated with decreased plant height and increases in both anther retention and FHB occurrence. However, Saville et al. (2012) reported that a Maris Huntsman near-isogenic line (NIL) carrying the *Rht-B1b* allele had less FHB symptoms than its NIL carrying the *Rht-B1a* allele in both indoor point inoculation and direct mycotoxin DON injection tests. The authors hypothesized that the *Rht-B1b* allele reduced Type I resistance and increased Type II and DON resistance. The objectives of the qRT-PCR study in Chapter 5 were to evaluate disease severity and relative gene expression of pathogen and plant defense genes in five genotypes under different inoculation treatments, spray *Fg* (sF), point inoculated *Fg* (iF) and point injected DON (iD) and Mock (water) at four time points (1.5, 3, 7 and 14 days after inoculation (dai)). The five genotypes (G) were Maris Huntsman *Rht-B1a* NIL and *Rht-B1b* NIL, 32c*17 (32c), Caledonia (Cal) and Sumai 3 (Su3) (**Figure 5.2**).

For the pathogen genes (*TRI5*, *TRI6*, *TRI12* and *TRI101*) examined, very different expression patterns of *TRI* genes were found between the inoculation treatments (iF and sF) (**Figures 5.3** and **5.4**). In the inoculated spikelets in the iF treatment, genotypes with high severity often had lower *TRI* gene expression, while in the spikelets below the inoculation point genotypes with less severity often had lower *TRI* gene expression. For host genes (*ABCC6*, *NFXL1*, *AOS*, *JAZ1*, *PR1b*, *PR4* and *PDF1.2*) examined, the timing of gene expression of some wheat genes tested might play an important role in FHB resistance (**Figure 5.5**). Higher expression of the three genes (*ABCC6*, *AOS* and *PR4*) at earlier time points (3 dai) and a lower expression level of *NFXL1* at the late time point may be associated with FHB resistance. Consistently, the *Rht-B1a* NIL and Caledonia had higher expression levels of *ABCC6*, *AOS* and *PR4* in the late time point (14 dai) in all three inoculation treatments, implying that late expression of these genes might be insufficient to reduce disease severity. Furthermore, the separation of the inoculated spikelets and the spikelets below the inoculation points might provide better resolution of gene expression than the simply grinding of the whole infected spikes.

All studies reported that 32c*17 has strong FHB and DON resistance. In the presence of the monomorphism in *Rht-B1* locus, several inconsistent QTL related to disease incidence were detected in the Chapter 3 QTL mapping study. In the presence of polymorphism in *Rht-B1* locus, the *Rht-B1a* allele in 32c*17 co-localized with a consistent source for Type I and DON resistance, in the Chapter 4 QTL mapping study. Furthermore, in chapter 5 an interesting phenomenon in the sF treatment showed that no visual disease symptoms occurred in 32c*17 at 3 dai, while the other four genotypes at least had some visible discoloration (**Figure 5.2 c**). This could correspond with 32c*17-derived QTL for Type I resistance detected in chapter 3 and 4. Since this phenomenon was

not detected on the *Rht-B1a* NIL, it implies that strong Type I resistance contributing to this phenomenon in 32c*17 might be a resistance source tightly linked with the *Rht-B1a* allele.

Sumai 3 is one of the paternal lines for 32c*17. Several QTL and *Fhb* genes contributing Type II resistance derived from Sumai 3 were mentioned in some review articles (Gilbert and Tekauz 2000; Bai and Shaner 2004; Buerstmayr et al. 2009, 2019; Zhu et al. 2019). Notably, the chapter 5 also detected that no increase of severity in Sumai 3 from 7 dai to 14 dai in both the iF and sF treatments (**Figure 5.2 a** and **c**), which could be explained by strong Type II resistance in Sumai 3. With the limited genes tested in Chapter 5, the FHB resistance in 32c*17 and Sumai 3 could not be fully explain, and future studies with more genes are required to reveal their role in FHB resistance. On the other hand, a susceptible winter wheat cultivar, McClintock, is the maternal line for 32c*17, which could still potentially contribute good FHB resistance to 32c*17. As an example of a FHB resistant line derived from two susceptible parents, the resistant winter wheat cultivar, Emerson, inherited FHB resistance from its parental lines McClintock and CDC Osprey, which both McClintock and CDC Osprey were indicated as low FHB resistance in Alberta seed guide in 2013 and 2014 (Alberta seed guide 2013, 2014; Graf et al. 2013).

All three studies demonstrate complexity of FHB resistance in wheat and show that the elite winter wheat breeding line 32c*17 possesses a potential breeding value for FHB resistance. The two QTL mapping studies show that different QTL for FHB resistance derived from 32c*17 could be identified after crossing this line into different genetic backgrounds. When two parental lines (32c*17 and Peregrine) were monomorphic for the *Rht-B1* locus in the 3CPR population, three main QTL for FHB resistance on chromosomes 4D, 6A and 6D were detected across with

resistance derived from 32c*17 in the 3CPR population. Several other FHB QTL on chromosomes 1A, 1B, 2A, 2D, 3A, 4A, 5D, 6B, 7A and 7B were inconsistently detected in different individual environments. In the reciprocal cross, PR3C, markers below peaks of QTL on chromosomes 4D, 6B and 6D, consistently and accurately predicted FHB resistance in the PR3C lines across both site years.

When the two parental lines (18i*45 and 32c*17) were polymorphic for the *Rht-B1* locus in the 8I3C population, the 32c*17 allele at that region of the *Rht-B1* locus on chromosome 4B increased plant height, reduced anther retention, disease incidence and DON content. Notably, 32c*17-derived 6D QTL for Type I and DON resistance were relatively consistently detected in both populations. Eight markers in the current 3CPR 6D QTL region were mapped within 6.13 cM in linkage group 6D, where the rest of 103 markers in the same linkage group were at least 25.8 cM away from the eight markers. The same eight markers in the current 8I3C 6D QTL region were mapped within 19.74 cM in the linkage group 6D.1, where the rest of 161 markers in the same chromosomes were mapped in the linkage group 6D.2. In the future, more markers could be added into chromosome 6D to fill the gap between the eight markers under 6D QTL region and the rest of markers in chromosome 6D. In addition, validation of this 6D QTL region in the other crosses with the common parental line 32c*17 in different genetic backgrounds are recommended before fine mapping this 6D QTL region. Since all previously reported QTL on chromosome 6D were associated with disease severity, further genomic and genetic research will be important to identify whether the 32c*17-derived alleles for this 6D QTL is novel. There was heterogeneity in this 6D region in both parents (McClintock and Sumai 3) after genotyping multiple times (unpublished data), thus further genetic studies could help to track down which parental line contributed FHB

resistance to 32c*17 on chromosome 6D. Also, it is important to study QTL for anther retention/extrusion or floral structure in 32c*17 in future field and greenhouse trials. In addition, the 8I3C 4D QTL for height and the 3CPR 4D QTL for Type I and DON resistance could be further characterized to study the relationship among 8I3C *QHt*, 3CPR *QFhb* and the *Rht-D1* loci. Furthermore, the 18i*45 allele at QTL for height on chromosomes 1D, 2B and 7B in the 8I3C population could be used to reduce height without altering FHB resistance.

The phenotyping data in gene expression revealed that there were no disease symptoms in 32c*17 at 3 dai under an indoor spray inoculation method. Expression of *TRI5*, *TRI6* and *TRI101* in 32c*17 3 dai in the spray treatment was generally lower than expression in Caledonia and Sumai 3, confirming that good FHB resistance possessed in 32c*17. The limited genes tested in this study implied that low expression of NFXL1 at 3 dai might associate with FHB resistance in 32c*17. Future gene expression studies (like RNA-seq, microarray and qRT-PCR etc.) on other JA-response genes and SA-response genes could help better understand FHB resistance in 32c*17. To better characterize good DON resistance in 32c*17, a DON injection experiment should be conducted in 32c*17 and measurement of DON conjugation in 32c*17 is recommended. Overall, it is important to combine multiple disciplines including field and greenhouse trials, QTL mapping and qRT-PCR gene expression studies to fully understand the wheat-*Fg* pathosystem and FHB resistance in wheat.

References

Aboukhaddour R, Fetch T, McCallum BD, et al (2020) Wheat diseases on the prairies: A Canadian story. Plant Pathol 69:418–432. doi: 10.1111/ppa.13147

Agriculture and Agri-Food Canada (2021) G003 - Supply and Dispositions Table Report - Agricultural Industry Market Information System (AIMIS) - Agriculture and Agri-Food Canada (AAFC) https://aimis-simia.agr.gc.ca/rp/index-eng.cfm?action=pR&r=244&pdctc=. Accessed 18 Mar 2021

Akbari M, Wenzl P, Caig V, et al (2006) Diversity arrays technology (DArT) for high-throughput profiling of the hexaploid wheat genome. Theor Appl Genet 113:1409–1420. doi: 10.1007/s00122-006-0365-4

Akram S, Arif MAR, Hameed A (2021) A GBS-based GWAS analysis of adaptability and yield traits in bread wheat (Triticum aestivum L.). J Appl Genet 62:27–41. doi: 10.1007/s13353-020-00593-1

Alberta seed guide (2013) https://www.seed.ab.ca/asg_flipbook_spring2013/files/inc/d28b268881.pdf. Accessed 03 Aug 2022

Alberta seed guide (2014) https://www.seed.ab.ca/asg_flipbook_spring2014/files/inc/e9b5aa69c7.pdf. Accessed 03 Aug 2022

Alexander NJ, McCormick SP, Waalwijk C, et al (2011) The genetic basis for 3-ADON and 15-ADON trichothecene chemotypes in Fusarium. Fungal Genet Biol 48:485–495. doi: 10.1016/j.fgb.2011.01.003

Alipour H, Bai G, Zhang G, et al (2019) Imputation accuracy of wheat genotyping-by-sequencing (GBS) data using barley and wheat genome references. PLoS One 14:1–20. doi: 10.1371/journal.pone.0208614

Allen AM, Barker GLA, Berry ST, et al (2011) Transcript-specific, single-nucleotide polymorphism discovery and linkage analysis in hexaploid bread wheat (Triticum aestivum L.). Plant Biotechnol J 9:1086–1099. doi: 10.1111/j.1467-7652.2011.00628.x

Amarasinghe CC, Sharanowski B, Dilantha Fernando WGD (2019) Molecular phylogenetic relationships, trichothecene chemotype diversity and aggressiveness of strains in a global collection of *Fusarium graminearum* species. Toxins (Basel) 11:1–17. doi: 10.3390/toxins11050263

Amarasinghe CC, Fernando WGD (2016) Comparative analysis of deoxynivalenol biosynthesis related gene expression among different chemotypes of *Fusarium graminearum* in spring wheat. Front Microbiol 7:1–10. doi: 10.3389/fmicb.2016.01229

Amarasinghe CC, Simsek S, Brûlé-Babel A, Fernando WGD (2016) Analysis of deoxynivalenol and deoxynivalenol-3-glucosides content in Canadian spring wheat cultivars inoculated with *Fusarium graminearum*. Food Addit Contam Part A Chem Anal Control Expo Risk Assess 33:1254–1264. doi: 10.1080/19440049.2016.1198050

Amarasinghe CC, Tittlemier SA, Fernando WGD (2015) Nivalenol-producing *Fusarium cerealis* associated with Fusarium head blight in winter wheat in Manitoba, Canada. Plant Pathol 64:988–995. doi: 10.1111/ppa.12329

Anderson JA, Stack RW, Liu S, et al (2001) DNA markers for Fusarium head blight resistance QTLs in two wheat populations. Theor Appl Genet 102:1164–1168. doi: 10.1007/s001220000509

Anonymous (2014) Harnessing genomics to help meet global food demand. Innov. Express 5:1–12

Aoki T, O'Donnell K (1999) Morphological and molecular characterization of *Fusarium pseudograminearum* sp. nov., formerly recognized as the Group 1 population of *F. graminearum*. Mycologia 91:597–609. doi: 10.2307/3761245

Arruda MP, Brown P, Brown-Guedira G, et al (2016) Genome-wide association mapping of Fusarium head blight resistance in wheat using genotyping-by-sequencing. Plant Genome 9:1-14. doi: 10.3835/plantgenome2015.04.0028

Aviles AC, Harrison SA, Arceneaux KJ, et al (2020) Identification of QTLs for resistance to Fusarium head blight using a doubled haploid population derived from southeastern United States soft red winter wheat varieties AGS 2060 and AGS 2035. Genes (Basel) 11:1–18. doi: 10.3390/genes11060699

Bai G, Kolb FL, Shaner G, Domier LL (1999) Amplified fragment length polymorphism markers linked to a major quantitative trait locus controlling scab resistance in wheat. Phytopathology 89:343–348. doi: 10.1094/PHYTO.1999.89.4.343

Bai G, Shaner G (2004) Management and resistance in wheat and barley to Fusarium head blight. Annu Rev Phytopathol 42:135–161. doi: 10.1146/annurev.phyto.42.040803.140340

Bai GH, Desjardins AE, Plattner RD (2002) Deoxynivalenol-nonproducing *Fusarium graminearum* causes initial infection, but does not cause disease spread in wheat spikes. Mycopathologia 153:91–98. doi: 10.1023/A:1014419323550

Basnet BR, Glover KD, Ibrahim AMHH, et al (2012) A QTL on chromosome 2DS of "Sumai 3" increases susceptibility to Fusarium head blight in wheat. Euphytica 186:91–101. doi: 10.1007/s10681-011-0495-x

Bayer PE, Petereit J, Durant É, et al (2022) Wheat Panache: A pangenome graph database representing presence–absence variation across sixteen bread wheat genomes. Plant Genome. doi: 10.1002/tpg2.20221

Becher R, Weihmann F, Deising HB, Wirsel SGR (2011) Development of a novel multiplex DNA microarray for *Fusarium graminearum* and analysis of azole fungicide responses. BMC Genomics 12:1–17. doi: 10.1186/1471-2164-12-52

Berens ML, Berry HM, Mine A, et al (2017) Evolution of hormone signaling networks in plant defense. Annu Rev Phytopathol 55:401–425. doi: 10.1146/annurev-phyto-080516-035544

Berraies S, Knox RE, Depauw RM, et al (2020) Effectiveness of multigenerational transfer of sumai 3 Fusarium head blight resistance in hard red spring wheat breeding populations. Can J Plant Sci 100:156–174. doi: 10.1139/cjps-2019-0066

Berthiller F, Dall'Asta C, Schuhmacher R, et al (2005) Masked mycotoxins: Determination of a deoxynivalenol glucoside in artificially and naturally contaminated wheat by liquid chromatography-tandem mass spectrometry. J Agric Food Chem 53:3421–3425. doi: 10.1021/jf047798g

Blackburn A, Sidhu G, Schillinger WF, et al (2021) QTL mapping using GBS and SSR genotyping reveals genomic regions controlling wheat coleoptile length and seedling emergence. Euphytica 217:1–12. doi: 10.1007/s10681-021-02778-z

Blandino M, Haidukowski M, Pascale M, et al (2012) Integrated strategies for the control of Fusarium head blight and deoxynivalenol contamination in winter wheat. F Crop Res 133:139–149. doi: 10.1016/j.fcr.2012.04.004

Brauer EK, Balcerzak M, Rocheleau H, et al (2020) Genome editing of a deoxynivalenol-induced transcription factor confers resistance to *Fusarium graminearum* in wheat. Mol Plant-Microbe Interact 33:553–560. doi: 10.1094/MPMI-11-19-0332-R

Brauer EK, Rocheleau H, Balcerzak M, et al (2019) Transcriptional and hormonal profiling of *Fusarium graminearum*-infected wheat reveals an association between auxin and susceptibility. Physiol Mol Plant Pathol 107:33–39. doi: 10.1016/j.pmpp.2019.04.006

Brown DW, McCormick SP, Alexander NJ, et al (2002) Inactivation of a cytochrome P-450 is a determinant of trichothecene diversity in *Fusarium* species. Fungal Genet Biol 36:224–233. doi: 10.1016/S1087-1845(02)00021-X

Brown NA, Bass C, Baldwin TK, et al (2011) Characterisation of the Fusarium graminearum - Wheat Floral Interaction. J Pathog 2011:1–9. doi: 10.4061/2011/626345

Buerstmayr H, Adam G, Lemmens M (2012) Resistance to head blight caused by *Fusarium spp.* in wheat. In: Sharma I (ed) Disease Resistance in Wheat,. Centre for Agriculture and Bioscience International, UK, pp 236–276

Buerstmayr H, Ban T, Anderson JA (2009) QTL mapping and marker-assisted selection for Fusarium head blight resistance in wheat: a review. Plant Breed 128:1–26. doi: 10.1111/j.1439-0523.2008.01550.x

Buerstmayr H, Lemmens M, Hartl L, et al (2002) Molecular mapping of QTLs for Fusarium head blight resistance in spring wheat. I. Resistance to fungal spread (Type II resistance). Theor Appl Genet 104:84–91. doi: 10.1007/s00122-003-1272-6

Buerstmayr H, Steiner B, Hartl L, et al (2003) Molecular mapping of QTLs for Fusarium head blight resistance in spring wheat. II. Resistance to fungal penetration and spread. Theor Appl Genet 107:503–508. doi: 10.1007/s00122-003-1272-6

Buerstmayr M, Buerstmayr H (2015) Comparative mapping of quantitative trait loci for Fusarium head blight resistance and anther retention in the winter wheat population Capo × Arina. Theor Appl Genet 128:1519–1530. doi: 10.1007/s00122-015-2527-8

Buerstmayr M, Buerstmayr H (2016) The semidwarfing alleles *Rht-D1b* and *Rht-B1b* show marked differences in their associations with anther-retention in wheat heads and with Fusarium head blight susceptibility. Phytopathology 106:1544–1552. doi: 10.1094/PHYTO-05-16-0200-R

Buerstmayr M, Huber K, Heckmann J, et al (2012) Mapping of QTL for Fusarium head blight resistance and morphological and developmental traits in three backcross populations derived from Triticum dicoccum × Triticum durum. Theor Appl Genet 125:1751–1765. doi: 10.1007/s00122-012-1951-2

Buerstmayr M, Lemmens M, Steiner B, Buerstmayr H (2011) Advanced backcross QTL mapping of resistance to Fusarium head blight and plant morphological traits in a Triticum macha x T. aestivum population. Theor Appl Genet 123:293–306. doi: 10.1007/s00122-011-1584-x

Buerstmayr M, Steiner B, Buerstmayr H (2019) Breeding for Fusarium head blight resistance in wheat—progress and challenges. Plant Breed 1–26. doi: 10.1111/pbr.12797

Buerstmayr M, Wagner C, Nosenko T, et al (2021) Fusarium head blight resistance in European winter wheat: insights from genome-wide transcriptome analysis. BMC Genomics 22:1–17. doi: 10.1186/s12864-021-07800-1

Buhrow LM, Cram D, Tulpan D, et al (2016) Exogenous abscisic acid and gibberellic acid elicit opposing effects on *Fusarium graminearum* infection in wheat. phytopathology 106:986–996. doi: 10.1094/PHYTO-01-16-0033-R

Cabral AL, Jordan MC, McCartney CA, et al (2014) Identification of candidate genes, regions and markers for pre-harvest sprouting resistance in wheat (Triticum aestivum L.). BMC Plant Biol 14:1–12. doi: 10.1186/s12870-014-0340-1

Cai J, Bai G (2014) Quantitative trait loci for Fusarium head blight resistance in Huangcandou × 'Jagger' wheat population. Crop Sci 54:2520–2528. doi: 10.2135/cropsci2013.12.0835

Cai J, Wang S, Su Z, et al (2019) Meta-analysis of QTL for Fusarium head blight resistance in Chinese wheat landraces. Crop J 7:784–798. doi: 10.1016/j.cj.2019.05.003

Cainong JC, Bockus WW, Feng Y, et al (2015) Chromosome engineering, mapping, and transferring of resistance to Fusarium head blight disease from Elymus tsukushiensis into wheat. Theor Appl Genet 128:1019–1027. doi: 10.1007/s00122-015-2485-1

Canadian Grain Commission (2019) Canadian wheat classes. https://www.grainscanada.gc.ca/wheat-ble/classes/classes-eng.htm. Accessed 18 Mar 2021

Canadian Grain Commission (2020) Grain varieties by acreage insured. https://www.grainscanada.gc.ca/en/grain-research/statistics/varieties-by-acreage/. Accessed 18 Dec 2020

Canadian Grain Commission (2021) Frequency and severity of Fusarium damaged kernels (FDK) in Canada Western Red Spring (CWRS) wheat samples from the Harvest Sample Program. https://www.grainscanada.gc.ca/en/grain-research/exportquality/cereals/wheat/western/annual-fusarium-damage/canada-western-red-spring/. Accessed 26 May 2022

Cavanagh CR, Chao S, Wang S, et al (2013) Genome-wide comparative diversity uncovers multiple targets of selection for improvement in hexaploid wheat landraces and cultivars. Proc Natl Acad Sci USA 110:8057–8062. doi: 10.1073/pnas.1217133110

Chan YK, Savard ME, Reid LM, et al (2009) Identification of lipopeptide antibiotics of a Bacillus subtilis isolate and their control of *Fusarium graminearum* diseases in maize and wheat. BioControl 54:567–574. doi: 10.1007/s10526-008-9201-x

Chao S, Sharp PJ, Worland AJ, et al (1989) RFLP-based genetic maps of wheat homoeologous group 7 chromosomes. Theor Appl Genet 78:495–504. doi: 10.1007/BF00290833

Charmet G (2011) Wheat domestication: Lessons for the future. Comptes Rendus - Biol 334:212–220. doi: 10.1016/j.crvi.2010.12.013

Chen H, Moakhar NP, Iqbal M, et al (2016) Genetic variation for flowering time and height reducing genes and important traits in western Canadian spring wheat. Euphytica 208:377–390. doi: 10.1007/s10681-015-1615-9

Chen Y, Kistler HC, Ma Z (2019) *Fusarium graminearum* trichothecene mycotoxins: Biosynthesis, regulation, and management. Annu Rev Phytopathol 57:15–39. doi: 10.1146/annurev-phyto-082718-100318

Chetouhi C, Bonhomme L, Lasserre-Zuber P, et al (2016) Transcriptome dynamics of a susceptible wheat upon Fusarium head blight reveals that molecular responses to *Fusarium graminearum* infection fit over the grain development processes. Funct Integr Genomics 16:183–201. doi: 10.1007/s10142-016-0476-1

Chini A, Fonseca S, Chico JM, et al (2009) The ZIM domain mediates homo- and heteromeric interactions between Arabidopsis JAZ proteins. Plant J 59:77–87. doi: 10.1111/j.1365-313X.2009.03852.x

Chini A, Fonseca S, Fernández G, et al (2007) The JAZ family of repressors is the missing link in jasmonate signalling. Nature 448:666–671. doi: 10.1038/nature06006

Clear RM, Abramson D (1986) Occurrence of Fusarium head blight and deoxynivalenol (vomitoxin) in two samples of Manitoba wheat in 1984. Can Plant Dis Surv 66:9–12

Cowger C, Ward TJ, Nilsson K, et al (2020) Regional and field-specific differences in Fusarium species and mycotoxins associated with blighted North Carolina wheat. Int J Food Microbiol 323:. doi: 10.1016/j.ijfoodmicro.2020.108594

Crismani W, Baumann U, Sutton T, et al (2006) Microarray expression analysis of meiosis and microsporogenesis in hexaploid bread wheat. BMC Genomics 7:1–17. doi: 10.1186/1471-2164-7-267

Cui F, Zhang N, Fan XL, et al (2017) Utilization of a Wheat660K SNP array-derived high-density genetic map for high-resolution mapping of a major QTL for kernel number. Sci Rep 7:1–12. doi: 10.1038/s41598-017-04028-6

Cuomo CA, Güldener U, Xu JR, et al (2007) The *Fusarium graminearum* genome reveals a link between localized polymorphism and pathogen specialization. Science 317:1400–1402. doi: 10.1126/science.1143708

Cuthbert PA, Somers DJ, Brulé-Babel A (2007) Mapping of Fhb2 on chromosome 6BS: A gene controlling Fusarium head blight field resistance in bread wheat (Triticum aestivum L.). Theor Appl Genet 114:429–437. doi: 10.1007/s00122-006-0439-3

Cuthbert PA, Somers DJ, Thomas J, et al (2006) Fine mapping Fhb1, a major gene controlling Fusarium head blight resistance in bread wheat (Triticum aestivum L.). Theor Appl Genet 112:1465–1472. doi: 10.1007/s00122-006-0249-7

Daba SD, Tyagi P, Brown-Guedira G, Mohammadi M (2020) Genome-wide association study in historical and contemporary U.S. winter wheats identifies height-reducing loci. Crop J 8:243–251. doi: 10.1016/j.cj.2019.09.005

Díaz A, Zikhali M, Turner AS, et al (2012) Copy number variation affecting the photoperiod-B1 and vernalization-A1 genes is associated with altered flowering time in wheat (Triticum aestivum). PLoS One 7:e33234. doi: 10.1371/journal.pone.0033234

Dill-Macky R, Jones RK (2000) The effect of previous crop residues and tillage on Fusarium head blight of wheat. Plant Dis 84:71–76. doi: 10.1094/PDIS.2000.84.1.71

Ding L, Xu H, Yi H, et al (2011) Resistance to hemi-biotrophic *F. graminearum* infection is associated with coordinated and ordered expression of diverse defense signaling pathways. PLoS One 6:e19008. doi: 10.1371/journal.pone.0019008

Draeger R, Gosman N, Steed A, et al (2007) Identification of QTLs for resistance to Fusarium head blight, DON accumulation and associated traits in the winter wheat variety Arina. Theor Appl Genet 115:617–625. doi: 10.1007/s00122-007-0592-3

Eckard JT, Gonzalez-Hernandez JL, Caffe M, et al (2015) Native Fusarium head blight resistance from winter wheat cultivars ‘Lyman,’ ‘Overland,’ ‘Ernie,’ and ‘Freedom’ mapped and pyramided onto ‘Wesley’-Fhb1 backgrounds. Mol Breed 35:1-16. doi: 10.1007/s11032-015-0200-1

El Baidouri M, Murat F, Veyssiere M, et al (2017) Reconciling the evolutionary origin of bread wheat (Triticum aestivum). New Phytol 213:1477–1486. doi: 10.1111/nph.14113

Ellis M, Rebetzke G, Azanza F, et al (2005) Molecular mapping of gibberellin-responsive dwarfing genes in bread wheat. Theor Appl Genet 111:423–430. doi: 10.1007/s00122-005-2008-6

Elshire RJ, Glaubitz JC, Sun Q, et al (2011) A robust, simple genotyping-by-sequencing (GBS) approach for high diversity species. PLoS One 6:1–10. doi: 10.1371/journal.pone.0019379

Fabre F, Rocher F, Alouane T, et al (2020) Searching for FHB resistances in bread wheat: Susceptibility at the crossroad. Front Plant Sci 11:1–8. doi: 10.3389/fpls.2020.00731

Fauteux F, Wang Y, Rocheleau H, et al (2019) Characterization of QTL and eQTL controlling early *Fusarium graminearum* infection and deoxynivalenol levels in a Wuhan 1 x Nyubai doubled haploid wheat population. BMC Plant Biol 19:1–9. doi: 10.1186/s12870-019-2149-4

Foroud NA, Baines D, Gagkaeva TY, et al (2019) Trichothecenes in cereal grains - An update. Toxins (Basel) 11:634–682. doi: 10.3390/toxins11110634

Foroud NA, Eudes F (2009) Trichothecenes in cereal grains. Int J Mol Sci 10:147–173. doi: 10.3390/ijms10010147

Foroud NA, Shank RA, Kiss D, et al (2016) Solvent and water mediated structural variations in deoxynivalenol and their potential implications on the disruption of ribosomal function. Front Microbiol 7:1–15. doi: 10.3389/fmicb.2016.01239

Fowler DB (2010) Peregrine hard red winter wheat. Can J Plant Sci 90:853–856. doi: 10.4141/CJPS10069

Gale LR, Bryant JD, Calvo S, et al (2005) Chromosome complement of the fungal plant pathogen *Fusarium graminearum* based on genetic and physical mapping and cytological observations. Genetics 171:985–1001. doi: 10.1534/genetics.105.044842

Garreau De Loubresse N, Prokhorova I, Holtkamp W, et al (2014) Structural basis for the inhibition of the eukaryotic ribosome. Nature 513:517–522. doi: 10.1038/nature13737

Garvin DF, Porter H, Blankenheim ZJ, et al (2015) A spontaneous segmental deletion from chromosome arm 3DL enhances Fusarium head blight resistance in wheat. Genome 58:479–488. doi: 10.1139/gen-2015-0088

Garvin DF, Stack RW, Hansen JM (2009) Quantitative trait locus mapping of increased Fusarium head blight susceptibility associated with a wild emmer wheat chromosome. Phytopathology 99:447–452. doi: 10.1094/PHYTO-99-4-0447

Gervais L, Dedryver F, Morlais JY, et al (2003) Mapping of quantitative trait loci for field resistance to Fusarium head blight in an European winter wheat. Theor Appl Genet 106:961–970. doi: 10.1007/s00122-002-1160-5

Gilbert J, Fernando WGD (2004) Epidemiology and biological control of *Gibberella zeae* /*Fusarium graminearum*. Can J Plant Pathol 26:464–472. doi: 10.1080/07060660409507166

Gilbert J, Guerrieri AT, Clear RM, et al (2014) Ratio of 3-ADON and 15-ADON isolates of *Fusarium graminearum* recovered from wheat kernels in Manitoba from 2008 to 2012. Can J Plant Pathol 36:54–63. doi: 10.1080/07060661.2014.887033

Gilbert J, Haber S (2013) Overview of some recent research developments in Fusarium head blight of wheat. Can J Plant Pathol 35:149–174. doi: 10.1080/07060661.2013.772921

Gilbert J, Tekauz A (2000) Review: Recent developments in research on Fusarium head blight of wheat in Canada. Can J Plant Pathol 22:1–8. doi: 10.1080/07060660009501155

Glazebrook J (2005) Contrasting mechanisms of defense against biotrophic and necrotrophic pathogens. Annu Rev Phytopathol 43:205–227. doi: 10.1146/annurev.phyto.43.040204.135923

Gooding RW, Lafever HN, Campbell KG, Herald LD (1997) Registration of 'Freedom' wheat. Crop Sci 37:1007–1007. doi: 10.2135/cropsci1997.0011183x003700030057x

Goutam U, Kukreja S, Yadav R, et al (2015) Recent trends and perspectives of molecular markers against fungal diseases in wheat. Front Microbiol 6:1–14. doi: 10.3389/fmicb.2015.00861

Government of Alberta (2021) Alberta Fusarium graminearum management plan. https://www.alberta.ca/alberta-fusarium-graminearum-management-plan.aspx. Accessed 26 Jul 2022

Graf RJ, Beres BL, Laroche A, et al (2013) Emerson hard red winter wheat. Can J Plant Sci 93:741–748. doi: 10.4141/CJPS2012-262

Griffiths J, Murase K, Rieu I, et al (2006) Genetic characterization and functional analysis of the GID1 gibberellin receptors in Arabidopsis. Plant Cell 18:3399–3414. doi: 10.1105/tpc.106.047415

Guedira M, Brown-Guedira G, van Sanford D, et al (2010) Distribution of Rht genes in modern and historic winter wheat cultivars from the eastern and central USA. Crop Sci 50:1811–1822. doi: 10.2135/cropsci2009.10.0626

Guenther JC, Trail F (2005) The development and differentiation of *Gibberella zeae* (anamorph: *Fusarium graminearum*) during colonization of wheat. Mycologia 97:229–237. doi: 10.3852/mycologia.97.1.229

Gunupuru LR, Perochon A, Doohan FM (2017) Deoxynivalenol resistance as a component of FHB resistance. Trop Plant Pathol 42:175–183. doi: 10.1007/s40858-017-0147-3

Guo J, Zhang X, Hou Y, et al (2015) High-density mapping of the major FHB resistance gene Fhb7 derived from Thinopyrum ponticum and its pyramiding with Fhb1 by marker-assisted selection. Theor Appl Genet 128:2301–2316. doi: 10.1007/s00122-015-2586-x

Guo PG, Bai GH, Shaner GE (2003) AFLP and STS tagging of a major QTL for Fusarium head blight resistance in wheat. Theor Appl Genet 106:1011–1017. doi: 10.1007/s00122-002-1129-4

Guo XW, Fernando WGD, Bullock P, Sapirstein H (2010) Quantifying cropping practices in relation to inoculum levels of *Fusarium graminearum* on crop stubble. Plant Pathol 59:1107–1113. doi: 10.1111/j.1365-3059.2010.02353.x

Häberle J, Schmolke M, Schweizer G, et al (2007) Effects of two major Fusarium head blight resistance QTL verified in a winter wheat backcross population. Crop Sci 47:1823–1831. doi: 10.2135/cropsci2006.12.0800

Häberle J, Schweizer G, Schondelmaier J, et al (2009) Mapping of QTL for resistance against Fusarium head blight in the winter wheat population Pelikan//Bussard/Ning8026. Plant Breed 128:27–35. doi: 10.1111/j.1439-0523.2008.01540.x

Haldar A, Tekieh F, Balcerzak M, et al (2021) Introgression of Thinopyrum elongatum DNA fragments carrying resistance to Fusarium head blight into Triticum aestivum cultivar Chinese Spring is associated with alteration of gene expression. Genome 1020:1–12. doi: 10.1139/gen-2020-0152

Hallen-Adams HE, Wenner N, Kuldau GA, Trail F (2011) Deoxynivalenol biosynthesis-related gene expression during wheat kernel colonization by *Fusarium graminearum*. Phytopathology 101:1091–1096. doi: 10.1094/PHYTO-01-11-0023

Harris LJ, Balcerzak M, Johnston A, et al (2016) Host-preferential *Fusarium graminearum* gene expression during infection of wheat, barley, and maize. Fungal Biol 120:111–123. doi: 10.1016/j.funbio.2015.10.010

Hauvermale AL, Ariizumi T, Steber CM (2012) Gibberellin signaling: A theme and variations on DELLA repression. Plant Physiol 160:83–92. doi: 10.1104/pp.112.200956

He X, Singh PK, Dreisigacker S, et al (2016) Dwarfing genes Rht-B1b and Rht-D1b are associated with both type I FHB susceptibility and low anther extrusion in two bread wheat populations. PLoS One 11:1–18. doi: 10.1371/journal.pone.0162499

Hedden P (2003) The genes of the Green Revolution. Trends Genet 19:5–9. doi: 10.1016/S0168-9525(02)00009-4

Hedden P, Sponsel V (2015) A century of gibberellin research. J. Plant Growth Regul. 34:740–760. doi: 10.1007/s00344-015-9546-1

Henriquez MA, Derksen H, Doherty J, et al (2018a) Fusarium head blight of spring wheat in Manitoba in 2017. Can Plant Dis Surv 98:121–122. https://phytopath.ca/wp-content/uploads/2018/11/CPDS_2018_Vol_98_revised-Nov-2018.pdf. Accessed 21 Mar 2021

Henriquez MA, Derksen H, Doherty J, et al (2018b) Fusarium head blight of winter wheat in Manitoba in 2017. Can Plant Dis Surv 98:123–124. https://phytopath.ca/wp-content/uploads/2018/11/CPDS_2018_Vol_98_revised-Nov-2018.pdf. Accessed 21 Mar 2021

Henriquez MA, Derksen H, Doherty J, et al (2019a) Fusarium head blight of spring wheat in Manitoba in 2018. Canadian plant disease survey 2019 Volume 99: Disease highlights 2018. Can J Plant Pathol 41:96–97. doi: 10.1080/07060661.2019.1619270

Henriquez MA, Derksen H, Doherty J, et al (2019b) Fusarium head blight of winter wheat in Manitoba in 2018. Canadian plant disease survey 2019 Volume 99: Disease highlights 2018. Can J Plant Pathol 41:96–97. doi: 10.1080/07060661.2019.1619270

Henriquez MA, Kaminski D, Doherty J, et al (2020a) Fusarium head blight of spring wheat in Manitoba in 2019. Canadian plant disease survey 2020 Volume 100: Disease highlights 2019. Can J Plant Pathol 42:71–72. doi: /10.1080/07060661.2020.1752524

Henriquez MA, Kaminski D, Doherty J, et al (2020b) Fusarium head blight of spring wheat in Manitoba in 2019. Canadian plant disease survey 2020 Volume 100: Disease highlights 2019. Can J Plant Pathol 42:73–74. doi: /10.1080/07060661.2020.1752524

Henriquez MA, Soliman A, Li G, et al (2016) Molecular cloning, functional characterization and expression of potato (Solanum tuberosum) 1-deoxy-d-xylulose 5-phosphate synthase 1 (StDXS1) in response to Phytophthora infestans. Plant Sci 243:71–83. doi: 10.1016/j.plantsci.2015.12.001

Herter CP, Ebmeyer E, Kollers S, et al (2018) Rht24 reduces height in the winter wheat population 'Solitär × Bussard' without adverse effects on Fusarium head blight infection. Theor Appl Genet 131:1263–1272. doi: 10.1007/s00122-018-3076-8

Holzapfel J, Voss HH, Miedaner T, et al (2008) Inheritance of resistance to Fusarium head blight in three European winter wheat populations. Theor Appl Genet 117:1119–1128. doi: 10.1007/s00122-008-0850-z

Hou X, Lee LYC, Xia K, et al (2010) DELLAs modulate jasmonate signaling via competitive binding to JAZs. Dev Cell 19:884–894. doi: 10.1016/j.devcel.2010.10.024

Inch SA, Gilbert J (2003) Survival of Gibberella zeae in Fusarium-damaged wheat kernels. Plant Dis 87:282–287. doi: 10.1094/PDIS.2003.87.3.282

International Wheat Genome Sequencing Consortium (IWGSC) (2018) Shifting the limits in wheat research and breeding using a fully annotated reference genome. Science 361:6403. doi: 10.1126/science.aar7191

Jansen C, Von Wettstein D, Schäfer W, et al (2005) Infection pattern in barley and wheat spikes inoculated with wild-type and trichodiene synthase gene disrupted F*usarium graminearum*. Proc Natl Acad Sci USA 102:16892–16897. doi: 10.1073/pnas.0508467102

Jia H, Zhou J, Xue S, et al (2018) A journey to understand wheat Fusarium head blight resistance in the Chinese wheat landrace Wangshuibai. Crop J 6:48–59. doi: 10.1016/j.cj.2017.09.006

Jing Y, Liu J, Liu P, et al (2019) Overexpression of TaJAZ1 increases powdery mildew resistance through promoting reactive oxygen species accumulation in bread wheat. Sci Rep 9:1–15. doi: 10.1038/s41598-019-42177-y

Jochum CC, Osborne LE, Yuen GY (2006) Fusarium head blight biological control with Lysobacter enzymogenes strain C3. Biol Control 39:336–344. doi: 10.1016/j.biocontrol.2006.05.004

Joehanes R, Nelson JC (2008) QGene 4.0, an extensible Java QTL-analysis platform. Bioinformatics 24:2788–2789. doi: 10.1093/bioinformatics/btn523

Kang J, Clark A, Van Sanford D, et al (2011) Exotic scab resistance quantitative trait loci effects on soft red winter wheat. Crop Sci 51:924–933. doi: 10.2135/cropsci2010.06.0313

Kang Z, Buchenauer H (1999) Immunocytochemical localization of fusarium toxins in infected wheat spikes by *Fusarium culmorum*. Physiol Mol Plant Pathol 55:275–288. doi: 10.1006/pmpp.1999.0233

Kazan K, Gardiner DM (2018) Transcriptomics of cereal-Fusarium graminearum interactions: What we have learned so far. Mol Plant Pathol 19:764–778. doi: 10.1111/mpp.12561

King R, Urban M, Hammond-Kosack MCU, et al (2015) The completed genome sequence of the pathogenic ascomycete fungus *Fusarium graminearum*. BMC Genomics 16:544–565. doi: 10.1186/s12864-015-1756-1

Kluger B, Bueschl C, Lemmens M, et al (2013) Stable isotopic labelling-assisted untargeted metabolic profiling reveals novel conjugates of the mycotoxin deoxynivalenol in wheat. Anal Bioanal Chem 405:5031–5036. doi: 10.1007/s00216-012-6483-8

Koornneef A, Pieterse CMJ (2008) Cross talk in defense signaling. Plant Physiol 146:839–844. doi: 10.1104/pp.107.112029

Kosambi DD (1943) The estimation of map distances from recombination values. Ann Eugen 12:172–175. doi: 10.1111/j.1469-1809.1943.tb02321.x

Kulik T (2008) Detection of *Fusarium tricinctum* from cereal grain using PCR assay. J Appl Genet 49:305–311. doi: 10.1007/BF03195628

Lagudah ES, Krattinger SG (2019) A new player contributing to durable Fusarium resistance. Nat Genet 51:1070–1071. doi: 10.1038/s41588-019-0454-3

Langevin F, Eudes F, Comeau A (2004) Effect of trichothecenes produced by Fusarium graminearum during Fusarium head blight development in six cereal species. Eur J Plant Pathol 110:735–746. doi: 10.1023/B:EJPP.0000041568.31778.ad

Lanning SP, Martin JM, Stougaard RN, et al (2012) Evaluation of near-isogenic lines for three height-reducing genes in hard red spring wheat. Crop Sci 52:1145–1152. doi: 10.2135/cropsci2011.11.0625

Lee J, Jurgenson JE, Leslie JF, Bowden RL (2008) Alignment of genetic and physical maps of *Gibberella zeae*. Appl Environ Microbiol 74:2349–2359. doi: 10.1128/AEM.01866-07

Lee T, Lee S-H, Shin JY, et al (2014) Comparison of trichothecene biosynthetic gene expression between *Fusarium graminearum* and *Fusarium asiaticum*. Plant Pathol J 30:33–42. doi: 10.5423/PPJ.OA.11.2013.0107

Lemmens M, Scholz U, Berthiller F, et al (2005) The ability to detoxify the mycotoxin deoxynivalenol colocalizes with a major quantitative trait locus for Fusarium head blight resistance in wheat. Mol Plant-Microbe Interact 18:1318–1324. doi: 10.1094

Li A, Yang W, Li S, et al (2013) Molecular characterization of three gibberellin-insensitive dwarf1 homologous genes in hexaploid wheat. J Plant Physiol 170:432–443. doi: 10.1016/j.jplph.2012.11.010

Li G, Yen Y (2008) Jasmonate and ethylene signaling pathway may mediate Fusarium head blight resistance in wheat. Crop Sci 48:1888. doi: 10.2135/cropsci2008.02.0097

Li G, Zhou J, Jia H, et al (2019) Mutation of a histidine-rich calcium-binding-protein gene in wheat confers resistance to Fusarium head blight. Nat Genet 51:1106–1112. doi: 10.1038/s41588-019-0426-7

Li H, Ribaut JM, Li Z, Wang J (2008a) Inclusive composite interval mapping (ICIM) for digenic epistasis of quantitative traits in biparental populations. Theor Appl Genet 116:243–260. doi: 10.1007/s00122-007-0663-5

Li S, Jochum CC, Yu F, et al (2008b) An antibiotic complex from Lysobacter enzymogenes strain C3: Antimicrobial activity and role in plant disease control. Phytopathology 98:695–701. doi: 10.1094/PHYTO-98-6-0695

Liu H, Timko MP (2021) Jasmonic acid signaling and molecular crosstalk with other phytohormones. Int J Mol Sci 22:1–24. doi: 10.3390/ijms22062914

Liu S, Christopher MD, Griffey CA, et al (2012) Molecular characterization of resistance to Fusarium head blight in U.S. soft red winter wheat breeding line VA00W-38. Crop Sci 52:2283–2292. doi: 10.2135/cropsci2012.03.0144

Liu S, Hall MD, Griffey CA, McKendry AL (2009) Meta-analysis of QTL associated with Fusarium head blight resistance in wheat. Crop Sci 49:1955–1968. doi: 10.2135/cropsci2009.03.0115

Liu S, Pumphrey MO, Gill BS, et al (2008) Toward positional cloning of fhb1, a major QTL for Fusarium head blight resistance in wheat. Cereal Res Commun 36:195–201. doi: 10.1556/CRC.36.2008.Suppl.B.15

Liu S, Zhang X, Pumphrey MO, et al (2006) Complex microcolinearity among wheat, rice, and barley revealed by fine mapping of the genomic region harboring a major QTL for resistance to Fusarium head blight in wheat. Funct Integr Genomics 6:83–89. doi: 10.1007/s10142-005-0007-y

Liu X, Yu F, Schnabel G, et al (2011) Paralogous *cyp51* genes in *Fusarium graminearum* mediate differential sensitivity to sterol demethylation inhibitors. Fungal Genet Biol 48:113–123. doi: 10.1016/j.fgb.2010.10.004

Liu Z, Sun Q, Ni Z, Yang T (1999) Development of SCAR markers linked to the Pm21 gene conferring resistance to powdery mildew in common wheat. Plant Breed 118:215–219. doi: 10.1046/j.1439-0523.1999.118003215.x

Livak KJ, Schmittgen TD (2001) Analysis of relative gene expression data using real-time quantitative PCR and the 2-ΔΔCT method. Methods 25:402–408. doi: 10.1006/meth.2001.1262

Löffler M, Schön CC, Miedaner T (2009) Revealing the genetic architecture of FHB resistance in hexaploid wheat (Triticum aestivum L.) by QTL meta-analysis. Mol Breed 23:473–488. doi: 10.1007/s11032-008-9250-y

Lorieux M (2012) MapDisto: fast and efficient computation of genetic linkage maps. Mol Breed 30:1231–1235. doi: 10.1007/s11032-012-9706-y

Lu Q, Lillemo M, Skinnes H, et al (2013) Anther extrusion and plant height are associated with Type I resistance to Fusarium head blight in bread wheat line "Shanghai-3/Catbird." Theor Appl Genet 126:317–334. doi: 10.1007/s00122-012-1981-9

Luo MC, Gu YQ, Puiu D, et al (2017) Genome sequence of the progenitor of the wheat D genome Aegilops tauschii. Nature 551:498–502. doi: 10.1038/nature24486

Lv C, Song Y, Gao L, et al (2014) Integration of QTL detection and marker assisted selection for improving resistance to Fusarium head blight and important agronomic traits in wheat. Crop J 2:70–78. doi: 10.1016/J.CJ.2013.10.004

Ma HX, Bai GH, Gill BS, Hart LP (2006a) Deletion of a chromosome arm altered wheat resistance to Fusarium head blight and deoxynivalenol accumulation in Chinese spring. Plant Dis 90:1545–1549. doi: 10.1094/PD-90-1545

Ma HX, Bai GH, Zhang X, Lu WZ (2006b) Main effects, epistasis, and environmental interactions of quantitative trait loci for Fusarium head blight resistance in a recombinant inbred population. Phytopathology 96:534–541. doi: 10.1094/PHYTO-96-0534

Ma Z, Xie Q, Li G, et al (2020) Germplasms, genetics and genomics for better control of disastrous wheat Fusarium head blight. Theor Appl Genet 133:1541–1568. doi: 10.1007/s00122-019-03525-8

Makhoul M, Rambla C, Voss-Fels KP, et al (2020) Overcoming polyploidy pitfalls: a user guide for effective SNP conversion into KASP markers in wheat. Theor Appl Genet 133:2413–2430. doi: 10.1007/s00122-020-03608-x

Malihipour A, Gilbert J, Fedak G, et al (2017) Mapping the A genome for QTL conditioning resistance to Fusarium head blight in a wheat population with Triticum Timopheevii background. Plant Dis 101:11–19. doi: 10.1094/PDIS-02-16-0144-RE

Mao SL, Wei YM, Cao W, et al (2010) Confirmation of the relationship between plant height and Fusarium head blight resistance in wheat (Triticum aestivum L.) by QTL meta-analysis. Euphytica 174:343–356. doi: 10.1007/s10681-010-0128-9

Marcussen T, Sandve SR, Heier L, et al (2014) Ancient hybridizations among the ancestral genomes of bread wheat. Science 345:1250092. doi: DOI: 10.1126/science.1250092

Mardi M, Pazouki L, Delavar H, et al (2006) QTL analysis of resistance to Fusarium head blight in wheat using a 'Frontana'-derived population. Plant Breed 125:313–317. doi: 10.1111/j.1439-0523.2006.01228.x

Marone D, Laidò G, Gadaleta A, et al (2012) A high-density consensus map of A and B wheat genomes. Theor Appl Genet 125:1619–1638. doi: 10.1007/s00122-012-1939-y

Mayer E, Novak B, Springler A, et al (2017) Effects of deoxynivalenol (DON) and its microbial biotransformation product deepoxy-deoxynivalenol (DOM-1) on a trout, pig, mouse, and human cell line. Mycotoxin Res 33:297–308. doi: 10.1007/s12550-017-0289-7

McCallum BD, Tekauz A, Gilbert J (2004) Reaction of a diverse collection of barley lines to Fusarium head blight. Plant Dis 88:167–174. doi: 10.1094/PDIS.2004.88.2.167

McCartney CA, Brûlé-Babel AL, Fedak G, et al (2016) Fusarium head blight resistance QTL in the spring wheat cross Kenyon/86ISMN 2137. Front Microbiol 7:1542. doi: 10.3389/fmicb.2016.01542

McCartney CA, Somers DJ, Fedak G, et al (2007) The evaluation of FHB resistance QTLs introgressed into elite Canadian spring wheat germplasm. Mol Breed 20:209–221. doi: 10.1007/s11032-007-9084-z

McCartney CA, Somers DJ, Fedak G, Cao W (2004) Haplotype diversity at Fusarium head blight resistance QTLs in wheat. Theor Appl Genet 109:261–271. doi: 10.1007/s00122-004-1640-x

McCormick SP, Harris LJ, Alexander NJ, et al (2004) *Tri1* in *Fusarium graminearum* encodes a P450 oxygenase. Appl Environ Microbiol 70:2044–2051. doi: 10.1128/AEM.70.4.2044–2051.2004

McCormick SP, Stanley AM, Stover NA, Alexander NJ (2011) Trichothecenes: from simple to complex mycotoxins. Toxins (Basel) 3:802–814. doi: 10.3390/toxins3070802

McLaughlin JE, Bin-Umer MA, Tortora A, et al (2009) A genome-wide screen in Saccharomyces cerevisiae reveals a critical role for the mitochondria in the toxicity of a trichothecene mycotoxin. Proc Natl Acad Sci USA 106:21883–21888. doi: 10.1073/pnas.0909777106

McMullen M, Bergstrom G, De Wolf E, et al (2012) A unified effort to fight an enemy of wheat and barley: Fusarium head blight. Plant Dis 96:1712–1728. doi: 10.1094/PDIS-03-12-0291-FE

McMullen M, Jones R, Gallenberg D, et al (1997) Scab of wheat and barley: a re-emerging disease of devastating impact. Plant Dis 81:1340–1348. doi: 10.1094/PDIS.1997.81.12.1340

Meier I, Gruissem W (1994) Novel conserved sequence motifs in plant G-box binding proteins and implications for interactive domains. Nucleic Acids Res 22:470–478. doi: 10.1093/nar/22.3.470

Meng L, Li H, Zhang L, Wang J (2015) QTL IciMapping: Integrated software for genetic linkage map construction and quantitative trait locus mapping in biparental populations. Crop J 3:269–283. doi: 10.1016/j.cj.2015.01.001

Mesterhazy A (2020) Updating the breeding philosophy of wheat to Fusarium head blight (FHB): Resistance components, QTL identification, and phenotyping—A review. Plants 9:1702–1735. doi: 10.3390/plants9121702

Mesterházy A (1995) Types and components of resistance to Fusarium head blight of wheat. Plant Breed 114:377–386. doi: 10.1111/j.1439-0523.1995.tb00816.x

Miedaner T, Lenhardt M, Grehl J, et al (2022) Dwarfing gene Rht24 does not affect Fusarium head blight resistance in a large European winter wheat diversity panel. Euphytica. 218:1-10. doi: 10.1007/s10681-022-03028-6

Miedaner T, Voss HH (2008) Effect of dwarfing Rht genes on Fusarium head blight resistance in two sets of near-isogenic lines of wheat and check cultivars. Crop Sci 48:2115–2122. doi: 10.2135/cropsci2008.02.0107

Mudge AM, Dill-Macky R, Dong Y, et al (2006) A role for the mycotoxin deoxynivalenol in stem colonisation during crown rot disease of wheat caused by *Fusarium graminearum* and *Fusarium pseudograminearum*. Physiol Mol Plant Pathol 69:73–85. doi: 10.1016/j.pmpp.2007.01.003

Murase K, Hirano Y, Sun TP, Hakoshima T (2008) Gibberellin-induced DELLA recognition by the gibberellin receptor GID1. Nature 456:459–463. doi: 10.1038/nature07519

Mwaniki A (2017) Molecular mapping of quantitative trait loci controlling Fusarium head blight resistance and deoxynivalenol accumulation in two winter wheat double haploid populations. Doctoral Thesis. University of Manitoba.

Nasmith CG, Walkowiak S, Wang L, et al (2011) Tri6 is a global transcription regulator in the phytopathogen fusarium graminearum. PLoS Pathog 7:1–12. doi: 10.1371/journal.ppat.1002266

Nathanail AV, Varga E, Meng-Reiterer J, et al (2015) Metabolism of the Fusarium mycotoxins T-2 toxin and HT-2 toxin in wheat. J Agric Food Chem 63:7862–7872. doi: 10.1021/acs.jafc.5b02697

Navarro L, Bari R, Achard P, et al (2008) DELLAs control plant immune responses by modulating the balance of jasmonic acid and salicylic acid signaling. Curr Biol 18:650–655. doi: 10.1016/j.cub.2008.03.060

Nelson JC, Sorrells ME, Van Deynze AE, et al (1995) Molecular mapping of wheat: Major genes and rearrangements in homoeologous groups 4, 5, and 7. Genetics 141:721–731. doi: 10.1093/genetics/141.2.721

Nelson SK, Steber CM (2016) Gibberellin hormone signal perception: down-regulating DELLA repressors of plant growth and development. In: Hedden P & Thomas SG (ed) Annual Plant Reviews: The Gibberellins, 49th edn. Wiley Blackwell, Chichester, England, pp 153–188

Nowakowski G (2018) Mitigation of Fusarium head blight in wheat caused by *Fusarium graminearum* through the use of host resistance genes and biological controls. Masters Thesis. University of Manitoba

O'Donnell K, Kistler HC, Tacke BK, Casper HH (2000) Gene genealogies reveal global phylogeographic structure and reproductive isolation among lineages of *Fusarium graminearum*, the fungus causing wheat scab. Proc Natl Acad Sci USA 97:7905–7910. doi: 10.1073/pnas.130193297

O'Donnell K, Ward TJ, Aberra D, et al (2008) Multilocus genotyping and molecular phylogenetics resolve a novel head blight pathogen within the *Fusarium graminearum* species complex from Ethiopia. Fungal Genet Biol 45:1514–1522. doi: 10.1016/j.fgb.2008.09.002

O'Donnell K, Ward TJ, Geiser DM, et al (2004) Genealogical concordance between the mating type locus and seven other nuclear genes supports formal recognition of nine phylogenetically distinct species within the *Fusarium graminearum* clade. Fungal Genet Biol 41:600–623. doi: 10.1016/j.fgb.2004.03.003

Okubara PA, Blechl AE, McCormick SP, et al (2002) Engineering deoxynivalenol metabolism in wheat through the expression a fungal trichothecene acetyltransferase gene. Theor Appl Genet 106:74–83. doi: 10.1007/s00122-002-1066-2

Paillard S, Schnurbusch T, Tiwari R, et al (2004) QTL analysis of resistance to Fusarium head blight in Swiss winter wheat (Triticum aestivum L.). Theor Appl Genet 109:323–332. doi: 10.1007/s00122-004-1628-6

Palazzini JM, Dunlap CA, Bowman MJ, Chulze SN (2016) Bacillus velezensis RC 218 as a biocontrol agent to reduce Fusarium head blight and deoxynivalenol accumulation: Genome sequencing and secondary metabolite cluster profiles. Microbiol Res 192:30–36. doi: 10.1016/j.micres.2016.06.002

Pan Y, Liu Z, Rocheleau H, et al (2018) Transcriptome dynamics associated with resistance and susceptibility against Fusarium head blight in four wheat genotypes. BMC Genomics 19:1–26. doi: 10.1186/s12864-018-5012-3

Park JH, Halitschke R, Kim HB, et al (2002) A knock-out mutation in allene oxide synthase results in male sterility and defective wound signal transduction in Arabidopsis due to a block in jasmonic acid biosynthesis. Plant J 31:1–12. doi: 10.1046/j.1365-313X.2002.01328.x

Paudel B, Zhuang Y, Galla A, et al (2020) WFhb1-1 plays an important role in resistance against Fusarium head blight in wheat. Sci Rep 10:1–15. doi: 10.1038/s41598-020-64777-9

Paul PA, Lipps PE, Hershman DE, et al (2008) Efficacy of triazole-based fungicides for Fusarium head blight and deoxynivalenol control in wheat: A multivariate meta-analysis. Phytopathology 98:999–1011. doi: 10.1094/PHYTO-98-9-0999

Paul RA, Lipps PE, Hershman DE, et al (2007) A quantitative review of tebuconazole effect on Fusarium head blight and deoxynivalenol content in wheat. Phytopathology 97:211–220. doi: 10.1094/PHYTO-97-2-0211

Pearce S, Saville R, Vaughan SP, et al (2011) Molecular characterization of Rht-1 dwarfing genes in hexaploid wheat. Plant Physiol 157:1820–1831. doi: 10.1104/pp.111.183657

Peng J, Richards DE, Hartley NM, et al (1999) “Green revolution” genes encode mutant gibberellin response modulators. Nature 400:256–261. doi: 10.1038/22307

Peng JH, Sun D, Nevo E (2011) Domestication evolution, genetics and genomics in wheat. Mol Breed 28:281–301. doi: 10.1007/s11032-011-9608-4

Petersen S, Lyerly JH, Maloney P V., et al (2016) Mapping of Fusarium head blight resistance quantitative trait loci in winter wheat cultivar NC-Neuse. Crop Sci 56:1473–1483. doi: 10.2135/cropsci2015.05.0312

Petersen S, Lyerly JH, McKendry AL, et al (2017) Validation of Fusarium head blight resistance QTL in US winter wheat. Crop Sci 57:1–12. doi: 10.2135/cropsci2015.07.0415

Pierron A, Mimoun S, Murate LS, et al (2016) Intestinal toxicity of the masked mycotoxin deoxynivalenol-3-β-d-glucoside. Arch Toxicol 90:2037–2046. doi: 10.1007/s00204-015-1592-8

Pritsch C, Muehlbauer GJ, Bushnell WR, et al (2000) Fungal development and induction of defense response genes during early infection of wheat spikes by *Fusarium graminearum*. Mol Plant-Microbe Interact 13:159–169. doi: 10.1094/MPMI.2000.13.2.159

Proctor RH, Hohn TM, McCormick SP (1995) Reduced virulence of *Gibberella zeae* caused by disruption of a trichothecene toxin biosynthetic gene. Mol Plant-Microbe Interact 8:593–601. doi: 10.1094/MPMI-8-0593

Puranik S, Sahu PP, Srivastava PS, Prasad M (2012) NAC proteins: Regulation and role in stress tolerance. Trends Plant Sci 17:369–381. doi: 10.1016/j.tplants.2012.02.004

Puri KD, Zhong S (2010) The 3ADON population of *Fusarium graminearum* found in North Dakota is more aggressive and produces a higher level of DON than the prevalent 15ADON population in spring wheat. Phytopathology 100:1007–1014. doi: 10.1094 /PHYTO-12-09-0332

Qi LL, Pumphrey MO, Friebe B, et al (2008) Molecular cytogenetic characterization of alien introgressions with gene *Fhb3* for resistance to Fusarium head blight disease of wheat. Theor Appl Genet 117:1155–1166. doi: 10.1007/s00122-008-0853-9

Qi PF, Balcerzak M, Rocheleau H, et al (2016) Jasmonic acid and abscisic acid play important roles in host-pathogen interaction between *Fusarium graminearum* and wheat during the early stages of Fusarium head blight. Physiol Mol Plant Pathol 93:39–48. doi: 10.1016/j.pmpp.2015.12.004

Qi PF, Jiang YF, Guo ZR, et al (2019) Transcriptional reference map of hormone responses in wheat spikes. BMC Genomics 20:1–13. doi: 10.1186/s12864-019-5726-x

Qi PF, Johnston A, Balcerzak M, et al (2012) Effect of salicylic acid on *Fusarium graminearum*, the major causal agent of Fusarium head blight in wheat. Fungal Biol 116:413–426. doi: 10.1016/j.funbio.2012.01.001

Qi T, Huang H, Wu D, et al (2014) Arabidopsis DELLA and JAZ proteins bind the WD-Repeat/ bHLH/MYB complex to modulate gibberellin and jasmonate signaling synergy. Plant Cell 26:1118–1133. doi: 10.1105/tpc.113.121731

Ramarathnam R, Bo S, Chen Y, et al (2007) Molecular and biochemical detection of fengycin- and bacillomycin D-producing Bacillus spp., antagonistic to fungal pathogens of canola and wheat. Can J Microbiol 53:901–911. doi: 10.1139/W07-049

Randhawa HS, Asif M, Pozniak C, et al (2013) Application of molecular markers to wheat breeding in Canada. Plant Breed 132:458–471. doi: 10.1111/pbr.12057

Ravensdale M, Rocheleau H, Wang L, et al (2014) Components of priming-induced resistance to Fusarium head blight in wheat revealed by two distinct mutants of *Fusarium graminearum*. Mol Plant Pathol 15:948–956. doi: 10.1111/mpp.12145

Rawat N, Pumphrey MO, Liu S, et al (2016) Wheat Fhb1 encodes a chimeric lectin with agglutinin domains and a pore-forming toxin-like domain conferring resistance to Fusarium head blight. Nat Genet 48:1576–1580. doi: 10.1038/ng.3706

Röder MS, Korzun V, Wendehake K, et al (1998) A microsatellite map of wheat. Genetics 149:2007–2023. doi: 10.1093/genetics/149.4.2007

Ruan J, Zhou Y, Zhou M, et al (2019) Jasmonic acid signaling pathway in plants. Int J Mol Sci 20:2479. doi: 10.3390/ijms20102479

Ruan Y, Zhang W, Knox RE, et al (2020) Characterization of the genetic architecture for Fusarium head blight resistance in durum wheat: The complex association of resistance, flowering time, and height genes. Front Plant Sci 11:592064. doi: 10.3389/fpls.2020.592064

Saito H, Oikawa T, Hamamoto S, et al (2015) The jasmonate-responsive GTR1 transporter is required for gibberellin-mediated stamen development in Arabidopsis. Nat Commun 6:6095. doi: 10.1038/ncomms7095

Salameh A, Buerstmayr M, Steiner B, et al (2011) Effects of introgression of two QTL for Fusarium head blight resistance from Asian spring wheat by marker-assisted backcrossing into European winter wheat on Fusarium head blight resistance, yield and quality traits. Mol Breed 28:485–494. doi: 10.1007/s11032-010-9498-x

Sari E, Berraies S, Id REK, et al (2018) High density genetic mapping of Fusarium head blight resistance QTL in tetraploid wheat. PLoS One 13:e0204362. doi: 10.1371/journal.10.1371/journal.pone.0204362

Sarver BAJ, Ward TJ, Gale LR, et al (2011) Novel Fusarium head blight pathogens from Nepal and Louisiana revealed by multilocus genealogical concordance. Fungal Genet Biol 48:1096–1107. doi: 10.1016/j.fgb.2011.09.002

Saville RJ, Gosman N, Burt CJ, et al (2012) The "Green Revolution" dwarfing genes play a role in disease resistance in Triticum aestivum and Hordeum vulgare. J Exp Bot 63:1271–1283. doi: 10.1093/jxb/err350

Schisler DA, Slininger PJ, Boehm MJ, Paul PA (2011) Co-culture of yeast antagonists of fusarium head blight and their effect on disease development in wheat. Plant Pathol J 10:128–137. doi: 10.2923-ppj.2011.128.137

Schmolke M, Zimmermann G, Buerstmayr H, et al (2005) Molecular mapping of Fusarium head blight resistance in the winter wheat population Dream/Lynx. Theor Appl Genet 111:747–756. doi: 10.1007/s00122-005-2060-2

Schweiger W, Steiner B, Vautrin S, et al (2016) Suppressed recombination and unique candidate genes in the divergent haplotype encoding Fhb1, a major Fusarium head blight resistance locus in wheat. Theor Appl Genet 129:1607–1623. doi: 10.1007/s00122-016-2727-x

Semagn K, Babu R, Hearne S, Olsen M (2014) Single nucleotide polymorphism genotyping using Kompetitive Allele Specific PCR (KASP): Overview of the technology and its application in crop improvement. Mol Breed 33:1–14. doi: 10.1007/s11032-013-9917-x

Semagn K, Skinnes H, Bjørnstad Å, et al (2007) Quantitative trait loci controlling Fusarium head blight resistance and low deoxynivalenol content in hexaploid wheat population from "Arina" and NK93604. Crop Sci 47:294–303. doi: 10.2135/cropsci2006.02.0095

Seong KY, Pasquali M, Zhou X, et al (2009) Global gene regulation by Fusarium transcription factors *Tri6* and *Tri10* reveals adaptations for toxin biosynthesis. Mol Microbiol 72:354–367. doi: 10.1111/j.1365-2958.2009.06649.x

Sheard LB, Tan X, Mao H, et al (2010) Jasmonate perception by inositol-phosphate-potentiated COI1-JAZ co-receptor. Nature 468:400–407. doi: 10.1038/nature09430

Shewry PR (2009) Wheat. J Exp Bot 60:1537–1553. doi: 10.1093/jxb/erp058

Shigenaga AM, Argueso CT (2016) No hormone to rule them all: Interactions of plant hormones during the responses of plants to pathogens. Semin Cell Dev Biol 56:174–189. doi: 10.1016/j.semcdb.2016.06.005

Shimada A, Ueguchi-Tanaka M, Nakatsu T, et al (2008) Structural basis for gibberellin recognition by its receptor GID1. Nature 456:520–523. doi: 10.1038/nature07546

Silverstone AL, Jung H, Dill A, et al (2001) Repressing a repressor : Gibberellin-induced rapid reduction of the RGA Protein in arabidopsis. Plant Cell 13:1555–1565. doi: 10.1105/tpc.010047.

Singh L, Anderson JA, Chen J, et al (2019) Development and validation of a perfect KASP marker for Fusarium head blight resistance gene Fhb1 in wheat. Plant Pathol J 35:200–207. doi: 10.5423/PPJ.OA.01.2019.0018

Skinnes H, Semagn K, Tarkegne Y, et al (2010) The inheritance of anther extrusion in hexaploid wheat and its relationship to Fusarium head blight resistance and deoxynivalenol content. Plant Breed 129:149–155. doi: 10.1111/j.1439-0523.2009.01731.x

Sobrova P, Adam V, Vasatkova A, et al (2010) Deoxynivalenol and its toxicity. Interdiscip Toxicol 3:94–99. doi: 10.2478/v10102-010-0019-x

Somers DJ, Isaac P, Edwards K (2004) A high-density microsatellite consensus map for bread wheat (Triticum aestivum L.). Theor Appl Genet 109:1105–1114. doi: 10.1007/s00122-004-1740-7

Somers DJ, Thomas J, DePauw R, et al (2005) Assembling complex genotypes to resist Fusarium in wheat (Triticum aestivum L.). Theor Appl Genet 111:1623–1631. doi: 10.1007/s00122-005-0094-0

Sorrells ME, Benscher D, Cox WJ (2004) Registration of 'Caledonia' wheat. Crop Sci 44:1471–1472. doi: 10.2135/cropsci2004.1471

Srinivasachary, Gosman N, Steed A, et al (2009) Semi-dwarfing Rht-B1 and Rht-D1 loci of wheat differ significantly in their influence on resistance to Fusarium head blight. Theor Appl Genet 118:695–702. doi: 10.1007/s00122-008-0930-0

Srinivasachary, Gosman N, Steed A, et al (2008a) Susceptibility to Fusarium head blight is associated with the Rht-D1b semi-dwarfing allele in wheat. Theor Appl Genet 116:1145–1153. doi: 10.1007/s00122-008-0742-2

Srinivasachary, Gosman N, Steed A, et al (2008b) Mapping of QTL associated with Fusarium head blight in spring wheat RL4137. Czech J Genet Plant Breed 44:147–159. doi: 10.17221/70/2008-cjgpb

Starkey DE, Ward TJ, Aoki T, et al (2007) Global molecular surveillance reveals novel Fusarium head blight species and trichothecene toxin diversity. Fungal Genet Biol 44:1191–1204. doi: 10.1016/j.fgb.2007.03.001

Statistics Canada (2020) Estimated areas, yield, production, average farm price and total farm value of principal field crops, in metric and imperial units. https://www150.statcan.gc.ca/t1/tbl1/en/tv.action?pid=3210035901.Accessed 18 Mar 2021

Steiner B, Buerstmayr M, Michel S, et al (2017) Breeding strategies and advances in line selection for Fusarium head blight resistance in wheat. Trop Plant Pathol 42:165–174. doi: 10.1007/s40858-017-0127-7

Steiner B, Buerstmayr M, Wagner C, et al (2019) Fine-mapping of the Fusarium head blight resistance QTL Qfhs.ifa-5A identifies two resistance QTL associated with anther extrusion. Theor Appl Genet 132:2039–2053. doi: 10.1007/s00122-019-03336-x

Steiner B, Lemmens M, Griesser M, et al (2004) Molecular mapping of resistance to Fusarium head blight in the spring wheat cultivar Frontana. Theor Appl Genet 109:215–224. doi: 10.1007/s00122-004-1620-1

Su Z, Bernardo A, Tian B, et al (2019) A deletion mutation in TaHRC confers Fhb1 resistance to Fusarium head blight in wheat. Nat Genet 51:1099–1105. doi: 10.1038/s41588-019-0425-8

Sun Y, Xiao J, Jia X, et al (2016) The role of wheat jasmonic acid and ethylene pathways in response to Fusarium graminearum infection. Plant Growth Regul 80:69–77. doi: 10.1007/s10725-016-0147-1

Suzuki T, Sato M, Takeuchi T (2012) Evaluation of the effects of five QTL regions on Fusarium head blight resistance and agronomic traits in spring wheat (Triticum aestivum L.). Breed Sci 62:11–17. doi: 10.1270/jsbbs.62.11

Szabó-Hevér Á, Lehoczki-Krsjak S, Tóth B, et al (2012) Identification and validation of Fusarium head blight and Fusarium -damaged kernel QTL in a Frontana/Remus DH mapping population. Can J Plant Pathol 34:224–238. doi: 10.1080/07060661.2012.676571

Tamburic-Ilincic L (2012) Effect of 3B, 5A and 3A QTL for Fusarium head blight resistance on agronomic and quality performance of Canadian winter wheat. Plant Breed 131:722–727. doi: 10.1111/pbr.12005

Tamburic-Ilincic L, Rosa SB (2017) Alleles on the two dwarfing loci on 4B and 4D are main drivers of FHB-related traits in the Canadian winter wheat population "Vienna" × "25R47." Plant Breed 136:1–10. doi: 10.1111/pbr.12527

Tamburic-Ilincic L, Somers D, Fedak G, Schaafsma A (2009) Different quantitative trait loci for Fusarium resistance in wheat seedlings and adult stage in the Wuhan/Nyubai wheat population. Euphytica 165:453–458. doi: 10.1007/s10681-008-9747-9

Thambugala D, Brûlé-Babel AL, Barbara B, et al (2020) Genetic analyses of native Fusarium head blight resistance in two spring wheat populations identifies QTL near the B1, Ppd-D1, Rht-1, Vrn-1, Fhb1, Fhb2, and Fhb5 loci. Theor Appl Genet 133:2775–2796. doi: 10.1007/s00122-020-03631-y

Thapa G, Gunupuru LR, Hehir JG, et al (2018) A pathogen-responsive leucine rich receptor like kinase contributes to Fusarium resistance in cereals. Front Plant Sci 9:1–15. doi: 10.3389/fpls.2018.00867

Thines B, Katsir L, Melotto M, et al (2007) JAZ repressor proteins are targets of the SCFCOI1 complex during jasmonate signalling. Nature 448:661–665. doi: 10.1038/nature05960

Thomas SG (2017) Novel Rht-1 dwarfing genes: tools for wheat breeding and dissecting the function of DELLA proteins. J Exp Bot 68:354–358. doi: 10.1093/jxb/erw509

Thomas SG, Blázquez MA, Alabadí D (2016) Della proteins: Master regulators of gibberellin-responsive growth and development. In: Hedden P & Thomas SG (ed) Annual Plant Reviews: The Gibberellins, 49th edn. Wiley Blackwell, Chichester, England, pp 189–228

Tian X, Wen W, Xie L, et al (2017) Molecular mapping of reduced plant height gene Rht24 in bread wheat. Front Plant Sci 8:1–9. doi: 10.3389/fpls.2017.01379

Torres AM, Palacios SA, Yerkovich N, et al (2019) Fusarium head blight and mycotoxins in wheat: Prevention and control strategies across the food chain. World Mycotoxin J 12:333–355. doi: 10.3920/WMJ2019.2438

Toth J, Pandurangan S, Burt A, et al (2019) Marker-assisted breeding of hexaploid spring wheat in the Canadian prairies. Can J Plant Sci 99:111–127. doi: 10.1139/cjps-2018-0183

Trail F (2009) For blighted waves of grain: *Fusarium graminearum* in the postgenomics era. Plant Physiol 149:103–110. doi: 10.1104/pp.108.129684

Trail F, Gaffoor I, Guenther JC, Hallen HE (2005a) Using genomics to understand the disease cycle of the Fusarium head blight fungus, Gibberella zeae (anamorph *Fusarium graminearum*). Can J Plant Pathol 27:486–498. doi: 10.1080/07060660509507250

Trail F, Gaffoor I, Vogel S (2005b) Ejection mechanics and trajectory of the ascospores of Gibberella zeae (anamorph *Fusarium graminearum*). Fungal Genet Biol 42:528–533. doi: 10.1016/j.fgb.2005.03.008

Valverde-Bogantes E, Bianchini A, Herr JR, et al (2020) Recent population changes of Fusarium head blight pathogens: drivers and implications. Can J Plant Pathol 42:315-329. doi: 10.1080/07060661.2019.1680442

Verma V, Worland AJ, Sayers EJ, et al (2005) Identification and characterization of quantitative trait loci related to lodging resistance and associated traits in bread wheat. Plant Breed 124:234–241. doi: 10.1111/j.1439-0523.2005.01070.x

Vogelgsang S, Beyer M, Pasquali M, et al (2019) An eight-year survey of wheat shows distinctive effects of cropping factors on different *Fusarium* species and associated mycotoxins. Eur J Agron 105:62–77. doi: 10.1016/j.eja.2019.01.002

Voss HH, Holzapfel J, Hartl L, et al (2008) Effect of the Rht-D1 dwarfing locus on Fusarium head blight rating in three segregating populations of winter wheat. Plant Breed 127:333–339. doi: 10.1111/j.1439-0523.2008.01518.x

Vujanovic V, Goh YK, Daida P (2012) Heat- and cold-shock responses in *Fusarium graminearum* 3 acetyl- and 15 acetyl-deoxynivalenol chemotypes. J Microbiol 50:97–102. doi: 10.1007/s12275-012-1381-5

Waldron BL, Moreno-Sevilla B, Anderson JA, et al (1999) RFLP mapping of QTL for fusarium head blight resistance in wheat. Crop Sci 39:805–811. doi: 10.2135/cropsci1999.0011183X003900030032x

Walkowiak S, Gao L, Monat C, et al (2020) Multiple wheat genomes reveal global variation in modern breeding. Nature 588:277–283. doi: 10.1038/s41586-020-2961-x

Walkowiak S, Rowland O, Rodrigue N, Subramaniam R (2016) Whole genome sequencing and comparative genomics of closely related Fusarium head blight fungi: F*usarium graminearum, F. meridionale* and *F. asiaticum*. BMC Genomics 17:1–15. doi: 10.1186/s12864-016-3371-1

Wang L, Li Q, Liu Z, et al (2018) Integrated transcriptome and hormone profiling highlight the role of multiple phytohormone pathways in wheat resistance against Fusarium head blight. PLoS One 13:1–24. doi: 10.1371/journal.pone.0207036

Wang R, Chen J, Anderson JA, et al (2017a) Genome-wide association mapping of Fusarium head blight resistance in spring wheat lines developed in the Pacific Northwest and CIMMYT. Phytopathology 107:1486–1495. doi: 10.1094/PHYTO-02-17-0073-R

Wang Y, Zhao J, Lu W, Deng D (2017b) Gibberellin in plant height control: old player, new story. Plant Cell Rep 36:391–398. doi: 10.1007/s00299-017-2104-5.

Wang S, Wong D, Forrest K, et al (2014) Characterization of polyploid wheat genomic diversity using a high-density 90 000 single nucleotide polymorphism array. Plant Biotechnol J 12:787–796. doi: 10.1111/pbi.12183

Ward TJ, Clear RM, Rooney AP, et al (2008) An adaptive evolutionary shift in Fusarium head blight pathogen populations is driving the rapid spread of more toxigenic *Fusarium graminearum* in North America. Fungal Genet Biol 45:473–484. doi: 10.1016/j.fgb.2007.10.003

Warth B, Fruhmann P, Wiesenberger G, et al (2015) Deoxynivalenol-sulfates: Identification and quantification of novel conjugated (masked) mycotoxins in wheat. Anal Bioanal Chem 407:1033–1039. doi: 10.1007/s00216-014-8340-4

Willyerd KT, Li C, Madden L V., et al (2012) Efficacy and stability of integrating fungicide and cultivar resistance to manage Fusarium head blight and deoxynivalenol in wheat. Plant Dis 96:957–967. doi: 10.1094/PDIS-09-11-0763

Windels CE (2000) Economic and social impacts of Fusarium head blight: Changing farms and rural communities in the Northern Great Plains. Phytopathology 90:17–21. doi: 10.1094/PHYTO.2000.90.1.17

Winfield MO, Allen AM, Burridge AJ, et al (2016) High-density SNP genotyping array for hexaploid wheat and its secondary and tertiary gene pool. Plant Biotechnol J 14:1195–1206. doi: 10.1111/pbi.12485

Worland AJ, Börner A, Korzun V, et al (1998a) The influence of photoperiod genes on the adaptability of European winter wheats. Euphytica 100:385–394. doi: 10.1023/a:1018327700985

Worland AJ, Korzun V, Röder MS, et al (1998b) Genetic analysis of the dwarfing gene Rht8 in wheat. Part II. The distribution and adaptive significance of allelic variants at the Rht8 locus of wheat as revealed by microsatellite screening. Theor Appl Genet 96:1110–1120. doi: doi.org/10.1007/s001220050846

Wu D, Dong J, Yao YJ, et al (2015) Identification and evaluation of endogenous control genes for use in quantitative RT-PCR during wheat (Triticum aestivum L.) grain filling. Genet Mol Res 14:10530–10542. doi: 10.4238/2015.September.8.15

Würschum T, Langer SM, Longin CFH, et al (2017) A modern Green Revolution gene for reduced height in wheat. Plant J 92:892–903. doi: 10.1111/tpj.13726

Xiao J, Jin X, Jia X, et al (2013) Transcriptome-based discovery of pathways and genes related to resistance against Fusarium head blight in wheat landrace Wangshuibai. BMC Genomics 14:197. doi: 10.1186/1471-2164-14-197

Xie D, Feys BF, James S, et al (1998) COI1 : An arabidopsis gene required for jasmonate-regulated defense and fertility. Science 280:1091–1094. doi: 10.1126/science.280.5366.1091

Xiong H, Li Y, Guo H, et al (2021) Genetic mapping by integration of 55K SNP array and KASP markers reveals candidate genes for important agronomic traits in hexaploid wheat. Front Plant Sci 12:1–16. doi: 10.3389/fpls.2021.628478

Xu H, Liu Q, Yao T, Fu X (2014) Shedding light on integrative GA signaling. Curr Opin Plant Biol 21:89–95. doi: 10.1016/j.pbi.2014.06.010

Xu K, He X, Dreisigacker S, et al (2020) Anther extrusion and its association with Fusarium. Agronomy 10:47. doi: 10.3390/agronomy1001004

Xue AG, Voldeng HD, Savard ME, et al (2009) Biological control of Fusarium head blight of wheat with Clonostachys rosea strain ACM941. Can J Plant Pathol 31:169–179. doi: 10.1080/07060660909507590

Xue S, Li G, Jia H, et al (2010a) Fine mapping Fhb4, a major QTL conditioning resistance to Fusarium infection in bread wheat (Triticum aestivum L.). Theor Appl Genet 121:147–156. doi: 10.1007/s00122-010-1298-5

Xue S, Li G, Jia H, et al (2010b) Marker-assisted development and evaluation of near-isogenic lines for scab resistance QTLs of wheat. Mol Breed 25:397–405. doi: 10.1007/s11032-009-9339-y

Xue S, Xu F, Tang M, et al (2011) Precise mapping Fhb5, a major QTL conditioning resistance to Fusarium infection in bread wheat (Triticum aestivum L.). Theor Appl Genet 123:1055–1063. doi: 10.1007/s00122-011-1647-z

Yabwalo DN, Mergoum M, Berzonsky WA (2011) Further characterization of the scab resistance of "Frontana" spring wheat and the relationships between resistance mechanisms. Plant Breed 130:521–525. doi: 10.1111/j.1439-0523.2011.01883.x

Yan W, Li HB, Cai SB, et al (2011) Effects of plant height on type I and type II resistance to Fusarium head blight in wheat. Plant Pathol 60:506–512. doi: 10.1111/j.1365-3059.2011.02426.x

Yang DL, Yao J, Mei CS, et al (2012) Plant hormone jasmonate prioritizes defense over growth by interfering with gibberellin signaling cascade. Proc Natl Acad Sci USA 109:7152-7153. doi: 10.1073/pnas.1201616109

Yang J, Duan G, Li C, et al (2019) The crosstalks between jasmonic acid and other plant hormone signaling highlight the involvement of jasmonic acid as a core component in plant response to biotic and abiotic stresses. Front Plant Sci 10:1349. doi: 10.3389/fpls.2019.01349

Yang M, Wang X, Dong J, et al (2021) Proteomics reveals the changes that contribute to Fusarium head blight resistance in wheat. Phytopathology 111:386–397. doi: 10.1094/PHYTO-05-20-0171-R

Yang Z, Gilbert J, Fedak G, Somers DJ (2005) Genetic characterization of QTL associated with resistance to Fusarium head blight in a doubled-haploid spring wheat population. Genome 48:187–196. doi: 10.1139/G04-104

Yli-Mattila T, Gagkaeva T, Ward TJ, et al (2009) A novel Asian clade within the *Fusarium graminearum* species complex includes a newly discovered cereal head blight pathogen from the Russian far east. Mycologia 101:841–852. doi: 10.3852/08-217

Zanke CD, Ling J, Rg Plieske J, et al (2014) Whole genome association mapping of plant height in winter wheat (Triticum aestivum L.). PLoS One 9:e113287. doi: 10.1371/journal.pone.0113287

Zhai Q, Yan C, Li L, et al (2017) Jasmonates. In: Li J, Li C, Smith SM (ed) Hormone Metabolism and Signaling in Plants : Biosynthesis and Mechanisms of Action, 1st edn. Elsevier, San Diego, pp 243–272

Zhang W, Boyle K, Brûlé-Babel AL, et al (2020) Genetic characterization of multiple components contributing to Fusarium head blight resistance of FL62R1, a Canadian bread wheat developed using systemic breeding. Front Plant Sci 11:1–16. doi: 10.3389/fpls.2020.580833

Zhao L, Ma X, Su P, et al (2018a) Cloning and characterization of a specific UDP-glycosyltransferase gene induced by DON and *Fusarium graminearum*. Plant Cell Rep 37:641–652. doi: 10.1007/s00299-018-2257-x

Zhao M, Wang G, Leng Y, et al (2018b) Molecular mapping of Fusarium head blight resistance in the spring wheat line nd2710. Phytopathology 108:972–979. doi: 10.1094/PHYTO-12-17-0392-R

Zhao Y, Selvaraj JN, Xing F, et al (2014) Antagonistic action of Bacillus subtilis strain SG6 on *Fusarium graminearum*. PLoS One 9:1–11. doi: 10.1371/journal.pone.0092486

Zhou W, Kolb FL, Bai G, et al (2002) Genetic analysis of scab resistance QTL in wheat with microsatellite and AFLP markers. Genome 45:719–727. doi: 10.1139/g02-034

Zhu T, Wang L, Rimbert H, et al (2021) Optical maps refine the bread wheat Triticum aestivum cv. Chinese Spring genome assembly. Plant J 107:303–314. doi: 10.1111/tpj.15289

Zhu X, Zhong S, Cai X (2016) Effects of D-genome chromosomes and their A/B-genome homoeologs on Fusarium head blight resistance in durum wheat. Crop Sci 56:1049–1058. doi: 10.2135/cropsci2015.09.0535

Zhu Z, Hao Y, Mergoum M, et al (2019) Breeding wheat for resistance to Fusarium head blight in the Global North: China, USA, and Canada. Crop J 7:730–738. doi: 10.1016/j.cj.2019.06.003

Ziesman B, Bawolin C, Sliva T, et al (2019) Fusarium head blight in common and durum wheat in Saskatchewan in 2018.Canadian plant disease survey 2019 Volume 99: Disease highlights 2018. Can J Plant Pathol 41:102–103. doi: 10.1080/07060661.2019.1619270

Ziesman B, Hartley S, Peru C, et al (2018) Fusarium head blight in common and durum wheat in Saskatchewan in 2016 and 2017. Can Plant Dis Surv 98:131–134

Zou Z, Liu F, Huang S, Fernando WGD (2021) Genome-wide identification and analysis of the valine-glutamine motif-containing gene family in brassica napus and functional characterization of BnMKS1 in response to leptosphaeria maculans. Phytopathology 111:281–292. doi: 10.1094/PHYTO-04-20-0134-R

Appendix 3.1 Markers associated with common semi-dwarf genes or common FHB resistance genes/QTL screened on the parental lines and 3CPR doubled haploid population where appropriate.

Chr[1]	Locus	Marker name	Marker Type	Parental lines	3PCRDHs[2]	Reference
2D	*Rht8*	Gwm261	SSR[3]	Monomorphic		
		Gwm261	Flash Gel	Monomorphic		
3B	*Fhb1*	Umn10	KASP[4]	Monomorphic		(Liu et al. 2008)
		Fhb1/Umn10	SSR	Monomorphic		
4B	*Rht-B1*	RhtB1	KASP	Monomorphic		
		wMAS000001	KASP	Monomorphic		http://www.cerealsdb.uk.net/cerealgenomics/CerealsDB/kasp_download.php?URL
4D	*Rht-D1*	RhtD1	KASP	Monomorphic		
		wMAS000002	KASP	Monomorphic		http://www.cerealsdb.uk.net/cerealgenomics/CerealsDB/kasp_download.php?URL
5A	*Qfhs.ifa*	Barc186	SSR	Polymorphic	Tested	(Steiner et al. 2019)
		Barc100	SSR	Polymorphic		(Xue et al. 2011)
		Gwm293	SSR	Polymorphic	Tested	(Steiner et al. 2019)
		Gwm304	SSR	Polymorphic	Tested	(Steiner et al. 2019)
6B	*Fhb2*	Gwm133	SSR	Polymorphic	Tested	(Cuthbert et al. 2007)
		Gwm644	SSR	Polymorphic	Tested	(Cuthbert et al. 2007)
		Wmc398	SSR	Polymorphic	Tested	
		Wmc397	SSR	Polymorphic	Tested	

[1]Chromsome; [2]Markers were screened in the 3CPR population; [3]Simple sequence repeat (SSR) is one type of molecular marker used in this study; [4]Kompetitive allele-specific PCR (KASP) is another type of molecular marker used

Appendix 3.2 Analysis of variance for anthesis date (Anth), height (Ht), incidence (Inc), severity (Sev) and visual rating index (VRI) for the 3CPR population in each of six site years in Manitoba.

Site year: Carman 2015										
Source of Variation	**Anth**		**Ht**		**Inc**		**Sev**		**VRI**	
	DF[1]	**MS[2]**	**DF**	**MS**	**DF**	**MS**	**DF**	**MS**	**DF**	**MS**
G[3]	106	4.38****	106	161.85****	106	622.02****	106	387.05****	106	397.60****
Rep[4]	2	147.54****	2	2432.98****	2	10812.00****	2	1364.60****	2	2252.35****
Residual	212	1.61	212	29.96	211	314.58	211	78.65	211	86.72
Site year: Carman 2016										
Source of Variation	**Anth**		**Ht**		**Inc**		**Sev**		**VRI**	
	DF	**MS**	**DF**	**MS**	**DF**	**MS**	**DF**	**MS**	**DF**	**MS**
G	106	4.08****	106	66.55****	106	219.56****	106	252.78****	106	102.84****
Rep	2	32.90****	2	3615.99****	2	733.46****	2	2581.05****	2	157.64****
Residual	212	1.63	212	12.73	212	46.20	212	51.78	212	9.40
Site year: Carman 2017										
Source of Variation	**Anth**		**Ht**		**Inc**		**Sev**		**VRI**	
	DF	**MS**	**DF**	**MS**	**DF**	**MS**	**DF**	**MS**	**DF**	**MS**
G	125	12.02****	125	76.01****	125	294.74****	125	324.72****	125	101.95****
Rep	2	14.09	2	212.72****	2	57.36	2	266.72	2	3.26
Residual	238	6.51	233	19.20	230	47.58	230	145.98	230	8.08
Site year: Winnipeg 2015										
Source of Variation	**Anth**		**Ht**		**Inc**		**Sev**		**VRI**	
	DF	**MS**	**DF**	**MS**	**DF**	**MS**	**DF**	**MS**	**DF**	**MS**
G	106	4.49****	106	150.88****	106	402.26**	106	249.38****	106	164.42****
Rep	2	80.28****	2	432.83****	2	2930.99****	2	626.03****	2	595.13****
Residual	212	1.37	212	15.28	212	263.46	212	64.37	212	44.64
Site year: Winnipeg 2016										
Source of Variation	**Anth**		**Ht**		**Inc**		**Sev**		**VRI**	
	DF	**MS**	**DF**	**MS**	**DF**	**MS**	**DF**	**MS**	**DF**	**MS**
G	106	4.20****	106	85.91****	106	174.28****	106	160.61****	106	42.18****

Rep	2	7.73***	2	27.47	2	38.98	2	80.45	2	5.58
Residual	212	1.06	212	18.91	212	27.88	212	34.25	212	2.89

Site year: Winnipeg 2017

Source of Variation	**Anth**		**Ht**		**Inc**		**Sev**		**VRI**	
	DF	**MS**	**DF**	**MS**	**DF**	**MS**	**DF**	**MS**	**DF**	**MS**
G	125	5.32****	125	113.57****	125	253.59****	125	552.17****	125	109.62****
Rep	2	15.37**	2	103.94**	2	873.94****	2	1045.02*	2	321.30****
Residual	250	2.16	250	16.76	249	59.84	249	256.47	249	21.98

[1]DF Degrees of freedom; [2]MS Mean squares; [3]G Genotype; [4]Rep Replicate;
****P value< 0.0001; ***P value< 0.001; **P value < 0.01; *P value < 0.05

Appendix 3.3 Mean phenotype for anthesis date (Anth), height (Ht), incidence (Inc), severity (Sev), visual rating index (VRI), Fusarium damaged kernel (FDK), deoxynivalenol (DON), greenhouse anthesis (GAnth) and greenhouse severity (GSev1 and GSev2) or six checks based on least squares means in the combined field data and one year greenhouse data.

Genotype[1]	Anth[2] (Julian)	Ht (cm)	Inc (%)	Sev (%)	VRI (%)	FDK (%)	DON (ppm[3])	GAnth[3] (days)	GSev1 (%)	GSev2 (%)
FHB148 (R)	168.54	110.70	19.12	16.32	3.35	5.01	9.05	88.27	27.68	39.19
Emerson (R)	167.39	90.98	33.44	21.66	7.64	5.69	8.94	62.35	39.29	49.76
43I*18 (I)	169.81	96.10	41.30	34.01	15.43	12.72	18.28	76.92	26.36	37.21
Freedom (I)	167.49	86.21	55.33	31.86	19.17	12.80	18.19	82.67	22.52	27.41
Caledonia (S)	166.04	72.14	59.00	63.31	39.67	21.95	38.18	57.53	49.48	63.81
Hanover (S)	167.22	85.20	75.44	69.88	54.17	23.71	38.98	80.50	43.63	59.90

[1]Letters (R, I and S) refer to FHB resistant, intermediate and susceptible checks, respectively; [2]Anthesis date in field tests were calculated based on Julian calendar date;[3]ppm part per million; [4]Greenhouse anthesis date was calculated as the number of days between transplanting into pots and the date at 30-50% anthesis stage.

Appendix 3.4 Pearson correlation of anthesis date (Anth), height (Ht), incidence (Inc), severity (Sev), visual rating index (VRI), Fusarium damaged kernel (FDK), deoxynivalenol (DON), greenhouse anthesis (GAnth) and greenhouse severity (GSev1 and GSev2) for the 3CPR population based on means in the combined field data and one year greenhouse data.

		Anth	Ht	Inc	Sev	VRI	FDK	DON	GAnth	GSev1
Ht	***r*[1]**	0.31**								
	N[2]	118								
Inc	***r***	0.18	0.19*							
	N	118	118							
Sev	***r***	0.16	0.01	0.07						
	N	118	118	118						
VRI	***r***	0.28**	0.13	0.74**	0.65**					
	N	118	118	118	118					
FDK	***r***	0.15	0.16	0.79**	0.19*	0.71**				
	N	118	118	118	118	118				
DON	***r***	0.22*	0.19*	0.87**	0.14	0.75**	0.88**			
	N	118	118	118	118	118	118			
GAnth	***r***	0.35**	0.27**	-0.01	0.02	0.09	0.09	0.12		
	N	99	99	99	99	99	99	99		
GSev1	***r***	-0.15	0.04	0.00	0.36**	0.18	0.16	0.13	-0.25*	
	N	99	99	99	99	99	99	99	99	
GSev2	***r***	-0.11	0.08	0.01	0.40**	0.20*	0.19	0.15	-0.27*	0.97**
	N	99	99	99	99	99	99	99	99	99

[1]*r* means correlation coefficient; [2]N means number of 3CPR doubled haploid lines used for testing a correlation between two traits;
*indicated the *P*-value (<0.05) of probability of correlation
**indicated the *P*-value (<0.01) of probability of correlation

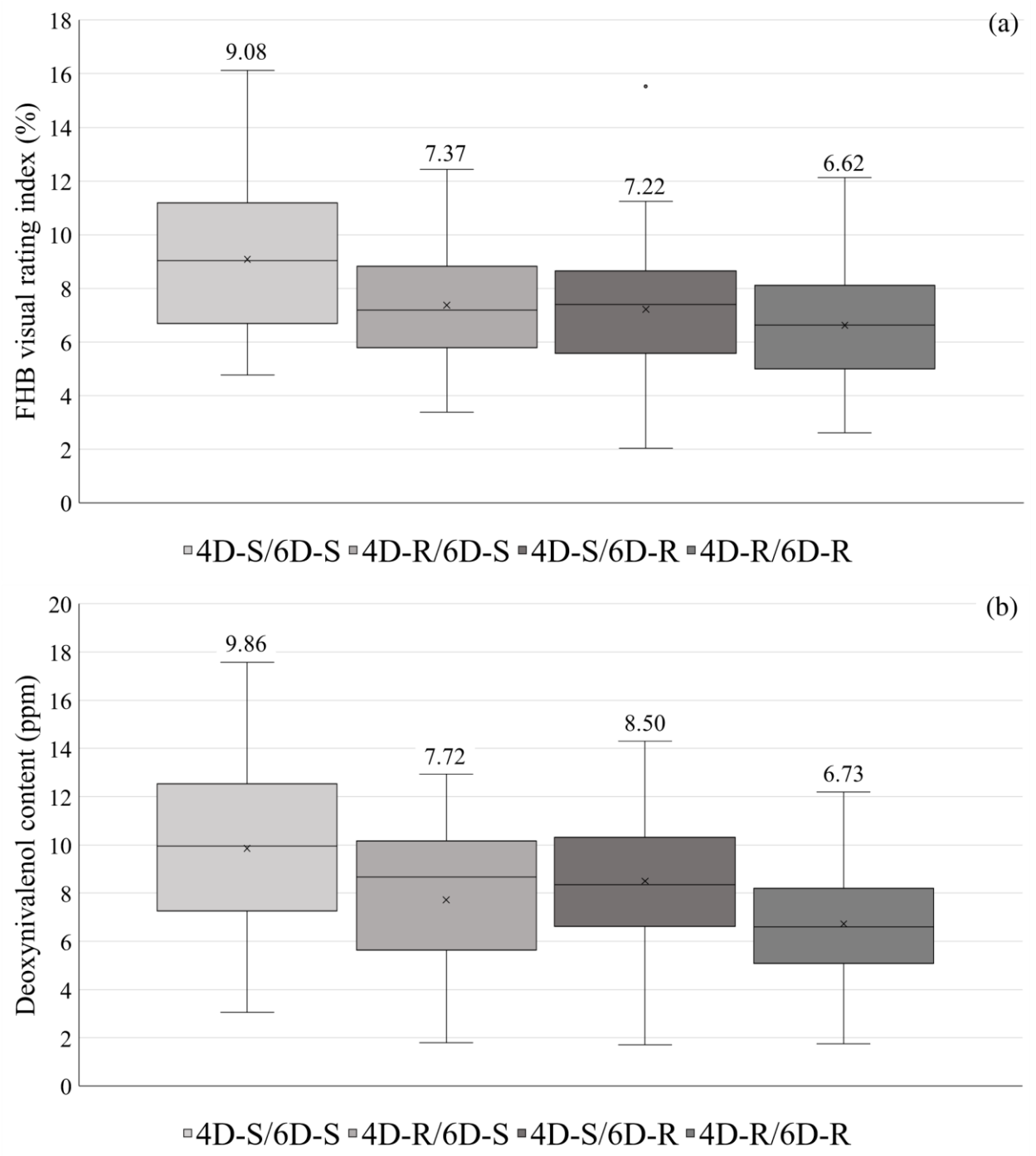

Appendix 3.5 Boxplot distribution of genotypic classes grouped according to presence of specific allele combinations at QTL located on chromosomes 4D and 6D for FHB visual rating index (VRI) (a) and deoxynivalenol content (DON) (b). The boxplots are based on number of DHs with the corresponding allele combination for each trait in the 3CPR population. Data of each trait is based on QTL analysis on the combined site years. Boxes show 1st and 3rd quartiles (as top and bottom edges, respectively), median values (as solid middle lines) and mean values (indicated by x as well as numbers above boxes). Outliers are dots outside the boxes.

Appendix 4.1 Markers associated with common semi-dwarf genes or common FHB resistance genes/QTL screened on the parental lines and 8I3C doubled haploid population where appropriate.

Chr[1]	Locus	Marker name	Marker Type	Parental lines	8I3CDHs[2]	Reference
2D	*Rht8*	Gwm261	SSR[3]	Monomorphic		
		Gwm261	Flash Gel	Monomorphic		
3B	*Fhb1*	Umn10	KASP[4]	Monomorphic		(Liu et al. 2008)
		Fhb1/Umn10	SSR	Monomorphic		
4B	*Rht-B1*	RhtB1	KASP	Polymorphic	Tested	
		wMAS000001	KASP	Polymorphic		http://www.cerealsdb.uk.net/cerealgenomics/CerealsDB/kasp_download.php?URL
4D	*Rht-D1*	RhtD1	KASP	Monomorphic		
		wMAS000002	KASP	Monomorphic		http://www.cerealsdb.uk.net/cerealgenomics/CerealsDB/kasp_download.php?URL
5AS	*Qfhs.ifa*	Barc186	SSR	Polymorphic	Tested	(Steiner et al. 2019)
		Barc100	SSR	Polymorphic		(Xue et al. 2011)
		Gwm293	SSR	Polymorphic	Tested	(Steiner et al. 2019)
		Gwm304	SSR	Polymorphic	Tested	(Steiner et al. 2019)
6B	*Fhb2*	Gwm133	SSR	Polymorphic	Tested	(Cuthbert et al. 2007)
		Gwm644	SSR	Polymorphic	Tested	(Cuthbert et al. 2007)
		Wmc398	SSR	Polymorphic	Tested	
		Wmc397	SSR	Polymorphic	Tested	

[1]Chromsome; [2]Markers were screened in the 8I3C population; [3]Simple sequence repeat (SSR) is one type of molecular marker used in this study; [4]Kompetitive allele-specific PCR (KASP) is another type of molecular marker used

Appendix 4.2 Analysis of variance for anthesis date (Anth), height (Ht), incidence (Inc), severity (Sev) and visual rating index (VRI) for the 8I3C population in each of six site years in Manitoba.

Site year: Carman 2015										
Source of Variation	**Anth**		**Ht**		**Inc**		**Sev**		**VRI**	
	DF[1]	**MS[1]**	**DF**	**MS**	**DF**	**MS**	**DF**	**MS**	**DF**	**MS**
G[2]	207	11.06****	207	602.53****	207	1325.23****	207	557.71****	207	637.31****
Rep[2]	2	125.15****	2	879.27****	2	9057.62****	2	1224.55****	2	2134.82****
Residual	413	1.41	413	21.72	413	254.15	413	74.17	413	83.81
Site year: Carman 2016										
Source of Variation	**Anth**		**Ht**		**Inc**		**Sev**		**VRI**	
	DF	**MS**	**DF**	**MS**	**DF**	**MS**	**DF**	**MS**	**DF**	**MS**
G[2]	207	7.88****	207	200.65****	207	190.99****	207	169.65****	207	52.11****
Rep[2]	2	34.26****	2	909.15****	2	596.48****	2	15.04	2	17.47*
Residual	414	1.13	413	19.48	414	46.74	414	44.71	414	4.95
Site year: Carman 2017										
Source of Variation	**Anth**		**Ht**		**Inc**		**Sev**		**VRI**	
	DF	**MS**	**DF**	**MS**	**DF**	**MS**	**DF**	**MS**	**DF**	**MS**
G[2]	207	15.53****	207	264.72****	207	256.65****	207	230.15****	207	56.96****
Rep[2]	2	292.97****	2	603.55****	2	1969.71****	2	1772.42****	2	326.80****
Residual	388	8.53	376	29.00	367	75.03	367	101.57	367	12.45
Site year: Winnipeg 2015										
Source of Variation	**Anth**		**Ht**		**Inc**		**Sev**		**VRI**	
	DF	**MS**	**DF**	**MS**	**DF**	**MS**	**DF**	**MS**	**DF**	**MS**
G[2]	207	10.17****	207	597.47****	207	1029.44****	207	309.97****	207	301.06****
Rep[2]	2	29.25****	2	122.52**	2	1910.45***	2	354.77**	2	170.20*
Residual	414	1.85	414	18.99	413	230.01	413	52.21	413	38.86
Site year: Winnipeg 2016										
Source of Variation	**Anth**		**Ht**		**Inc**		**Sev**		**VRI**	
	DF	**MS**	**DF**	**MS**	**DF**	**MS**	**DF**	**MS**	**DF**	**MS**
G[2]	207	10.37****	207	283.76****	207	415.75****	207	176.42****	207	56.60****

Rep[2]	2	68.18****	2	297.96****	2	787.95****	2	105.33	2	51.34**
Residual	414	1.23	413	17.70	414	79.93	414	69.21	414	8.58

Site year: Winnipeg 2017

Source of Variation	**Anth**		**Ht**		**Inc**		**Sev**		**VRI**	
	DF	**MS**	**DF**	**MS**	**DF**	**MS**	**DF**	**MS**	**DF**	**MS**
G[2]	207	11.39****	207	368.88****	207	327.06****	207	552.52****	207	131.88****
Rep[2]	2	26.30****	2	150.04****	2	1106.42****	2	1692.97***	2	337.64****
Residual	411	2.06	411	14.72	408	57.97	408	231.73	408	18.79

[1]DF Degrees of freedom; [2]MS Mean squares; [3]G Genotype; [4]Rep Replicate;
****P value< 0.0001; ***P value< 0.001; **P value < 0.01; *P value < 0.05

Appendix 4.3 Mean phenotype for anthesis date (Anth), height (Ht), incidence (Inc), severity (Sev), visual rating index (VRI), Fusarium damaged kernel (FDK), deoxynivalenol (DON), 2016 greenhouse anthesis (GAnth), 2016 greenhouse severity (GSev1 and GSev2), 2019 greenhouse anthesis (GAnth2), 2019 greenhouse height (GHt) and anther retention (GAR) of six checks based on least squares means in the combined field data and two year greenhouse data.

Genotype[1]	Anth[2] (Julian)	Ht (cm)	Inc (%)	Sev (%)	VRI (%)	FDK (%)	DON (ppm[3])	GAnth[4] (days)	GSev1 (%)	GSev2 (%)	GAnth2[5] (days)	GHt (cm)	GAR (%)
FHB148 (R)	168.13	110.74	20.88	18.87	4.10	7.33	8.72	60.90	37.71	47.53	59.88	96.05	32.08
Emerson (R)	167.14	89.89	32.08	22.08	7.48	6.80	8.13	47.04	40.14	56.01			
43I*18 (I)	169.10	95.61	40.78	35.94	16.82	15.69	16.78	58.06	51.49	66.99	80.75	87.92	54.17
Freedom (I)	167.74	85.52	60.51	33.64	22.14	13.69	16.04	52.06	28.71	34.48	119.87	75.81	55.14
Caledonia (S)	165.86	73.98	64.94	66.35	44.96	26.61	44.64	41.81	66.64	82.64	86.81	73.08	34.91
Hanover (S)	167.54	86.16	74.82	68.54	53.18	27.28	34.56	51.86	57.13	75.54	66.00	93.67	50.00

[1]Letters (R, I and S) implied FHB resistant, intermediate and susceptible checks, respectively; [2]Anthesis date in field tests were calculated based on Julian calendar; [3]ppm part per million; [4]Greenhouse anthesis date was calculated between the date of transplanting into pots and the date at 30-50% anthesis stage in 2016; [5]Greenhouse anthesis date was calculated between the date of transplanting into pots and the date at 30-50% anthesis stage in 2019

Appendix 4.4 Pearson correlation of anthesis date (Anth), height (Ht), incidence (Inc), severity (Sev), visual rating index (VRI), Fusarium damaged kernel (FDK), deoxynivalenol (DON), 2016 greenhouse anthesis (GAnth), 2016 greenhouse severity (GSev1 and GSev2), 2019 greenhouse anthesis (GAnth2), 2019 greenhouse height (GHt) and anther retention (GAR) for the 8I3C population based on means in the combined field data and two year greenhouse data.

		Anth	Ht	Inc	Sev	VRI	FDK	DON	GAnth	GSev1	GSev2	GAnth2	GHt
Ht	***r*[1]**	0.45**											
	N[2]	199											
Inc	***r***	0.18**	-0.54**										
	N	200	199										
Sev	***r***	0.31**	-0.08	0.70**									
	N	200	199	200									
VRI	***r***	0.27**	-0.37**	0.92**	0.87**								
	N	200	199	200	200								
FDK	***r***	0.08	-0.53**	0.89**	0.71**	0.88**							
	N	200	199	200	200	200							
DON	***r***	0.15*	-0.46**	0.89**	0.70**	0.88**	0.92**						
	N	200	199	200	200	200	200						
GAnth	***r***	0.66**	0.22**	0.16*	0.17*	0.21**	0.14	0.16*					
	N	200	199	200	200	200	200	200					
GSev1	***r***	-0.15*	0.06	0.05	0.38**	0.17*	0.15*	0.12	-0.17*				
	N	200	199	200	200	200	200	200	200				
GSev2	***r***	-0.08	0.17*	0.02	0.43**	0.17*	0.13	0.11	-0.15*	0.94**			
	N	200	199	200	200	200	200	200	200	200			
GAnth2	***r***	0.33**	-0.03	0.19*	0.07	0.17*	0.18*	0.16*	0.36**	-0.14	-0.16*		
	N	176	176	176	176	176	176	176	176	176	176		
GHt	***r***	0.13	0.82**	-0.53**	-0.15	-0.41**	-0.53**	-0.43**	-0.09	0.02	0.12	-0.23**	
	N	176	176	176	176	176	176	176	176	176	176	176	
GAR	***r***	0.15*	-0.24**	0.57**	0.34**	0.51**	0.54**	0.54**	0.23**	-0.14	-0.11	0.15	-0.29**
	N	176	176	176	176	176	176	176	176	176	176	176	176

[1]*r* means correlation coefficient; [2]N means number of 8I3C doubled haploid lines used for testing a correlation between two traits;
*indicated the *P*-value (<0.05) of probability of correlation
**indicated the *P*-value (<0.01) of probability of correlation

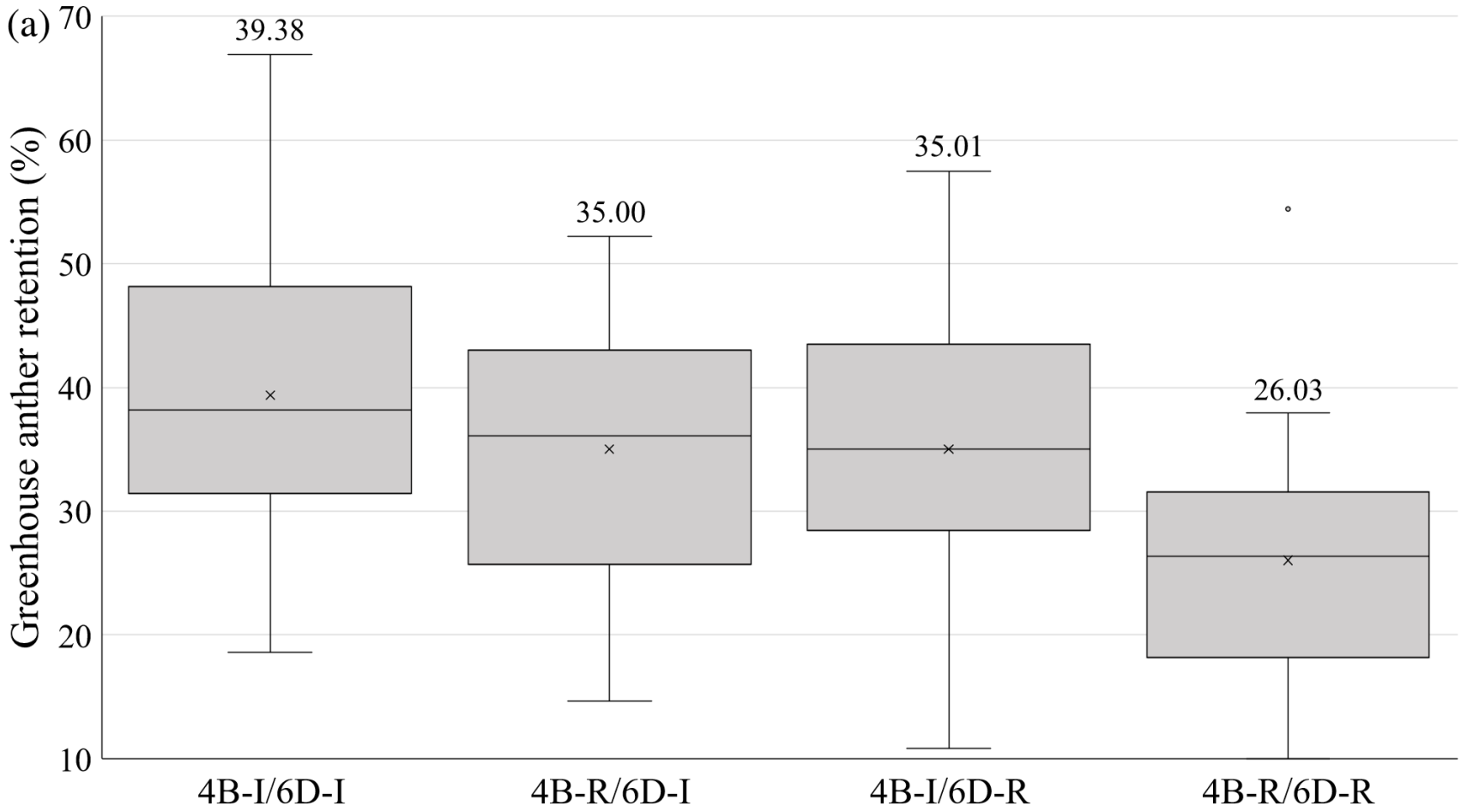
(a)
Greenhouse anther retention (%)
70
60
50
40
30
20
10
39.38
35.00
35.01
26.03
4B-I/6D-I
4B-R/6D-I
4B-I/6D-R
4B-R/6D-R

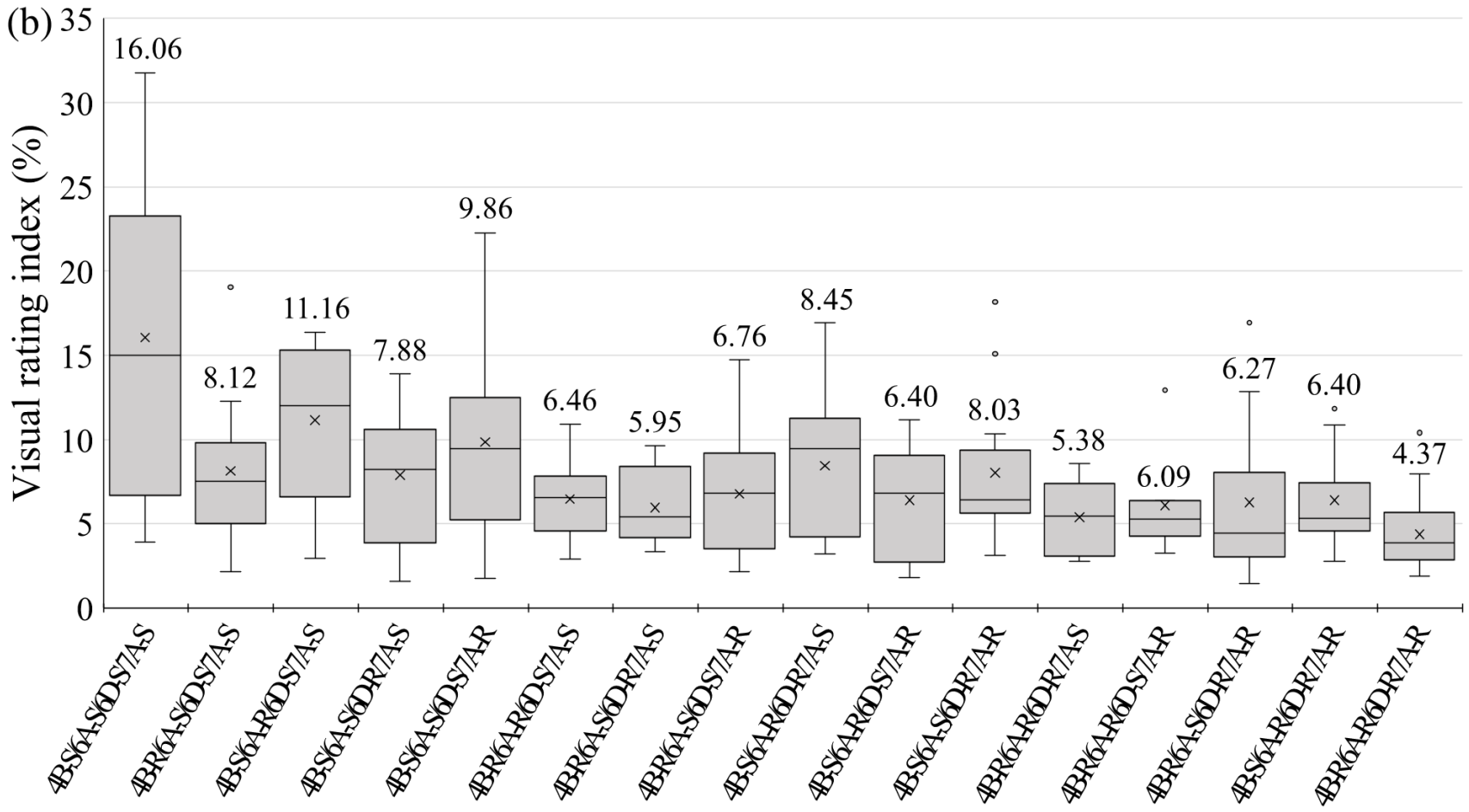
(b)
Visual rating index (%)
35
30
25
20
15
10
5
0
16.06
8.12
11.16
7.88
9.86
6.46
5.95
6.76
8.45
6.40
8.03
5.38
6.09
6.27
6.40
4.37
4BS6A-S6DS7A-S
4BR6A-S6DS7A-S
4BS6A-R6DS7A-S
4BS6A-S6DR7A-S
4BS6A-S6DS7A-R
4BR6A-R6DS7A-S
4BR6A-S6DR7A-S
4BR6A-S6DS7A-R
4BS6A-R6DR7A-S
4BS6A-R6DS7A-R
4BS6A-S6DR7A-R
4BR6A-R6DR7A-S
4BR6A-R6DS7A-R
4BR6A-S6DR7A-R
4BS6A-R6DR7A-R
4BR6A-R6DR7A-R

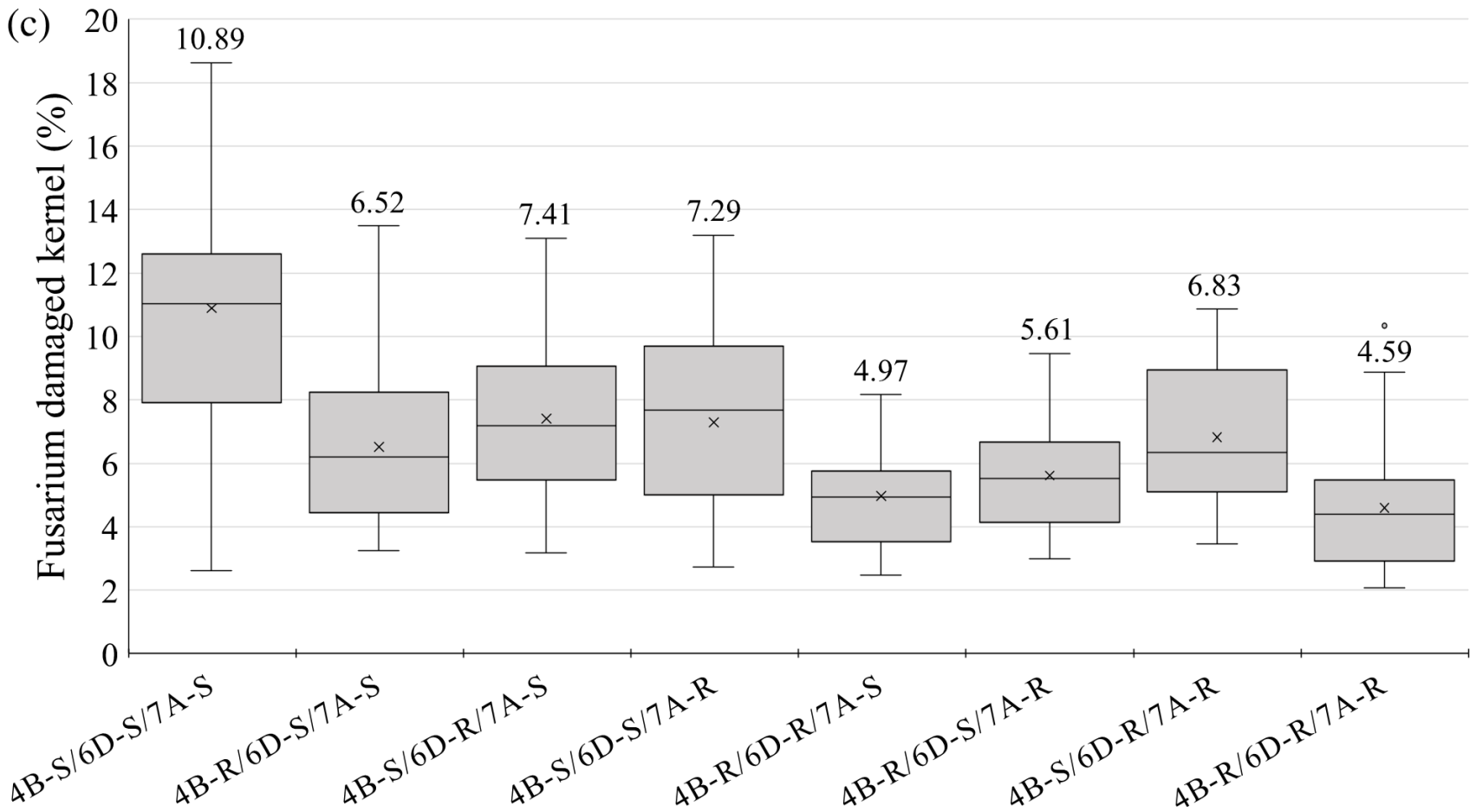
(c)
Fusarium damaged kernel (%)
20
18
16
14
12
10
8
6
4
2
0
10.89
6.52
7.41
7.29
4.97
5.61
6.83
4.59
4B-S/6D-S/7A-S
4B-R/6D-S/7A-S
4B-S/6D-R/7A-S
4B-S/6D-S/7A-R
4B-R/6D-R/7A-S
4B-R/6D-S/7A-R
4B-S/6D-R/7A-R
4B-R/6D-R/7A-R

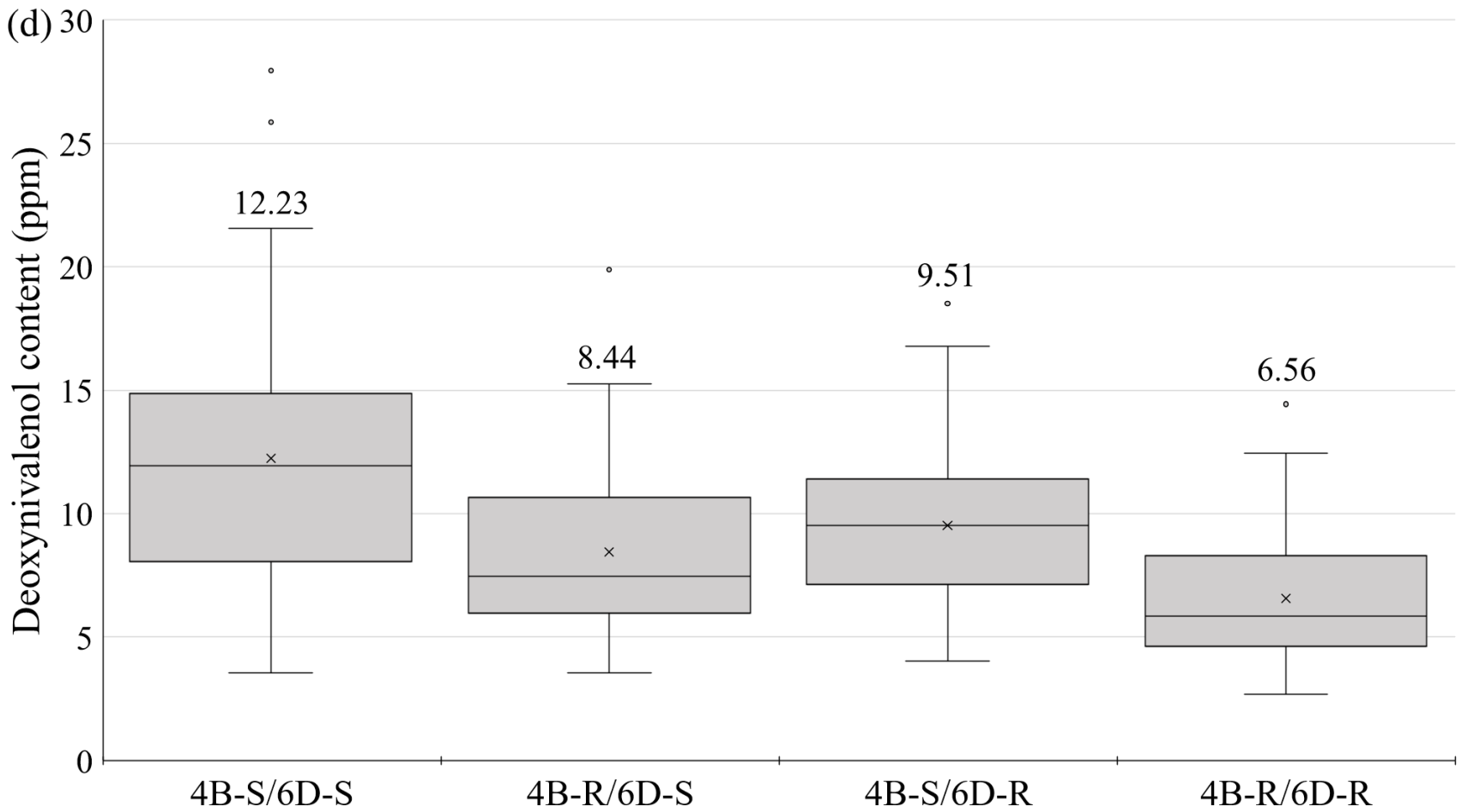

Appendix 4.5 Boxplot distribution of the 8I3C population genotypic classes grouped according to presence of specific allele combinations at QTL of interest for phenotypic traits. The boxplots are based on number of DHs with the corresponding allele combination for each trait in the 8I3C population. Data of each trait are based on QTL analysis on the combined site years. Boxes show 1st and 3rd quartiles (as top and bottom edges, respectively), median values (as solid middle lines) and mean values (indicated by x as well as numbers above boxes). Outliers are dots outside the boxes.

Appendix 5.1 Selected genes studied for gene expression in the *Fusarium*-wheat pathosystem. Four genes in deoxynivalenol (DON) biosynthesis were tested for pathogen genes, while seven genes involved in DON response and jasmonic acid (JA) pathway were examined for wheat genes.

Catalogue	Gene	Gene function	Reference[5]
DON[1] biosynthesis in *Fusarium*	*TRI5*	the early stage of DON biosynthesis pathway	(Mudge et al. 2006)
	TRI6	the global transcription regulator activating through the whole DON biosynthesis pathway	(Lee et al. 2014; Amarasinghe and Fernando 2016)
	TRI12	the end stage of DON biosynthesis pathway	(Nasmith et al. 2011)
	TRI101	the middle stage of DON biosynthesis pathway	(Lee et al. 2014; Amarasinghe and Fernando 2016)
DON response in wheat	*ABCC6*	ABC[2] transporter related to DON response	(Brauer et al. 2020)
	NFXL1	transcription factor related to DON response	(Brauer et al. 2020)
JA pathway in wheat	*AOS*	JA[3]-biosynthesis gene	(Qi et al. 2016)
	JAZ1	the key repressor of all JA-response and JA signaling gene	(Jing et al. 2019)
	*PR1b**	SA[4]- and JA-response gene	(Qi et al. 2016)
	PR4	JA-response gene	(Qi et al. 2016)
	PDF1.2	JA-response gene	(Qi et al. 2016)
Internal reference	*GAPDH*	*Fusarium* house-keeping gene	(Qi et al. 2016; Harris et al. 2016)
	EF-1α	Wheat house-keeping gene	(Crismani et al. 2006; Wu et al. 2015)

[1]DON deoxynivalenol; [2]ABC ATP-binding cassette; [3]JA jasmonic acid; [4]SA salicylic acid; [5]Primer sequences of the chosen genes were selected from those publications mentioned in this column

*The *PR1b* gene were not tested on the three checks in this qPCR study.

Appendix 5.2 Height (Ht) of infected wheat spikes of five genotypes in a series of time points (0, 1.5, 3, 7 and 14 days after inoculation (dai)). The five genotypes are Maris Huntsman *Rht-B1a* NIL (1a) and *Rht-B1b* NIL (1b), 32c*17(32c), Caledonia (Cal) and Sumai 3 (Su3). The multiple means comparison test for the interaction between genotype and time points on height was conducted in a combined analysis across all treatments. Letters indicate significant differences ($P < 0.05$) among genotypes at individual time points using Fisher's least significant difference (LSD) test. Means of Ht across all time points for each genotype were also included.

Genotype	Mean Ht (cm)	Ht (cm) at five time points				
		0 dai	1.5 dai	3 dai	7 dai	14 dai
1a	63.61^{c}	64.18^{ef}	63.38^{ef}	64.08^{ef}	64.18^{ef}	62.75^{f}
1b	45.08^{e}	47.43^{hi}	45.55^{ij}	44.27^{j}	44.82^{ij}	45.19^{ij}
32c	67.41^{b}	72.65^{c}		64.45^{ef}	69.28^{d}	66.35^{de}
Cal	50.76^{d}	49.92^{gh}		51.88^{g}	52.13^{g}	48.69^{h}
Su3	84.80^{a}	87.20^{a}		83.83^{b}	84.81^{ab}	85.09^{ab}

Appendix 5.3 Analysis of variance of log10 transformed relative expression of four *Fusarium* and seven wheat genes under a controlled environment on two parts (Part) of five genotypes (G) at four time points (T) under different treatments (Trt). *Fusarium* gene (*TRI5*, *TRI6*, *TRI12* and *TRI101*) were tested under both spray and point inoculated Fg treatments, while wheat genes (*ABCC6*, *NFXL1*, *AOS*, *JAZ1*, *PR1b*, *PR4* and *PDF1.2*) were tested under all four treatments. The four treatments were point inoculated *Fusarium* spore suspension, point injected deoxynivalenol solution, point injected water and spray inoculated *Fusarium* suspension.

Source of	***TRI5***		***TRI6***		***TRI12***		***TRI101***		***ABCC6***		***NFXL1***	
Variation	**DF**[1]	***P* value**[2]	**DF**	***P* value**	**DF**	***P* value**	**DF**	***P* value**	**DF**	***P* value**	**DF**	***P* value**
Trt	1	0.35	1	<0.01	1	0.05	1	0.04	3	<0.01	3	<0.01
G	4	0.02	4	0.36	4	0.03	4	<0.01	4	<0.01	4	<0.01
Trt*G	4	0.09	4	0.49	4	0.47	4	0.16	4	0.14	4	0.05
T	9	<0.01	9	0.03	9	<0.01	9	0.22	9	<0.01	9	<0.01
Trt*T	9	0.32	8	0.05	8	0.61	9	0.08	9	0.17	9	0.96
G*T	1	0.07	1	0.05	1	<0.01	1	0.45	1	<0.01	1	<0.01
Trt*G*T	3	<0.01	3	<0.01	3	<0.01	3	<0.01	3	<0.01	3	<0.01
Part	3	0.45	3	0.03	3	0.19	3	0.23	3	<0.01	3	<0.01
Trt*Part	4	0.22	4	0.13	4	0.42	4	1.00	9	<0.01	9	<0.01
G*Part	4	0.77	4	0.31	4	0.85	4	0.89	9	0.48	9	0.58
Trt*G*Part	9	<0.01	8	<0.01	9	0.02	9	<0.01	21	0.01	21	<0.01
T*Part	8	0.51	7	0.85	6	0.49	8	0.04	20	0.95	20	1.00
Trt*T*Part	1	0.07	1	0.28	1	0.21	1	0.48	3	<0.01	3	<0.01
G*T*Part	3	0.02	3	<0.01	3	0.01	3	<0.01	9	<0.01	9	<0.01
Trt*G*T*Part	3	0.42	2	0.41	3	0.18	3	0.51	9	<0.01	9	0.04
Replicate(Trt)[3]	4	0.74	4	0.93	4	0.58	4	0.45	8	0.11	8	0.29

Source of	***AOS***		***JAZ1***		***PR1b***		***PR4***		***PDF1.2***	
Variation	**DF**	***P* value**	**DF**	***P* value**	**DF**	***P* value**	**DF**	***P* value**	**DF**	***P* value**
Trt	3	<0.01	3	<0.01	3	<0.01	3	<0.01	3	<0.01
G	4	<0.01	4	<0.01	1	0.04	4	<0.01	4	0.11
Trt*G	4	0.03	4	<0.01	1	<0.01	4	<0.01	4	0.36
T	9	<0.01	9	0.04	3	0.10	9	<0.01	9	<0.01
Trt*T	9	0.24	9	0.05	3	0.01	9	<0.01	9	0.06
G*T	1	0.24	1	0.63	1	0.85	1	0.71	1	<0.01
Trt*G*T	3	<0.01	3	<0.01	3	<0.01	3	<0.01	3	0.01
Part	3	0.60	3	0.97	3	0.49	3	1.00	3	0.05
Trt*Part	9	<0.01	9	0.09	3	0.27	9	0.16	9	0.17
G*Part	9	0.35	9	0.15	3	0.02	9	0.09	9	0.49
Trt*G*Part	21	0.01	21	0.04	9	0.83	21	<0.01	20	0.06
T*Part	20	0.96	17	0.68	8	0.41	20	0.45	14	0.14
Trt*T*Part	3	<0.01	3	0.01	3	<0.01	3	<0.01	3	<0.01
G*T*Part	9	<0.01	9	<0.01	9	0.04	9	<0.01	9	<0.01
Trt*G*T*Part	9	0.97	9	0.67	9	0.02	9	0.02	8	0.03
Replicate(Trt)	8	0.05	8	0.18	8	0.72	8	0.93	8	0.13

[1]DF Degrees of freedom; [2]*P* value indicates a probability value; [3]Replicate nested within individual treatment

Appendix 5.4 Analysis of variance of log10 transformed relative expression of four *Fusarium* genes (*TRI5, TRI6, TRI12* and *TRI101*) under a controlled environment on two parts (Part) of five genotypes (G) at four time points (T) under the following individual treatments: point inoculated Fusarium (iF) and spray inoculated Fusarium (sF).

Source of Variation	iF treatment								sF treatment							
	TRI5		*TRI6*		*TRI12*		*TRI101*		*TRI5*		*TRI6*		*TRI12*		*TRI101*	
	DF[1]	*P* value[2]	DF	*P* value	DF	*P* value	DF	*P* value	DF	*P* value	DF	*P* value	DF	*P* value	DF	*P* value
G	4	<0.01	4	<0.01	4	<0.01	4	0.01	4	0.87	4	0.84	4	0.91	4	0.25
T	3	<0.01	3	<0.01	3	<0.01	3	<0.01	3	<0.01	3	<0.01	3	<0.01	3	<0.01
G*T	9	<0.01	9	<0.01	9	<0.01	9	0.14	9	0.01	8	0.02	9	0.05	9	0.01
Part	1	<0.01	1	0.02	1	<0.01	1	0.81	1	0.95	1	0.41	1	0.42	1	0.34
G*Part	4	0.01	4	0.03	4	0.09	4	0.07	4	0.81	4	0.81	4	0.96	4	0.79
T*Part	3	0.07	2	<0.01	3	<0.01	3	0.02	3	0.72	3	0.54	3	0.96	3	0.95
G*T*Part	8	<0.01	7	0.01	7	0.17	8	<0.01	9	0.98	8	0.70	7	0.78	9	0.67
Replicate	2	0.19	2	0.47	2	0.43	2	0.27	2	0.86	2	0.98	2	0.51	2	0.46

[1]DF Degrees of freedom; [2]*P* value indicates a probability value;

Appendix 5.5 Analysis of variance of log10 transformed relative expression of seven wheat genes (*ABCC6*, *NFXL1*, *AOS*, *JAZ1*, *PR1b*, *PR4* and *PDF1.2*) under a controlled environment on two parts (Part) of five genotypes (G) at four time points (T) under the following individual treatments: point inoculated Fusarium (iF), point injected DON (iD) and spray inoculated Fusarium (sF).

Source of Variation	iF treatment						iD treatment						sF treatment					
	ABCC6		*NFXL1*		*AOS*		*ABCC6*		*NFXL1*		*AOS*		*ABCC6*		*NFXL1*		*AOS*	
	DF[1]	*P* value[2]	DF	*P* value	DF	*P* value	DF	*P* value	DF	*P* value	DF	*P* value	DF	*P* value	DF	*P* value	DF	*P* value
G	4	<0.01	4	<0.01	4	<0.01	1	0.01	1	0.56	1	0.36	4	<0.01	4	<0.01	4	<0.01
T	3	<0.01	3	<0.01	3	<0.01	3	<0.01	3	<0.01	3	0.05	3	<0.01	3	<0.01	3	<0.01
G*T	9	0.01	9	0.02	9	<0.01	3	0.46	3	<0.01	3	<0.01	9	<0.01	9	<0.01	9	<0.01
Part	1	<0.01	1	<0.01	1	<0.01	1	0.01	1	<0.01	1	<0.01	1	0.09	1	0.95	1	0.64
G*Part	4	0.13	4	0.07	4	0.01	1	0.14	1	0.41	1	0.10	4	0.23	4	0.48	4	0.27
T*Part	3	<0.01	3	0.01	3	0.28	3	<0.01	3	<0.01	3	0.57	3	0.43	3	0.35	3	0.93
G*T*Part	9	0.56	9	0.91	9	0.23	2	0.47	2	0.65	2	0.49	9	0.19	9	0.99	9	0.57
Replicate	2	0.90	2	0.77	2	0.38	2	0.06	2	0.01	2	0.97	2	0.14	2	0.79	2	0.01
Source of	***JAZ1***		***PR1b***		***PR4***		***JAZ1***		***PR1b***		***PR4***		***JAZ1***		***PR1b***		***PR4***	
Variation	**DF**	***P* value**	**DF**	***P* value**	**DF**	***P* value**	**DF**	***P* value**	**DF**	***P* value**	**DF**	***P* value**	**DF**	***P* value**	**DF**	***P* value**	**DF**	***P* value**
G	4	<0.01	1	0.36	4	<0.01	1	0.84	1	0.69	1	0.09	4	<0.01	1	0.01	4	0.02
T	3	<0.01	3	0.01	3	<0.01	3	0.20	3	<0.01	3	0.01	3	<0.01	3	0.02	3	<0.01
G*T	9	0.07	3	0.29	9	<0.01	3	0.01	3	0.40	3	<0.01	9	0.04	3	0.18	9	<0.01
Part	1	0.24	1	<0.01	1	<0.01	1	0.05	1	0.01	1	<0.01	1	0.01	1	0.85	1	0.62
G*Part	4	0.03	1	<0.01	4	<0.01	1	0.01	1	0.02	1	0.02	4	0.12	1	0.05	4	0.50
T*Part	3	0.41	3	<0.01	3	<0.01	3	0.66	3	0.32	3	<0.01	3	0.53	3	0.73	3	0.73
G*T*Part	8	0.52	3	0.19	9	0.01	1	<0.01	2	0.55	2	0.11	8	0.14	3	0.01	9	0.13
Replicate	2	0.91	2	0.35	2	0.78	2	0.44	2	0.59	2	0.33	2	0.08	2	0.53	2	0.58

Source of	*PDF1.2*		*PDF1.2*		*PDF1.2*	
Variation	DF	*P* value	DF	*P* value	DF	*P* value
G	4	0.04	1	0.95	4	0.20
T	3	<0.01	3	<0.01	3	0.11
G*T	9	0.03	2	0.04	9	0.01
Part	1	0.01	1	<0.01	1	0.48
G*Part	4	0.36	1	0.98	4	0.25
T*Part	3	<0.01	2	0.49	3	0.32
G*T*Part	4	0.03	2	0.52	8	0.12

Replicate	2	0.46	2	0.32	2	0.45

[1]DF Degrees of freedom; [2]*P* value indicates a probability value;

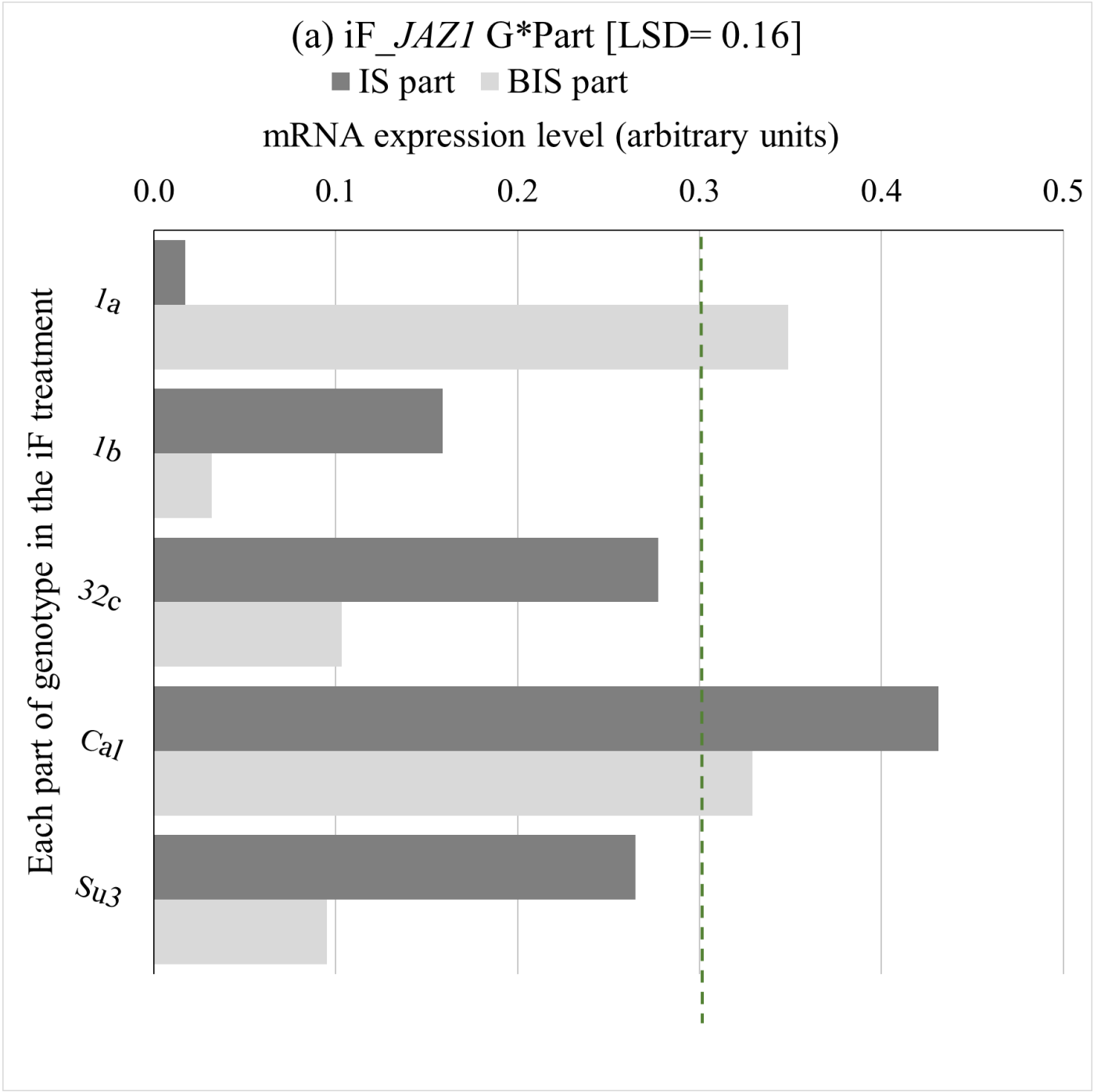
(a) iF_JAZ1 G*Part [LSD= 0.16]
IS part
BIS part
mRNA expression level (arbitrary units)
0.0
0.1
0.2
0.3
0.4
0.5
Each part of genotype in the iF treatment
1a
1b
32c
Cal
Su3

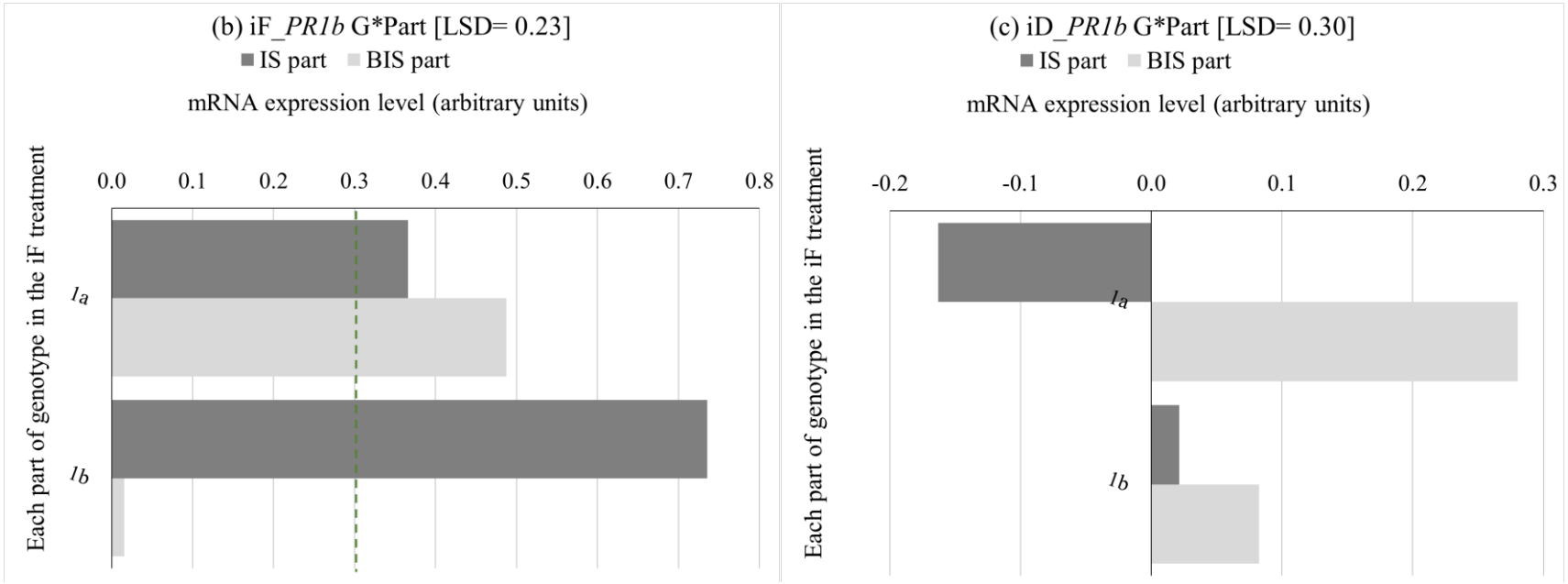

Appendix 5.6 Relative expression of wheat genes (*JAZ1* and *PR1b*) under a two-way interaction among part and genotype in individual treatments: (a) *JAZ1* and (b) *PR1b* in the point inoculated *Fusarium* treatment (iF) and (c) *PR1b* in the point inoculated deoxynivalenol treatment (iD). The two parts (IS and BIS part) are the inoculated and neighboring spikelets. The five genotypes (G) are Maris Huntsman *Rht-B1a* NIL (1a) and *Rht-B1b* NIL (1b), 32c*17(32c), Caledonia (Cal) and Sumai 3 (Su3). Mean of relative expression with log10 transformation for each part of each genotype is shown, and least significant difference (LSD) values are shown. Letters indicate significant differences ($P < 0.05$) among means comparisons of the G*Part interaction using Fisher's LSD test in each treatment.